OFFICE OF CIVILIAN RADIOACTIVE WASTE MANAGEMENT
SPECIAL INSTRUCTION SHEET

1. QA: QA

Complete Only Applicable Items

This is a placeholder page for records that cannot be scanned.

2. Record Date 06/04/2001	3. Accession Number MOL.20010613.0248
4. Author Name(s) S.F. ALEX DENG	5. Author Organization N/A

6. Title/Description
GENERIC DEGRADED CONFIGURATION PROBALILITY ANALYSIS FOR THE CODISPOSAL WASTE PACKAGE

7. Document Number(s) ANL-EDC-NU-000001	8. Version Designator REV. 00
9. Document Type REPORT	10. Medium OPTIC/PAPER

11. Access Control Code
PUB

12. Traceability Designator
DC #28615

13. Comments
THIS IS A ONE-OF-A-KIND DOCUMENT DUE TO THE COLORED GRAPHS ENCLOSED AND CAN BE LOCATED THROUGH THE RPC

OFFICE OF CIVILIAN RADIOACTIVE WASTE MANAGEMENT
ANALYSIS/MODEL COVER SHEET

Complete Only Applicable Items

1. QA: QA

Page: 1 of: 76

2. ☒ Analysis — Check all that apply		3. ☒ Model — Check all that apply	
Type of Analysis	☒ Engineering ☐ Performance Assessment ☐ Scientific	Type of Model	☒ Conceptual Model ☐ Abstraction Model ☐ Mathematical Model ☐ System Model ☐ Process Model
Intended Use of Analysis	☐ Input to Calculation ☐ Input to another Analysis or Model ☒ Input to Technical Document	Intended Use of Model	☐ Input to Calculation ☐ Input to another Model or Analysis ☒ Input to Technical Document
Describe use:		Describe use:	
Provides summary results on degraded configurations for DOE SNF types.		Provides screening criteria on degraded configurations for DOE SNF types.	

4. Title:

Generic Degraded Configuration Probability Analysis for DOE Codisposal Waste Package

5. Document Identifier (including Rev. No. and Change No., if applicable):

ANL-EDC-NU-000001 REV 00

6. Total Attachments:	7. Attachment Numbers - No. of Pages in Each:
4	I-15, II-42, III-7, IV-3

	Printed Name	Signature	Date
8. Originator	S.F. Alex Deng	S.F. Deng	05/23/01
	Mehmet Saglam	aaalsaed for M. Saglam	5/23/01
	Luca J. Gratton	Luca J. Gratton	5/23/01
9. Checker	Abbelhalim Alsaed	aaalsaed	5/23/01
	Pierre Macheret	P. Macht.	5/23/01
10. Lead/Supervisor	Abbelhalim Alsaed	aaalsaed	5/23/01
11. Responsible Manager	Dan Thomas	Douglas Brownson for Dan Thomas	5/23/01

12. Remarks:

OFFICE OF CIVILIAN RADIOACTIVE WASTE MANAGEMENT
ANALYSIS/MODEL REVISION RECORD

Complete Only Applicable Items

2. Analysis or Model Title:

Generic Degraded Configuration Probability Analysis for DOE Codisposal Waste Package

3. Document Identifier (including Rev. No. and Change No., if applicable):

ANL-EDC-NU-000001 REV 00

4. Revision/Change No.	5. Description of Revision/Change
00	Initial issue

CONTENTS

CONTENTS (Continued)

CONTENTS (Continued)

Page

FIGURES

Page

FIGURES (Continued)

Page

TABLES

Page

ACRONYMS AND ABBREVIATIONS

AMR	Analysis/Model Report
CDF	cumulative distribution function
CL	critical limit
CRWMS	Civilian Radioactive Waste Management System
DHLW	defense high-level waste
DFA	driver fuel assembly
DOE	U.S. Department of Energy
EDA	Enhanced Design Alternative
HLW	high-level waste
M&O	Management and Operations
MCNP	Monte Carlo N-Particle (transport code)
MCO	multi-canister overpacks
PWR	pressurized water reactor
Sh	Sherwood number
SNF	spent nuclear fuel
SS	stainless steel
TR	Technical Report
VA	viability assessment
wt%	weight percent

1. PURPOSE

In accordance with the technical work plan, *Technical Work Plan For: Department of Energy Spent Nuclear Fuel Work Packages* (CRWMS M&O 2000c), this Analysis/Model Report (AMR) is developed for the purpose of screening out degraded configurations for U.S. Department of Energy (DOE) spent nuclear fuel (SNF) types. It performs the degraded configuration parameter and probability evaluations of the overall methodology specified in the *Disposal Criticality Analysis Methodology Topical Report* (YMP 2000, Section 3) to qualifying configurations. Degradation analyses are performed to assess realizable parameter ranges and physical regimes for configurations. Probability calculations are then performed for configurations characterized by k_{eff} in excess of the Critical Limit (CL).

The scope of this document is to develop a generic set of screening criteria or models to screen out degraded configurations having potential for exceeding a criticality limit. The developed screening criteria include arguments based on physical/chemical processes and probability calculations and apply to DOE SNF types when codisposed with the high-level waste (HLW) glass inside a waste package. The degradation takes place inside the waste package and is long after repository licensing has expired. The emphasis of this AMR is on degraded configuration screening and the probability analysis is one of the approaches used for screening.

The intended use of the model is to apply the developed screening criteria to each DOE SNF type following the completion of the degraded mode criticality analysis internal to the waste package.

2. QUALITY ASSURANCE

An activity evaluation (CRWMS M&O 2000c, Addendum A), which was prepared per AP-2.21Q, *Quality Determinations and Planning for Scientific, Engineering, and Regulatory Compliance Activities*, determined that the Quality Assurance (QA) program (DOE 2000a) applies to the activity under which this analysis was developed. Control of the electronic management of data was accomplished in accordance with the controls specified by CRWMS M&O (2000c).

3. COMPUTER SOFTWARE AND MODEL USAGE

Microsoft Excel for Windows, Version 97 SR-2, was used in this document for graphic representation and arithmetical manipulations. Excel is commercial off-the-shelf software that is exempt in accordance with AP-SI.1Q, Section 2.1.

4. INPUTS

Various inputs are used to develop the screening criteria and the degradation configurations. These inputs, in terms of parameters and criteria, are discussed below.

4.1 PARAMETERS

The parameters for various inputs used in this AMR are described below. These parameters are appropriate for the intended use.

4.1.1 Waste Package Characteristics

As shown in Figure 1, the waste package consists of an outer and an inner barrier. The outer barrier is made of Alloy 22 and the inner barrier is made of 316 SS NG (CRWMS M&O 2000i; Pasupathi 1999). Inside the waste package, there is a web-shaped basket supporting structure that divides the interior of the waste package into six compartments, five around the periphery and one in the center (center tube). A HLW glass canister is placed in each of the five peripheral compartments. Codisposed with the five HLW glass canisters is the DOE SNF canister in the center of the waste package. Note that the variations in the waste package design from VA to EDA-II have had no impact on the current evaluation because all the degradation sequences of concern occur within the waste package volume, which has not significantly varied. The breach probability is the only parameter that varied, and the latest probabilities based on the EDA-II design are used in this report.

In the context of this analysis, the waste package degradation process is associated with the degradation of materials. The parameters that need to be considered for degradation analysis characterize the different components and associated materials inside the waste package. They are described below.

Waste Package Supporting Basket (Web) Structure–As discussed above, the basket structure shown in Figure 1 divides the waste package interior into six compartments, which provide the support and separation for the five peripheral HLW glass canisters and the DOE SNF canister in the center. The basket structure material is A516 CS.

HLW Glass Canister–As discussed above, there are five HLW glass canisters inside the waste package. An example of a HLW glass canister is shown in Figure 2. The glass canister shell is made of 304L SS (stainless steel) (CRWMS M&O 2000i; Pasupathi 1999). The glass chemical composition varies depending on where the HLW glass is made.

DOE SNF Canister–The DOE SNF canister is an 18- or a 24-inch-diameter cylindrical pipe; length is limited to no more than 3 m or 15 ft (depending on design). The 18-inch DOE SNF canister is to be placed in the center of the waste package (Figure 1). The 24-inch DOE SNF canister will replace one of the five HLW glass canisters. The design specification of the DOE SNF canister can be found in CRWMS M&O (2000i). The DOE SNF canister contains one of the various SNF types to be stored in the repository. The DOE SNF canister shell is made of 316L SS (CRWMS M&O 2000i, pp. 14-16).

Spent Nuclear Fuel–The DOE spent nuclear fuel is referred to as SNF. Six types of SNFs are used for screening examples in this report. Details of analyses are provided in Section 6. It should be noted that this screening is for internal criticality only. The subject of external criticality will be treated in another AMR.

Waste Form–Waste form refers to the DOE SNF. After the SNF matrix has degraded, the fissile material may be referred to as fissile waste form. As an example, Figure 1 shows the DOE-SNF canister with TRIGA SNF and 5 DHLW glass canisters inside the waste package (CRWMS M&O 2000a).

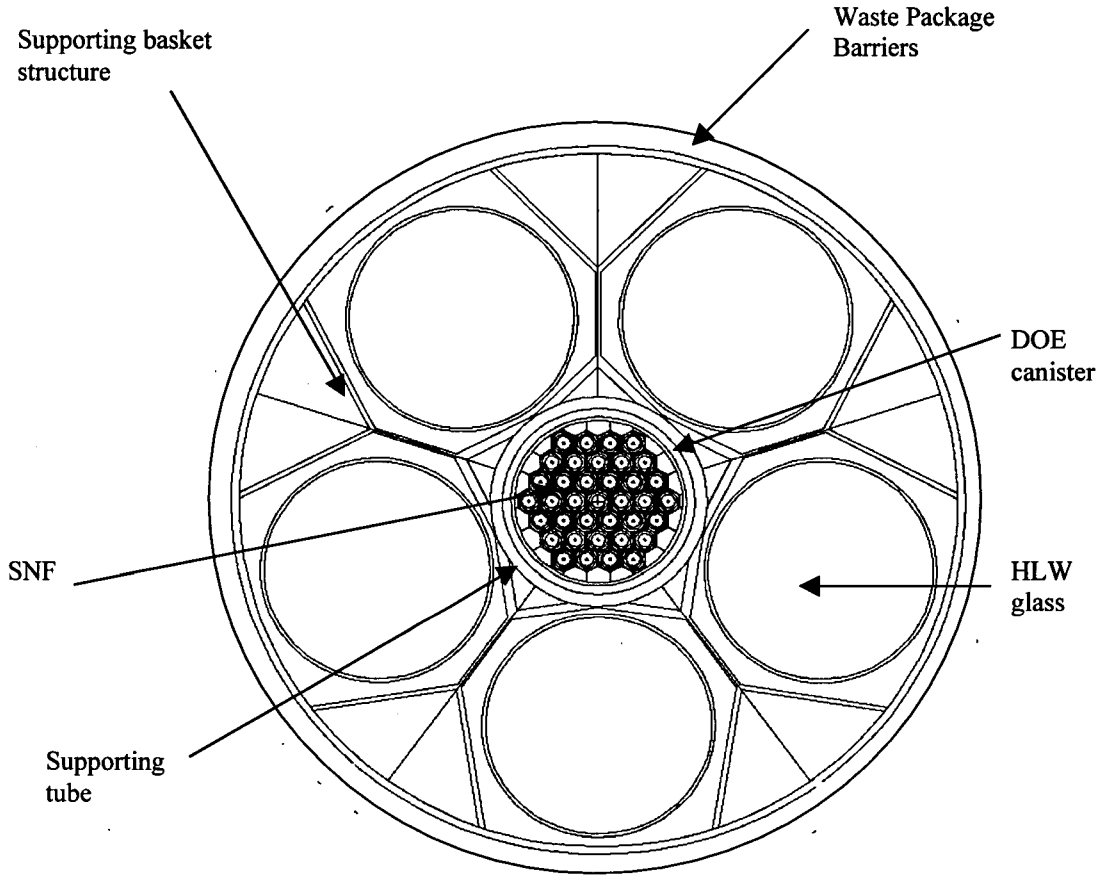

Figure 1. Cross Section of Codisposal Waste Package

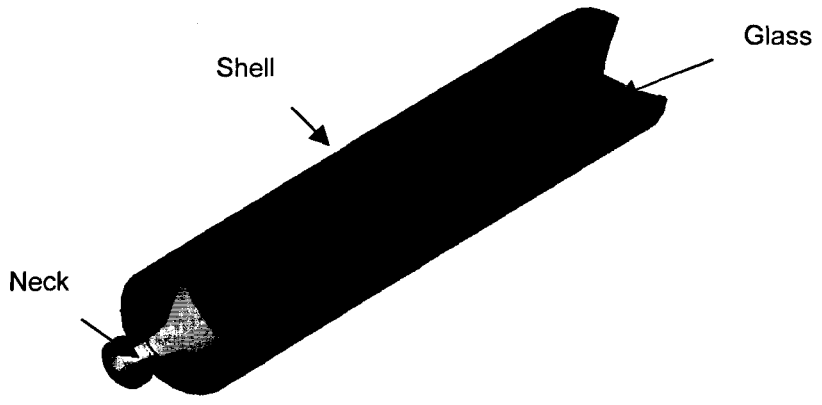

Figure 2. HLW Glass Canister

4.1.2 DOE Spent Nuclear Fuel

The following DOE SNF types (FFTF, Enrico Fermi, TRIGA, Shippingport PWR and LWBR, and N Reactor) were analyzed in this report. The details on the characteristics of these SNFs are provided in the respective technical report for each fuel type. For FFTF SNF, the dimensions of the Ident-69 are given in Section 6.2.1.2.3 and Figure 11. Note that for N Reactor SNF, multi-canister overpacks (MCOs) are used in lieu of DOE SNF canisters for codisposal in 2 HLW x 2 SNF arrays rather than the 5 HLW x 1 SNF array shown in Figure 1.

4.1.3 Degradation Rates

CRWMS M&O (1999a, pp. 19-20, Tables 2-17, 2-18, and 2-19; 1999b, p. 11, Table 4-1; 2000b, p. 22, Table 16) provides the degradation rates for the various materials used in the waste package and disposal canisters. The degradation rates for the materials of interest are provided in Table 1.

Table 1. Degradation Rates for Waste Package Components

Component	Material	Degradation Rate (moles/cm^2·s)
Waste Package Outer Barrier	Alloy 22	0.005
Waste Package Inner Barrier	316 SS	5.0E-13
Web Inside Waste Package	A516 CS	1.8E-11
HLW Glass	Glass	3.47E-13[a]
HLW Glass Canister	304L SS	8.6E-12
DOE SNF Canister	316L SS	5.0E-13
Fermi SNF	U-Mo	7.95E-14

NOTES: [a]High rate
[b]In units of (μm/yr)

4.1.4 Materials and Thicknesses

The various materials and associated thickness for the components used in the waste package and in the DOE SNF canister for the Enrico Fermi SNF are listed in Table 2 below.

Table 2. Materials and Thickness

Components	Material	Thickness (mm)
Waste package outer bracket	A 516 carbon steel	12.7
Waste package inner bracket	A 516 carbon steel	25.4
Waste package support pipe	A 516 carbon steel	31.75
HLW glass shell	304L SS	9.5
HLW glass	Glass	N/A
DOE SNF canister	316L SS	9.5
Spacer	316L SS	6.3
Lifting rod	316L SS	25.4
4-in. pipe	316L SS	4.8
Dividers A and B	316L SS	9.5
Base plate	316L SS	9.5
-01 shipping canister	Aluminum	3.175
-04 inner canister	Aluminum	1.651

Source: CRWMS M&O (1999c) and DOE (1999a)

4.2 CRITERIA

The design probability criterion states that the average criticality frequency will be less than 10^{-4} per year for the entire repository for the first 10,000 years (YMP 2000).

4.3 CODES AND STANDARDS

No specific codes and standards are required for this analysis.

5. ASSUMPTIONS

5.1 It is assumed that all the degrading solid surfaces are constantly exposed to a volume of water equal to the void space of the waste package. This corresponds to a waste package filled with water. The basis for this assumption is that this model is conservative with respect to the removal of neutron absorber by flushing because a smaller volume of water would have a higher concentration of dissolved material, thereby more easily reaching the solubility limit so that the material would be precipitated rather than remaining in solution to be flushed out. If there were several small ponds instead of a big one, the surface area of solids exposed to aqueous attack would be correspondingly decreased, so that the rate of dissolution would be decreased. The extreme case of localized ponding occurs when the waste package is penetrated at the bottom (as well as at the top). The water may then flow through the waste package as a thin film over a limited set of solid surfaces, without ever

ponding at all. Nevertheless, this film can be considered as a very localized pond with only a small fraction of the solid material contacting the water at any given time. Therefore, solid material would be dissolved at a slower rate than it would if the entire waste package were flooded. This assumption is used in Section 6.2.

5.2 Beginning of life pre-irradiation fuel compositions were used for all analyses. The basis of this assumption is that it is conservative to assume fresh fuel as it is more neutronically reactive than spent fuel. This assumption is used in Section 6.2.

5.3 It is assumed that the waste package barrier can maintain structural integrity indefinitely. The basis of this assumption is that it is conservative because intact waste package supports internal criticality. This assumption is used in Section 6.12.2.1.

5.4 For the TRIGA SNF (Figure 17), it is assumed that in order for the fuel to separate from the neutron absorber the absorber needs to break apart to at least 4 pieces. The basis of this assumption is that the fuel is 'encapsulated' by the basket pipes and absorber tubes. The way of freeing the fuel is by damaging (e.g. corrosion) the basket pipe and neutron absorber tube apart and it takes at least 4 pieces for the fuel rod to break free. The total number of particles is calculated from the number of fuel particles (1 per basket tube) and the number of pieces per basket tube (4 per tube) giving a total of 5 pieces per basket tube location. This assumption is used in Section 6.2.2.2.

6. ANALYSIS/MODEL

Based on the screening criteria provided in Attachment 1 of AP-3.15Q, this AMR does not include any "Principal Factors" or "Other Factors."

6.1 MODELS

This section discusses the general models used to develop the specific screening criteria used in Section 6.2. The models described in the following sections are based on physical/chemical analyses and probability calculations. Model validation consists of technical review on various publications in the open literature, which support the physical/chemical analyses and probability calculations. These publications are referenced throughout the report.

6.1.1 Degraded Configuration Screening

In performing the degraded mode criticality analysis, all possible degradation configurations are first identified using the methodology of the generic degradation scenario and configuration analysis report (CRWMS M&O 1999b) as a guide. Screening processes are then performed. The first screening is to eliminate any non-critical degraded configurations by MCNP calculations if the resulting k_{eff} for the degraded configuration is less than a prescribed critical limit (CL) of 0.93 (CRWMS M&O 1999a). In this report, the attainment of critical limit is regarded as condition equivalent to the observance of a nuclear critical state. Configurations with k_{eff} less than the CL are considered subcritical. The second screening is performed using some arguments and/or probability calculations. The arguments are used to screen out the impossible degraded configurations. The arguments are based on some physical/chemical

analysis and are used to provide the reasons why the critical configurations are impossible to occur. The probability calculation is used to indicate that the probability for a specific critical configuration to occur is very small.

6.1.2 Screening Models

The screening models are developed based on physics, geochemistry and probability. The physics part deals with the degradation processes that take place inside the waste package and the DOE SNF canister. The geochemistry deals with the nature of the different materials inside the waste package during degradation. One crucial information is the amount and form of the neutron absorber remaining in the waste package. The various degradation scenarios/processes lead to various degradation configurations. The configurations with the potential to become critical are the interest of this report. The probability part deals with the calculation on the probability of occurrence for the degraded configuration that could potentially lead to criticality.

6.1.2.1 Degradation Scenarios Development

The degradation scenarios consist of identifying the degradation process and associated sequence of events leading to some critical degraded configuration(s). Some degradation process may be applicable to only certain DOE SNF type. The degradation scenarios are determined by the materials and geometry of the individual DOE SNF types and of the supporting structures inside the waste package and the DOE SNF canister.

In this report, the generic degradation scenario and configuration analysis report (CRWMS M&O 1999b) was used as a guide for developing the degradation scenarios and the final critical degradation configurations. Various degraded configurations have been developed for different DOE SNF types. These configurations can be found in the respective Technical Report for each DOE SNF type (see Section 6.2). In general, the development consists of the following steps:

1. Identify the components and associated materials of the waste package, DOE SNF canister, and the SNF.

2. Identify the corrosion rates of the different materials.

3. Using the report CRWMS M&O (1999b) as a guide, postulate the possible combinations of degradation scenarios and configurations.

6.1.2.1.1 Degradation Processes and Configurations Development

In developing the list of degradation processes that make up the scenarios and lead to the resulting configurations, the following sequence can be used as a guide:

- Dripping on the waste package after drip shield failure

- Penetration of the waste package by dripping water

- Flooding of the waste package

- Degradation of the steel shells of the glass canisters and the supporting basket structure materials (external to the DOE SNF canister)
- Degradation of the HLW glass
- Degradation of the DOE SNF canister shell just sufficient to allow penetration and inflow of water (which leaves the canister shell otherwise intact, so that it may still be referred to as intact)
- Flooding of the DOE SNF canister
- Degradation of the supporting structure internal to the DOE SNF canister (called the basket and generally containing any neutron absorber added for criticality control)
- Processes that may separate the SNF from neutron absorber within the DOE SNF canister
- Degradation of the DOE SNF
- Complete degradation of the DOE SNF canister resulting in the contents of the waste package settling to the bottom of waste package
- Processes that separate the neutron absorber from the fissile material (from degraded SNF or in any remaining intact SNF).

It should be noted that the time sequence implied by the ordering in the above list is flexible. Indeed many of the processes overlap in time or may occur in a different order. It should be noted that the events listed above are generic in nature. Some events can not or will not occur. For example, there will be no neutron absorber separation if no neutron absorber is used or no fuel degradation if extremely durable fuel is used.

Note that various degraded configurations have been developed for different DOE SNF types. These configurations can be found in the Technical Reports (TR) for the respective DOE SNFs. References for these TRs can be found in Section 6.2. Only those configurations having potential for criticality are analyzed in this AMR and are discussed in Section 6.2

6.1.2.2 Probability Models

If a degraded configuration is identified to be critical, the probability of the scenario for reaching that configuration can be calculated. This scenario probability will be a combination of the individual probabilities of all the individual processes of the scenario leading to the configuration. Individual probability distributions may be time-dependent or non-time-dependent, according to the characteristics of the individual process. The various degradation process parameters may have different probability distributions depending on the degradation process. The individual probabilities can generally be combined in a Monte Carlo simulation. The methodology for the Monte Carlo simulation includes sampling for individual process parameters using the distributions appropriate to those parameters. Specialized analyses have used uniform, binomial, and Weibull distributions for sampling in the Monte Carlo process. The

limited probability analyses in this report have focused on only a few key parameters, so there is no need for a comprehensive Monte Carlo simulation. Furthermore, the uncertainty of estimating the probability of these parameters prevents the justification of any specialized probability distribution, so only the general binomial and Weibull distributions are used. For this report, only the probability of the event on the separation of SNF from neutron absorber is calculated for selected SNF. Due to lack of specific data for most of the degradation parameters, a range of parameters were used to perform the necessary analyses to bound the results.

Depending on the degradation processes, different sequences of events will take place to reach the final critical degraded configuration. In most cases, each event can be treated as an independent event, and the final probability will be the product of the probability for each individual event. Note that some external events, such as seismic or rockfall, are treated as initiating events which can also contribute to the final probability.

6.1.2.2.1 Degradation Events Necessary for Criticality

An abbreviated list of degradation events necessary (but not sufficient) for loss of the packaged Gd neutron absorber inventory and contributing to the possibility for internal criticality can be defined. The abbreviated sequence of events leads to transient waste package system states, labeled B, C and G for the analyses in Sections 6.2.1.2.4. The waste package states are defined as follows:

State B) Breach of the codisposal waste package and waste package flooding with water
State C) Breach of the DOE SNF canister during waste package flooding
State G) Consequential flushing of Gd from the standardized DOE SNF canister during waste package flooding

The consideration of only the necessary events provides a conservatively biased probability estimate (i.e., some "false positives" are admitted in the resulting statistics) because further refined estimates that consider additional events required for Gd loss must contribute to a lower overall probability.

The waste package system states are informed by the results of criticality evaluations. For example, assessments of the codisposal waste package containing FFTF SNF (CRWMS M&O 1999e; 1999f) indicate possibilities for degraded configurations with $k_{eff} \geq 0.93$ under situations involving both intact and degraded DOE SNF canisters. All configurations with $k_{eff} \geq 0.93$ require waste package breach, SNF canister breach and the complete loss of Gd and Fe-bearing degradation products while the waste package is flooded.

The probabilities for individual events in a degradation sequence are assessed using models for uncertain physical processes and random component failures. The 3 transient states B, C, and G are prerequisites to an ensemble of configurations with varying degrees of package damage. The probability for a degraded waste package state that is completely depleted of the Gd neutron absorber by a time t is assessed by integration of a double convolution:

$$P_{0-g}(t) = \int_0^t dt_b \frac{\partial P_{0-b}}{\partial t_b} \left[\int_0^{t-t_b} d\Delta t_b \frac{\partial P_{b-c}}{\partial \Delta t_b} \left[\int_0^{t-t_b-\Delta t_b} d\Delta t_c \frac{\partial P_{c-g}}{\partial \Delta t_c} \right] \right] \quad \text{(Eq. 1)}$$

where

P_{0-b} = probability for transition from initial state to state B
P_{0-c} = probability for transition from initial state to state C
P_{0-g} = probability for transition from initial state to state G
P_{b-c} = probability for transition from state B to state C
P_{c-g} = probability for transition from state C to state G
t = ellapsed time (years)
t_b = sampled time for transition to state B (years)
t_c = sampled time for transition to state C (years)
t_g = sampled time for transition to state G (years)
Δt_b = time difference between t_c and t_b (years)
Δt_c = time difference between t_g and t_c (years)

The probability for transition to state B is assigned as the product of the probability for the intersection of percolation drips with the waste package, the conditional probability for waste package barrier breach and the conditional probability for water pooling in the waste package,

$$P_{0-b}(t) = P_{bathtub} P_{breach}(t) \quad \text{(Eq. 2)}$$

$$P_{bathtub} = P_{drip} P_{pond} \quad \text{(Eq. 3)}$$

The probability that the waste package intersects seepage (P_{drip}) is a stationary value that is derived from performance assessment and accounts for the influence of the dripshield (McClure and Alsaed 2001, Table 8-9). The conditional water ponding probability assignment (P_{pond}) assumes that the waste package is flooded if there is no breach at the bottom, and that the package drains instantly upon breach at the bottom. The ponding assumption is conservative because it presumes instantaneous package flooding. The drainage assumption is reasonable, because the plugging of waste package barrier penetrations by corrosion products or debris is only a concern in the unlikely circumstance that the waste package becomes internally pressurized (CRWMS M&O 1999g, p. 6). The value P_{pond} is a conservative stationary estimate based on the maximum probability calculated in stochastic assessments for 6 different waste package designs (CRWMS M&O 1999g, Table 5.1.3-1 and p.18),

$$P_{drip} = 0.0694 \; ; \; P_{pond} = 0.4675$$

The conditional probability for codisposal waste package barrier breach is contingent upon barrier penetration within the scoping period, t. This probability is assessed using failure statistics for a waste package design for uncanistered commercial Pressurized Water Reactor (PWR) SNF assemblies (CRWMS M&O 1999g). Additionally, the probability assessment assumes that the waste package barrier can maintain structural integrity indefinitely, despite the

increasing probability that the waste package barrier will completely degrade (therefore, unable to support internal criticality) at a future time. Due to the lower package decay heat load, the codisposal waste package performance is expected to exceed that of the commercial SNF waste package. The use of 21 PWR failure statistics is, therefore, conservative.

The probability assignment is the Weibull Cumulative Distribution Function (CDF) for a parameter defined as the natural logarithm of time (CRWMS M&O 1999g, p. 8),

$$P_{breach}(t) = 1 - \exp\left[-\left(\frac{\ln(t) - \theta}{\alpha}\right)^{\beta}\right] \quad ; \quad \ln(t) \geq \theta \qquad \text{(Eq. 4)}$$

where the time t is assessed in years and the distribution parameters are obtained from CRWMS M&O (1999g, p. 8),

$$\begin{aligned} \alpha &= 2.347 \\ \beta &= 4.810 \\ \theta &= 10.820 \end{aligned}$$

The probability in Equation 4 is defined to be 0 for $\ln(t) < \theta$ (t is in years) and the distribution parameter values are determined by numerical regressions to the results of stochastic assessments for breach-times (CRWMS M&O 1999g, Table 5.1.2-1).

The probability for transition from state B to state C requires that sufficient time has elapsed since waste package breach (t_b) to allow penetration of the DOE SNF canister wall,

$$P_{b\text{-}c}(t) = P_{SS}(t) \qquad \text{(Eq. 5)}$$

If state C is considered the terminal state (instead of state G), evaluation of $P_{b\text{-}c}$ requires consideration of the conditional probability that the waste package flooding duration exceeds the time elapsed since waste package breach. When Gd loss is considered, the flooding duration probability modifies the state C to G transition probability (Equation 7).

P_{ss} in Equation 5 is assessed in terms of the conditional probability that a long-term average SS corrosion rate ($\tilde{N}_{ss}$:in mm per year) exceeds the ratio of the canister wall thickness (M_{ss}) to the elapsed time. M_{ss} has the value 9.525 mm (CRWMS M&O 1999a, p. 6). P_{ss}, can be calculated with a formalism for depletion under constant loss rate. In anticipation of $\tilde{N}_{ss}$ values less than 1 mm/yr, the variate for the conditional probability P_{ss} is assessed in terms of the negative natural logarithm of the rate. The conditional probability is given by the Weibull distribution,

$$P_{ss}(t-t_b) = 1-\exp\left[-\left(\frac{-\ln(\frac{M_{ss}}{t-t_b})-\theta}{\alpha}\right)^{\beta}\right] ; -\ln(\frac{M_{ss}}{t-t_b}) \geq \theta \qquad \text{(Eq. 6)}$$

where t and t_b are assessed in years and

$$\begin{aligned} \alpha &= 4.852 \\ \beta &= 4.041 \\ \theta &= 4.605 \end{aligned}$$

The distribution parameters listed above for Equation 6 are determined by regression to the results of stochastic assessments for the distributions of both SS304L and SS316L corrosion rates (CRWMS M&O 1999g, p. 16). The regression produces the distribution parameters for the variate defined as the negative natural logarithm of the corrosion rate.

The conditional probability for transition from state C to state G involves the complete loss of the packaged Gd by flushing while the package remains flooded. The transition to state G is dependent on the prevalence of highly unlikely chemical conditions and package flushing rates. The possibility of significant Gd loss is low because the Gd-bearing species are only very slightly soluble even under unlikely chemical conditions.

The probability for transition to state G is the product of the conditional probability for Gd loss within a relative time, t - t_c, and the probability that the waste package is flooded at the time of final loss,

$$P_{c\text{-}g}(t) = P(\tilde{N} > \frac{M}{t - t_c}) \; P(t < t_b + t_{flood}) \qquad \text{(Eq. 7)}$$

The condition for the elapsed time (t - t_c) sufficient to allow total loss requires the effective average $GdPO_4$ flushing rate ($\tilde{N}$ in kg per year) to exceed the ratio of the DOE SNF canister's initial $GdPO_4$ inventory (M) to the elapsed time. The $GdPO_4$ content of the DOE SNF canister basket material (SS316L) is greater than 11.43 kg, or 3 wt% of the basket mass for the most reactive configuration with 5 DFAs (CRWMS M&O 1999a, p. 68). Therefore, a minimum value for M is 11.43 kg. The $GdPO_4$ flushing rate can be expressed in terms of a $GdPO_4$ molality (μ) and a volumetric flushing rate ($\hat{U}$), assuming a nominal water mass density (ρ) of 1000 kg/m^3,

$$\tilde{N}\left[\frac{\text{kg - GdPO}_4}{\text{yr}}\right] = 252.22\left[\frac{\text{gm}}{\text{mole}}\right]\frac{\rho\left[\frac{\text{kg - H}_2\text{O}}{\text{m}^3}\right]}{1000\left[\frac{\text{gm}}{\text{kg}}\right]}\hat{U}\left[\frac{\text{m}^3}{\text{yr}}\right]\mu\left[\frac{\text{mole} - \text{GdPO}_4}{\text{kg} - \text{H}_2\text{O}}\right] = 252.22\,\hat{U}\,\mu$$

(Eq. 8)

where the atomic weights for $GdPO_4$ are from Parrington et al. (1996, p.16, 19, 36 and 37). Using Equation 8, the conditional probability for Gd flushing in Equation 7 can be expressed in terms of μ,

$$P(\tilde{N} > \frac{M}{t-t_c}) = 1 - P\left(\mu < \frac{M}{252.22\,\hat{U}\,(t-t_c)}\right) \qquad \text{(Eq. 9)}$$

An envelope bounding the pH dependence of μ is obtained from the results of transient, deterministic evaluations for the chemical degradation of a codisposal waste package containing FFTF SNF (CRWMS M&O 1999a, p. 55, Figure 6-10). The pH dependence of μ is strictly valid for in-package pH values between 5 and 9, though extrapolated in this analysis to higher pH. The extrapolation is reasonable because the evaluations include the peak value of $\hat{U}$ (0.15 m^3/year) and high values for the total dissolved phosphate concentration (10^{-2} mole/kg-H_2O), thereby shifting the chemical equilibrium towards high $GdPO_4$ concentrations,

$$\mu(pH) = \begin{cases} 10^{-11} & ;\ pH \le 7 \\ 10^{(pH-18)} & ;\ pH > 7 \end{cases} \qquad \text{(Eq. 10)}$$

Using Equation 10, the conditional probability for complete Gd flushing (Equation 9) can be expressed in terms of a randomly sampled in-package pH level,

$$P(\tilde{N} > \frac{M}{t-t_c}) = \begin{cases} 0 & ;\ pH \le 7 \\ 1 - P\left(pH < 18 + \log_{10}\left[\frac{M}{252.22\,\hat{U}\,(t-t_c)}\right]\right) & ;\ pH > 7 \end{cases} \qquad \text{(Eq. 11)}$$

where t and t_c are given in years. A zero probability results for pH $\le$ 7 because M (11.43 kg) and $\hat{U}$(0.15 m^3/year) are known, and because scoping times (t) less than 30 billion years render a deterministic result for this pH range in the envelope defined by Equation 10.

A Weibull distribution is the appropriate model for in-package pH level uncertainties,

$$P(pH < X) = 1 - \exp\left[-\left(\frac{X-\theta}{\alpha}\right)^{\beta}\right] ;\ X \ge \theta \qquad \text{(Eq. 12)}$$

where X is an arbitrary pH value and the distribution parameters for Equation 12 are regressed to in-package chemistry data provided in (CRWMS M&O 2000g),

α = 8.2038
β = 5.5416
θ = 0

Equations 11 and 12 establish that $P(\tilde{N}>M/(t-t_c)) = 0$ with a probability 0.34 determined by X=7 in Equation 12 and that $P(\tilde{N}>M//(t-t_c))$ is non-zero with the complimentary probability 0.66

$$P(\tilde{N} > \frac{M}{(t-t_c)}) = 0.66 \exp\left[-\left(\frac{18 + \log_{10}\left[\frac{M}{252.22\,\hat{U}\,(t-t_c)}\right]}{\alpha}\right)^{\beta}\right]; \quad \text{(Eq. 13)}$$

$$18 + \log_{10}\left[\frac{M}{252.22\,\hat{U}\,(t-t_c)}\right] \geq 7$$

Chemical forms other than $GdPO_4$ are under consideration for the engineered Gd bearing species (e.g, Gd-Al and Gd-Ni-Mo alloy). Alternate chemical forms may have degradation and solubility characteristics that differ from $GdPO_4$ sufficiently to modify the functional form and magnitude of the probability in Equation 13.

The probability that the waste package is flooded at the moment of complete Gd loss, $P(t < t_b + t_{flood})$, is assessed using the complimentary probability (i.e., $1 - P(t_b + t_{flood} < t)$) to a flooding duration distribution. The assessment gives $P(t < t_b + t_{flood})$ in terms of the variate defined as the natural log of time (CRWMS M&O 1999g, Table 5.1.3-1 and Figure 5.1.3-2),

$$P(t < t_b + t_{flood}) = \exp\left[-\left(\frac{\ln(t-t_b) - \theta}{\alpha}\right)^{\beta}\right]; \ \ln(t-t_b) \geq \theta \quad \text{(Eq. 14)}$$

where t and t_b are assessed in years and the distribution parameters for Equation 14 are given in CRWMS M&O (1999g, p. 13, Table 5.1.3-1),

α = 11.881
β = 10.218
θ = 0

6.1.3 Generic Screening Physics Models

Knowing the processes of reaching some degraded configurations as described above, some screening models can be developed based on some physical and/or chemical processes involved. Some of the screening models are generic and can be applied to screen out the critical degraded configurations for different DOE SNF types. These generic screening physics models are described below.

6.1.3.1 Generic Degradation Physical Phenomena

When analyzing the degradation processes for reaching the critical configurations, the following physical phenomena were identified:

- The effect of the neutron absorber is diminished due to separation from the fissile material. The separation was due to stratification.

- Geometry of the fuel is such that the fuel elements form an independent continuous array (e.g., are stratified from the other materials) and their arrangement/spacing is favorable to criticality. Note that the spacing of the fuel modeled for criticality calculations is not based on collapse but on optimum pitch. In addition, for the completely degraded state, generally the bounding cases are configurations with a truly homogenous mixture of fissile mass and moderator.

The phenomena of stratification and optimum spacing are further discussed below.

6.1.3.1.1 Separation of Fissile Material from Absorber Due to Density Variation

The following discussion postulates that the particles of interest are non-colloidal particles or droplets that are distributed in a continuous fluid and the only body force acting is gravity. The subsequent motion of the particles is governed by body forces (possibly allowing buoyancy), solid particle collisions, and hydrodynamic forces (such as Stokeian drag).

For a more explicit description consider the configuration sketched in Figure 3. This is a general depiction regarding this phenomena. This figure is for illustration only.

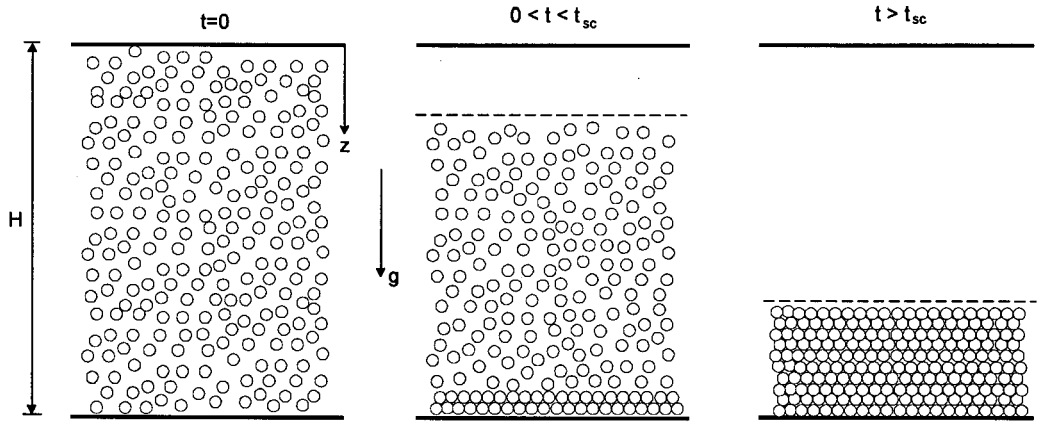

Figure 3. Settling of Heavy Particles by Gravity

Initially the suspension is mixed throughout the volume of interest and motionless. The gravitational body force is constant and acts in the vertical direction z. This is a hydrostatic steady state condition if the effective density of the particles is equal to the density of the continuum. However, if the particles are heavier than the fluid they will fall. The falling particles are stopped by a solid horizontal wall (a simplification that represents the bottom of the waste package, or DOE SNF canister) and concentrate in a sedimentation layer. The estimate of the terminal velocity of the particles can be obtained from the Stokes drag formula (Weast 1979, p. F-127):

$$V_{sep} = \left(\frac{\rho_D - \rho_C}{\rho_C} \right) \frac{2}{9} \frac{a^2}{\upsilon_0} g = \varepsilon \frac{2}{9} \frac{a^2}{\upsilon_0} g \qquad \text{(Eq. 15)}$$

Where ρ_D and ρ_C is the density of the particles and the surrounding fluid continuum, respectively (g/cm^3), a is the characteristic size of the particles (cm), ν_0 is the kinematic viscosity of the medium (poise), g is the gravitational constant and ε is defined by the formula as the relative density of the particles.

If the characteristic height for the system is H, then the time scale for separation (or stratification) is $t_{sep} = H / V_{sep}$. For a distribution of particle types, the individual velocities would define a time scale for sedimentation that would be proportional to their relative densities.

For illustrative purposes this can be demonstrated by doing a calculation for particles of different densities. The main challenge in using Equation 15 is to obtain appropriate values for the viscosity of the medium, which vary widely for different type of materials. For example, the viscosity of water is 10^{-2} poises at room temperature while the viscosity of resins and gums is 10^3 to 10^9 poises (Jastrzebski 1959, p. 3). For illustrative purposes, it is possible to assume that the kinematic viscosity of the medium is 10^6 poises and that the density of the medium is 1.5 g/cm^3. Table 3 shows settling times for particles with a characteristic size of 1 cm and varying densities that fall a distance of 1.0 m in such an environment.

Table 3. Particle Settling Times

Density (g/cm^3)	Settling Time (sec)
2.0	13770
2.5	6883
3.0	4589
3.5	3441
4.0	2753

The settling time is proportional to the square of the characteristic size of the particles. This means that a particle that has 1/10 of the size of another particle will have a settling time that is 100 times larger. The calculated values show that the time frames of interest are rather large for the settling process even if Stokes Law is valid.

In the case that a particle is buoyant in the continuum, it can rise, which is indicated by a negative V_{sep} in Equation 15. Figure 4 shows the case where two kinds of particles that are initially mixed do separate due to the difference in particle buoyancy.

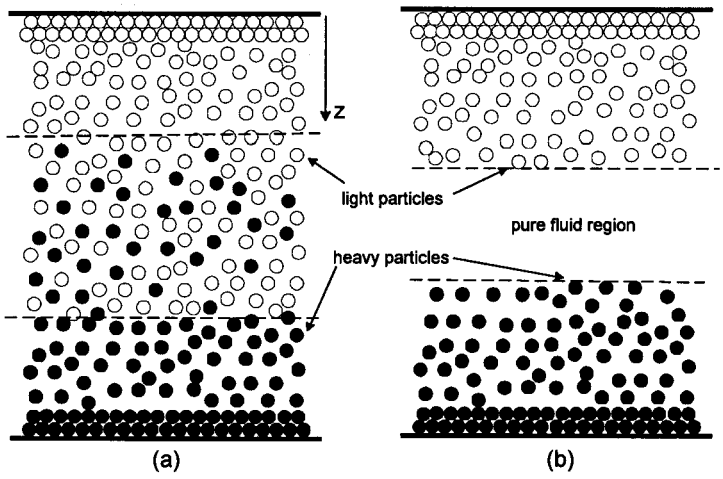

Figure 4. Separation of a Bidisperse Suspension into its Constituents

For the case in Figure 5, an effective tri-fluid stratification is evident. The particle bearing regions are treated as two distinct phases, each with its own continuity and momentum equations interacting with the continuous fluid phase. The straightforward extension of the correlation for a monodispersion to a polydispersion is an oversimplification but is shown to be valid for non-dense suspensions of particles with moderately different size and densities.

The physical situation described above is unstable and could only exist for a relatively short period of time. It could form from a collapse due to a sudden external event, such as an earthquake, provided the degraded material is already in a metastable state. Degradation is a gradual process and cannot lead directly to an unstable configuration. In any instant, effective separation as shown in Figure 4 is only possible if one constituent of the mixture has a smaller density than the fluid continuum. This is true, for example, if one of the components is SS and the other component is made of plastic. In this case, the plastic could separate due to having a density smaller than the fluid continuum. The neutron absorber particles and the fissile material on the other hand have densities that are significantly larger than the density of the fluid, which has density close to water (see Table 4 and Table 5 in the following section). Therefore, separation between fissile and neutron absorber is not possible because both will settle with similar velocities once they have degraded, and their degradation rates will be similar enough to guarantee that their individual degradation processes will have a significant overlap in time. This is further discussed in Section 6.1.3.1.2 below.

6.1.3.1.2 Separation of Fissile Material from Absorber Due to Sedimentation

The conceptual analysis of the possibility of separation of neutron absorber from fuel due to fall or sedimentation requires an understanding of the physical phenomena affecting the processes. An initial assessment, for the cases in which the basket materials degrade much faster than the SNF, can be made by using a conceptual model as shown in Figure 5.

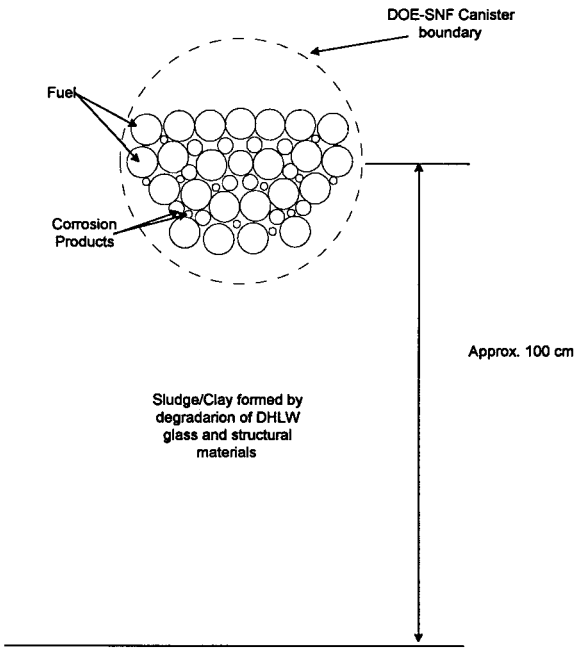

Figure 5. Conceptual Sketch of a 'Lump' of Material Formed by Corrosion Products and Fuel Inside the DOE SNF Canister

The separation of the neutron absorber particles and degradation products from the fuel can arise from the 'collapse' or 'disintegration' associated with the DOE SNF canister and its contents, e.g., basket, fuel assembly, and fuel matrix. In terms of the process, it is possible to distinguish between three different ways of sedimentation of the particles depending on the concentration (solid volume fraction) of the falling particles (Druitt 1995, p. 28).

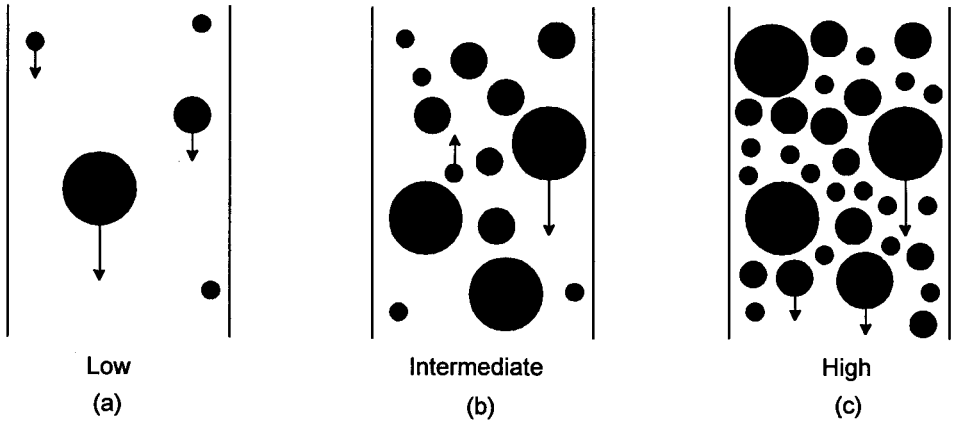

Figure 6. Schematic Particle Motions in Settling Dispersions of Three Concentrations

At low concentrations (typically a few percent or less), the particles settle according to their respective fall velocities in the fluid. Larger and/or denser particles settle faster than smaller and/or less dense particles, generating vertical gradients in concentration and size distribution in the initially homogenous dispersion. This is represented in Figure 6a. At intermediate

concentrations, (up to 30 percent) the rain of large particles causes a return flow of fluid, which flushes upward particles that are below a critical particle size (Figure 6b). This is called the hindered settling effect. But the magnitude of the settling time in the systems of interest to this analysis is large, in the order of hours, (see Table 3) and the velocity of the return fluid would correspondingly be small enough not to cause a significant concern for upward flush of particles. The detailed settling behavior depends in detail on solids concentration and on species sizes, densities, and relative proportions. The solid density contrast is a major factor in determining possible segregation. At concentrations greater than 30% solid fraction, segregation is increasingly suppressed and eventually no segregation occurs due to grain-fluid coupling (Figure 6c). A numerical illustration can be done by taking into account the probability of a particle falling into a swarm of other particles not hitting a particle. For simplicity, assume the situation shown in the Figure 7 where a particle needs to cross through other particles. It is possible to assume that the probability is 0.7 for the low limit (30% solid fraction) for a unit distance. In this case, the probability of the falling particle not to hit another particle over a distance of 5 units would correspond to $0.7^5=0.168$ e.g, 16.8 %. The probability of a subsequent particle to do the same would be a combined probability of the two, e.g. $0.168 \cdot 0.168=0.028$ and for a third particle to do the same would be $0.028\ \ 0.168=4.742 \cdot 10^{-3}$. The probability decreases rapidly with higher solids concentration and segregation becomes more unlikely in that case.

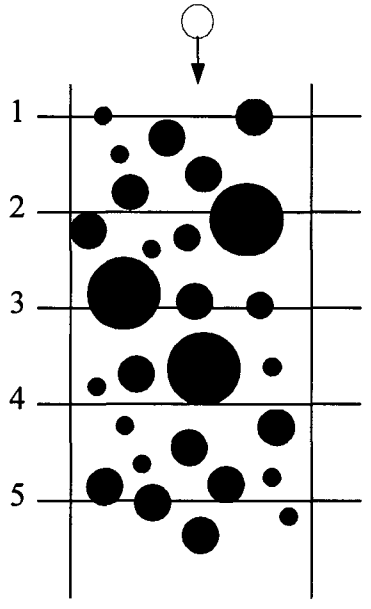

Figure 7. Particles Crossing Through Other Particles

Additionally, in the codisposal designs for the DOE SNF, use of the available space inside the waste package is maximized, and it is expected that volumetric expansion of the degradation products of the structural materials would reduce the available void space even further. Thus, the material concentration inside the waste package and DOE SNF canister do not allow for a low concentration regime as shown in Figure 6a. As fuel degrades incrementally, the solid fraction of the fuel matrix decreases, and this promotes mixing of the fuel with other degradation products. An additional factor affecting the possibility of separation is the neutron absorber

form. Separation is retarded if the neutron absorber form is such that it promotes mixing with the fuel elements, e.g., in the form of shot or plates/tubes between the fuel elements.

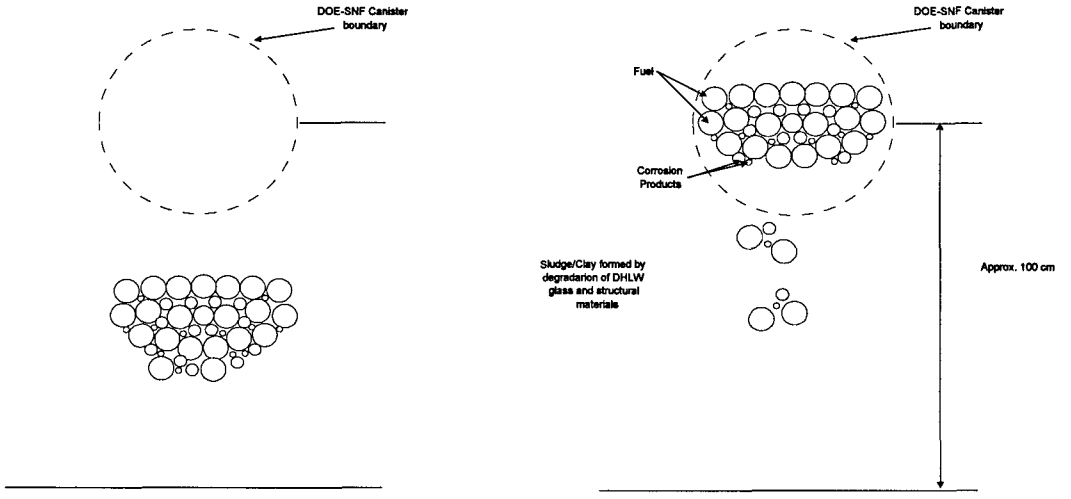

Figure 8. Schematic Representation of Fuel Rods and Other Material Falling Together (a) and Fuel Rods and Other Materials Falling in Batches (b).

Figure 8 is a depiction of two extreme cases of fuel and other materials (neutron absorber, degradation products, etc.) falling in a clay/sludge suspension. Catastrophic failure of the DOE SNF container implies a drop of all available components as a 'lump' as shown in Figure 8a. This failure needs to be initiated by an external event such as an earthquake following significant degradation. The concentration of this lump is similar to the close packing limit, e.g., greater than 75% solid fraction. As explained above, such a failure does not cause segregation of different particles and, thus, no separation of fuel and neutron absorber. The sequential sedimentation of a smaller number of particles as depicted in Figure 8b corresponds to a scenario where fractures in the DOE SNF canister wall allow a limited amount of dripping water to seep in. A delay between the different batches of particles falling out of the canister is conceivable. In this case the segregation of the particles would depend on the relative density difference(s) and the size ratios. But in the end the net effect of the sedimentation would again be mixing, and no separation would occur (from a neutronic standpoint). Considering separation of the first batch where the larger particles concentrate in the bottom of the waste package and the smaller particles sediment on top of the larger particles is conceivable, but any subsequent batch of particles would sediment on top of the previous layer(s) and, thus, a layer of larger particles would concentrate on top of the previous layer of smaller particles and form, in the extreme case, a layered structure as shown in Figure 9. Neutronically, this structure is not favorable for criticality since the neutron absorber and degradation products remain mixed. Furthermore, this case leads (generally) to a sub-optimally moderated fissile mass that can not support criticality in this configuration.

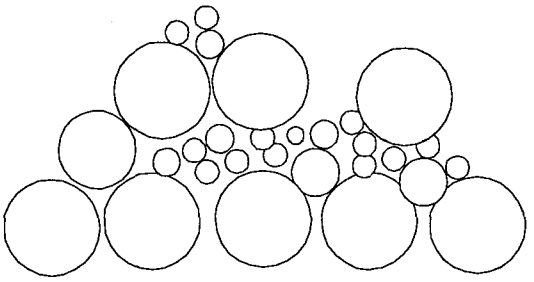

Figure 9. Conceptual Sketch of Sediment Layer Formed When Partial Segregation Due to Time Delayed Drop of Fuel/Absorber Particles as Shown in Figure 8b Occurs

In summary, a sedimentation scenario, which could account for significant separation such that the effectiveness of the neutron absorber is diminished, is not conceivable if the only force acting on the system is the gravitational force. Separation under this condition could only occur if the smaller particles have a density comparable to the surrounding environment (clay or sludge). Table 4 lists representative densities for the different materials of interest, such as Gd neutron absorber, carrier material, and degradation products. Densities for different clay/sludges are given in Table 5 in order to provide an order of magnitude estimate of the conceivable sludge/ clay density.

Table 4. Densities for Some In-Package Materials of Interest

Material	Density
Pure Gadolinium/$GdPO_4$	7.89 g/cm^3 to 5 g/cm^3
Alloy-22, SS, Carbon Steel, Iron	~7 to 8 g/cm^3
Goethite (FeOOH)	3.3 to 4.3 g/cm^3
Hematite (Fe_2O_3)	~5.26 g/cm^3
Gibbsite ($Al(OH)_3$)	~2.4 g/cm^3
Solid Glass	2-2.5 g/cm^3

Sources: Mills 1995; Roberts et al. 1990

Table 5. Typical Densities for Some Clay/Sludge Types

Clay type	Density
Typical Dry Soil	1.5 g/cm^3
Concrete stone mix (1-2-4 mix)	2.1 g/cm^3
Soil clay (SiC, SiCL etc.)	1.2-1.5 g/cm^3

Source: Mills (1995)

The values of Table 5 show that in any case the sludge/clay density is below 2 g/cm^3. None of the degradation products, except for Gibbsite, is comparable and, thus, any separation due to density effects of particles is not conceivable because all the solids have densities that are larger than clay, e.g., they will all sink eventually to the bottom of the canister.

6.1.3.1.3 Separation of Fissile Material From Absorber Due to Diffusion/Brownian Motion

Diffusion of particles into the clay is a mechanism that may allow for separation of neutron absorber from the fuel if the conditions are suitable. In some critical configurations, the neutron

absorber is postulated to be evenly distributed throughout the entire waste package by diffusion. Diffusion is a consequence of the constant thermal motion of particles, and results in material moving from areas of high to low concentration. Thus, the end result (limit) of diffusion is a uniform concentration, throughout available space, of each of the components of the system. Diffusion of solids through solids can be neglected for all conceivable conditions. Diffusion occurs at an atomic/molecular level and particulate do not lend themselves to mass transport by diffusion.

The speed of the diffusion process depends on:

- Temperature of the system.
- Size (mass) of the diffusing particles.
- Viscosity of the environment.

The formula for average distance moved by a particle during diffusion is (Bosworth 1956, p. 23):

$$< x^2 >= 2Dt \qquad \text{(Eq. 16)}$$

where $<x^2>$ is the mean square distance moved , D is the diffusion coefficient, and t is time. The diffusion coefficient can be estimated by using the Einstein equation (Bosworth 1956, p. 127) as given in Equation 17:

$$D = RT/6\pi N\nu r \qquad \text{(Eq. 17)}$$

where R is the gas constant (approx. 8.315 $J \cdot mol^{-1}K^{-1}$), T is the absolute temperature in Kelvin, N is Avogadro's number ($6.022 \cdot 10^{23}$ mol^{-1}), ν is the viscosity of the environments (0.001 for water in SI units), and r is the radius of the particle. As a computationally example consider a particle size of 1 μm; the numerical value of the diffusion constant in water at 100° C temperature is calculated to be approximately $3 \cdot 10^{-13}$ cm^2/sec. The mean distance traveled by a particle of this size is approximately $6 \cdot 10^{-7}$ cm per second. It would take more than 500 years for a particle to travel a distance of 10 cm under the conditions given in the example. This estimate shows that the size of the particle has to be much less than 1 μm to cause significant diffusion even if the environment has the same viscosity as water. The mean particle sizes for some clays is reported to be in the order of one μm in Coussot (1995). In the absence of any unrealistic external force it is plausible to assume that the size of the neutron absorber particles would be at least of the same order of magnitude. The mobility of the Gd before clay formation can be neglected based on the fact that the constituents are solid before degradation.

In reality, the viscosity of clays or sludges is much higher than the viscosity of water. A qualitative estimate can be obtained through the Einstein viscosity equation (Perry and Chilton 1973, p. 3-247)

$$\mu = \mu_0 \frac{1+\phi/2}{(1-\phi)^4} \qquad \text{(Eq. 18)}$$

where μ is the viscosity of the clay/sludge, μ_0 is the solvent viscosity, ϕ is the fraction of the clay/sludge occupied by particles. Increasing solid fraction of the particles in the clay/sludge results in a rapid increase of viscosity. A numerical value for aqueous dispersion of colloidal gibbsite platelets is given in Wierenga (1998). According to this work, even a 5% volume fraction of gibbsite suspended in water results in a threefold increase in the viscosity of the solution. A volume fraction of 20% results in a twentyfold increase of the value of the viscosity relative to water. In addition, the temperature of the waste package is most likely to be less than 100°C, the boiling point of water, at the time when the degradation phenomena takes place. This is due to the fact that a temperature over the boiling point would result in evaporation of residual water and, thus, solidify the environment. In summary, it is possible to conclude that separation due to diffusion is not a realistic process for the separation of neutron absorber from fuel under realistic repository conditions. The result of simple diffusion or brownian motion is a Gaussian distribution with a peak at the starting point; thus, there would still be a significant amount of absorber in the vicinity of the fissile material.

6.1.3.1.4 Optimum Spacing Between Fuel Rods

In many cases of degraded configurations, criticality requires a postulated optimum spacing of the SNF rods, which is generally larger than the nominal assembly spacing. In reality, it is extremely unlikely that the fuel pins could spread slightly further apart when the canister contents degrade. Generally, degradation leads to the 'collapse' of rod spacing, which lowers system reactivity due mostly to sub-optimal moderation.

A calculation was performed to investigate the possibility of increasing the spacing between fuel particles by differential settling velocity. The calculation uses empirical results from literature to calculate the separation of fuel elements during a sudden drop. The calculation is given in Attachment I. The main finding of the analysis is that the distance between fuel particles will either stay the same or will decrease during the drop within the confined space of the canister. This is due to the effective drag on a subsequent particle is less than the drag acting on the initial one for any configuration of wake augmentation of shadowing.

Additionally, in some potentially critical configurations with optimum or uniform spacing, pure water was postulated to occupy the spaces between the spent fuel rods or pins. This condition is very unlikely to occur because the volume of the degradation products inside the waste package is significant as discussed in Sections 6.2.2.2 and 6.2.3.2.. The degradation products, mainly iron oxide, have a primary criticality control function by displacing the moderator from the system. In addition to this criticality control of the degradation products, any water entering the waste package will mix with these products; thus, the environment surrounding the fissile material will have a higher neutron absorption than pure water as discussed in Section 6.2.1.2.3. Any natural accumulation of assembly rods or pieces would be random. In evaluating the optimum spacing of rods for the criticality parametric calculations, the accumulations are represented as uniform arrays. The criticality models represent the average spacing of any accumulation of fuel. Any reference to arrays actually represents any accumulation of fuel with similar average spacing or effective space between adjacent pieces.

6.1.3.1.5 Natural Circulation Within Degraded Waste Packages

Thermally-driven fluid circulation within a breached codisposal waste package system might augment the material degradation rates but only in an early or infantile waste package failure when substantial quantity of heat producing radionuclides still remain in the package. Clay formation in an early waste package failure will experience retarded circulation because of increasing viscosity as clay thickens. The possibility of enhanced degradation for materials containing neutron absorbers is a primary concern. Despite any mass transfer rate enhancements from buoyant convection, degradation must persist for centuries (see Section 6.2.1.2.5) to result in significant neutron absorber relocation. Therefore, the physical processes contributing to in-package circulation and supporting enhanced material degradation are adequately conceptualized as steady processes.

The possibility for consequential natural circulation is limited to quasi-steady processes and times when temperatures within waste package are below 100°C at approximately atmospheric pressure. Greater temperatures at the nominal pressure would allow bulk liquid vaporization and dry out the package. Likewise, significant pressurization of the package would allow increased liquid temperatures but would necessarily induce transient phenomena. The transient phenomena would ultimately lead to package dryout because the pressure differential would induce convective fluid losses and because work would be required to introduce makeup liquids into the package for the maintenance of a constant liquid inventory.

The in-package temperature gradient drives the buoyant convection and determines the rate of fluid circulation. For example, a credible maximum internal temperature difference for the TRIGA codisposal arrangement can be obtained by taking the difference between the SNF cladding surface temperature and the waste package external surface temperature (CRWMS M&O 1999d, p. 21, Table 6-2) at 1000 years after emplacement for the case of argon waste package fill. The use of the peak DHLW glass temperature in lieu of the TRIGA cladding temperature comparatively reduces the temperature difference by 10°C. The water and degradation product mixture filler is apt to have a lower effective thermal diffusivity than argon (leading to comparatively larger temperature gradients). However, no waste package breach is possible prior to 10,000 years (McClure and Alsaed 2001, Table 8-9) of residence and the remaining assumptions compensate to overestimate the magnitude of temperature gradient for this analysis. Principally, both the cladding and waste package surface temperatures at 1000 years are well above 100°C, leading to a conservative estimate for the thermal gradient corresponding to a time when no liquid can actually occupy the waste package. Additionally, the analysis uses a hot SNF canister surface temperature (close to the cladding temperature) and the slightly cooler waste package external surface temperature (the circulating fluid contacts the waste package interior) to maximize the assessed temperature difference. The peak temperature difference used for analysis is listed in Table 6.

Table 6. Credible Temperatures and Peak Difference for Circulation in the TRIGA Codisposal Waste Package

Location	Temperature or Difference
Cladding Temperature at 1,000 years[a]	162.0 °C
Waste Package Barrier Exterior at 1,000 years[a]	144.0 °C
Temperature Difference (ΔT)	18.0 °C

Source: [a]CRWMS M&O (1999d)

The hydrodynamic permeability of the degradation product mixture is unknown but is bounded by the maximum value given in Table 7 for wire crimps (Nield and Bejan 1992, p. 4, Table 1.1). System void fractions as large as 0.76 are attainable in media composed of wire crimps. Because void fractions for in-package degradation product layers are less than for wire crimps and because the hydrodynamic permeability generally scales as some power of the void fraction, the assessed permeability bounds the values appropriate to in-package obstructions.

Table 7. Assessed Maximum Hydrodynamic Permeability for Degradation Product Mixtures

Parameter	Value
Hydrodynamic Permeability (K)	$1.0 \cdot 10^{-4}$ m^2

Source: Nield and Bejan (1992, p. 4, Table 1.1)

The waste package region between the SNF canister wall and the internal barrier surface is exposed to the largest possible in-package temperature difference. Despite the possibility of internal structural degradation, the largest propensity for natural circulation is associated with the heated SNF canister occupying the position at the central waste package basket bay. This maximizes the nominal temperature gradient and maintains a uniform thermal resistance for heat dissipation. The smallest temperature difference is associated to a configuration with the SNF canister settled at the bottom of the waste package. With canister settling, the uniform resistance is shunted by eccentric location for the heated canister, leading to smaller overall temperature differences for equivalent heat dissipation. These considerations also motivate the use of a concentric arrangement for bounding thermal analyses of the TRIGA codisposal waste package in CRWMS M&O (1999d, p. 7, Assumption 3.23). The SNF canister diameter used is specified in CRWMS M&O (2000a) and the inner waste package barrier diameter used is given in CRWMS M&O (2000e). Dimensional specifications are listed in Table 8.

Table 8. Component Dimensions for Circulation in the TRIGA Codisposal Waste Package

Component	Diameter
Outer Surface of DOE SNF Canister (D_i)[a]	457.2 mm
Inner Surface of the Codisposal Waste Package Barrier (D_o)[b]	1880 mm
$\delta = (D_o - D_i)/2$	711.4 mm

Source: [a]CRWMS M&O (2000a)
[b]CRWMS M&O (2000e)

With minor exceptions, the fluid properties are those for pure water near the atmospheric boiling point and are listed in Table 9. To represent the transport properties of the degradation product and fluid mixture (i.e., slurry), the kinematic viscosity value used is that for SAE 50 oil at 300 K. The thermal diffusivity is derived using the kinematic viscosity for oil and Pr for water at the atmospheric boiling point. For the Sc number, approximate parity is assumed between Gd and benzoic acid at 300 K with consideration for the molecular weight difference between elemental Gd and acid. Note that Gd is insoluble as $GdPO_4$, with caveats at extreme values for solution pH. The equivalence to acid should overestimate Sc for Gd, which is an additional conservatism in subsequent analysis.

Table 9. Fluid properties for circulation in the TRIGA codisposal Waste Package.

Property	Value
Fluid Density (ρ_f)[a]	958 kg/m^3
Kinematic Viscosity (ν)[a]	$5.7 \cdot 10^{-4}$ m^2/s
Thermal Diffusivity (α)[a]	$3.2 \cdot 10^{-4}$ m^2/s
Schmidt ($Sc = \nu/D_{1,2}$)[b]	913
Volumetric Expansion Coefficient (β)[c]	$7.501 \cdot 10^{-4}$ 1/K

Source: Mills (1995, [a]Table A.8, [b]Table A.18 (assuming parity with Benzoic Acid) and [c]Table A.10b)

The Sherwood number (Sh) is a dimensionless parameter that quantifies the convective enhancement to mass transport beyond the contribution from molecular diffusion. It is defined by the enclosure gap width, $\delta = (D_o - D_i)/2$, between the outer cylinder with diameter, D_o, and the inner cylinder with diameter, D_i, by the mass conductance, G, by the fluid mixture density, ρ_f, and by the molecular diffusivity of the dilute species, $D_{1,2}$,

$$Sh = \frac{G\delta}{\rho_f D_{1,2}} \qquad \text{(Eq. 19)}$$

Invoking the heat and mass transfer analogy for an annular system with a heated internal cylinder, the apparent enhancement to the mass conductance across the annular cavity is a function of the Rayleigh number for the annular system, Ra_{ann} (Mills 1995, p. 305, Eq. 4.104),

$$Sh = \begin{cases} 1 & ; \ \zeta_a < 1 \\ \zeta_a & ; \ \zeta_a \geq 1 \end{cases}, \qquad \text{(Eq. 20)}$$

where,

$$\zeta_a = 0.386\left(\frac{Sc}{Sc+0.861}\right)^{\frac{1}{4}} Ra_{ann}^{\frac{1}{4}} \qquad \text{(Eq. 21)}$$

A Sh value of 1 indicates that there is no enhancement to rate of diffusive mass transfer. A Sh value > 1 indicates the effective enhancement to mass transport as a multiple of the prevailing diffusive transport rate. Sc is the fluid's Schmidt number and Equation 20 is accurate in the range $10^2 < Ra_{ann} < 10^7$. Re_{ann} incorporates a correction for geometric effects to the nominal Rayleigh number for the system, Ra (Mills 1995, p. 305, Eq. 4.104),

$$Ra_{ann} = \frac{\left(\ln(D_o / D_i)\right)^4}{\delta^3\left(D_o^{-\frac{3}{5}} + D_i^{-\frac{3}{5}}\right)^5} Ra \qquad \text{(Eq. 22)}$$

Assignments for the nominal Ra can be distinguished on the basis of assumptions for the in-package environment. If no obstructions to fluid circulation are present (i.e., clear fluid situation) in the annular region, Ra varies as the third power of δ,

$$Ra = \frac{g\,\beta\,\Delta T\,\delta^3}{\nu\,\alpha} \qquad \text{(Eq. 23)}$$

where g is the acceleration from terrestrial gravity, β is the volumetric coefficient of thermal expansion, ΔT is the system temperature difference, ν is the kinematic fluid viscosity, and α is the fluid thermal diffusivity.

If the annular region is occupied by porous medium composed of degradation products that obstruct any fluid circulation, Ra is necessarily defined differently (Nield and Bejan 1992, p. 107, Eq. 5.104),

$$Ra = \frac{g\,\beta\,\Delta T\,K\,\delta}{\nu\,\alpha} \qquad \text{(Eq. 24)}$$

where K is the hydraulic permeability of the porous degradation products. The use of Equation 23 in Equation 20 provides a maximum Sh estimate for the clear fluid situation. The use of Equation 24 in Equation 20 produces a maximum Sh estimate for the situation involving porous degradation product obstructions.

6.1.3.2 Generic Degradation Geochemistry Phenomena

As a part of the degraded mode criticality analysis for each SNF type, degraded mode geochemistry analysis is also performed using the EQ6 computer code. In the geochemistry analysis, the materials inside the waste package and DOE SNF canister including the waste form are degraded to analyze the effect of degradation on the fissile and neutron absorber materials. The effect focuses on the separation and loss of the neutron absorber and the rearrangement of the degradation products. Based on all the results analyzed so far for the different DOE SNFs, the loss of the neutron absorber material particularly $GdPO_4$ is not a concern. For conservatism, the loss of fissile materials from the waste package is assumed to be minimal if not zero because this will increase the potential for criticality.

6.1.4 Other Screening Models Based on Component Materials and Degradation Rates

For most of the degraded configurations analyzed showing a significant potential for criticality are due to the separation of neutron absorber from fissile material. Separation occurred when the fuel pins remain intact while the DOE SNF canister stays sufficiently intact to remain flooded and all other components have already degraded. Based on the values of the material thickness and degradation rates, some of the degradation configurations involving the events assuming intact components are not possible. This is further discussed in detail in the technical reports for different DOE SNF types. In general, the basket structure of waste package and the HLW glass will degrade first, followed by the degradation of the DOE SNF canister, then followed by the degradation of the components inside, including the SNF. It is very unlikely that the DOE SNF canister shell would stay intact while everything else would have already degraded including the SNF inside the DOE SNF canister. Another unlikely case would be that the SNF stays intact while everything else has degraded. These conditions affect the potential for criticality since they modify the geometry of the system during degradation.

6.2 ANALYSIS

The analysis is an application of the physics models described above. Applications have been performed for the following DOE SNF types: FFTF, Enrico Fermi, TRIGA, Shippingport PWR, Shippingport LWBR and N Reactor.

Using the developed physical models, the degraded configurations with potential for criticality have been screened out for the above fuel types. The screening is performed by physical impossibility and/or probability calculations if applicable. The details of screening are provided below.

6.2.1 FFTF SNF

The detailed characteristics and properties of the FFTF SNF are presented in CRWMS M&O (1999a). A unique feature of this fuel type is that, in addition to the fuel assemblies, there are also canisters with derodded fuel pins, called Ident-69 (referred to as Ident from here on), that need to be disposed of. Figure 10 is a drawing of the different constituents inside the DOE SNF canister. The current design calls for one position in the basket structure to be blocked before loading the DOE SNF canister.

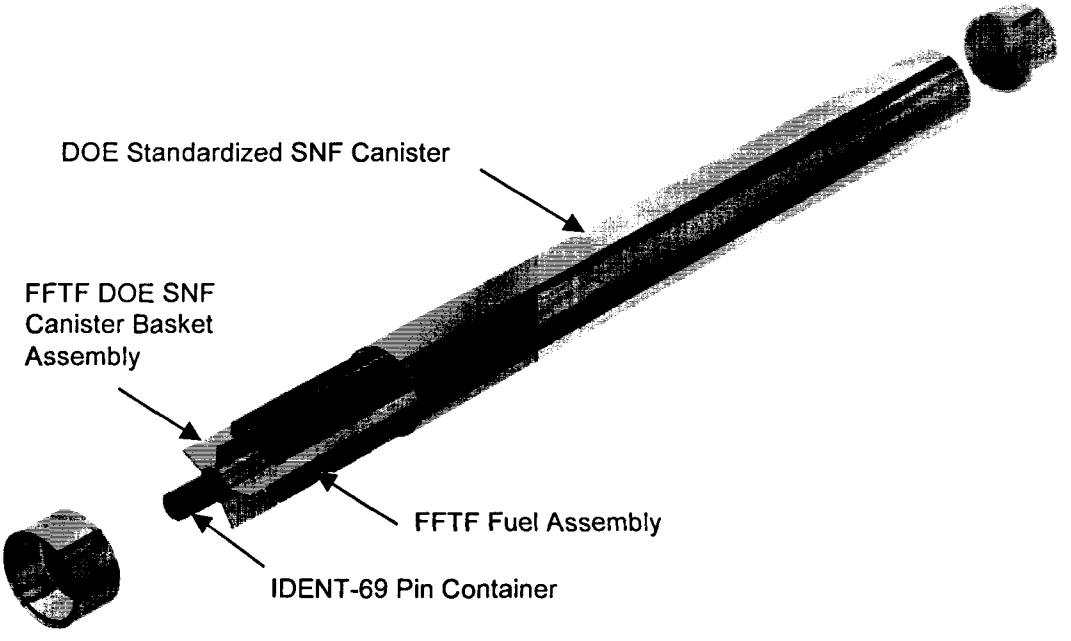

Figure 10. Three-Dimensional Exploded View of the DOE SNF Standard Canister, FFTF Basket Assembly, Fuel Assembly, and Ident-69 Pin Container

6.2.1.1 Critical Degraded Configurations

Criticality calculations with the FFTF fuel type need to take into account the change in fissile inventory due to decay of the Pu isotopes: Pu-239 to U-235 with $t_{1/2}$ of 24,400 years, Pu-240 to U-236 with $t_{1/2}$ of 6,560 years, and Pu-241 to Np-237 with $t_{1/2}$ of 447.1 years. Thus, the criticality calculations were done with isotopic contents corresponding to t=0, t=24,400 years, t=48,800 years and t=244,000 years. Results indicate that the most reactive cases occur for t=48,800 years (CRWMS M&O 1999a, pp. 67-68). Thus, the results indicated below are based on isotopic inventory at t=48,800 years. Some degraded configurations involving dissolved fuel show more reactivity for t=24,400 years, but the current analysis is also bounding these cases.

The geochemistry calculations for the different degraded cases show that the Gd loss is never greater than 0.7 % over 100,000 years for any of the scenarios (CRWMS M&O 1999a, pp. 56-57). This implies that if criticality is to be possible, there must be a separation between the

fissile material of the FFTF SNF and the Gd neutron absorber that was added to the DOE SNF canister in proximity with the fuel pins.

The criticality calculations for the degraded cases show that the most reactive configurations occur when the Ident-69 container stays intact, but internally flooded, and assuming worst case uniform distribution of pins. A sequence of events that may in effect allow the Ident-69 container to degrade slower than the other components inside the DOE SNF canister is postulated (CRWMS M&O 1999a, p. 66). The main premise of that scenario is that the degradation products from the support tube form a protective layer around the Ident-69 container, thereby, limiting the oxygen supply and reducing the amount of degradation of the Ident-69 container.

6.2.1.2 Critical Degraded Configuration Screening

6.2.1.2.1 Case with Four DFAs and One Ident-69 Canister

The design recommendation calls for four DFAs and one Ident-69 canister inside the codisposal waste package (CRWMS M&O 1999a, p. 80). The basket structure contains at least 2.75 wt% of $GdPO_4$ (1.714 wt% Gd) neutron absorber. One location of the basket is blocked in order to eliminate the possibility of loading 5th DFA's with an Ident-69 container. The calculations performed in support of the technical report show that there is no concern for exceeding the prescribed critical limit if the FFTF-SNF is disposed in this manner (CRWMS M&O 1999a, pp. 80-81).

6.2.1.2.2 Probability of Degradation with Five DFAs and Intact Ident 69

If 5 DFAs are used, the k_{eff} values for some degraded configurations exceed the CL of 0.93 (CRWMS M&O 1999e). The following probability calculation is performed to see if the loading scheme of using 5 DFAs and an intact Ident-69 can be screened. The probability calculation is focused on Ident-69 staying intact.

6.2.1.2.3 Probability of Ident-69 Staying Intact

The probability calculation performed below is to show that the probability of Ident-69 staying intact is very small or very unlikely. This is done by calculating the probabilities of degradation for the components inside the Ident-69 versus the spokes outside the Ident-69 under local corrosion, i.e., corrosion patches formed on the surfaces. Based on the results presented in Table 10 below, the Ident-69 would not stay intact. If the internal components of the Ident-69 degrades, no critical geometry will exist.

Probability that Ident-69 Dividers and Center Ring Degrade Faster Than the DOE SNF Canister Spokes –Surface Areas (CRWMS M&O 1999a, Sections 2.1.3 and 2.1.4):

- Center Ring (inside Ident-69)
  O.D. = 44.45 mm
  Length = 4145 mm

Surface area = π (44.45) (4145) = 578,823.52 mm^2

- Dividers (inside Ident-69)
  Thickness = (1.524 + 1.778)/2 = 1.651 mm (use average)
  Width = Inner diameter of the Ident-69 outer shell - Outer diameter of the center ring
  = (141.3 – 2 x 2.77) – 44.45 = 91.31 mm
  Length = 4145 mm
  Surface area per one divider = 91.31 (4145) (2) = 756,959.9 mm^2
  Area of 6 dividers = 756,959.9 (6) = 4,541,759.4 mm^2

- Surface area of 5 spokes (outside of Ident-69, Figure 11)

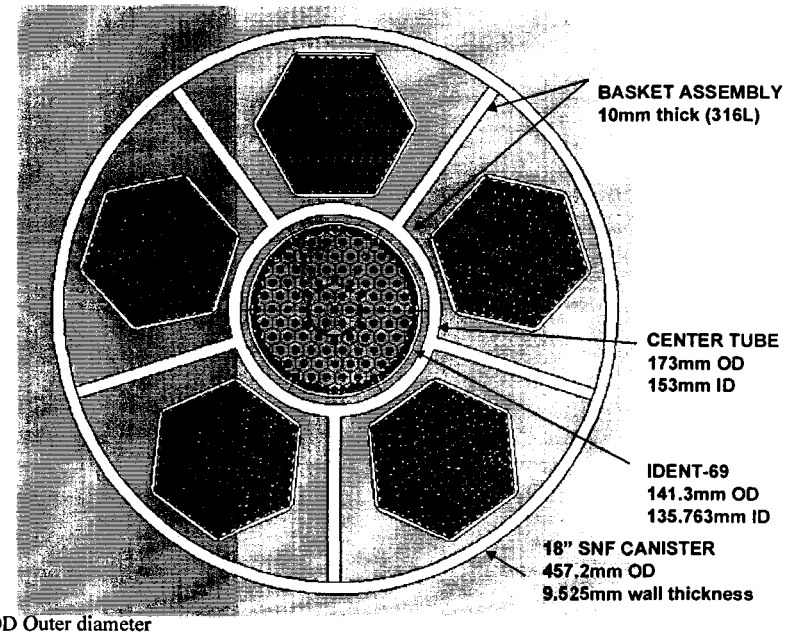

Figure 11. FFTF DOE SNF Canister (CRWMS M&O 1999a, Figure 2-4)

The width of one spoke = [(457.2-2·9.525)/2-173/2] = 132.575 mm
Surface area = As = 132.575·(4145)·(5)·(2) = 5,495,233.75 mm^2

Probability Calculation Using Negative Binomial Distribution–The negative binomial distribution calculates the probability on the number of failures (i) before the *mth* success in a sequence of (m+i) independent Bernoulli trials given that the probability of success (1-p) remains constant throughout the trials (Equation 25 can be derived from Scheaffer and McClave 1990).

$$P_{tot} = \sum_{i=0}^{i=k-1} \left(\frac{(m+i-1)!}{i!(m-1)!} \right) p^i (1-p)^m \qquad \text{(Eq. 25)}$$

The form of Equation 25 results for the total probability of terminal success (m individual success with an overall probability P_{tot}) by summation over all allowed values of (i) that do not attain or exceed the threshold for a competing secondary event (k).

To use the distribution in Equation 25, the probability that a corrosion patch preferentially forms on the Ident dividers and center ring or on the spokes can be calculated as follows.

- Probability of patch formation on the Ident (p):

  Let, Ai = surface area of 6 dividers + surface area of center ring
  As = surface area of the 5 spokes
  ti = thickness of the dividers and center ring
  ts = thickness of the spokes
  Ai/ti = Li = characteristic length of Ident-69
  As/ts= Ls = characteristic length of spoke

  Then, p = Li / (Ls + Li) = 1 if Ls = 0
  = 0 if Li = 0

  Or, $p/(1-p)$ = Li/Ls = Ai/As (ts/ti)

  Where,

  Ai = 4,541,759.4 + 578,823.52 = 5,120,582.92 mm^2

  Area ratio = Ai/(Ai+As) = 5,120,582.92 / 5,495,233.75 = 0.93

  Thickness ratio = ts/ ti = 10 / 1.651 = 6.057

  Thus, $p/(1-p)$ = Ai/As (ts/ti) = (0.93) (6.057) = 5.64

  Or, p = 0.85

  Note that the intermediate results shown here are rounded and do not reflect actual precision of the calculations.

The results of the negative binomial probability calculations with Equation 25 over a range of component failure threshold are shown in Table 10 below. The calculations are performed using Microsoft Excel software. In Table 10, as defined above, the parameter **k** is the required number of corrosion patches formed on the surface of the internal components, such as dividers and center ring, to fail the Ident. The parameter **m** is the required number of corrosion patches on the surface of the spokes (external to the Ident) for spoke failure. The values in Table 10 are the

complement of the probability that the Ident dividers and center ring would degrade slower than the spokes, i.e., they are the probabilities that the spokes would degrade faster than the dividers and the center ring (1-*p*). Thus in this application, *p* is defined as the probability of failure and (1-*p*) is defined as probability of success. Favorable low complement probability values are obtained when the value of **m** is much greater than **k**.

It should be noted that the degradation concern for the Ident-69 is **mostly** and the concern for spokes is **completely**. This is because the degradation of most of the Ident-69 will release the fuel pins contained therein, or at least put them in a much less reactive configuration. The degradation of nearly all the spokes will be necessary condition for a uniform distribution of the Gd throughout the water (rather than concentration of the Gd in the region with the pins from the assemblies). Since **k** represents only mostly degraded, while **m** represents completely degraded, the expectation is that the ratio of k/(m + k) would be smaller than p or Ai/(Ai+As) which is less than 1/2. Actually k/(m + k) can also be considered as a variate. Even though no static values of k and m are known, the proceeding argument provides the expectation that fewer patches are needed to corrode the Ident-69 than the spokes, i.e., the Ident-69 will degrade faster than spokes with k<m.

It should also be noted that some of the conditions for the degraded configurations to become critical are that the water inside the Ident-69 has no dissolved impurities and that the fuel pins inside the Ident-69 are in an optimum array (closely packed) (CRWMS M&O 1999e). As discussed in Section 6.3.2 of CRWMS M&O 1999h, for the Ident-69, the k_{eff} values decrease when the fuel pin pitch increases and when the shape of the fuel array changes from hexagon to square. Thus when the Ident-69 is breached, its contribution toward a critical geometry will diminish. Because only one corrosion patch is sufficient to breach the Ident-69, there is additional support for the reasoning that **k** implies **mostly compromised** and is **smaller** than m.

Table 10. Total Probability of Failure for Different Values of k and m (p=0.85)

	m= 5	m= 10	m= 20	m= 30	m = 50
k = 5	5.63e-03	3.22e-06	1.91e-13	4.75e-21	1.07 e-36
k = 10		1.44e-04	8.34e-11	9.92e-18	1.92e-32
k = 20			1.24e-07	1.85e-13	1.44e-26
k = 30				1.22e-10	2.12e-22
k = 50					1.35e-16

Sensitivity Analysis on Number of Patches – The results shown in Table 10 are for a range of k and m values. The results show that the complement probability values approach zero as the numbers of corrosion patches on the Ident-69 and on the spokes increase, i.e., for the probability values approaching the upper right corner of the table. The results also show that as the ratio of m/k decreases, the complement probability values become larger, i.e., for the probability values approaching the lower left corner of the table. However, based on the reasoning given in Section 6.2.1.2.3 above, the value of k/(m + k) is expected to be less than Ai/(Ai+As) or 0.44. It implies that the ratio of k/m would be less than 1.0. Thus only the probability values shown on the upper right corner of Table 10 need be considered. As can be seen, these probability values are approaching zero. Which implies that the dividers and center ring inside the Ident-69 will always degrade faster than the spokes.

Another observation can be made from the results shown in Table 11. In this table, a higher value on the probability of p is used, i.e., 0.90 as compared to the value of 0.85 used in Table 10. The higher p value can be obtained by including the difference in the corrosion rates of the 316L and 304 L SS materials. As can be seen from Table 11, the probability values are even smaller than those shown in Table 10. It implies that as p increases, the probability of spokes degrading faster than the Ident is getting smaller.

Table 11. Total Probability of Failure for Different Values of k and m (p=0.90)

	m=5	m= 10	m= 20	m= 30	m = 50
K=5	8.91e-04	6.84e-08	7.12e-17	3.09e-26	2.09e-45
k = 10		3.93e-06	4.07e-14	8.48e-23	4.97e-41
k = 20			1.03e-10	2.73e-18	6.52e-35
k = 30				3.11e-15	1.67e-30
k = 50					3.23e-24

6.2.1.2.4 Additional Probability Considerations

For a critical degraded configuration to occur, some sequence of events must take place. The following events are examples (CRMWS M&O 1999a, Section 6.0):

- Waste package dripped on
- Waste package breached
- Waste Package internally flooded
- Waste Package internal components degraded excluding DOE SNF canister
- DOE SNF canister breached
- DOE SNF canister shell stays intact
- DOE SNF canister internals flooded
- DOE SNF canister internal components degraded, including the SNF matrix
- SNF degraded and forming an optimum shape
- Ident-69 container stays intact

For each of events listed above a probability can be calculated. The probabilities for some of the key events are discussed as follows:

- Probability of Waste Package Being Dripped On

  This probability has been calculated in McClure and Alsaed 2001, Table 8-9. The probability is considered as fraction of packages being seeped on and the value is 0.0694.

- Probability of Waste Package Breach

  This probability has also been calculated in McClure and Alsaed 2001, Table 8-9. The probability is considered as time to first waste package failure and the value is $5 \cdot 10^{-4}$.

- Probability of Ident-69 Staying Intact

  This probability is discussed in section above and the results are shown in Table 10 for p=0.85 based on the actual area and thickness ratios. As can be seen from Table 10, the probability of Ident-69 staying intact depends on the k/m ratio and is generally very small. For k/m < 1.0, the probability values range from $1.44 \cdot 10^{-4}$ (k/m = 1 with the equivalent of more than one patch per spoke) to $1.07 \cdot 10^{-36}$ (k/m = 0.10).

Total Probability – The total probability is the product of each individual probability for each event presented above. The probability value for each individual event is expected to be small. Thus the product of each of the individual probability would bring the total probability to be even smaller. For example, by just considering the probabilities of waste package dripping, breaching and Ident staying intact, the overall probability for a degraded configuration resulting from the events listed above would range from $5.0 \cdot 10^{-9}$ to $3.7 \cdot 10^{-41}$ for the first 10,000 years. When considering the probability of all the individual event listed above, it is expected that the highest overall probability would be much less than 10^{-9} which meets the probability criterion of 10^{-4} for the first 10,000 years.

6.2.1.2.5 Probability Calculations for Gadolinium Loss

The time dependent probabilities for attaining transitory states (states B and C) and a terminal state involving the complete loss of Gd (state G) are assessed using the analytic techniques in Section 6.1.2.2.1. The probability estimates for the abbreviated event sequences allowing transitions among states (i.e., sequences that only consider *necessary* failures) are greater than would be observed if all of the events required to realize the degraded configurations were assessed (e.g., see Section 6.2.1.2.2). The analytic techniques used here indicate that the manifestation of these degraded configurations involving loss of the packaged Gd is impossible within a 60,000 year time period, and has a very small probability over a 100,000 year time period ($P_{0\text{-}g} < 8.0 \cdot 10^{-13}$). The worksheet in which the probability calculations are performed is provided as Attachment II.

The transient results for the probability of transition to waste package system state G, and for the probabilities of transitions to intermediate states B and C, are provided in Figure 12. The analysis produces congruent rises of the probabilities for the states of DOE SNF canister breach during flooding ($P_{0\text{-}c}$ in Figure 12) and Gd loss during flooding ($P_{0\text{-}g}$). For times less than 60,000 years, $P_{0\text{-}g}$ is identically zero because the probability for waste package breach and flooding with subsequent DOE SNF canister breach is zero within this time period. $P_{0\text{-}g}$ attains the limiting value of $4.1 \cdot 10^{-7}$ (per waste package) at 950,000 years.

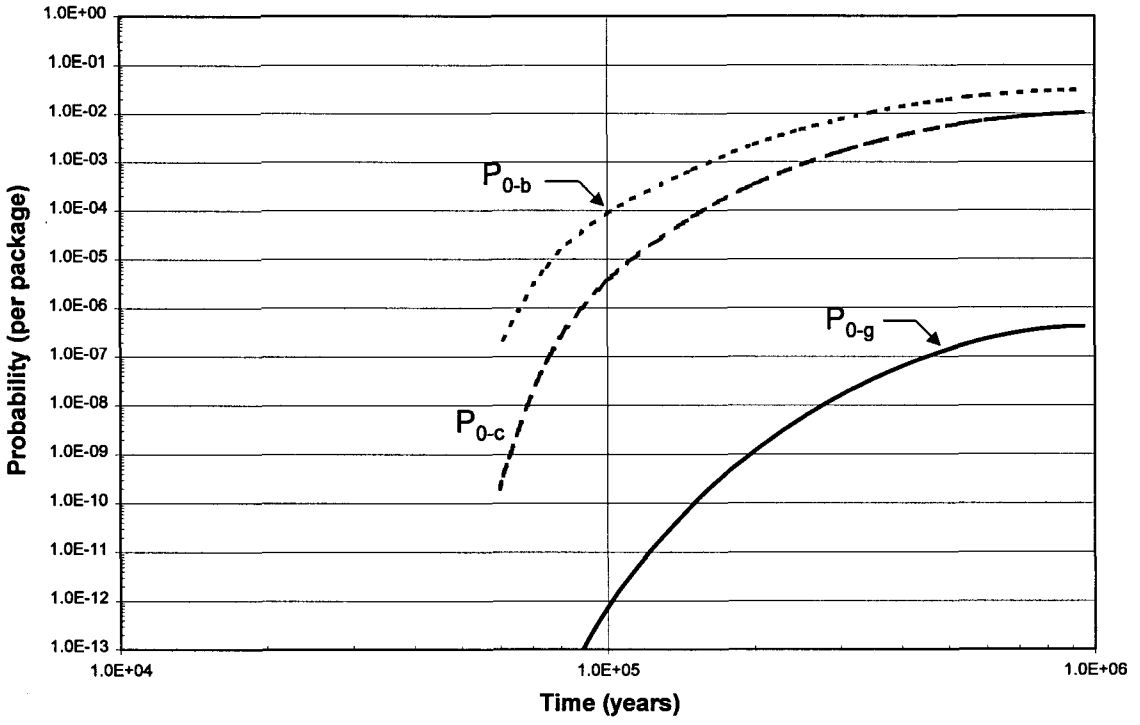

Figure 12. Transient Probabilities for Degraded Waste Package States Contributing to a Condition of Gd Loss are Assessed by an Analytic Technique

6.2.1.2.6 Ident-69 Degradation Based on Steel Degradation Rates

Ident-69 canister is made of SS type 304 whereas the DOE SNF canister and the basket structure with Gd are made of SS type 316 (CRWMS M&O 1999a, Sections 2.1.3 and 2.1.4). Comparison on the degradation rates of SS types 316 and 304 presented below indicates that Ident-69 canister shell will degrade always faster than the basket structure:

1. SS 316 is less susceptible to localized corrosion than SS type 304.

2. The general degradation rate of SS 316 is lower than SS 304 in similar environmental conditions. Thus we can assume such that the SS 304 degradation rate is either the same as SS 316 degradation rate or SS 304 degradation rate is worse.

3. Based on the two arguments above the only parameter determining whether the Ident-69 canister will be degraded before or after the steel basket is the thickness of the various components. CDFs for the degradation of the SS 316/304 is calculated based on the configuration given in CRWMS M&O 2000h (p. 45, Figure 11). The results are presented in Table 12 below. Table 13 shows the time of penetration for different thicknesses of steel layers based on the results shown in Table 12.

Table 12. CDF for Degradation of SS 304L/SS316L under Aqueous Environment Conditions

Percentile	SS304L	SS316L
15th percentile	15μm/year	0.15μm/year
50th percentile	40μm/year	1.8μm/year
95th percentile	200μm/year	30μm/year

Table 13. Time for Penetration of 0.3 cm Thick Layer of SS304L Compared to 1.0 cm Thick Layer of SS316L

Percentiles (SS304,SS316)	Time for 1 cm thick SS316L (0.5cm)	Time for 0.3 cm thick SS304L
(50,50)	5,556 years (2,778 years)	75 years
(95,95)	333 years (167 years)	15 years
(95,50)	333 years (167 years)	75 years

As shown in the Table 13, the Ident-69 canister shell will always degrade faster than the basket structure. This is true for even the conservative case of very high degradation rate of SS316L and average degradation rate of SS304L. The results presented here further support the results presented in Section 6.2.1.2.3 dealing with the probability of Ident-69 staying intact.

6.2.1.3 Summary

For FFTF SNF, the key element for any degraded configuration to exceed the CL of 0.93 is based on the postulation that the Ident-69 stays intact. The analysis results presented in the above sections show that Ident-69 will not stay intact based on steel material thickness and corrosion rates or the probability of staying intact is negligibly small. Another element for the degraded configuration to reach criticality is on the loss of Gd. Again the analysis results show that the probability of Gd loss is also negligibly small. Additionally the overall probability for reaching a specific critical configuration considering all the necessary sequence of events to reach the critical configuration is small enough to meet the probability criterion specified in the Topical Report.

6.2.2 TRIGA SNF

A detailed description of the TRIGA SNF is presented in CRWMS M&O (2000a). A drawing depicting the basket structure and DOE SNF canister is shown in Figure 13.

The Uranium-Zirconiumhydride (U-ZrH) used in the TRIGA fuel rods is a self-moderating fuel that provides inherent safety characteristics during reactor operation. The fuel has a large negative temperature coefficient of reactivity such that if all the available excess reactivity were suddenly inserted into the core, the resulting fuel temperature would automatically cause the power excursion to terminate before any core damage resulted (Simnad 1981).

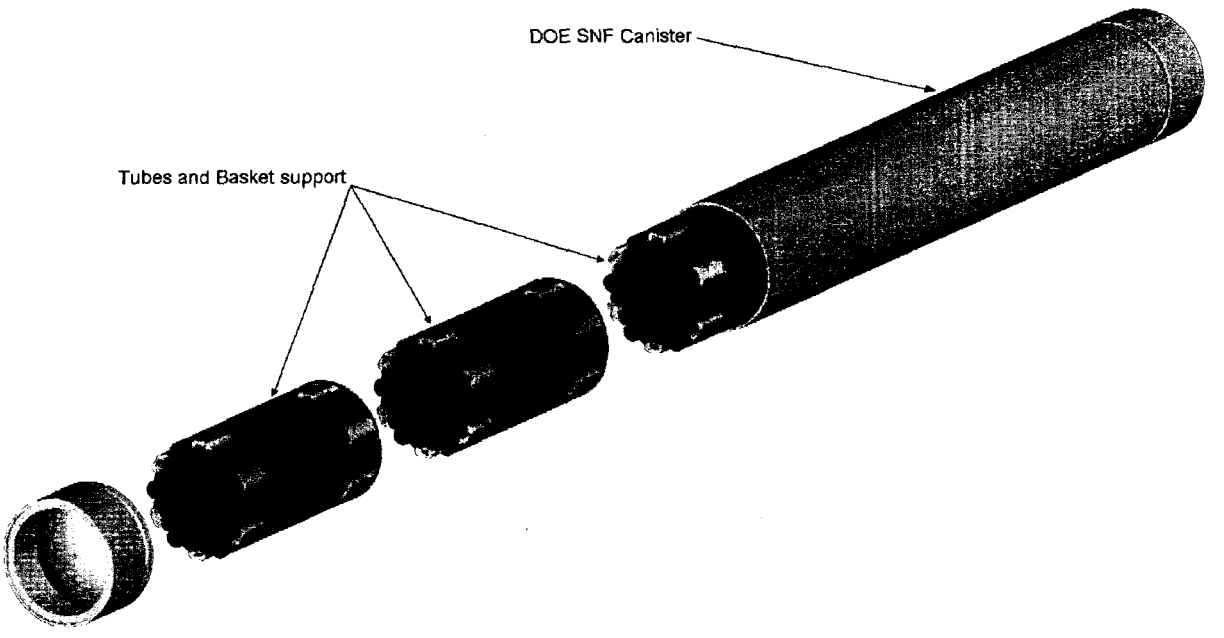

Figure 13. Drawing of TRIGA-SNF Inside the Standard DOE SNF canister

6.2.2.1 Critical Degraded Configuration

The MCNP calculations performed for the degraded configurations of the TRIGA SNF type show that the potential for criticality exists only for cases where the fuel does not degrade and the neutron absorber moves away from the fuel region (CRWMS M&O 2000a). The calculation for the case sketched in Figure 14 shows that the configuration in which the neutron absorber is diluted throughout the clay volume and the fuel rods are stacked together in a close packed hexagonal configuration is the most reactive configuration of concern. The maximum $k_{eff}+2\sigma$ is calculated as 1.0378 (CRWMS M&O 2000a, p. 82) when 2.7 kg of Gd is homogenized throughout the entire clay volume.

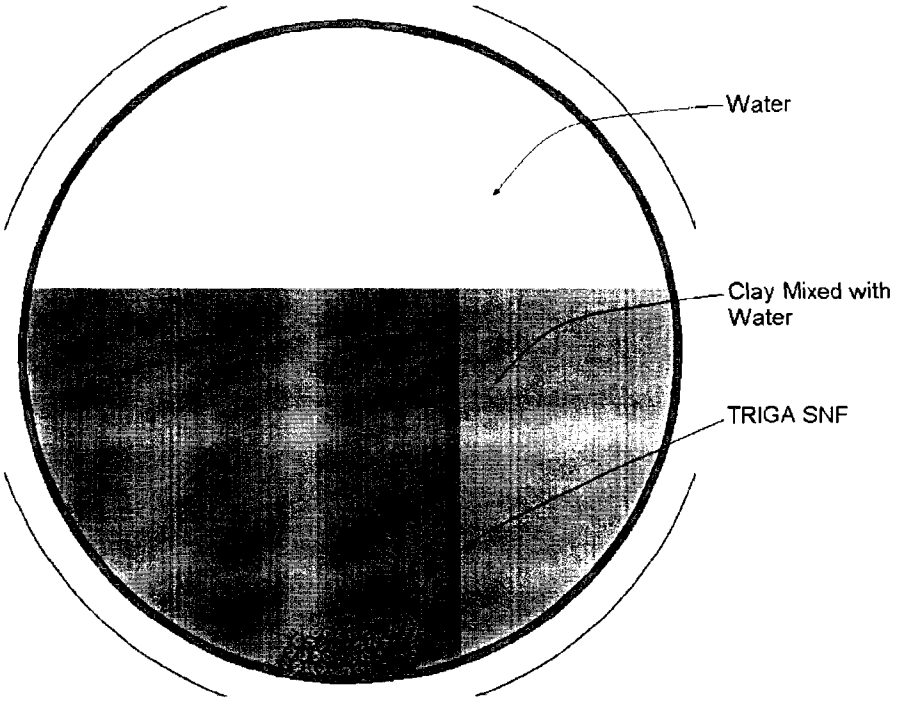

Figure 14. Waste Package Cross Section with the TRIGA SNF Intact on the Bottom

6.2.2.2 Critical Degraded Configuration Screening

The potential for criticality for the TRIGA fuel type arises if the amount of neutron absorber that stays in the vicinity of the fuel rods is significantly reduced by dispersion throughout the canister while the fuel pins remain in a cluster at the center, or bottom of the waste package, and if the geometric configuration of the fuel rods is favorable. It has also been shown that there is no potential for criticality of any configuration as long as there is no significant dispersion of the neutron absorber from the initial co-location together with fissile material. The analyses presented in Section 6.1 show that this kind of dispersion is not physically possible for three main reasons:

- Density of neutron absorber and carrier material is significantly larger than the surrounding clay/sludge so that enough of the neutron absorber will settle to the bottom of the waste package to remain largely mixed with the known waste forms.

- The concentration of the neutron absorber particles and fuel mixture is significantly larger than the low-concentration limit required for Stokian separation.

- The characteristic size of the neutron absorber particles and carrier material is larger than the size where molecular diffusion or brownian motion plays a role.

The formation of a close-packed array of fuel rods as depicted in Figure 15 implies an effective void fraction between the fuel rods of less than 30%. Based on literature, random drop or fall of

relatively large pieces such as cylindrical fuel rods do not result in void fractions of less than 40% even under optimum conditions (Coelho et al. 1997). This reference does not specifically discuss pins in sludge but provides information on void fraction as a function of length to diameter for cylindrical objects falling randomly inside a larger cylinder

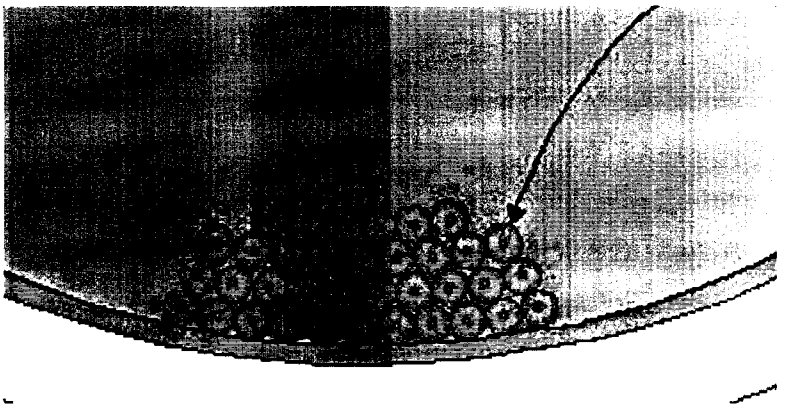

Figure 15. Cross Section of Close-Packed Lattice Formed by TRIGA Fuel Rods

Another feature of the disposal concept for the TRIGA fuel type is that the basket arrangement with the neutron absorber tubes favors homogenous mixing of neutron absorber, degradation products, and fuel rods. It is possible to obtain a very approximate first estimate of the likelihood of whether the settling particle will be a fuel rod or degradation product with neutron absorber by means of the area fraction of the constituents. Based on the intact areas of the basket and the fuel rods, the area fraction of the fuel rods is approximately 0.5. Assuming a volumetric expansion of about 2 times for the basket structure would result in an area fraction of approximately 0.36 (Attachment IV) for the fuel in the degraded mode. Thus, the probability of a single falling particle being a fuel particle is approximately 36% while the probability of the particle being a degradation product would be 64%. The probability of 37 fuel rods (Attachment IV) forming a close-packed array can be represented as a binomial probability. It should be noted that this statement would not be true if the disposal scheme for this fuel type did not result in the configuration as shown in Figure 16. The available void space for accumulation of water inside the DOE SNF canister as a fraction of the total can be estimated by using the area fraction of the materials to the area of the canister.

From the TRIGA technical report (CRWMS M&O 2000a), the diameter of a TRIGA fuel rod is approximately 3.755 cm. The diameters of the basket pipes and DOE SNF canister are shown in Figure 17. The intact case area fraction based on these values is as follows (see Attachment IV for the detailed calculations):

- Area of DOE-SNF canister=1508 cm^2
- Area of 37 fuel rods and basket tubes=759.8 cm^2
- Area fraction is 759.8/1508 which is approximately 0.5

Thus, the available void space inside the DOE SNF canister is approximately 0.5 of the total volume. In case of degradation of the basket structure only and assuming a two (2) times

volumetric expansion of the steel basket due to degradation, the available void fraction inside the DOE SNF canister reduces to approximately 0.25 (half of 0.5). This estimate shows that the solid fraction inside the DOE SNF canister is greater than 0.7 for the degraded case.

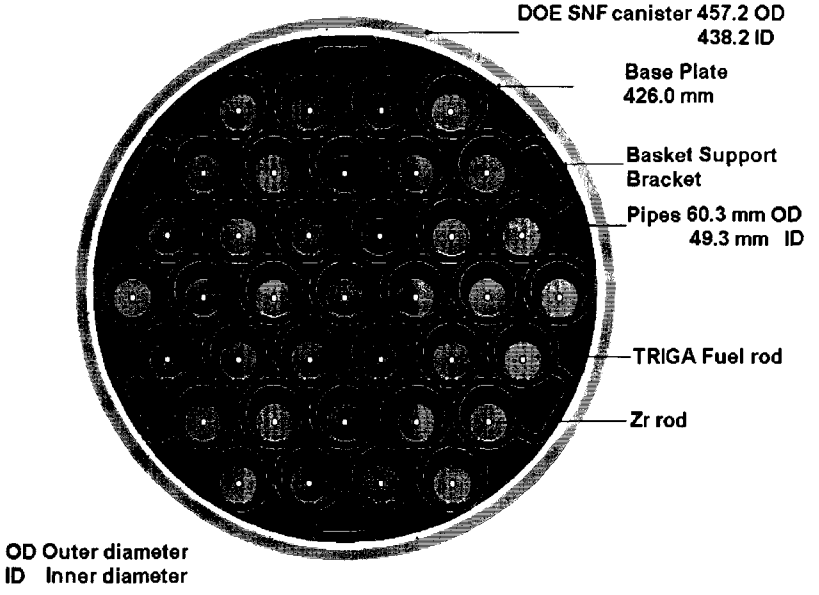

Figure 16. Cross Section of TRIGA SNF Basket Inside the DOE SNF Canister

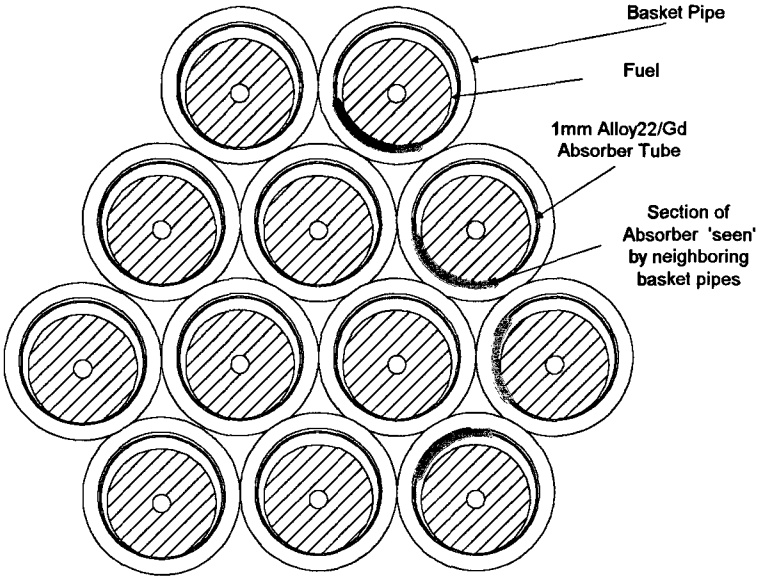

Figure 17. Expanded View of Part of Basket Structure that Would Be Subject to Loss of Neutron Absorber

The binomial distribution function of an event X, that has an individual probability of p, to have equal or less than i successes in a total of n trials is written as shown in Equation 26:

$$P\{X \le i\} = \sum_{k=0}^{i} \binom{n}{k} p^k (1-p)^{n-k}, i = 0,1,\ldots,n \qquad \text{(Eq. 26)}$$

A representative analysis can be made by using the 2-D cross section in Figure 16 as a basis. It is possible to assume that the number of particles (fraction of fuel rods) due to degradation will be at least 4 times the original number in order to allow the fuel rods to fall. The rationale behind this number is the fact that the pipes need to disintegrate at least to that many pieces before the rods can separate from the basket structure. Thus, the total number of particles of interest in the example is equal to the number of pipe pieces plus the fuel rod itself, i.e., 4+1=5. The total number of pieces in a single basket structure (there are three basket structures in the DOE SNF canister) is 5·37=185. Based on these numbers, the probability of having 37 fuel rods from a single basket stacked on top of each other due to one-by-one falling of the fuel rods from the DOE SNF would be equal to having at least 37 individual successes out of 185 tries when success of individual trial is 36%. The probability value calculated using Equation 26 above is about 10^{-6}. This probability in itself is not small enough to be inconceivable. However, the critical configuration would require a number of additional events, for example; dripping on the waste package and waste package breaching, retention of water in the waste package, or DOE SNF canister, etc. The combined probability considering waste package dripping and breaching only is about $3.47 \cdot 10^{-9}$ which is far less than 10^{-6}. Under real circumstances it is not conceivable that all the basket pipes will separate into 4 pieces due to degradation, but the more likely case is that due to degradation (e.g. oxidation) the pipes will become brittle and the basket structure collapses due to the weight of the fuel. The collapse would result in many more than 4 pieces per basket tube and actually promote mixing of the absorber and fuel. As such the probability calculation given is conservative because the binomial probability will be smaller when the number of pieces increases.

Based on the above argument it is not conceivable that the fuel rods form an array such as shown in Figure 15. In reality, it is expected that a very large fraction of the degradation products (including neutron absorber) accumulates with the fuel at the bottom of the waste package and that the average volume fractions of the 'pile' formed is similar to the initial volume fractions (e.g., approximately 64% volume fraction degradation products and 36% volume fraction fuel).

Causes for separation due to turbulent circulation of water inside the waste package or due to rotational motion (like a centrifuge) of the waste package are also considered. But none of these could occur inside the waste package because the void space, particularly after the expansion of the degraded products, is not sufficient for turbulent circulation. See Section 6.1.3.1.5 for detailed discussions.

Even if separation were possible due to some extreme event, the necessity to have a geometric arrangement favorable to the neutron economy of the system provides a second threshold for criticality concern. Based on the above arguments, it is not conceivable that neutron absorber and/or degradation products separate from the TRIGA fuel as long as the force acting on the system is the gravitational force only.

6.2.2.3 In-Package Natural Circulation Screening

Turbulent circulation of water inside the waste package can cause separation between the neutron absorber and the fuel. However the possibility for the enhancement of mass transport and accelerated neutron absorber relocation beyond the diffusion-controlled rate limit is unlikely. The enhancement is unlikely because the flow obstructions created by settled degradation products and sludge components severely limit the in-package temperature difference at which thermal instabilities can sustain buoyant recirculation. A quantitative demonstration for the influence of in-package circulation and degradation product settling is obtained using the method described in Section 6.1.3.1.5. The worksheet containing numerical calculations is provided as Attachment III.

The maximum Sh is a dimensionless parameter that scales the mass transport enhancement from buoyant convection to the diffusion contribution. Figure 18 illustrates the sensitivity of the maximum Sh (corrected for the annular waste package system geometry) under two TRIGA Codisposal waste package conditions and under increasing radial temperature drop. The maximum temperature difference of 18°C is a bounding maximum, as explained in Section 6.1.3.1.5.

The first condition corresponds to an absence of settled degradation products and precipitates (i.e., clear fluid). The maximum value of Sh is shown to be 5.67 at the bounding temperature drop, indicating an effective material relocation rate that is nominally 6 times the rate in a singular diffusion mode. Even in the absence of obstructions to flow, the mass relocation enhancement beyond a diffusive mode is less than an order of magnitude. With this modest enhancement to mass relocation, the second condition involving porous degradation product obstructions should ultimately result even where circulation is initiated under clear fluid conditions. Therefore, in the worst case, there could be a transition from the upper curve to the lower curve in Figure 18 following a brief and minor relocation of neutron absorber at accelerated rates.

Because most of the degradation products from package structural materials are insoluble, the second condition with settled porous degradation products will ultimately result, regardless of circulation initiation under either of the two conditions. For the porous system, a maximum intrinsic (uncorrected) Ra = 50 is observed and transport enhancements by natural circulation do not occur. The maximum intrinsic Ra is well under the threshold value of 250 (the threshold is specific to TRIGA Codisposal waste package arrangement and conditions) required to perpetuate instabilities.

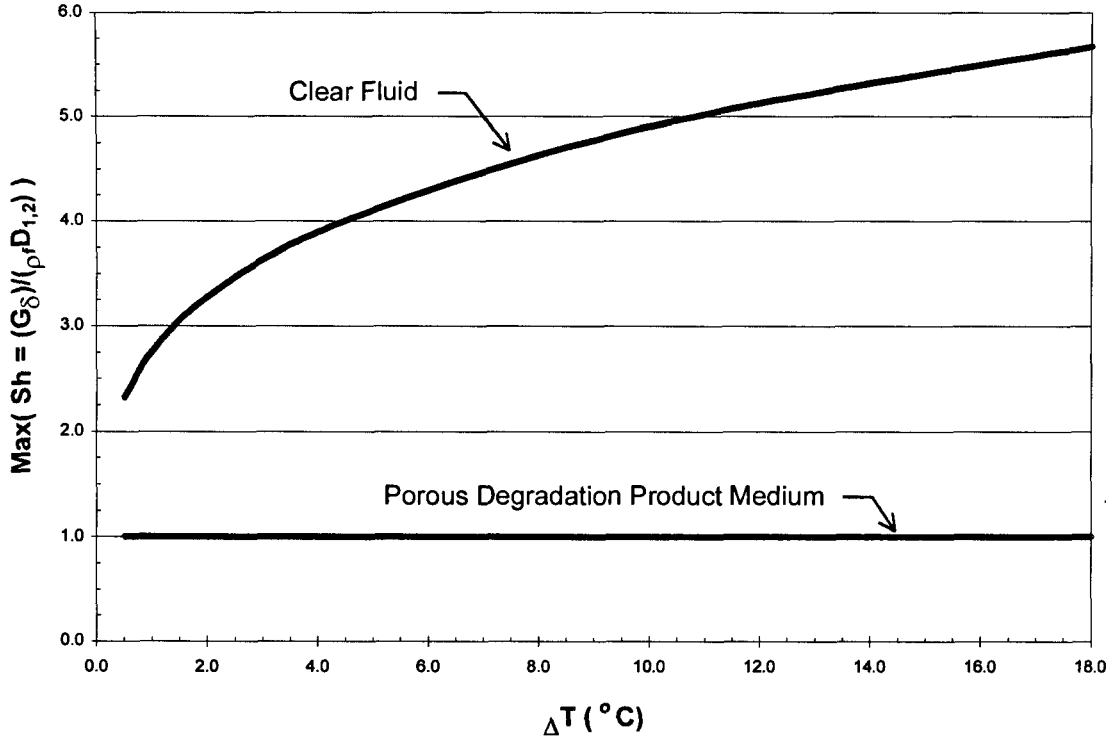

Figure 18. Maximum Sh as Function of Temperature for Settled Porous Degradation Products

6.2.2.4 Summary

For TRIGA SNF, the most reactive degraded configuration is the one with all the intact fuel rods clustered together at the bottom of the waste package and the neutron absorber dispersed throughout the waste package. The configuration can be screened out based on the arguments that there is no physical mechanism for dispersion and that fuel rods clustering is not possible because random drop or fall of relatively large pieces such as cylindrical fuel rods does not result in void fractions of less than 40% even under optimum conditions. The probability of fuel rods clustering is also very small utilizing a binomial distribution calculation. Additionally separation of neutron absorber from the fuel by thermal induced internal circulation is also investigated. The calculation results shown in Attachment III indicate that the possibility for the enhancement of mass transport and accelerated neutron absorber relocation beyond the diffusion-controlled rate limit is unlikely. The enhancement is unlikely because the flow obstructions created by settled degradation products and sludge components severely limit the in-package temperature difference at which thermal instabilities can sustain buoyant recirculation. The internal circulation screening process can also be applied for other DOE SNF types.

6.2.3 Enrico Fermi SNF

A detailed description of the Fermi SNF is presented in CRWMS M&O (2000b). For codisposal in the waste package, the Fermi SNF will be placed inside a steel basket made of 4-inch diameter pipes. Figure 20 shows a sketch of the cross section of the DOE SNF canister, steel basket

structure, and fuel. The fuel is stored in dual aluminum containers called -04 and -01 containers. The -04 aluminum containers each contain 140 zirconium-clad fuel pins from 191 derodded (clad) fuel sections,. The -04 containers are placed inside the -01 aluminum containers for on-site storage. These dual canisters are then loaded into basket/canister prior to shipment to the repository. Figure 20 is a sketch of the cross section of Fermi fuel pin canisters inside a basket pipe. The space between the steel basket pipes will be filled with iron shot in order to provide structural support for the basket and to mainly act as moderator displacer during degradation. The iron shot is also the medium for carrying the $GdPO_4$ neutron absorber.

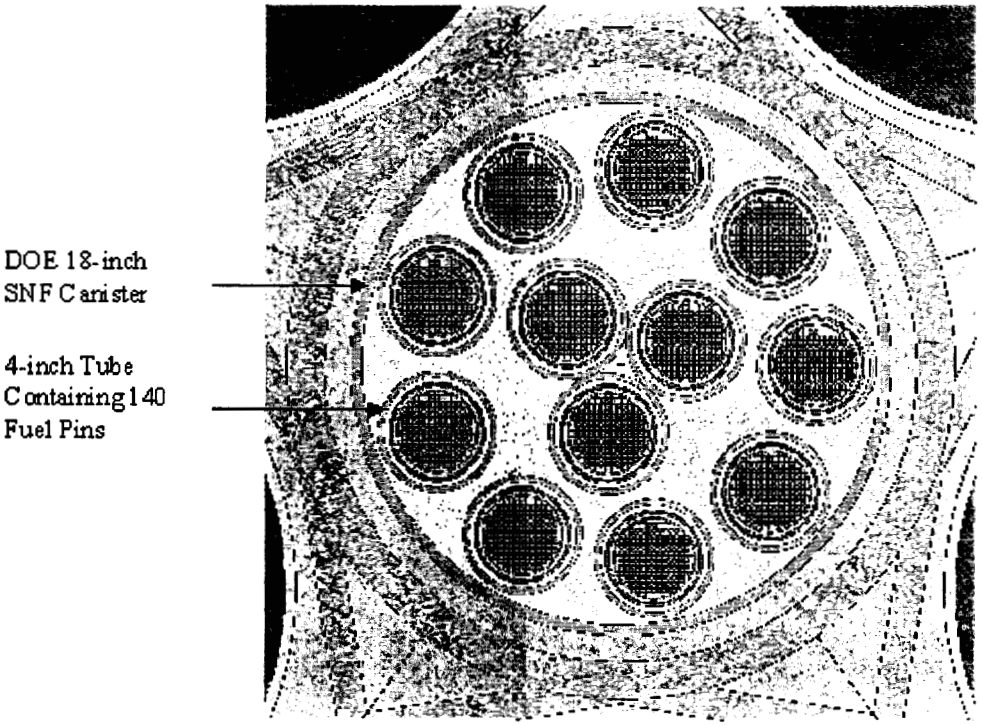

Figure 19. Cross Section of DOE SNF Canister with Enrico fermi Type Fuel

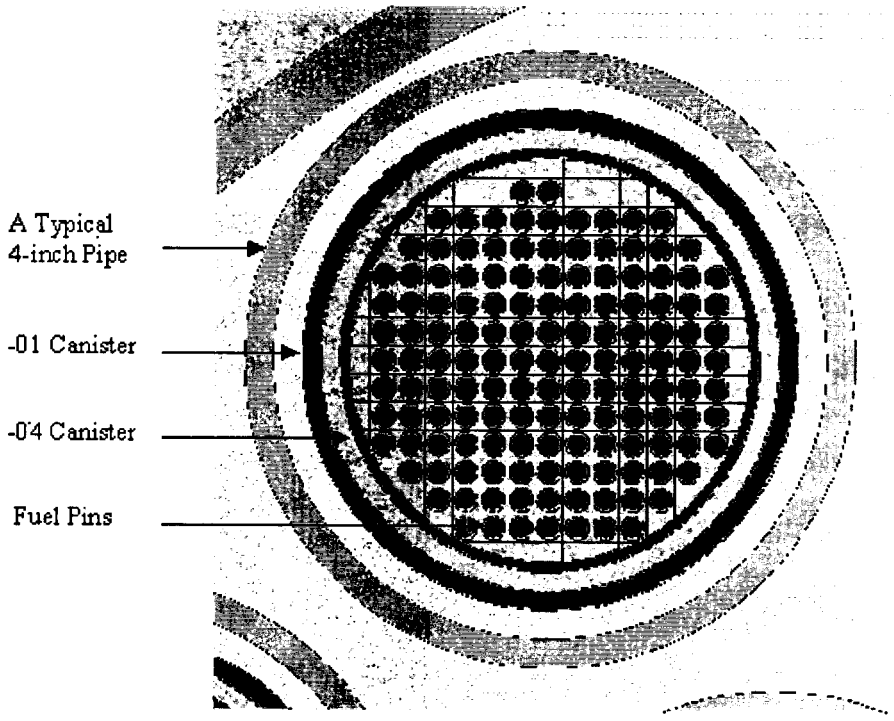

Figure 20. Enrico Fermi Fuel Pins in -04,-01 Containers, Which are Then Inserted in 4-Inch Diameter Steel Pipe

6.2.3.1 Critical Degraded Configurations

6.2.3.1.1 Codisposal Design

The design for the Enrico Fermi SNF calls for criticality control by placing iron shot containing 3% by volume $GdPO_4$ (14.5 kg per 737.9 kg of iron or 9.0 kg Gd per 737.9 kg of iron) in the available space in and around the steel pipes but outside the aluminum -01 canister.

The degraded configuration that is the most limiting case (baseline for design) is given in CRWMS-M&O (2000b, p. 75) and is based on the following conditions as shown in Figure 21:

- DOE SNF canister shell remains intact.
- Waste Package basket structure and HLW glass have degraded to iron oxide and clay
- Zirconium cladding degrades completely
- Fuel is degraded to UO_2 and remains in the intact DOE-SNF canister.

- Goethite, diaspore, and neutron absorber are partially mixed with the UO_2. There may also be complete separation between the neutron absorber and the fissile material, such that none of the neutron absorber remains in the vicinity of the fissile material.

- Gd loss renders an inventory below 9 kg distributed inside the DOE-SNF canister. The Gd is initially distributed in Fe shot, and a 9 kg inventory ensures that $k_{eff}+2\sigma$ is below the critical limit of 0.93 in the most reactive degraded configuration.

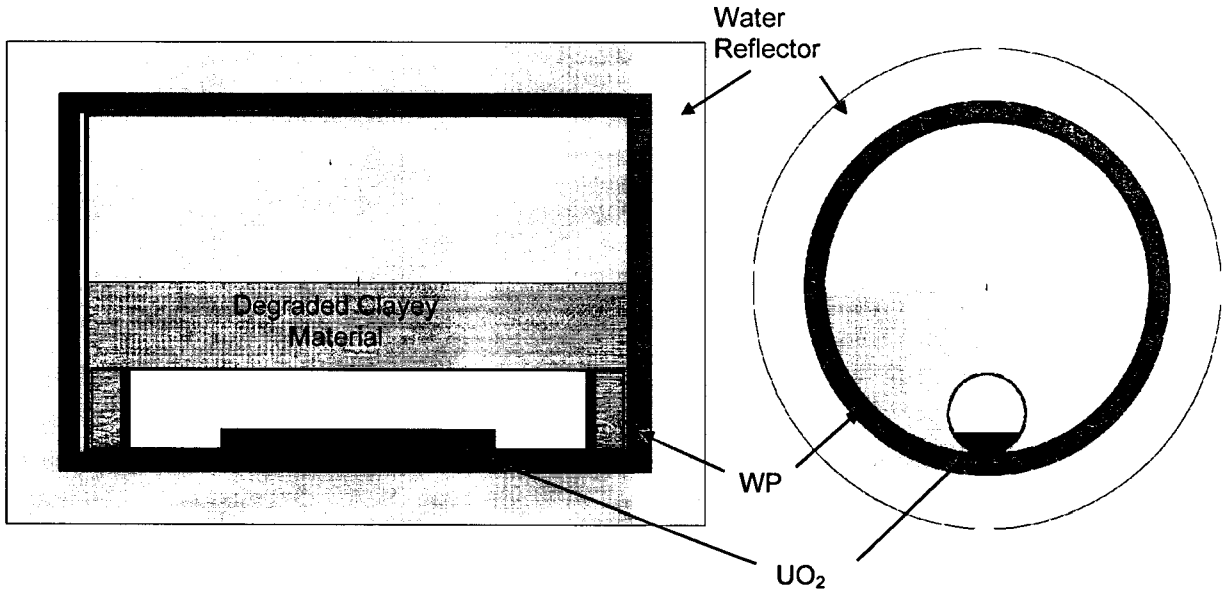

WP = Waste Package

Figure 21. Cross Sectional View of the Breached Waste Package But Otherwise Sufficiently Intact to Support Ponding

6.2.3.1.2 Additional Degraded Configurations that may Support Criticality

Figure 22 shows a cross section of the waste package for this additional configuration . The neutron absorber and carrier material are significantly separated from the intact fuel pins and distributed uniformly at the bottom of the waste package. Significant Gd loss is necessary to achieve this configuration, because a minimum of 3.5 kg of Gd distributed uniformly throughout the goethite layer maitains $k_{eff}+2\sigma$ below 0.93 for the 'most reactive pitch' (CRWMS M&O 2000b, p. 76). Additionally, the effective mean pitch between fuel elements must be greater than approximately 0.5 cm to have $k_{eff} > CL$, even with total Gd loss from the package.

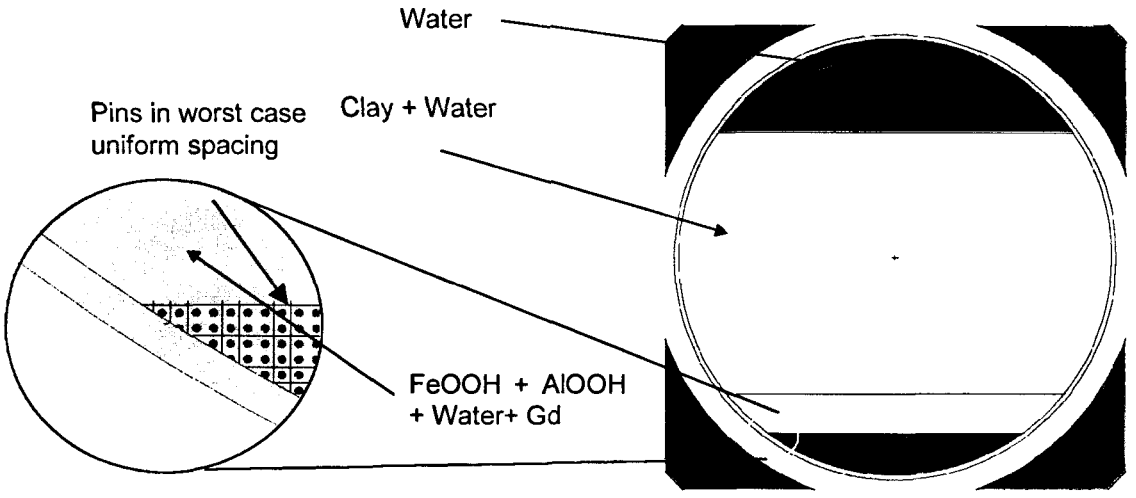

Figure 22. Configuration with Enrico Fermi Fuel Pins Distributed Uniformly at Bottom of Waste Package

Another case where Enrico Fermi pins are stacked at the bottom of the waste package in a pyramidal shape is shown in Figure 23. In this case, the Gd inventory is less than 9 kg (or less than 14.5 kg $GdPO_4$), which corresponds to the initial loading. A reduction of the Gd inventory below this value is required to increase $k_{eff}+2\sigma$ above 0.93 for the 'most reactive' pitch configuration. The neutron absorber is in effect largely separated from the SNF due to the fact that only a limited amount of Gd remains between fuel pins as an optimal effective mean fuel element pitch is attained. This configuration alsor requires an effective mean pitch greater than approximately 0.5 cm to have $k_{eff} > CL$, even with no Gd.

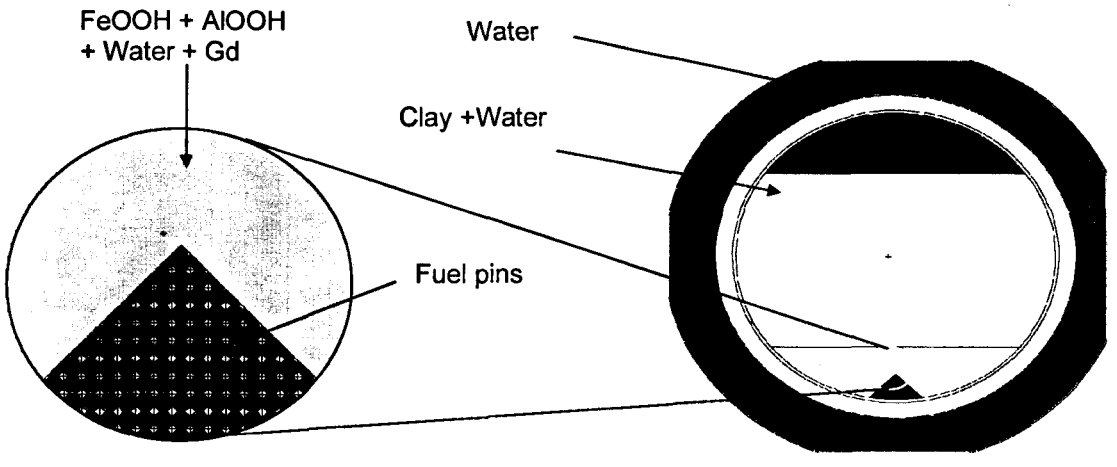

Figure 23. Cross Section of Enrico Fermi Fuel Pins Forming a Triangular Pile at the Bottom of the Waste Package

6.2.3.2 Criticality Degraded Configurations Screening

Deterministic and probabilistic arguments do not support the occurrence of the Enrico Fermi SNF configurations depicted in Figures 21, 22 and 23. Any configurations resembling those

shown are apt to be subcritical if realized. The critical configurations are highly improbable for the following reasons:

1. stratification or removal of fuel from the neutron absorber is improbable

2. fuel pin arrays with geometries and pitches in the ranges supporting criticality cannot result from degradation processes alone.

Buoyancy considerations preclude any stable stratification of the neutron absorber and/or degradation products and the fuel inside the waste package under the influence of gravity. Based on the mass density information presented in Tables 4 and 5 of Section 6.1.3.1.2, neither the fuel, degradation products, nor the neutron absorber would be buoyant or neutrally-buoyant in a water or hydrated clay environment. Additionally, the neutron absorber in the form of $GdPO_4$ is mixed with the iron shot. The confined space inside the DOE SNF canister, the distribution of the iron shot throughout the canister, and the volumetric expansion of the iron shot as it is converted to degradation products all bind the fuel pins and ensure that the neutron absorber remains with the fuel. Neutron absorber stratification under the influence of gravity does not serve as a mechanism for relative separation of the neutron absorber and fuel.

The most feasible case is that the degraded iron oxide volume fully occupies the void within the DOE canister and effectively binds the fuel, $GdPO_4$ and the DOE canister so that they behave as an integral component. If subsequent degradation of the fuel and stratification of the absorber could occur while the intact canister settles in the package, the configuration of section 6.2.3.1.1 would be realized. Alternately, the configurations in Section 6.2.3.1.2 would occur with subsequent degradation of the SNF canister and separation of the neutron absorber while the fuel elements remains intact. However, the prior degradation and expansion of the iron shot impedes relative transport of the neutron absorber. Therefore, neutron absorber stratification by mechanisms other than gravity are also excluded for relative separation of the neutron absorber and fuel. For criticality to occur under any of the configurations shown in Sections 6.2.3.1.1 and 6.2.3.1.2, vertical translation of the fuel within the package must be accompanied by removal of both the engineered neutron absorber and structural degradation products away from the fuel mass. The $GdPO_4$ inventory has an order of magnitude greater reactivity worth than the position of the SNF canister within the package or the canister water content (CRWMS M&O 2000j, p. 39, Table 6-18, pg. 40, Table 6-19).

The geometric arrangement of the fuel pins is such that, even if batch sedimentation were possible, a significant amount of neutron absorber and degradation products would either fall with or on top of the fuel pins. Subsequent sedimentation would result in a configuration that has no potential for criticality since the engineered neutron absorber (Gd) and other neutron absorbing degradation products (e.g., oxidized iron) are retained and homogeneously distributed throughout the fuel mass and interstices. Calculations for Enrico Fermi SNF package component degradation, with worst-case parameter values for material degradation rates and in-package chemistry, indicate that the maximum Gd loss does not exceed 2.3% for periods exceeding 250,000 years (CRWMS M&O 2000b pg. 61). The analysis for the removal of the $GdPO_4$, under an FFTF arrangement with the method described in the Section 6.1.2.2.1, gives an indication of

the terminal probability for relocation of the $GdPO_4$ provided in Section 6.2.1.2.5. Under this approximation, the bounding probability of significant $GdPO_4$ relocation for all time is $4.1 \cdot 10^{-7}$.

Configurations of the type shown in Figures 22 and 23, and possessing sufficient interstitial goethite or diaspore to provide moderation with $k_{eff} > CL$, have vanishingly small probabilities for occurrence. In addition to the low probability for significant Gd loss or separation, effective system-averaged rod pitches must exceed a threshold to allow $k_{eff} > CL$. The pyramid-shaped pile shown in Figure 23 is only metastable for potential energy minimization, and all of the configurations are likely to undergo rod consolidation that precludes criticality. Disturbances from package settling or seismic activity flatten the piles, and displace interstitial moderator as the rod pitches are minimized under the force of gravity. A physically consolidated fuel mass has a solid fraction approaching the close packing limit (i.e., greater than 75%) and promotes low system reactivity. For a system at the close packing limit, the pitch between intact fuel elements is approximately 0.4 cm and k_{eff} does not exceed the CL, even with complete removal of Gd from the clay layer (CRWMS M&O 2000j, pp. 41-42, Table 6-21, p. 43, Table 6-23). Additionally, no separation among the fuel rods is expected if the rods drop inside a viscous sludge/clay (e.g., see the results of the quantitative evaluation for intact fuel element translation and separation for an analagous configuration in Attachment I). The conditional probabilities of establishing the specified fuel element array geometries at the bottom of a waste package are very low, and would modify the small probabilities for Gd loss or separation. The estimate is based on the same approach used in Section 6.2.2.2 for TRIGA SNF, except the probability is much less than 10^{-6} because the number of fuel elements (i.e., the number of successes in the statistical population of possible states) considered increases from 37 to 3360. Therefore, the probability of achieving the configurations with intact rods, and based only on necessary considerations for Gd loss and fuel element geometry, is less than 10^{-12}.

6.2.3.3 Summary

For Enrico Fermi SNF, three degraded configurations are identified as the worst cases and are characterized by k_{eff} in excess of the CL. The first configuration involves an intact DOE SNF canister with all other components degraded (i.e., everything else inside and outside the canister, including the fuel pins). The intact canister sits at the bottom of the waste package. The second and third configurations require degradation of all components inside the waste package and intact fuel elements with sufficient rod spacings (i.e., separated by sufficient neutron moderating materials) in a settled assembly at the bottom of the package. In the second configuration, the fuel pins and degradation products form a uniform array in the package trough. The third configuration is similar to the second, except that the fuel pins form a crown shaped pile. None of these configurations can occur without significant separation of the Gd neutron absorber from the fuel, and the conditional probability for such separation is already low at a value less than $4.1 \cdot 10^{-7}$.

The possibility for differential stratification of neutron absorber and fissile material in the first configuration is screened out based on the gravitational stratification arguments supported by the information in Section 6.1. Stratification by mechanical perturbation of the fluidic environment is also screened. The conditional probability for Gd loss by leaching and aqueous flushing is less

than $4.1 \cdot 10^{-7}$. The point-estimate probability for Gd loss is based on the results presented in Section 6.2.1.2.5.

The second and third configurations are also precluded by the low probability for Gd losses by aqueous flushing, as discussed above. Additionally, the effective mean rod pitch may not decrease below an approximate value of 0.5 cm (fuel mass solid fraction in excess of 75%) to observe k_{eff} in excess of the CL, even with the complete loss of $GdPO_4$ from the interstitial goethite and diaspore mixture. The conditional probability of realizing either settled intact rod array geometry is less than 10^{-6}, making the probability for attaining either configuration less than 10^{-12}. This point-estimate conditional probability is based on the probability calculation performed for the TRIGA fuel for forming the clustered fuel pin pile at the bottom of a package utilizing the binomial distribution. In the case of the Fermi fuel, the probability will be even smaller because there are more intact fuel pins in the degraded configurations for Fermi than for TRIGA.

6.2.4 Shippingport PWR SNF

A detailed description of the Shippingport PWR SNF is presented in CRWMS M&O (2000d). Figure 24 below shows a isometric view of the DOE SNF canister containing the SNF. The Shippingport PWR was a "seed and blanket" reactor, which underwent multiple modifications to provide higher power outputs. The blankets will be shipped and handled as bare assemblies. Two seeds, Seed 1 (S1) and Seed 2 (S2), which had identical geometrical dimensions but different U-235 enrichment and chemical composition, were designed for Shippingport PWR Core 2 (C2) operation. The Shippingport PWR C2 S2 fuel assembly is shown in Figure 25 below (DOE 1999b). The assembly is composed of Zircaloy-4 and consists of four sub-assemblies and a cruciform-shaped channel in the center that accommodated a control rod when in the reactor.

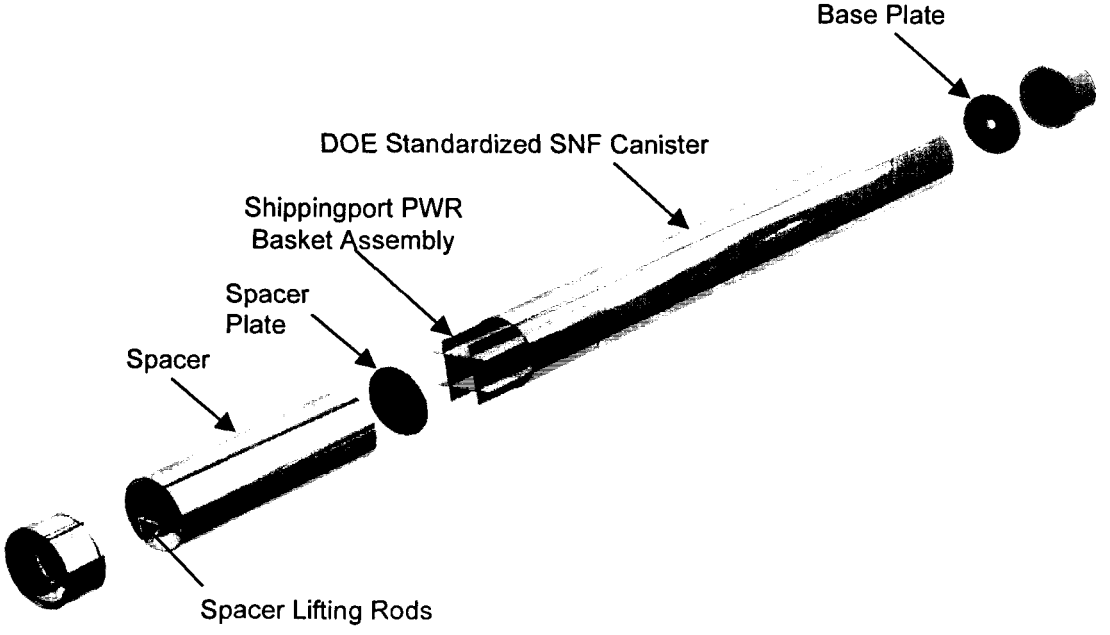

Figure 24. Isometric View of the Shippingport PWR DOE SNF Canister

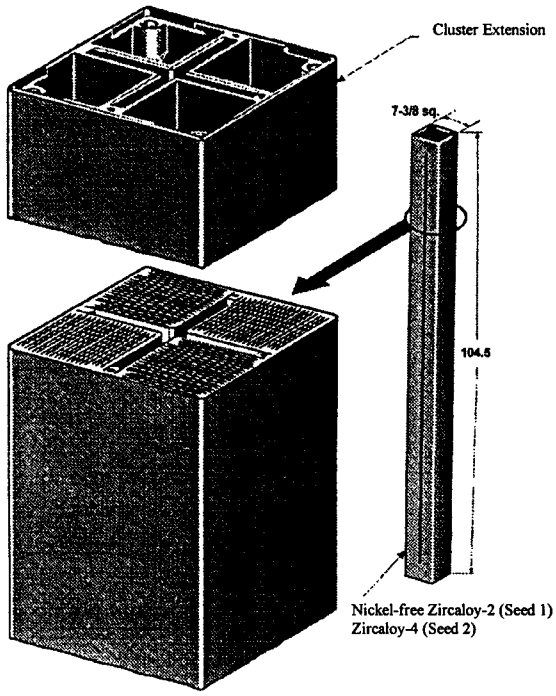

Figure 25. Shippingport C2 S2 SNF Assembly

6.2.4.1 Critical Degraded Configurations

A number of degraded configurations were presented in the technical report for the Shippingport PWR SNF (CRWMS M&O 2000d). As a result of the criticality analyses for the degraded configurations, none of the configurations has exceeded the interim critical limit of 0.93. Thus, there is no criticality concern for any of the degraded configurations analyzed.

6.2.4.2 Critical Degraded Configurations Screening

Since none of the configurations has exceeded the interim critical limit of 0.93, no screening is required.

6.2.4.3 Summary

No screening is required since there are no critical degraded configurations.

6.2.5 Shippingport LWBR SNF

A detailed description of the Shippingport LWBR SNF is presented in CRWMS M&O (2000e). Figure 26 below shows a cross-sectional view of the DOE SNF canister containing the SNF and Figure 27 shows the isometric view. The LWBR core was fueled with fertile Th-232 and fissile U-233, the relative concentrations of which varied axially and radially across the core to promote high neutron economy. The design called for vertical fuel rods on a triangular pitch (i.e., the distance between the centers of two adjacent rods) with the space between taken up by

circulating cooling water. The fuel rods featured cladding tubes loaded with cylindrical fuel pellets of thoria (ThO_2) or a binary mixture of thoria and UO_2 and backfilled with helium at one atmosphere during welding. The as-built core was conceptually segregated into four regions. The relative concentrations of fissile and fertile material varied axially and radially within each region. The four regions are Seed, Standard Blanket, Power Flattening Blanket, and Reflector.

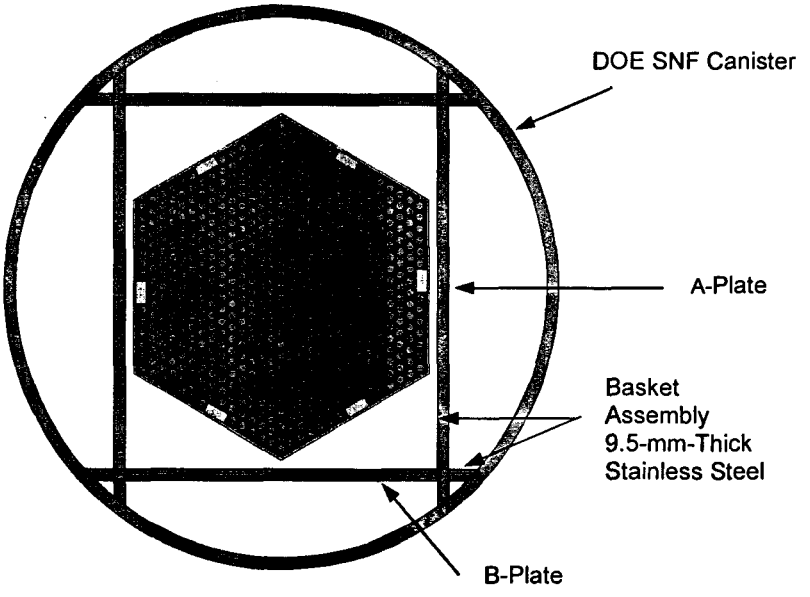

Figure 26. Cross-Section of the Shippingport LWBR DOE SNF Canister

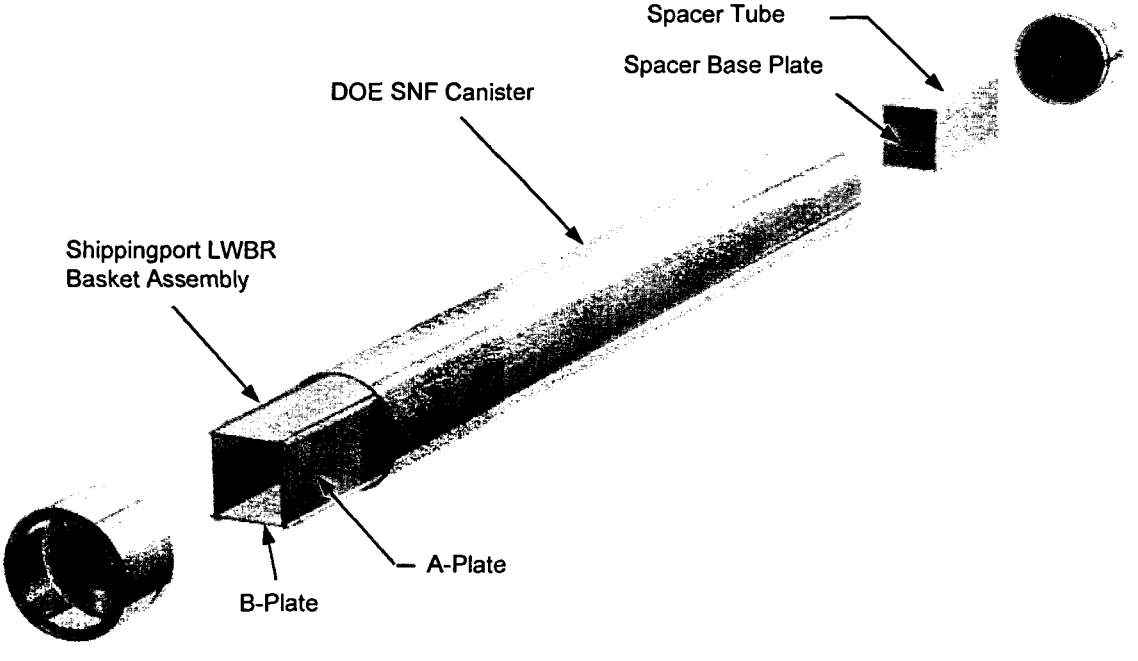

Figure 27. Isometric View of the Shippingport LWBR DOE SNF Canister

6.2.5.1 Critical Degraded Configurations

Two degraded configurations were identified as being critical, i.e., with k_{eff} exceeding the CL of 0.93 (CRWMS M&O 2000e). In the configuration shown in Figure 28, the supporting basket plates and contents inside the DOE SNF canister have totally degraded except the fuel pins. The canister shell is assumed to be breached but structurally intact. The degradation products resulting from degradation of the canister internals (mainly FeOOH [goethite from basket degradation] and AlOOH [diaspore from Al/Gd poison addition]) are distributed among the loose fuel pins. The neutron absorber, however, is distributed in the upper diaspore region and is, therefore, totally separated from the fuel pins. The greatest effect on k_{eff} of the system results from changes in the fuel pin pitch. The pitch producing the largest value of k_{eff} occurs at about 1.25 cm.

In the configuration shown in Figure 29, all the components inside the DOE SNF canister have degraded including the fuel pins. The canister shell is assumed to be breached but structurally intact. The degraded products from layers with the neutron absorber are distributed in the upper diaspore region. The highest values of k_{eff} (> 0.93) for the system occur when the fuel without thoria is mixed with goethite and water and rests at the bottom of the SNF canister. The values of k_{eff} for the system increase with increasing water volume fraction, though increasing the amount of water in the mixture also increases the probability that these configurations will attempt to float a higher density layer over a lower density layer, thus defying gravity.

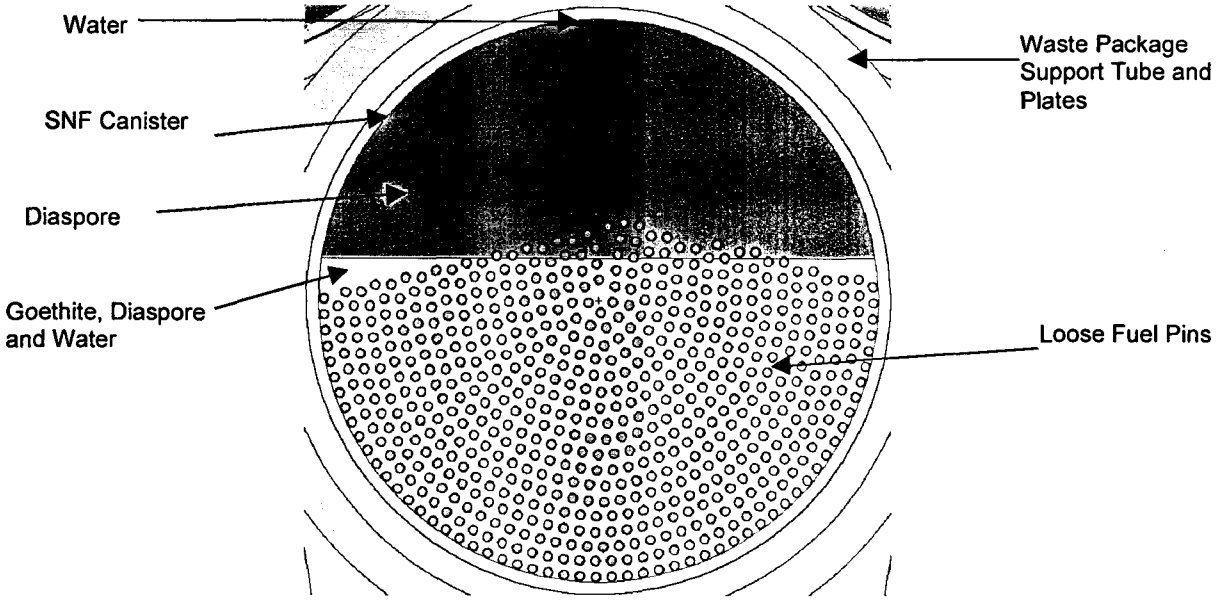

Figure 28. Cross-Sectional View of the Degraded Configuration with Intact Fuel Pins Dispersed (at optimum pitch) within the DOE SNF canister Shell

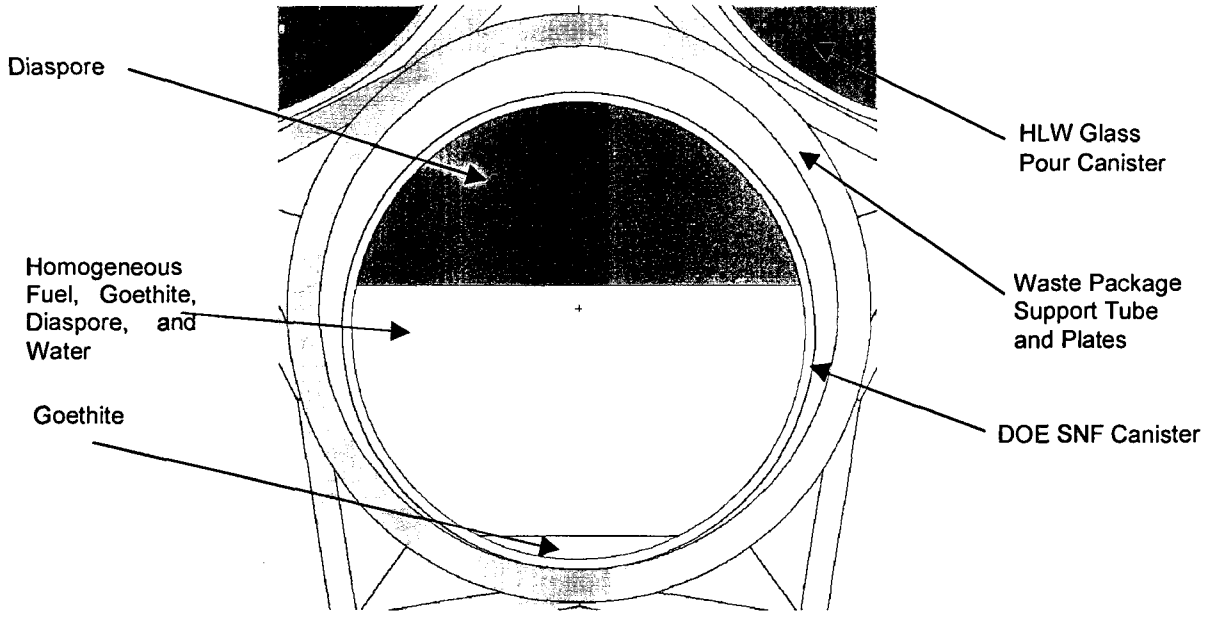

Figure 29. Cross-Sectional View of the Breached Intact DOE SNF Canister Containing Fully Degraded Fuel

The thickness of the bottom goethite layer shown in Figure 29 is based on the amount of the structural material that is degraded within the DOE SNF canister.

6.2.5.2 Critical Degraded Configurations Screening

The results of the screening process for the SLWBR fuel type show that separation of the $GdPO_4$ neutron absorber from the region containing the SNF, or its degradation product, is necessary for the occurrence of criticality. In Figure 28, the degradation product, which is a mixture of diaspore and $GdPO_4$, is on top of the fuel pins, which are spread out in a regular array having the optimum pitch. Based on the analysis done in Section 6.1, the following apply:

1. The separation of the diaspore requires a stage where it can separate by density difference inside a fluid continuum. The requirement is that the diaspore has less density than the continuum. Based on the analysis done in Section 6.1, there is no basis for such a density difference. The density of the diaspore will always be larger than the density of a fluid continuum.

2. The formation of a fuel array inside the DOE SNF canister that has close to optimum pitch requires a mechanism for the fuel elements to 'fan out.' A conceivable mechanism would be the expansion of structural material due to corrosion. It is not conceivable that the gadolinium that is originally trapped between the fuel pins can migrate toward the top section as shown in Figures 28 and 29. Diffusion has been ruled out as a valid mechanism based on the analysis given in Section 6.1.3.1.3.

3. Criticality calculations show that only 3% of the total Gd inventory staying in the fuel pin region is sufficient to reduce $k_{eff}+2\sigma$ well below the interim critical limit (CRWMS M&O 2000e, p. 73).

The above findings illustrate that the configuration where the fuel pins form an optimum pitch array inside the DOE SNF canister and the neutron absorber is completely separated is not possible and can be screened out from further consideration.

Configurations that have a degraded waste package and degraded DOE SNF canister internals but with an intact DOE SNF canister shell have shown to raise criticality concerns only when more fuel than actually present has been modeled in the calculation (CRWMS M&O 2000e, Table 40). In all other cases, $k_{eff}+2\sigma$ is shown to be below the interim critical limit. Thus, this particular configuration class has no criticality concern and can be screened out from consideration.

6.2.5.3 Summary

For Shippingport LWBR SNF, one degraded configuration has potential for criticality. In this configuration, the supporting basket plates and contents inside the DOE SNF canister have totally degraded except the fuel pins. The fuel pins form an optimum pitch array. The canister shell is assumed to be breached but structurally intact. The degradation products are distributed among the loose fuel pins. The neutron absorber is distributed in the upper diaspore region and is totally separated from the fuel pins. This configuration can be screened out based on the arguments presented in Section 6.1 that separation of neutron absorber and diaspore due to stratification is not possible. In addition, the density of diaspore is always larger than the fluid continuum. Also there is no mechanism for the fuel pins to "fan out" to form optimum array.

6.2.6 N Reactor SNF

A detailed description of the N Reactor SNF is presented in DOE (2000b). The codisposal waste package for N reactor SNF differs from that used for the other DOE spent nuclear fuel types. The N Reactor waste package contains two defense high-level waste (DHLW) canisters and two canisters filled with N Reactor SNF (for historical reasons called multi-canister overpacks (MCO)). The other SNF waste packages have five DHLW canisters surrounding the single DOE spent nuclear fuel canister. Thus, the DOE SNF canister is not used in the N Reactor waste package as shown in Figure 30.

The N Reactor fuel elements feature two basic designs, Mark IA and Mark IV. Mark IV fuel elements used two concentric tubes of uranium metal co-extruded into Zircaloy-2 cladding. The uranium enrichment for both layers was specified to be 0.947 wt% U-235, yielding an average uranium weight of 22.7 kg (50 lb.) per element. These fuels had an outer diameter of 6.147 cm (2.42 in.) and lengths varied (to facilitate reactor fuel loading configurations) as follows: 44, 59, 62, and 66 cm (17.4, 23.2, 24.6, and 26.1 in.). The Mark IV fuel inner and outer elements have Zircaloy-2 end caps with an axial length of 0.48 cm (0.19 in.) on each end.

The Mark IA fuels are differentiated from the Mark IV fuel elements in that the outer concentric tube of uranium metal consists of 1.25 wt% enriched in U-235; the inner concentric tube still consists of a 0.947 wt% uranium enrichment. These fuels have a diameter of 6.096 cm (2.40 inches), slightly smaller than the Mark IV fuels, and their U-metal weight of 16.3 kg (35.9 lbs.) is somewhat less than that found in the average Mark IV elements. Fuel lengths varied by the following values: 38, 50, or 53 cm (14.9, 19.6, and 20.9 in.). The Mark IA fuel element inner and outer elements have Zircaloy-2 end caps with an axial length of 0.483 cm (0.190 in.) on each end. Detailed information about the Mark IV and Mark IA fuel elements is provided in the characteristics report for the N Reactor SNF (DOE 2000b).

The N Reactor SNFs are loaded into MCOs. The MCOs are constructed out of 304L SS having an outside diameter 60.92 cm (23.985 inches) and a wall thickness of 1.27 cm (0.5 inches). The top portion of the MCO has a slightly larger diameter than the overall tube body in order to accommodate the top mechanical closure device. The overall length of the MCO is 422.707 cm (166.42 inches) with an inner cavity height to the top of the stacked baskets of 356.545 cm (140.372 inches). The bottom plate has a thickness of 5.11 cm (2.01 inches). There is a metal structure that adds another 57.91 cm (22.80 inches) to the top of the MCO above the basket that is best approximated as a solid, 304L SS shield plug. In addition, a central process post made of 304L SS is present in the MCOs. This central post is associated with the stacked baskets, and each post is drilled to facilitate water removal from the bottom of the MCO after underwater loading. Detailed description of the disposal scheme for this fuel type is given in the technical report for the N Reactor (CRWMS M&O 2001). Figure 30 shows an example of loading N Reactor fuel elements in the MCOs.

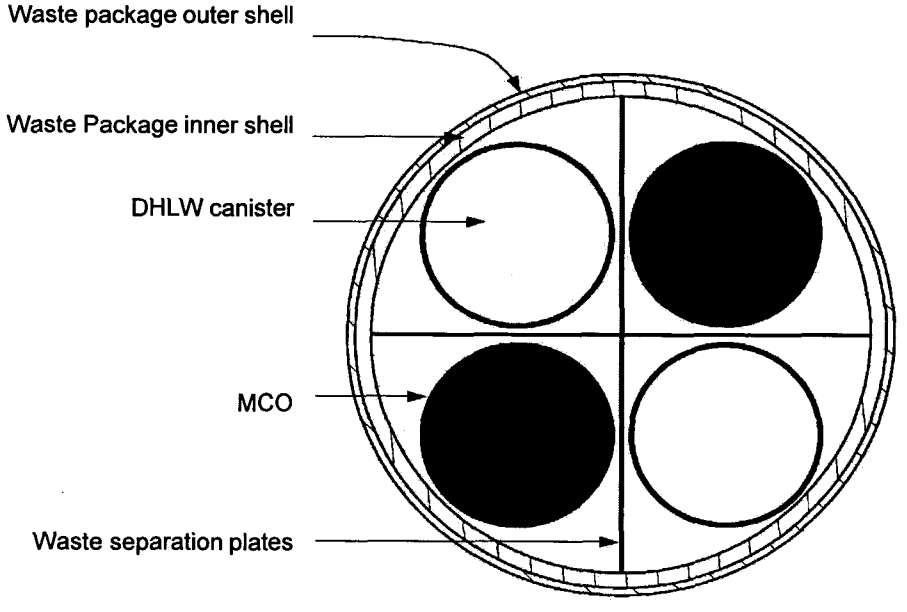

Figure 30. Cross-Sectional View of the 2-MCO/2-DHLW Waste Package in an As-Loaded Position

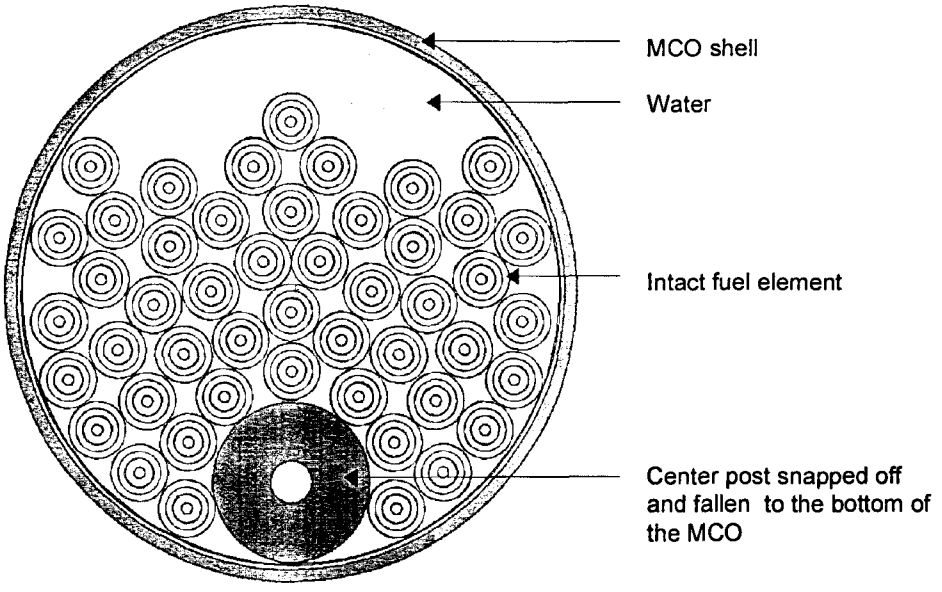

Figure 31. Center Post Fallen to the Bottom of the MCO

6.2.6.1 Critical Degraded Configurations

As a result of the degraded mode criticality analysis (CRWMS M&O 2001), two degraded configurations have been identified as being potentially critical. In the configuration shown in Figure 31, the MCO is breached but not degraded, all the internal components have degraded except the fuel elements and the center post. The center post has fallen to the bottom of each MCO in the waste package and the fuel elements are distributed uniformly over the entire available volume. A common mode failure mechanism promoting the simultaneous defeat of multiple center posts has not been identified. For this configuration with a single post failure, k_{eff} exceeds 0.93.

In the configuration shown in Figure 32a, the two MCO shells are partially degraded and fused together. If the canister pair is vertically oriented, gravity could cause the contents of the two MCOs to combine within the cavity formed by the degraded shells. Since the U-metal degrades much faster than the steel, once the MCO shell degrades, the fuel element either stays intact (cladded, Figure 32a) or is degraded (sludge, Figures 32b and 32c). Water contents in the mixture resulting from the degradation of the baskets and/or fuel were varied from 0 to a content such that the mixture is uniformly distributed over the entire volume available. Results show (CRWMS M&O 2001, Section 6.2.1.3) that the k_{eff} values exceed 0.93 only when the goethite resulting from the degradation of the basket is fully neglected (which would correspond to complete loss of iron oxide from the canister/waste package, an extremely unlikely event, given the low solubility of iron oxide), and the fully degraded outer fuel elements are distributed throughout the entire cavity ($k_{eff} + 2\sigma = 0.9614$; $k_{eff} + 2\sigma = 0.9259$ if the goethite is not neglected). The k_{eff} ranking of the configuration given in Figure 32 is k_{eff} (a) > k_{eff} (b) > k_{eff} (c).

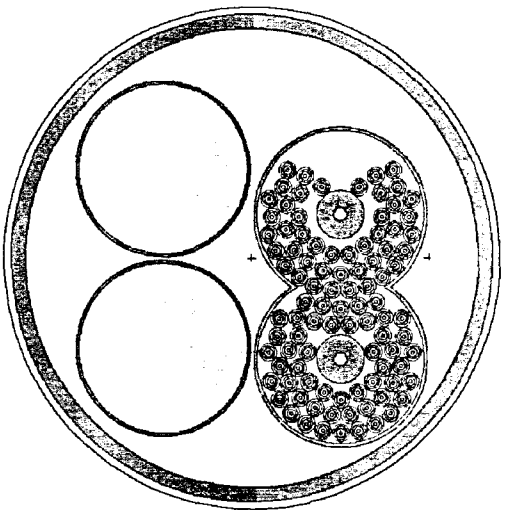

a. Intact Basket

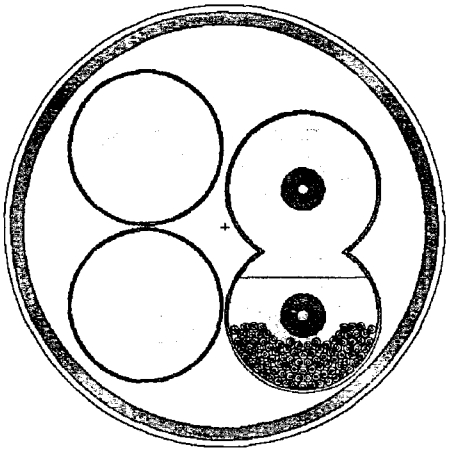

b. Partially Degraded Fuel Elements

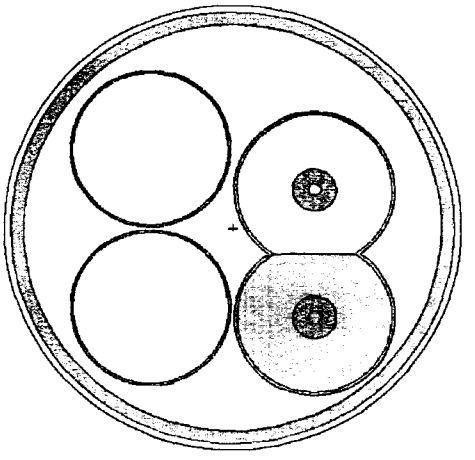

c. Fully Degraded Fuel Elements

Figure 32. Configurations Where 2 MCOs Combine

6.2.6.2 Critical Degraded Configurations Screening

The principal factors affecting the criticality potential for N Reactor type fuel are the mode and sequence of degradation of the waste package components. All the configurations that show potential for criticality are based on degradation rates that are not realistic. For example, in the configuration shown in Figure 32, the fuel in the canister is represented as spheres and distributed throughout the basket. However, it is not possible for the fuel to form particles distributed throughout the MCO after degradation. Uranium metal is chemically very reactive, and the products of uranium-water reaction are uranium oxide (UO_2) and hydrogen gas (H_2). The molecular hydrogen is dissociated by uranium and forms uranium hydride (UH_3) (Huang

1996). Therefore, the formation of solid uranium metal spheres due to degradation is physically not achievable and the homogeneous mixture resulting from oxidation of the uranium metal is much less reactive. Also, there are no physical mechanisms for the fuel in the basket to be uniformly distributed over the entire volume available in the basket and for the center post to snap and settle down through the fuel elements. The center post is twice as thick as the basket bottom plate and more than sixty times thicker than the basket shell and would be the last component to degrade. No mechanism for shearing off the center post has been identified. In summary, the conditions leading to the critical configurations are not realistic based on material properties.

The formation of a 'combined MCO' is an extremely unlikely phenomena, which would require selective corrosion and subsequent collapse of the line of contact of the two MCOs. Even in that event, the results show (CRWMS M&O 2001, Section 7.4.3) that the k_{eff} values exceed 0.93 only when the goethite resulting from the degradation of the basket is fully neglected (less absorption), and the fully degraded outer fuel elements are distributed over the entire cavity ($k_{eff} + 2\sigma = 0.9614$; $k_{eff} + 2\sigma = 0.9259$ if the goethite is not neglected). The iron oxide density is much larger than the density of any fluid continuum that may exist inside the MCO. Thus, loss by 'flushing out' of goethite is not feasible. The degradation rate of uranium metal would imply that goethite and fuel would be mixed inside the MCO, and any loss of goethite by any mechanism would also result in loss of fuel. Thus, these configurations are impossible since there is no physical mechanism to separate the iron oxide from the degraded fuel inside the cavity; therefore, it is not possible that the iron oxide be flushed out of the MCO without flushing out some degraded fuel as well. Also, there is no physical mechanism to distribute the degraded outer fuel elements over the entire cavity based on the arguments presented in Section 6.1.

6.2.6.3 Summary

For N Reactor SNF, two degraded configurations are considered as having potential for criticality. The first one is associated with the center post having snapped off and fallen to the bottom of the MCO with intact fuel element inside the intact MCO. The second one is associated with two MCOs being fused together while the fuel elements inside the MCOs either stay intact, or partially or totally degraded. In addition, it is assumed that the fuel element forms spheres after degradation. The screening is based on the fact that it is impossible for the center post to snap because the center post is twice as thick as the basket bottom plate and more than sixty times thicker than the basket shell and would be the last component to degrade. No mechanism for shearing off the center post has been identified. The formation of a 'combined MCO' is an extremely unlikely phenomena, which would require selective corrosion and subsequent collapse of the line of contact of the two MCOs. Finally, it is impossible for the fuel to form distributed particles after degradation. Uranium metal is chemically very reactive, and the products of uranium-water reaction are uranium oxide (UO_2) and hydrogen gas (H_2). The molecular hydrogen is dissociated by uranium and forms uranium hydride (UH_3) (Huang 1996). Therefore, the formation of uranium particles distributed throughout the MCO due to degradation is physically not achievable

7. CONCLUSIONS

The configurations that have potential for $k_{eff}+2\sigma$ exceeding the prescribed critical limit have two features in common:

- The neutron absorber is separated from the fissile material (with the exception of N Reactor SNF because there is no neutron absorber added).
- The geometric arrangement of the fissile material is favorable to the neutron economy.

The analysis given in Section 6 shows that no mechanism exists for the separation between neutron absorber and fissile material as long as their initial (intact) configuration is 'mixed' and no forces other than gravity affect the waste package. Table 14 summarizes the findings presented in this analysis.

Table 14. Summary of Findings for Screening of DOE SNF Degraded Configurations

SNF Type	Mechanism for $k_{eff}+2\sigma$ in excess of the CL	$k_{eff}+2\sigma$	Comment (p=probability)	Design Mitigation
FFTF SNF	5 DFA's degraded while Ident-69 canister is intact.	0.95634 for 6wt% Gd in basket	Intact Ident-69 drop ($p < 5.0 \cdot 10^{-9}$) and $GdPO_4$ loss ($p \leq 4.1 \cdot 10^{-7}$) are unlikely (Section 6.2.1).	Dispose 4 DFA's with Ident-69 only
Enrico Fermi SNF	Separation of neutron absorber from fuel region due to density stratification.	> 0.95	Improbable because of the low conditional probabilities for $GdPO_4$ loss ($p \leq 4.1 \cdot 10^{-7}$)and intact fuel element geometries ($p << 10^{-6}$). Buoyant $GdPO_4$ stratification cannot occur (Section 6.2.3).	N/A
TRIGA SNF	Separation of neutron absorber due to mode of collapse.	>0.95	The fuel geometry necessary for criticality is unlikely ($p < 10^{-6}$). Natural fluid circulation does not occur with porous degradation products (Section 6.2.2).	N/A
Shippingport PWR	None	<0.93	N/A	N/A
Shippingport LWBR	Separation of neutron absorber from fuel due to density stratification	>0.95	No neutron absorber separation is feasible due to component density differences (Section 6.1).	N/A
N Reactor	Degradation of center post and MCO	> 0.95	Degradation rates and common mode failure requirements do not allow configurations to occur (Section 6.2.6).	N/A

Based on the physical parameters, stratification and separation due to density difference of fissile materials and the neutron absorber and/or carrier can only occur if:

- Particle density during sedimentation/drop is less than 10 % of void fraction.
- Particle size for neutron absorber and/or carrier is significantly smaller than for fissile material.

- Neutron absorber and/or carrier particle density is equal or less than that of the environment (sludge/clay) in which the particles sediment.

As discussed in Section 6.1.3.1.2 that between the two extremes, of particles sedimenting as a lumped aggregate or in batches, there is no mechanism to allow for separation. In lumped aggregate sedimentation the particles will have the same mixing characteristics as before the drop while the case of batch sedimentation may result in localized stratification. However, for both cases the end result would still be a mix of neutron absorber and fissile material in terms of neutron absorption.

In summary, it can be concluded that:

For the FFTF fuel type, if four DFAs are used with one compartment in the DOE SNF canister blocked, there will be no criticality concern, based on the initial loading of the fissile material. This is the recommended design. If five DFAs are used, the critical degraded configurations can be screened out based on the physical arguments presented in Section 6.1 and the low probabilities for $GdPO_4$ loss and for intact Ident-69 container drop.

For the Enrico Fermi fuel type, all of the critical degraded configurations have low conditional probabilities of $GdPO_4$ loss, and the configurations involving intact fuel elements have subsequently reduced conditional probabilities for attainment of the necessary fuel geometries and moderator distributions. Critical configurations cannot occur for close-packed fuel geometries, despite any assumed $GdPO_4$ loss.

In the case of the TRIGA fuel type, the critical degraded configurations have low conditional probabilities. Degradation rate enhancements from in-package natural convection can be screened out if porous degradation products exist in the waste package.

The Shippingport PWR fuel type is screened out directly since none of the configurations analyzed show concern for $k_{eff}+2\sigma$ exceeding the prescribed critical limit.

For the Shippingport LWBR fuel type, the critical degraded configurations can be screened out based on the arguments presented in Section 6.1 that separation of neutron absorber and diaspore due to stratification is not possible. Also there is no mechanism for the fuel pins to "fan out" to form an optimum array.

For the N Reactor fuel type, the screening is based on the fact that it is impossible for the center post to snap prior to other components because the center post is twice as thick as the basket bottom plate and more than sixty times thicker than the basket shell. A common mode failure involving the simultaneous failure of all of the posts in all MCO and scrap baskets cannot be identified. The post is the last component to degrade. The formation of a 'combined MCO' is an extremely unlikely phenomena, which would require selective corrosion and subsequent collapse of the line of contact of the two MCOs. Finally, it is impossible for the fuel to from an array of particles distributed through MCO after degradation because of the uranium metal reaction rate.

8. INPUTS AND REFERENCES

8.1 DOCUMENTS CITED

Bosworth, R.C.L. 1956. *Transport Processes in Applied Chemistry.* New York, New York: John Wiley & Sons. On Order Library Tracking Number-249831

Chen, R.C. and Wu, J.L. 2000. "The Flow Characteristics Between Two Interactive Spheres." *Chemical Engineering Science, 55,* ([6]), 1143-1158. [New York, New York]: Elsevier. TIC: 249633.

Coelho, D.; Thovert, J.-F.; and Adler, P.M. 1997. "Geometrical and Transport Properties of Random Packings of Spheres and Aspherical Particles." *Physical Review E, 55,* (2), 1959-1978. [New York, New York]: American Physical Society. TIC: 249557.

Coussot, P. 1995. "Structural Similarity and Transition from Newtonian to Non-Newtonian Behavior for Clay-Water Suspensions." *Physical Review Letters, 74,* (20), 3971-3974. [Woodbury, New York]: American Physical Society. TIC: 249554.

CRWMS M&O 1999a. *Evaluation of Codisposal Viability for MOX (FFTF) DOE-Owned Fuel.* BBA000000-01717-5705-00023 REV 00. Las Vegas, Nevada: CRWMS M&O. ACC: MOL.19991014.0235.

CRWMS M&O 1999b. *Generic Degradation Scenario and Configuration Analysis for DOE Codisposal Waste Package.* BBA000000-01717-0200-00071 REV 00. Las Vegas, Nevada: CRWMS M&O. ACC: MOL.19991118.0180.

CRWMS M&O 1999c. *EQ6 Calculations for Chemical Degradation of Enrico Fermi Spent Nuclear Fuel Waste Packages.* BBA000000-01717-0210-00029 REV 00. Las Vegas, Nevada: CRWMS M&O. ACC: MOL.19990702.0030.

CRWMS M&O 1999d. *Thermal Evaluation of the TRIGA Codisposal Waste Package.* BBAA00000-01717-0210-00022 REV 00. Las Vegas, Nevada: CRWMS M&O. ACC: MOL.19990712.0195.

CRWMS M&O 1999e. *Fast Flux Test Facility (FFTF) Reactor Fuel Degraded Criticality Calculations: Intact SNF Canister.* BBA000000-01717-0210-00051 REV 00. Las Vegas, Nevada: CRWMS M&O. ACC: MOL.19990607.0075.

CRWMS M&O 1999f. Attachment X of "Fast Flux Test Facility (FFTF) Reactor Fuel Degraded Criticality Calculation: Degraded SNF Canister". BBA000000-01717-0210-00033 REV 01. Las Vegas, Nevada: CRWMS M&O. ACC: MOL.19990601.0234.

CRWMS M&O 1999g. *Probability of PWR UCF WP Postclosure Criticality for Enhanced Design Alternatives.* BBA000000-01717-0210-00072 REV 00. Las Vegas, Nevada: CRWMS M&O. ACC: MOL.19990927.0365.

CRWMS M&O 1999h. *Fast Flux Test Facility (FFTF) Reactor Fuel Criticality Calculations.* BBA000000-01717-0210-00016 REV 00. Las Vegas, Nevada: CRWMS M&O. ACC: MOL.19990426.0142.

CRWMS M&O 2000a. *Evaluation of Codisposal Viability for UZrH (TRIGA) DOE-Owned Fuel.* TDR-EDC-NU-000001 REV 00. Las Vegas, Nevada: CRWMS M&O. ACC: MOL.20000207.0689.

CRWMS M&O 2000b. *Evaluation of Codisposal Viability for U-Zr/U-Mo Alloy (Enrico Fermi) DOE-Owned Fuel.* TDR-EDC-NU-000002 REV 00. Las Vegas, Nevada: CRWMS M&O. ACC: MOL.20000815.0317.

CRWMS M&O 2000c. *Technical Work Plan For: Department of Energy Spent Nuclear Fuel Work Packages.* TWP-MGR-MD-000010 REV 00. Las Vegas, Nevada: CRWMS M&O. ACC: MOL.20001107.0305.

CRWMS M&O 2000d. *Evaluation of Codisposal Viability for HEU Oxide (Shippingport PWR) DOE-Owned Fuel.* TDR-EDC-NU-000003 REV 00. Las Vegas, Nevada: CRWMS M&O. ACC: MOL.20000227.0240.

CRWMS M&O 2000e. *Evaluation of Codisposal Viability for Th/U Oxide (Shippingport LWBR) DOE-Owned Fuel.* TDR-EDC-NU-000005 REV 00. Las Vegas, Nevada: CRWMS M&O. ACC: MOL.20001023.0055.

CRWMS M&O 2000f. *Drift Degradation Analysis.* ANL-EBS-MD-000027 REV 00 ICN 01. Las Vegas, Nevada: CRWMS M&O. ACC: MOL.20001103.0004.

CRWMS M&O 2000g. *In-Package Chemistry Abstraction for TSPA-LA.* Input Transmittal 00163.T. Las Vegas, Nevada: CRWMS M&O. ACC: MOL.20000327.0214.

CRWMS M&O 2000h. *Degradation of Stainless Steel Structural Material.* ANL-EBS-MD-000007 REV 00. Las Vegas, Nevada: CRWMS M&O. ACC: MOL.20000329.1188.

CRWMS M&O 2000i. *Design Analysis for the Defense High-Level Waste Disposal Container.* ANL-DDC-ME-000001 REV 00. Las Vegas, Nevada: CRWMS M&O. ACC: MOL.20000627.0254.

CRWMS M&O 2000j. *Enrico Fermi Fast Reactor Spent Nuclear Fuel Criticality Calculations: Degraded Mode.* CAL-EDC-NU-000001 REV 00. Las Vegas, Nevada: CRWMS M&O. ACC: MOL.20000802.0002.

CRWMS M&O 2001. *Evaluation of Codisposal Viability for U-Metal (N-Reactor) DOE-Owned Fuel.* TDR-EDC-NU-000004 REV 00. Las Vegas, Nevada: CRWMS M&O. ACC: MOL.20010314.0004.

Davis, R.H. 1992. "Effects of Surface Roughness on a Sphere Sedimenting Through a Dilute Suspension of Neutrally Buoyant Spheres." *Physics of Fluids A, Fluid Dynamics, 4,* (12), 2607-2619. [New York, New York]: American Institute of Physics. TIC: 249635.

DOE (U.S. Department of Energy) 1999a. *Fermi (U-Mo) Fuel Characteristics for Disposal Criticality Analysis.* DOE/SNF/REP-035, Rev. 0. Washington, D.C.: U.S. Department of Energy. TIC: 242461.

DOE (U.S. Department of Energy) 1999b. *Shippingport PWR (HEU Oxide) Fuel Characteristics for Disposal Criticality Analysis.* DOE/SNF/REP-040, Rev. 0. Washington, D.C.: U.S. Department of Energy. TIC: 243528.

DOE (U.S. Department of Energy) 2000a. *Quality Assurance Requirements and Description.* DOE/RW-0333P, Rev. 10. Washington, D.C.: U.S. Department of Energy, Office of Civilian Radioactive Waste Management. ACC: MOL.20000427.0422.

DOE (U.S. Department of Energy) 2000b. *N Reactor (U-Metal) Fuel Characteristics for Disposal Criticality Analysis.* DOE/SNF/REP-056, Rev. 0. [Washington, D.C.]: U.S. Department of Energy, Office of Environmental Management. TIC: 247956.

Druitt, T.H. 1995. "Settling Behaviour of Concentrated Dispersions and Some Volcanological Applications." *Journal of Volcanology and Geothermal Research, 65,* ([1-2]), 27-39. [New York, New York]: Elsevier. TIC: 249553.

Feng, J.; Huang, P.Y.; and Joseph, D.D. 1996. "Dynamic Simulation of Sedimentation of Solid Particles in an Oldroyd-B Fluid." *Journal of Non-Newtonian Fluid Mechanics, 63,* ([1]), 63-88. [Amsterdam, The Netherlands]: Elsevier. TIC: 249641.

Gheissary, G. and van den Brule, B.H.A.A. 1996. "Unexpected Phenomena Observed in Particle Settling in Non-Newtonian Media." *Journal of Non-Newtonian Fluid Mechanics, 67,* ([1-3]), 1-18. [Amsterdam], The Netherlands: Elsevier. TIC: 249642.

Huang, F.H. 1996. "Container Materials in Environments of Corroded Spent Nuclear Fuel." *Journal of Nuclear Materials, 231,* ([1-2]), 74-82. [New York, New York]: Elsevier. TIC: 249579.

Jastrzebski, Z.D. 1959. *Nature and Properties of Engineering Materials.* New York, New York: John Wiley & Sons. TIC: 249621.

McClure, J.A. and Alsaed, A.A. 2001. *External Criticality Risk of Immobilized Plutonium Waste Form in a Geologic Repository.* TDR-EBS-MD-000019 REV 00. Las Vegas, Nevada: Bechtel SAIC Company. ACC: MOL.20010314.0001.

Mills, A.F. 1995. *Heat and Mass Transfer.* Chicago, Illinois: Irwin. TIC: 249568.

Nield, D.A. and Bejan, A. 1992. *Convection in Porous Media.* New York, New York: Springer-Verlag. TIC: 249632.

Parrington, J.R.; Knox, H.D.; Brenenman, S.L.; Baum, E.M.; and Feiner, F. 1996. *Nuclides and Isotopes.* 15th Edition. San Jose, California: Lockheed Martin. TIC: 233705.

Pasupathi, V. 1999. "Waste Package Structural Material." Interoffice correspondence from V. Pasupathi (CRWMS M&O) to T.W. Doering, May 7, 1999, LV.WP.VP.05/99-073. ACC: MOL.19990518.0316.

Perry, R.H. and Chilton, C.H., eds. 1973. *Chemical Engineers' Handbook.* 5th Edition. New York, New York: McGraw-Hill. TIC: 242591.

Roberts, W.L.; Campbell, T.J.; and Rapp, G.R., Jr. 1990. *Encyclopedia of Minerals.* 2nd Edition. New York, New York: Van Nostrand Reinhold. TIC: 242976.

Scheaffer, R.L. and McClave, J.T. 1990. *Probability and Statistics for Engineers.* 3rd Edition. Boston, Massachusetts: PWS-Kent Publishing Company. On Order Library Tracking Number-249631

Schlichting, H. 1987. *Boundary-Layer Theory.* 7th Edition. New York, New York: McGraw-Hill. TIC: 241144.

Simnad, M.T. 1981. "The U-ZRH_x Alloy: Its Properties and Use in Triga Fuel." *Nuclear Engineering and Design, 64,* 403-422. [Amsterdam, The Netherlands]: North-Holland Publishing. TIC: 243927.

Weast, R.C., ed. 1979. *CRC Handbook of Chemistry and Physics.* 60th Edition, 1979 - 1980. Boca Raton, Florida: CRC Press. TIC: 245312.

Wierenga, A.M.; Lenstra, T.A.J.; and Philipse, A.P. 1998. "Aqueous Dispersions of Colloidal Gibbsite Platelets: Synthesis, Characterisation and Intrinsic Viscosity Measurements." *Colloids and Surfaces A: Physicochemical and Engineering Aspects, 134,* ([3]), 359-371. [New York, New York]: Elsevier. TIC: 249556.

Wu, J. and Manasseh, R. 1998. "Dynamics of Dual-Particles Settling Under Gravity." *International Journal of Multiphase Flow, 24,* ([8]), 1343-1358. New York, New York: Elsevier. TIC: 249634.

YMP (Yucca Mountain Site Characterization Project) 2000. *Disposal Criticality Analysis Methodology Topical Report.* YMP/TR-004Q, Rev. 01. Las Vegas, Nevada: Yucca Mountain Site Characterization Office. ACC: MOL.20001214.0001.

8.2 CODES, STANDARDS, REGULATIONS, AND PROCEDURES

AP-2.21Q, Rev. 1, ICN 0, BSCN 1. *Quality Determinations and Planning for Scientific, Engineering, and Regulatory Compliance Activities.* Washington, D.C.: U.S. Department of Energy, Office of Civilian Radioactive Waste Management. ACC: MOL.20010212.0018.

AP-SI.1Q, Rev. 3, ICN 1. *Software Management.* Washington, D.C.: U.S. Department of Energy, Office of Civilian Radioactive Waste Management. ACC: MOL.20010515.0126.

ATTACHMENT I

FIRST ANALYSIS OF THE MAXIMUM TRANSIENT SNF ROD PITCH FOR NUCLEAR CRITICALITY INITIATION

ATTACHMENT I

FIRST ANALYSIS OF THE MAXIMUM TRANSIENT SNF ROD PITCH FOR NUCLEAR CRITICALITY INITIATION

I-1. INTRODUCTION

An evaluation of a hypothetical nuclear criticality initiation mechanism is performed. The hypothesis pertains to a partially degraded and flooded canister or waste package containing spent nuclear fuel (SNF) with fully deteriorated assembly ducts and grid spacers. The unconstrained, intact fuel rods rest in a pile at the lowpoint in the canister or waste package, surrounded by a viscous sludge/fluid composed of water and the degradation products from the structural materials. Some rapid mechanical disturbance, such as an earthquake or a sudden structural collapse, accelerates the canister or waste package. The system response to acceleration may give rise to differential relative velocities for the internal components. A hypothetical concern is that an increase in the relative transverse center-to-center separation between many neighboring fuel rods may allow the transient establishment of a geometry that supports nuclear criticality.

The transient criticality hazard is contingent upon the dynamic interactions of the SNF rods and sludge solution allowing the momentary establishment of a mean inter-rod separation distance within the narrow range of values that correspond to critical configurations. The physics affecting the interactions among rods is identical to that affecting component settling in dilute fluid-particle suspensions (e.g., clays and slurries) and affecting fluid flow around cascades of stationary obstructions at low or moderate Reynolds numbers. The introduction of literature concerning these analogous applications is valid and useful in demonstrating that SNF rod separation will not occur even under the most pessimistic conditions.

The potential for rod separation is determined by the directions and magnitudes of forces arising in direct (i.e., rod collisions) and indirect (i.e., fluid-rod interactions) transient rod interactions. For a system of equi-dimensional and equally massive SNF rods, the indirect interactions dominate the potential for rod separation after the initial impulse, unless unrealistically large accelerations are imparted (e.g., it requires much less effort to clap one's hands in air than under water).

The fluid physics influencing the relative translations of the system of SNF rods following a disturbance are adequately resolved with a conceptual model for flow around a tandem cascade. The comparative magnitude of fluid drag on the aft body determines the magnitude of the force affecting relative rod motions, and is determined by the characteristics of the fluid shear layer leaving the forward body and impinging on the aft body. If the streamline perturbations or vortex in the wake of the leading body produce a situation where the flow just outside of the shear layer is channeled around the aft body, thereby positioning an adverse pressure gradient in the wake immediately forward of the rear body, the resultant forces would reduce the separation. This is the flow-shadowing effect. Conversely, if the characteristics of the wake flow do not position an adverse pressure gradient immediately ahead of the rear body, then the aft body sees a relative drag force that would maintain or increase the separation. Over the broad range of

Reynolds numbers ($Re_D > 4$) where an attached vortex or vortex-shedding exists in the wake of the forward body, the streamwise length of the vortex is roughly equivalent to the length of the region of neutral or adverse pressure gradient. For the equi-dimensional bodies, the relative fluid drag is a function of the impinging flow speed, the distance of separation, and the relative orientation of the axis of the tandem cascade to the principal direction of fluid flow.

This document evaluates the fluid-rod interactions in an accelerated canister or waste package that would presumably allow the establishment of rod separations. Sections I-2 and I-3 of this attachment provide an assessment with a 1-D model for the dynamic translation of the SNF rods within a canister barrier. The results of the assessment indicate that the rod separations do not occur. Section I-4 introduces authoritative literature on many-body interactions in fluids, and provides additional support for the conclusion (Section I-5) that rod separation is impossible.

I-2. THEORY

Subsequent modeling treats component and system momenta and energy within a 2-D cross-sectional plane of the canister or waste package (Figure I-1). Only displacements in the vertical coordinate direction are considered. The waste package system is assumed to be comprised of three types of components. The outer component is the effective barrier with total mass, m_b, and inner diameter, $D_{b,i}$. The barrier encloses a total of N_r free SNF rods, each with mass, m_r, outer diameter, $D_{r,o}$ and axial length, L_r. The third type of component is the incompressible sludge/fluid mixture that fills the remaining space within the package. The sludge has total mass, m_s, and total volume, V_s.

Upon mechanical disturbance, the barrier and contents react as a fully dynamic system. Models for the disturbance and system response are categorized in 3 sequential phases. Phase I (Section I-2.1) pertains to the external initiator with the system in an inertial state of rest. Phase II (Section I-2.2) corresponds to the initial system response and distribution of momenta among components. For Phase III (Section I-2.3), the relative transient rod movements that may result from the disturbance are modeled.

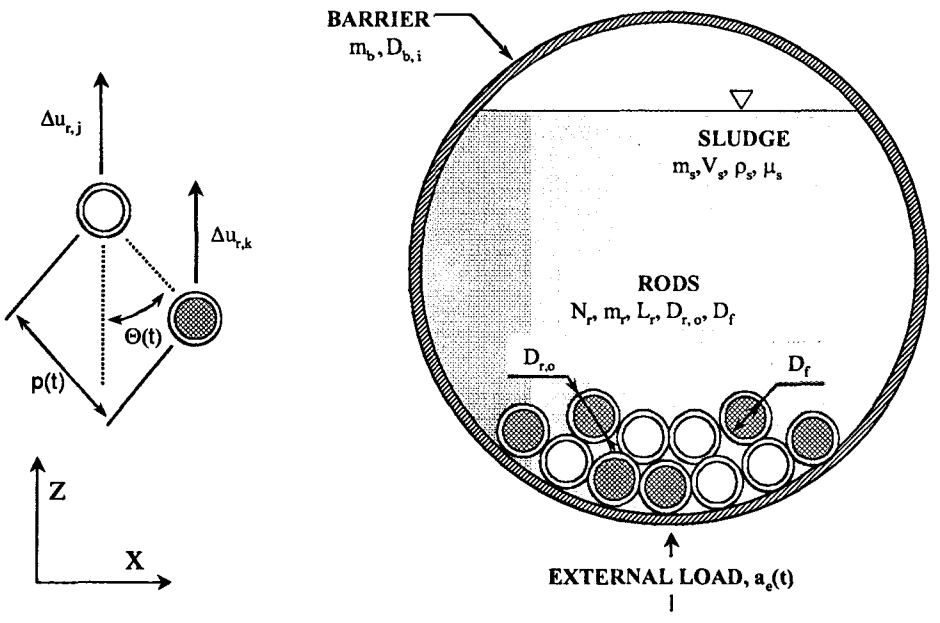

Figure I-1. System Component Types, Component Characteristics, and Coordinate Definitions for the Theoretical Model

I-2.1 Phase I–External Initiation

The external disturbance is assumed to jolt the system from an initial state of rest, accelerating the system centroid vertically in the inertial frame. The acceleration is presumed to be time-dependent, but to act for a sufficiently short duration (t_e) to qualify an impulse assumption formulation later in Phase II,

$$P_c(t_e) - 0 = \int_0^{t_e} \frac{dP_c}{dt} dt = \int_0^{t_e} m_c a_e(t) dt \qquad \text{(Eq. I-1)}$$

where the integration on the right-hand-side of Equation (I-1) is intended to performed only over either the positive or negative acceleration phase (i.e., integration ends where $a_e(t)$ changes sign), and where,

$a_e(t)$ = external acceleration of waste package centroid [m/s^2]
m_b = total waste package barrier mass [kg]
m_c = total waste package system mass [kg]
$= m_b + m_s + N_r m_r$
m_r = single SNF rod mass [kg]

m_s = total sludge and water mass [kg]
N_r = total number of SNF rods [-]
P_c = momentum of the waste package system centroid [N·s]

$$= m_b u_b + m_s u_s + \sum_{j=1}^{N_r} m_r u_{r,j}$$

t = time [s]
t_e = disturbance duration [s]
u_b = vertical velocity of waste package barrier [m/s]
$u_{r,}$ = jvertical velocity of single SNF rod with label j [m/s]
u_s = mass-average vertical velocity of sludge [m/s]

I-2.2 Phase II – Force Transmission

The external disturbance is assumed to act on a small time scale and to translate the entire system of components uniformly. In reality, relative differential forces may act on components because the system is undergoing a transient response and is not a rigid body. If the rods occupy a small fraction of the total volume, then the distance between the mass centroids of the barrier and filling sludge remains small and constant. It follows that the sludge and barrier velocities are equal,

$$u_b = u_s \quad . \tag{Eq. I-2}$$

As the SNF rods are initially coalesced in a compact pile, it is assumed that they are displaced as a coherent group until cessation of the external disturbance,

$$u_{r,j}(t_e) = u_r(t_e)\,;\, 1 \le j \le N_r \tag{Eq. I-3}$$

Note that the assumption of coherence for Equation I-3 is highly accurate for an external loading that acts opposite the direction of gravity. In a center-of-mass coordinate frame, the net momentum is zero,

$$(m_b + m_s)(u_b(t_e) - u_c(t_e)) = -N_r m_r (u_r(t_e) - u_c(t_e)) \tag{Eq. I-4}$$

where,

$$u_c = \frac{P_c}{m_c} \quad . \tag{Eq. I-5}$$

If the initial motion of the waste package system is fully coherent through time t_e, and if there is no relative differential motion among the SNF rods at later times, the system energy is expressed in terms of the system centroid momenta and the relative velocity of the SNF rods,

$$\frac{P_c^2(t_e)}{2m_c} = \frac{P_c^2(t)}{2m_c} + \frac{N_r m_r}{2}\left(1 + \frac{N_r m_r}{m_b + m_s}\right)(u_r(t) - u_c(t))^2 \tag{Eq. I-6}$$

or, rearranging terms in Equation I-6,

$$u_r(t) - u_c(t) = G(t, t_e) \qquad \text{(Eq. I-7)}$$

where,

$$G(t,t_e) = \left(\frac{P_c^2(t_e) - P_c^2(t)}{N_r\, m_r\, m_c \left(1 + \frac{N_r m_r}{m_b + m_s}\right)} \right)^{\frac{1}{2}} \quad . \qquad \text{(Eq. I-8)}$$

Subsequent use of the COM momentum balance (Equation I-4) allows calculation of the remaining component velocities,

$$u_b(t) - u_c(t) = u_s(t) - u_c(t) = -\frac{N_r m_r}{m_b + m_s} G(t,t_e) \quad . \qquad \text{(Eq. I-9)}$$

The maximum possible velocity differential corresponds to a time when the system centroid momentum is zero (this would occur near the time of maximum elevation for a positive vertical displacement of the waste package system). The maximum velocity differential corresponds to a maximum value of $G(t,t_e)$,

$$G_{\max} = \left(\frac{P_c^2(t_e)}{N_r\, m_r\, m_c \left(1 + \frac{N_r m_r}{m_b + m_s}\right)} \right)^{\frac{1}{2}} \quad . \qquad \text{(Eq. I-10)}$$

I-2.3 Phase III – Differential SNF Rod Displacements

The problem of relative movements among the rods is generalized in terms of a two-body problem. The rods are immersed in the sludge, which is viscous and conveys fluidic force interactions among the rods. The objective of the Phase III calculation is to determine the relative rod separations that can occur vertically, the coordinate direction transverse to the axes of the rods (Figure I-1).

The Phase II models (Eqs. I-7 and I-9) are used to obtain the velocity differential between rod and sludge in a situation where the SNF rods are displaced coherently,

$$\Delta u_r(t) = u_r(t) - u_s(t) = \left(1 + \frac{N_r m_r}{m_b + m_s}\right) G(t,t_e) \quad . \qquad \text{(Eq. I-11)}$$

The force of fluid resistance on the j^{th} rod is a function of the differential velocity, the total drag coefficient, and the projected area of the rod normal to the flow (Schlichting 1987, p. 16),

$$F_j(t) = \frac{\rho_s D_{r,o} L_r}{2} C_{D,j}\left(\theta, \frac{p}{D_{r,o}}, \mathrm{Re}_D\right) \Delta u_{r,j}^2 \qquad \text{(Eq. I-12)}$$

where the rod pitch , angle and relative velocities are shown schematically in Figure I-1, and where,

$C_{D,j}$ = fluid drag coefficient for rod j in the presence of other rods [-]
$D_{r,o}$ = SNF rod outer diameter [m]
F_j = fluid drag force on rod j [N]
L_r = SNF rod length [m]
p = center-to-center rod pitch [m]
Re_D = Reynolds number for rod j [-]

$$= \frac{\rho_s \Delta u_{r,j} D_{r,o}}{\mu_s}$$

μs = dynamic viscosity of sludge [Pa·s]
ρ_s = mass density of sludge[kg/m^3]
Θ = angle between rod j and neighboring rod k measured from vertical direction in which fluid drag acts [deg]

The appropriate values or functional dependencies of $C_{D,j}$ are obtained from empirical relationships, as discussed in Section I-3.1. Physical aspects of the fluid flow in the wake of the leading SNF rod (e.g., streamline divergence, flow channeling, attached fluid recirculation in the rod wake, and downstream vortex-rod interactions) are inherently quantified in this experimentally measured parameter. The fluid drag on rod acts opposite the direction of motion through the fluid, decelerating the rod,

$$\frac{d\Delta u_{r,j}}{dt} = -\frac{F_j}{m_r} \quad . \qquad \text{(Eq. I-13)}$$

The magnitude of $C_{D,j}$ depends upon the instantaneous rod velocity and orientation of rod j relative to rod k. If rods j and k respectively have unequal values of $C_{D,j}$ and $C_{D,k}$, a transient increase in the rod pitch may result. Because the drag coefficient depends on velocity and orientation angle, it varies with time. Temporal integration of the variable $C_{D,j}$ is involved for determination of the instantaneous rod velocity,

$$\Delta u_{r,j}(t) = \left(\frac{1}{\Delta u_{r,j}(t_{III})} + \frac{\rho_s D_{r,o} L_r}{2 m_r} \int_{t_{III}}^{t} C_{D,j}\, dt' \right)^{-1} \qquad \text{(Eq. I-14)}$$

where,

t_{III} = time for incipient differential movement of SNF rods (i.e., Phase III initiation) [s]

The Phase II results (Equation I-11) are used for the initial condition and simplify the right hand side of Equation I-14,

$$\Delta u_{r,j}(t_{III}) = \Delta u_r(t_{III}) = \left(1 + \frac{N_r m_r}{m_b + m_s} \right) G(t_{III}, t_e) \quad . \qquad \text{(Eq. I-15)}$$

The transient elevation difference between rods is a function of the relative difference in rod velocities,

$$p_z(t) = \cos(\Theta(t_{III}))p(t_{III}) + \int_{t_{III}}^{t}\left(\Delta u_{r,j}(t') - \Delta u_{r,k}(t')\right)dt' \quad . \qquad \text{(Eq. I-16)}$$

The transient orientation angle is measured from vertical to rod k with vertex on rod j,

$$\Theta(t) = \tan^{-1}\left(\frac{\sin(\Theta(t_{III}))\,p(t_{III})}{p_z(t)}\right) \quad . \qquad \text{(Eq. I-17)}$$

Finally, the transient pitch is calculated,

$$p(t) = \frac{p_z(t)}{\cos(\Theta(t))} \quad . \qquad \text{(Eq. I-18)}$$

I-3. NUMERICAL MODELING

The numerical model consists of a Microsoft Excel spreadsheet solution to Equations I-1, I-10, I-11, and I-14 through I-18. The use of Equation I-10, in lieu of other possible forms of Equation I-8, to render G_{max} is an inherent conservatism in the numerical implementation that should overestimate the $\Delta u_{r,j}(t_{III})$ and p(t) in all calculations. All spreadsheet calculations were performed with the file "MaxRodPitch.xls" on a Dell *Optiplex* personal computer with Microsoft Excel version *97*. Section I-3.1 provides the input parameters for the numerical assessments, including detailed descriptions of the $C_{D,j}$ calculations. Section I-3.2 presents the results for a constant disturbance magnitude with discrete variations of the initial rod orientation angle values. One additional calculation for a heuristic drag coefficient model with an anomalous dependence on Θ is also presented in Section 3.2 as a sensitivity study for the only hypothetical fluid drag conditions allowing SNF rod separations.

I-3.1 Parameter Values

Parameter values for the physical properties of the components are adapted or calculated from the information in CRWMS M&O (2000a, pp. 5-23) for a DOE SNF canister containing TRIGA SNF and are listed in Table I-1. The SNF rod and fuel dimensions correspond to standard SS-clad TRIGA fuel elements, with 1 exception. The SNF basket design accepts 37 rods, as counted across an arbitrary canister cross section. However, disposal configurations and component dimensions vary with the TRIGA SNF type and may allow up to 3 axially separated SNF zones within a canister for a total of 111 rods. From the standpoint of the transient establishment of a critical configuration, it is conservative to neglect axial variations and to assume that one SNF fuel rod has axial length equivalent to the internal length of the canister. The SNF rod mass neglects the minor contribution from cladding. The sludge density is taken to be the median of nominal water and wet clay densities. The sludge dynamic viscosity is conservatively taken to be the nominal value for water, which is a lower value than for clay. The assignment of a

minimum value for μ_s renders maximum values for Re_D, and therefore maximum differences of the F_j that lead to a potential increase of the SNF rod pitch.

Table I-1. Physical Input Parameters for TRIGA SNF Canister Components

Parameter	Parameter Type	Value
m_b [kg]	constant	330
$D_{b,i}$ [m]	constant	0.50
m_s [kg]	formula	$= \rho_s V_s$
V_s [m^3]	constant	0.49
ρ_s [kg/m^3]	constant	$1.50\ 10^3$
μ_s [Pa-s]	constant	$1.10\ 10^{-3}$
N_r [-]	constant	37
m_r [kg]	formula	$= \rho_r \frac{\pi}{4} D_f^2 L_r$
$D_{r,o}$ [m]	constant	$3.75\ 10^{-2}$
D_f [m]	constant	$3.65\ 10^{-2}$
L_r [m]	constant	2.50
ρ_r [kg/m^3]	constant	$8.37\ 10^3$
$\Theta(t_{III})$ [deg]	discrete variable	0, 30, 45, 60, and 89
$p(t_{III})$ [m]	formula	$= 1.001 \cdot D_{r,o}$

The parameters affecting the external initiator magnitude are representative of a 1-g square-wave positive-acceleration histogram of 10 [s] duration and are given in Table I-2. The external impulse assumed here is arbitrary and at least 20 times the impulse magnitude from a credible seismic disturbance recurring once every 10^4 years.

With the high seismic wavelength to drift diameter ratio, it is likely that the drift and surrounding rock mass would move as a rigid body under free-field acceleration. It is unlikely that underground openings could move independently of the surrounding medium or be subjected to vibrational amplifications. Therefore, the accelerations at the package pedestal are not likely to exceed the peak ground acceleration, which is estimated to be 0.43-g in the principal frequency range of 1-10 [Hz] (acceleration phase durations from 1 to 0.1 [s]) for a Category 2 (i.e., 1 in 10^4 years) seismic event (CRWMS M&O 2000f, pgs. 17 and 32). The assumed acceleration and duration are highly conservative for seismic disturbances.

Table I-2. Parameters for the External Disturbance (Phase I) and Force Transmission (Phase II) Calculations.

Parameter	Parameter Type	Value
$a_e(t)$ [m/s^2]; $0 \le t \le t_e$	constant	10
t_e [s]	constant	10
t_{III} [s]	arbitrary	$P_c(t_{III}) \rightarrow 0$; $G(t_{III},t_e) \cong G_{max}$

Chen and Wu (2000) perform experiments measuring the drag characteristics of a test sphere in a Newtonian fluid and in the presence of one neighboring sphere of equivalent diameter. Measurements in the laminar boundary-layer flow regime at moderate Re_D (≤ 100) indicate drag coefficient dependencies on Re_D, on the relative orientation of the axis of the array of spheres to the flow ($0° \le \Theta \le 180°$), and on the separation distance between the spheres ($1 \le p/D \le 4$). The magnitude of the scaled drag interaction is moderated with an increase of Re_D over

approximately an order of magnitude (Chen and Wu 2000, pg. 1147) or increasing p/D to a value of 4 (Chen and Wu 2000, p. 1149, Figures 5, 9, 12). Therefore, the model is conservatively limited to reproduce the primary sensitivity to Θ that is observed in the experiments, while neglecting the reduction in the magnitude of the interactions between the pair of spheres that occurs with increasing values of p. The drag coefficient required in Equation I-12 is calculated as the product of two functions,

$$C_{D,j}(\Theta, \tfrac{p}{D_{r,o}}, \mathrm{Re}_D) = \frac{C_D}{C_{D0}}(\Theta) \cdot C_{D0}(\mathrm{Re}_D) \qquad \text{(Eq. I-19)}$$

where,

C_D/C_{D0} = scaled drag coefficient for an obstruction with an interacting neighbor [-]
C_{D0} = drag coefficient for an individual obstruction in a free fluid stream

The angular dependence of the scaled drag coefficient for spheres (Chen and Wu 2000, Figure 5c, l/d=1/3) is here applied to the cylindrical geometry of the SNF rods. This extension is valid because the third-dimensional flow effects that arise for individual spheres, but are negligible for flow around individual cylinders with large $L_r/D_{r,o}$ at low and moderate Re_D, result in a uniform shift of the drag coefficient values over a broad range of Re_D ($0.1 \le Re_D \le 10^6$) between the two obstruction geometries (see Schlichting 1987, pg. 17). The regression for the angular dependence of the scaled drag coefficient incorporates the hydrodynamic effects of divergent streamlines and vortex-particle interactions at various orientations of the tandem cascade to the impinging flow that are inherent in the basis data. The Re_D range of formal applicability is necessarily limited by the range evaluated in experiment. The regression for the angular dependence is a superposition of linear and sinusoidal terms,

$$\frac{C_D}{C_{D0}} = 0.95 - 0.55\left(\frac{\Theta}{180}\right) + 0.525\left(\sin(\Theta)\right)^{1.06868} \qquad \text{(Eq. I-20)}$$

Note that in application of Equation I-20 evaluation only need be performed in the range ($0° \le \Theta \le 90°$) for the leading particle, and the corresponding complimentary range ($90° \le \Theta \le 180°$) for the trailing particle, to examine all possible relative orientations of equi-dimensional particles. Symmetries are commonly exploited in investigations of sedimentation in dilute suspensions with smooth equi-dimensional particles (Davis 1992, pg. 2614).

The drag coefficient for an independent cylinder in cross flow is calculated with an empirical expression that is valid in the range $1 \le Re_D \le 10^4$ (Mills 1995, pg. 285, Eq. 4.69),

$$C_D = 1 + \frac{10}{\mathrm{Re}_D^{2/3}} \qquad \text{(Eq. I-21)}$$

I-3.2 Results

The numerical spreadsheet model "MaxRodPitch.xls" indicates that the center-to-center rod pitch, p, remains constant after the disturbance for evaluations with the parameters specified in Table I-1, Table I-2, and Eqs. I-19 through I-21 (Figure I-2). This result is insensitive to the initial orientation angle of the rods, as no dynamic increase of p is observed for any of the initial $\Theta = 0°, 30°, 45°, 60°$, or 89°.

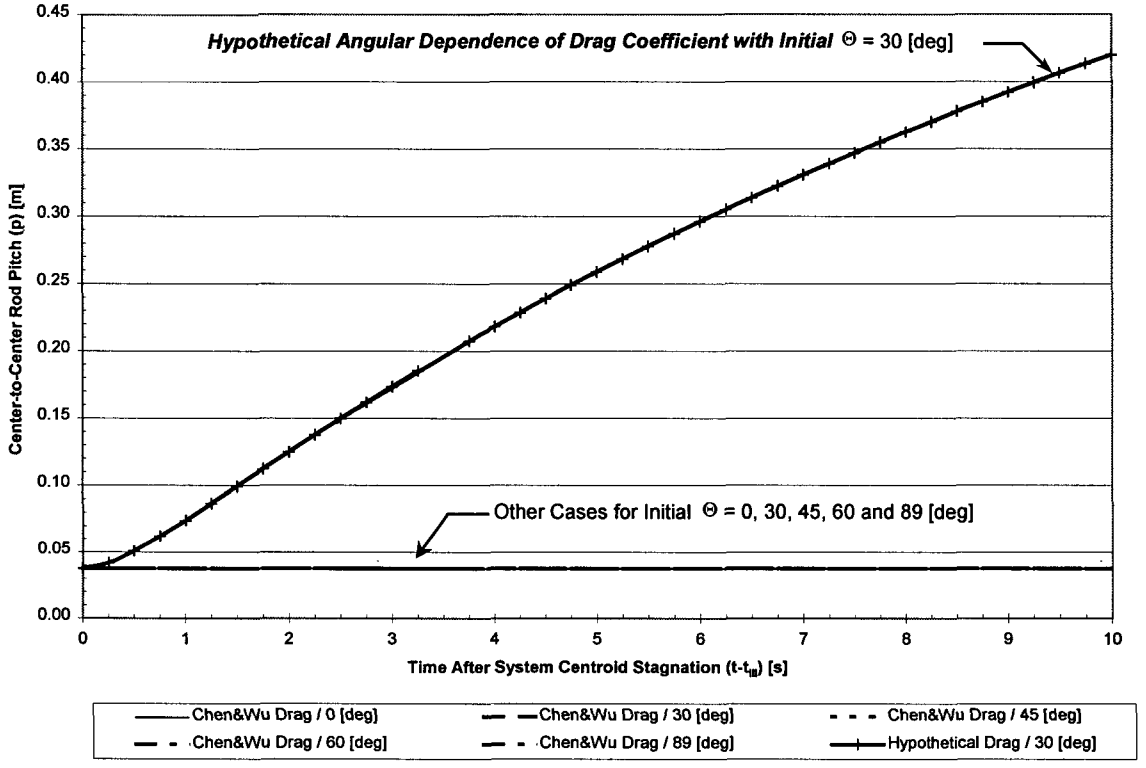

Figure I-2. The Chen and Wu (2000) Drag Model Gives No Rod Separation Over the Range of Initial Orientation Angles

To test the model performance, a hypothetical case is run with an intentional misappropriation of the angular dependence (i.e., swap) of the drag coefficient values for the forward and aft rods, respectively. Under these hypothetical conditions, an increase in the rod pitch would be possible if the forward rod were to experience the drag force appropriate for the aft rod, which cannot occur in reality (upper curve, Figure I-2). An extended discussion of the impossibility for rod separation is given in Section I-4.1.

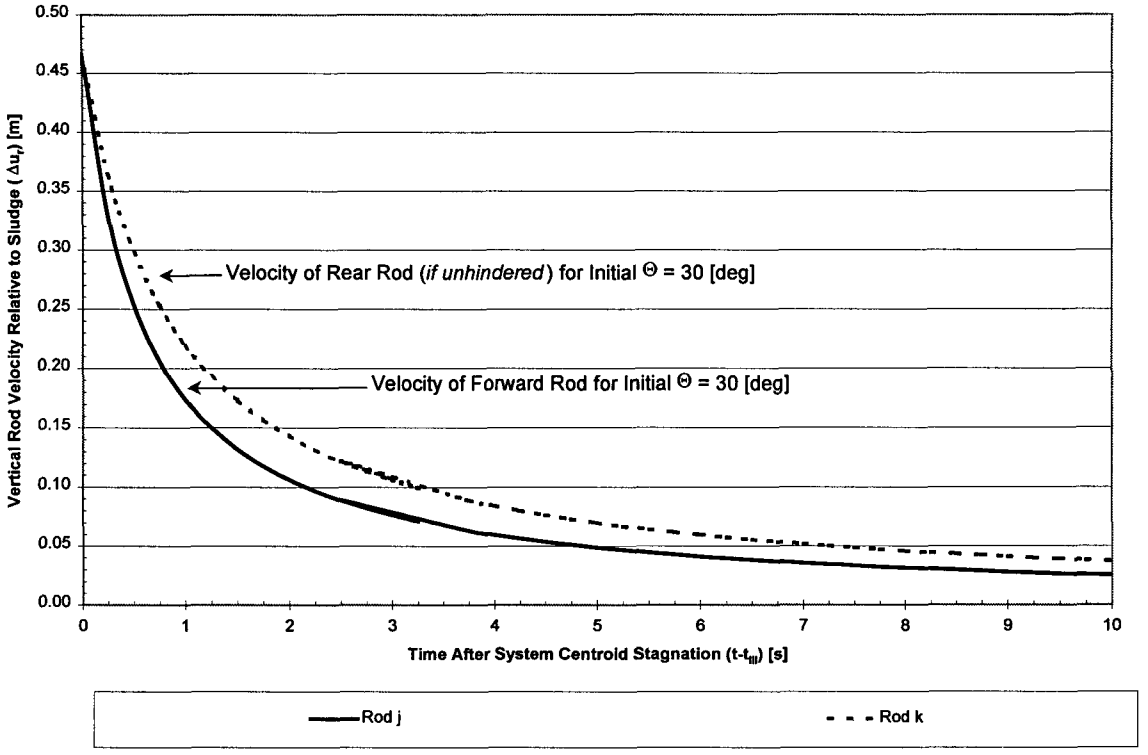

NOTE: Fluid Drag on the aft rod is lower than on the forward rod because of flow-shadowing. The rear rod can therefore maintain larger velocities than the forward rod until physical contact of the rods occurs at p(t)/Dr,o = 1.

Figure I-3. Fluid Drag on the Aft Rod is Lower Than on the Forward Rod

Figure I-3 provides velocity histograms for the forward and aft rods with the Chen and Wu (2000) drag model at initial $\Theta = 30°$. Velocity profiles for the other initial values of Θ are not shown, but are qualitatively similar. The range of Reynolds numbers corresponding to the velocity profiles is $10^3 < Re_D < 2.4 \cdot 10^3$, and Equation I-21 is valid throughout most of the simulated transient. The aft rod should experience less fluid drag resistance in all cases due to the separation of the impinging flow stream from the surface of the forward rod and the alteration of the rod-boundary-pressure field (i.e., flow-shadowing) induced by the presence of the leading rod. Therefore, the rear rod experiences lower deceleration and maintains greater velocity. The influences of the maximum allowable rod displacement within a container or waste package (i.e., $D_{b,i}$), and rod collision from the rear rod impacting the first, are physical constraints that are not directly accounted for in the velocity profiles of Figure I-3. However, the model does indicate the experimentally observed phenomena of incipient collision between the forward and aft bodies (Davis 1992; Feng et al. 1996; Gheissary et al. 1996; and Wu and Manasseh 1998). The relative difference between instantaneous forward and aft rod velocity decreases as a non-linear function of increasing the initial Θ, such that there is no vertical velocity profile distinction when the rods are initially side-by-side ($\Theta = 89°$). The model prediction for the maintenance of a common vertical velocity for particles in the same horizontal plane is a characteristic that is also observed in experiment (Wu and Manasseh 1998, pp. 1351-1352, Figure 8c).

I-4. DISCUSSION

The possibility of SNF rod separation following canister agitation is addressed in two ways. First the modeling results of Section 3 are interpreted. Second, the results of a literature survey of research on particle settling and many-body fluid-dynamical interactions are provided.

I-4.1 Numerical Modeling

The results of the numerical modeling in Section 3 indicate that no increase of the relative vertical separation between SNF fuel rods occurs after a large magnitude disturbance. This observation is strictly valid for equi-dimensional rods of identical mass, and effective rod material densities much greater than sludge (i.e., buoyancy has been neglected). Furthermore, the results indicate that the rods should dynamically reconsolidate for a range of initial rod pitches because the aft rod can generally maintain a greater relative velocity than the forward rod because of flow-shadowing effects. Therefore, the possibility for a transient in-package criticality from SNF rod separation following a mechanical disturbance currently has no physical basis in the modeling results. The conclusion is valid despite the conservatism of assumptions for the large magnitude of the initial disturbance, for the low sludge viscosity (a viscosity identical to water gives the highest Re_D estimates), and for the high sensitivity of the drag coefficient to rod orientation angle (i.e., angular dependence appropriate to low $p/D_{r,o}$).

The difficulty in obtaining rod separation is a characteristic of the influence of flow-shadowing effects at low to moderate low $p/D_{r,o}$. Partial diversion of the fluid flow by the forward rod around the trailing rod reduces the comparative drag resistance for the rod in the wake. This effect is captured in the Θ dependence of the drag coefficient (Equation I-19) because the drag coefficient on the forward rod ($CD(\Theta,Re_D)$) is consistently greater than or equal to the corresponding value for rod in the wake ($CD(\pi-\Theta,Re_D)$) for any discrete orientation Θ in the interval (0°, 90°). As demonstrated in the hypothetical case (Figure I-2 at $\Theta = 30°$), the only possibility for dynamic rod separation is in the non-physical situation that the shadowing effect is reversed.

I-4.2 Authoritative Work

The following brief literature review is performed in support of the analysis done for the possibility of transient separation of a pile of particles that has undergone a seismic disruption. Emphasis is placed on literature that investigates the settling of interacting pair of particles.

Publication: "Unexpected Phenomena Observed in Particle Setting in Non-Newtonian Media." *Journal of Non-Newtonian Fluid Mechanics (67)* (Gheissary et al. 1996, pp.1-18).

This paper investigates the settling of two or more particles in viscous Newtonian and non-Newtonian liquids. Major findings related to current topic are: In the Newtonian fluid the well known 'drafting, kissing, and tumbling motion' phenomena are observed. A trailing sphere is caught in the wake of a leading sphere and speeds up until they touch. By this time the vertical

dumbbell is unstable and they turn around and tumble. This finding supports the analysis given in the previous sections.

The same experiment in a non-Newtonian fluid (Boger fluid), gave an opposite result. The authors state that since the only difference between the Newtonian and the Boger fluid is the added elasticity, only the elastic forces could drive the spheres apart.

Publication: "Dynamic Simulation of Sedimentation of Solid Particles in an Oldroyd-B Fluid." *Journal of Non-Newtonian Fluid Mechanics (63)* (Feng et al. 1996, pp. 63-88).

This paper presents a two dimensional numerical study of the viscoelastic effects on the sedimentation of particles in the presence of solid walls or another particle. Major findings are: Two particles settling one on top of the other attract and form a doublet if their initial separation is not too large. Two particles settling side by side approach each other and the doublet rotates till the line of centers is aligned with the direction of sedimentation. This paper supports the conclusions derived from the current analysis.

Publication: "Dynamics of Dual-Particles Settling Under Gravity." *International Journal of Multiphase Flow (24)* (Wu and Manasseh 1998, pp. 1343-1358).

The motion of two spherical particles settling in close proximity under gravity in Newtonian fluids is investigated for a range of Reynolds numbers. The major finding is that the particles undergo horizontal repulsion for $Re_D > 0.1$ and that the separation distance between particles is dependent on the magnitude of the Reynolds number. However, this separation occurs only in the horizontal plane, and only after the aft particle accelerates into and contacts the lead particle, rotating the pair into a horizontal orientation (Wu and Manasseh 1998, pg. 1351). Flow channeling between the contacting particles thereafter pries the bodies apart horizontally. The data presented by Wu and Manasseh (1998, pg. 1347, Figure 2a) indicate that the channeling results in final horizontal separations greater than 3 particle diameters for $Re_D > 1$. Horizontal separations are not the primary concern for SNF rod separation, because the canister curvature limits the lateral spacing both at the base and top of the vertical trajectory.

An additional complication for the horizontal separation finding is the experimental method, which employs a sloping plate mounted on top of a tank. The spheres are introduced to the test section by rolling them over the plates, thus providing rotational momentum to each of the 2 particles. The initial 'rotational' effect may increase the dynamic separation, as the rotation generates a transverse 'lift' in conjunction with the translational cross flow over the spheres during settling. Thus, the findings in this particular paper may not precisely apply to the current analysis, but are supportive of the conclusion that vertical rod separations do not occur.

These experiments and studies confirm the general finding that identical particles that sediment in a viscoelastic fluid do not separate during sedimentation under the influence of gravity unless the fluid is highly non-Newtonian and elastic effects dominate. Elasticity is not anticipated to characterize any sludge filling the SNF disposal canister or waste package.

I-5. CONCLUSIONS

A significant increase of the center-to-center spacing among a consolidated pile of SNF rods is impossible to achieve by agitation of a flooded and partially degraded SNF canister or waste package. This conclusion is supported by physical models and experimental evidence. Numerical assessments for an initiating disturbance of magnitude and duration much greater than any credible earthquake demonstrate that no relative vertical separations among the SNF fuel rods can occur over the range of all possible initial rod orientations. The curvature of the barrier wall limits the horizontal separation of the rods. The conclusion that rod separation will not occur is also supported in authoritative literature on experiments for particle settling and fluid dynamical interactions for many-body systems. The only possible caveats to this conclusion involve considerations for non-negligible mechanical elasticity of the sludge and for axial counter-rotations of neighboring SNF rods. Complications from sludge elasticity or rod rotations are not applicable to the repository situations.

ATTACHMENT II

ANALYTIC PROBABILITY CALCULATIONS FOR THE LOSS OF PACKAGED GADOLINIUM NEUTRON ABSORBER: WORKSHEETS "RIGOR-InnerConvolutions" and "RIGOR-OuterConvolution" IN MICROSOFT EXCEL 97 SR-2 SPREADSHEET GdLossProbRIGOR2.xls

Attachment II

ANALYTIC PROBABILITY CALCULATIONS FOR THE LOSS OF PACKAGED GADOLINIUM NEUTRON ABSORBER :WORKSHEETS "RIGOR-InnerConvolutions" and "RIGOR-OuterConvolution" IN MICROSOFT EXCEL 97 SR-2 SPREADSHEET GdLossProbRIGOR.xls

	A	B	C	D	E	F
1	NUMERICAL TREATMENT FOR CONVOLVED P(BCG) - OuterConvolution by finite difference method					
2	Pdrip	Ppond				Alpha-breach
3	6.94E-02	0.4675				2.347
4						Beta-breach
5	tscope [years]				P0-b(tscope)	4.81
6	60,001				V	Theta-breach
7	1.89337E-19	<- P0-g(tscope)	1.98296E-10	<- P0-c(tscope)	2.20763E-07	10.82
8			SAMPLE COLUMN C = IF(($A$6-$B10)>=0,($A$6-$B10),0)	SAMPLE COLUMN D = IF($B10>0,($A10/$B10),0)	SAMPLE COLUMN E = IF((LN($B10+1E-99)-$F$7)>=0,(LN($B10)-$F$7),0)	SAMPLE COLUMN F = IF(AND($C10>0,$E10>0),WEIBULL($E10,$F$5,$F$3,FALSE),0). This is a differential form of Eq. 4 in AMR.
9	d(tb) [years]	tb [years]	tscope-tb [years]	Jacobian*d(tb)=d(tb)/tb	(ln(tb)-Theta-breach)	pdf in ln(tb) for Pbreach
10	0	0	6.00010E+04	0.00000E+00	0	0.00000E+00
11	1000	1000	5.90010E+04	1.00000E+00	0	0.00000E+00
12	1000	2000	5.80010E+04	5.00000E-01	0	0.00000E+00
13	1000	3000	5.70010E+04	3.33333E-01	0	0.00000E+00
14	1000	4000	5.60010E+04	2.50000E-01	0	0.00000E+00
15	1000	5000	5.50010E+04	2.00000E-01	0	0.00000E+00
16	1000	6000	5.40010E+04	1.66667E-01	0	0.00000E+00
17	1000	7000	5.30010E+04	1.42857E-01	0	0.00000E+00
18	1000	8000	5.20010E+04	1.25000E-01	0	0.00000E+00
19	1000	9000	5.10010E+04	1.11111E-01	0	0.00000E+00
20	1000	10000	5.00010E+04	1.00000E-01	0	0.00000E+00
21	2.00E+03	12000	4.80010E+04	1.66667E-01	0	0.00000E+00
22	2.00E+03	14000	4.60010E+04	1.42857E-01	0	0.00000E+00
23	2.00E+03	16000	4.40010E+04	1.25000E-01	0	0.00000E+00
24	2.00E+03	18000	4.20010E+04	1.11111E-01	0	0.00000E+00
25	2.00E+03	20000	4.00010E+04	1.00000E-01	0	0.00000E+00
26	2.00E+03	22000	3.80010E+04	9.09091E-02	0	0.00000E+00
27	2.00E+03	24000	3.60010E+04	8.33333E-02	0	0.00000E+00
28	2.00E+03	26000	3.40010E+04	7.69231E-02	0	0.00000E+00
29	2.00E+03	28000	3.20010E+04	7.14286E-02	0	0.00000E+00
30	2.00E+03	30000	3.00010E+04	6.66667E-02	0	0.00000E+00
31	2.00E+03	32000	2.80010E+04	6.25000E-02	0	0.00000E+00
32	2.00E+03	34000	2.60010E+04	5.88235E-02	0	0.00000E+00
33	2.00E+03	36000	2.40010E+04	5.55556E-02	0	0.00000E+00
34	2.00E+03	38000	2.20010E+04	5.26316E-02	0	0.00000E+00
35	2.00E+03	40000	2.00010E+04	5.00000E-02	0	0.00000E+00
36	2.00E+03	42000	1.80010E+04	4.76190E-02	0	0.00000E+00
37	2.00E+03	44000	1.60010E+04	4.54545E-02	0	0.00000E+00
38	2.00E+03	46000	1.40010E+04	4.34783E-02	0	0.00000E+00
39	2.00E+03	48000	1.20010E+04	4.16667E-02	0	0.00000E+00
40	2.00E+03	50000	1.00010E+04	4.00000E-02	0	0.00000E+00
41	2.00E+03	52000	8.00100E+03	3.84615E-02	0.038998998	3.40323E-07
42	2.00E+03	54000	6.00100E+03	3.70370E-02	0.076739326	4.48638E-06
43	2.00E+03	56000	4.00100E+03	3.57143E-02	0.11310697	1.96685E-05
44	2.00E+03	58000	2.00100E+03	3.44828E-02	0.14819829	5.50667E-05
45	2.00E+03	60000	1.00000E+00	3.33333E-02	0.182099841	1.20713E-04
46	2.00E+03	62000	0.00000E+00	3.22581E-02	0.214889664	0.00000E+00
47	2.00E+03	64000	0.00000E+00	3.12500E-02	0.246638362	0.00000E+00
48	2.00E+03	66000	0.00000E+00	3.03030E-02	0.277410021	0.00000E+00
49	2.00E+03	68000	0.00000E+00	2.94118E-02	0.307262984	0.00000E+00
50	2.00E+03	70000	0.00000E+00	2.85714E-02	0.336250521	0.00000E+00
51	2.00E+03	72000	0.00000E+00	2.77778E-02	0.364421398	0.00000E+00
52	2.00E+03	74000	0.00000E+00	2.70270E-02	0.391820372	0.00000E+00
53	2.00E+03	76000	0.00000E+00	2.63158E-02	0.418488619	0.00000E+00
54	2.00E+03	78000	0.00000E+00	2.56410E-02	0.444464106	0.00000E+00
55	2.00E+03	80000	0.00000E+00	2.50000E-02	0.469781914	0.00000E+00
56	2.00E+03	82000	0.00000E+00	2.43902E-02	0.494474526	0.00000E+00
57	2.00E+03	84000	0.00000E+00	2.38095E-02	0.518572078	0.00000E+00
58	2.00E+03	86000	0.00000E+00	2.32558E-02	0.542102575	0.00000E+00

	G	H	I	J
1				
2				
3				
4				
5				
6				
7				
8	SAMPLE COLUMN G = IF(434+MATCH($C10,'RIGOR-InnerConvolutions'!$A$435:$A$505)>=435,434+MATCH($C10,'RIGOR-InnerConvolutions'!$A$435:$A$505), 435). This column facilitates interpolation of data from sheet RIGOR-InnerConvolutions.	SAMPLE COLUMN H = IF($G10<505,$G10+1,505). This column facilitates interpolation of data from sheet RIGOR-InnerConvolutions.	SAMPLE COLUMN I = ADDRESS($G10,2,1,TRUE,"RIGOR-InnerConvolutions"). This column facilitates interpolation of data from sheet RIGOR-InnerConvolutions.	SAMPLE COLUMN J = CELL("contents",INDIRECT($I10)). This column facilitates interpolation of data from sheet RIGOR-InnerConvolutions.
9	Upper Row Index from Pb-g Table	Lower Row Index from Pb-g Table	ADDRESS for Upper Index Pb-g Bound	Upper Indexed Pb-g Bound
10	4.67000E+02	4.68000E+02	'RIGOR-InnerConvolutions'!$B$467	6.61023E-07
11	4.66000E+02	4.67000E+02	'RIGOR-InnerConvolutions'!$B$466	5.09177E-07
12	4.66000E+02	4.67000E+02	'RIGOR-InnerConvolutions'!$B$466	5.09177E-07
13	4.66000E+02	4.67000E+02	'RIGOR-InnerConvolutions'!$B$466	5.09177E-07
14	4.66000E+02	4.67000E+02	'RIGOR-InnerConvolutions'!$B$466	5.09177E-07
15	4.66000E+02	4.67000E+02	'RIGOR-InnerConvolutions'!$B$466	5.09177E-07
16	4.65000E+02	4.66000E+02	'RIGOR-InnerConvolutions'!$B$465	3.78596E-07
17	4.65000E+02	4.66000E+02	'RIGOR-InnerConvolutions'!$B$465	3.78596E-07
18	4.65000E+02	4.66000E+02	'RIGOR-InnerConvolutions'!$B$465	3.78596E-07
19	4.65000E+02	4.66000E+02	'RIGOR-InnerConvolutions'!$B$465	3.78596E-07
20	4.65000E+02	4.66000E+02	'RIGOR-InnerConvolutions'!$B$465	3.78596E-07
21	4.64000E+02	4.65000E+02	'RIGOR-InnerConvolutions'!$B$464	2.69387E-07
22	4.64000E+02	4.65000E+02	'RIGOR-InnerConvolutions'!$B$464	2.69387E-07
23	4.63000E+02	4.64000E+02	'RIGOR-InnerConvolutions'!$B$463	1.81238E-07
24	4.63000E+02	4.64000E+02	'RIGOR-InnerConvolutions'!$B$463	1.81238E-07
25	4.63000E+02	4.64000E+02	'RIGOR-InnerConvolutions'!$B$463	1.81238E-07
26	4.62000E+02	4.63000E+02	'RIGOR-InnerConvolutions'!$B$462	1.13335E-07
27	4.62000E+02	4.63000E+02	'RIGOR-InnerConvolutions'!$B$462	1.13335E-07
28	4.61000E+02	4.62000E+02	'RIGOR-InnerConvolutions'!$B$461	6.41775E-08
29	4.61000E+02	4.62000E+02	'RIGOR-InnerConvolutions'!$B$461	6.41775E-08
30	4.61000E+02	4.62000E+02	'RIGOR-InnerConvolutions'!$B$461	6.41775E-08
31	4.60000E+02	4.61000E+02	'RIGOR-InnerConvolutions'!$B$460	3.15466E-08
32	4.60000E+02	4.61000E+02	'RIGOR-InnerConvolutions'!$B$460	3.15466E-08
33	4.59000E+02	4.60000E+02	'RIGOR-InnerConvolutions'!$B$459	1.24945E-08
34	4.59000E+02	4.60000E+02	'RIGOR-InnerConvolutions'!$B$459	1.24945E-08
35	4.59000E+02	4.60000E+02	'RIGOR-InnerConvolutions'!$B$459	1.24945E-08
36	4.58000E+02	4.59000E+02	'RIGOR-InnerConvolutions'!$B$458	6.95690E-09
37	4.57000E+02	4.58000E+02	'RIGOR-InnerConvolutions'!$B$457	3.42980E-09
38	4.56000E+02	4.57000E+02	'RIGOR-InnerConvolutions'!$B$456	1.41630E-09
39	4.55000E+02	4.56000E+02	'RIGOR-InnerConvolutions'!$B$455	4.42212E-10
40	4.55000E+02	4.56000E+02	'RIGOR-InnerConvolutions'!$B$455	4.42212E-10
41	4.53000E+02	4.54000E+02	'RIGOR-InnerConvolutions'!$B$453	1.25125E-10
42	4.51000E+02	4.52000E+02	'RIGOR-InnerConvolutions'!$B$451	2.06988E-11
43	4.49000E+02	4.50000E+02	'RIGOR-InnerConvolutions'!$B$449	1.06239E-12
44	4.46000E+02	4.47000E+02	'RIGOR-InnerConvolutions'!$B$446	7.64850E-16
45	4.36000E+02	4.37000E+02	'RIGOR-InnerConvolutions'!$B$436	0.00000E+00
46	4.35000E+02	4.36000E+02	'RIGOR-InnerConvolutions'!$B$435	0.00000E+00
47	4.35000E+02	4.36000E+02	'RIGOR-InnerConvolutions'!$B$435	0.00000E+00
48	4.35000E+02	4.36000E+02	'RIGOR-InnerConvolutions'!$B$435	0.00000E+00
49	4.35000E+02	4.36000E+02	'RIGOR-InnerConvolutions'!$B$435	0.00000E+00
50	4.35000E+02	4.36000E+02	'RIGOR-InnerConvolutions'!$B$435	0.00000E+00
51	4.35000E+02	4.36000E+02	'RIGOR-InnerConvolutions'!$B$435	0.00000E+00
52	4.35000E+02	4.36000E+02	'RIGOR-InnerConvolutions'!$B$435	0.00000E+00
53	4.35000E+02	4.36000E+02	'RIGOR-InnerConvolutions'!$B$435	0.00000E+00
54	4.35000E+02	4.36000E+02	'RIGOR-InnerConvolutions'!$B$435	0.00000E+00
55	4.35000E+02	4.36000E+02	'RIGOR-InnerConvolutions'!$B$435	0.00000E+00
56	4.35000E+02	4.36000E+02	'RIGOR-InnerConvolutions'!$B$435	0.00000E+00
57	4.35000E+02	4.36000E+02	'RIGOR-InnerConvolutions'!$B$435	0.00000E+00
58	4.35000E+02	4.36000E+02	'RIGOR-InnerConvolutions'!$B$435	0.00000E+00

	K	L	M	N
1				
2				
3				
4				
5				
6				
7				
8	SAMPLE COLUMN K = ADDRESS($H10,2,1,TRUE,"RIGOR-InnerConvolutions"). This column facilitates interpolation of data from sheet RIGOR-InnerConvolutions.	SAMPLE COLUMN L = CELL("contents",INDIRECT ($K10)). This column facilitates interpolation of data from sheet RIGOR-InnerConvolutions.	SAMPLE COLUMN M =ADDRESS($G10,1,1,TRUE,"RIGOR-InnerConvolutions"). This column facilitates interpolation of data from sheet RIGOR-InnerConvolutions.	SAMPLE COLUMN N = CELL("contents",INDIRECT ($M10)). This column facilitates interpolation of data from sheet RIGOR-InnerConvolutions.
9	ADDRESS for Lower Index Pb-g Bound	Lower Indexed Pb-g Bound	ADDRESS for Upper Index (t-tb) Bound	Upper Indexed (t-tb) Bound
10	'RIGOR-InnerConvolutions'!$B$468	8.33686E-07	'RIGOR-InnerConvolutions'!$A$467	6.00000E+04
11	'RIGOR-InnerConvolutions'!$B$467	6.61023E-07	'RIGOR-InnerConvolutions'!$A$466	5.50000E+04
12	'RIGOR-InnerConvolutions'!$B$467	6.61023E-07	'RIGOR-InnerConvolutions'!$A$466	5.50000E+04
13	'RIGOR-InnerConvolutions'!$B$467	6.61023E-07	'RIGOR-InnerConvolutions'!$A$466	5.50000E+04
14	'RIGOR-InnerConvolutions'!$B$467	6.61023E-07	'RIGOR-InnerConvolutions'!$A$466	5.50000E+04
15	'RIGOR-InnerConvolutions'!$B$467	6.61023E-07	'RIGOR-InnerConvolutions'!$A$466	5.50000E+04
16	'RIGOR-InnerConvolutions'!$B$466	5.09177E-07	'RIGOR-InnerConvolutions'!$A$465	5.00000E+04
17	'RIGOR-InnerConvolutions'!$B$466	5.09177E-07	'RIGOR-InnerConvolutions'!$A$465	5.00000E+04
18	'RIGOR-InnerConvolutions'!$B$466	5.09177E-07	'RIGOR-InnerConvolutions'!$A$465	5.00000E+04
19	'RIGOR-InnerConvolutions'!$B$466	5.09177E-07	'RIGOR-InnerConvolutions'!$A$465	5.00000E+04
20	'RIGOR-InnerConvolutions'!$B$466	5.09177E-07	'RIGOR-InnerConvolutions'!$A$465	5.00000E+04
21	'RIGOR-InnerConvolutions'!$B$465	3.78596E-07	'RIGOR-InnerConvolutions'!$A$464	4.50000E+04
22	'RIGOR-InnerConvolutions'!$B$465	3.78596E-07	'RIGOR-InnerConvolutions'!$A$464	4.50000E+04
23	'RIGOR-InnerConvolutions'!$B$464	2.69387E-07	'RIGOR-InnerConvolutions'!$A$463	4.00000E+04
24	'RIGOR-InnerConvolutions'!$B$464	2.69387E-07	'RIGOR-InnerConvolutions'!$A$463	4.00000E+04
25	'RIGOR-InnerConvolutions'!$B$464	2.69387E-07	'RIGOR-InnerConvolutions'!$A$463	4.00000E+04
26	'RIGOR-InnerConvolutions'!$B$463	1.81238E-07	'RIGOR-InnerConvolutions'!$A$462	3.50000E+04
27	'RIGOR-InnerConvolutions'!$B$463	1.81238E-07	'RIGOR-InnerConvolutions'!$A$462	3.50000E+04
28	'RIGOR-InnerConvolutions'!$B$462	1.13335E-07	'RIGOR-InnerConvolutions'!$A$461	3.00000E+04
29	'RIGOR-InnerConvolutions'!$B$462	1.13335E-07	'RIGOR-InnerConvolutions'!$A$461	3.00000E+04
30	'RIGOR-InnerConvolutions'!$B$462	1.13335E-07	'RIGOR-InnerConvolutions'!$A$461	3.00000E+04
31	'RIGOR-InnerConvolutions'!$B$461	6.41775E-08	'RIGOR-InnerConvolutions'!$A$460	2.50000E+04
32	'RIGOR-InnerConvolutions'!$B$461	6.41775E-08	'RIGOR-InnerConvolutions'!$A$460	2.50000E+04
33	'RIGOR-InnerConvolutions'!$B$460	3.15466E-08	'RIGOR-InnerConvolutions'!$A$459	2.00000E+04
34	'RIGOR-InnerConvolutions'!$B$460	3.15466E-08	'RIGOR-InnerConvolutions'!$A$459	2.00000E+04
35	'RIGOR-InnerConvolutions'!$B$460	3.15466E-08	'RIGOR-InnerConvolutions'!$A$459	2.00000E+04
36	'RIGOR-InnerConvolutions'!$B$459	1.24945E-08	'RIGOR-InnerConvolutions'!$A$458	1.75000E+04
37	'RIGOR-InnerConvolutions'!$B$458	6.95690E-09	'RIGOR-InnerConvolutions'!$A$457	1.50000E+04
38	'RIGOR-InnerConvolutions'!$B$457	3.42980E-09	'RIGOR-InnerConvolutions'!$A$456	1.25000E+04
39	'RIGOR-InnerConvolutions'!$B$456	1.41630E-09	'RIGOR-InnerConvolutions'!$A$455	1.00000E+04
40	'RIGOR-InnerConvolutions'!$B$456	1.41630E-09	'RIGOR-InnerConvolutions'!$A$455	1.00000E+04
41	'RIGOR-InnerConvolutions'!$B$454	2.46831E-10	'RIGOR-InnerConvolutions'!$A$453	8.00000E+03
42	'RIGOR-InnerConvolutions'!$B$452	5.57338E-11	'RIGOR-InnerConvolutions'!$A$451	6.00000E+03
43	'RIGOR-InnerConvolutions'!$B$450	5.85723E-12	'RIGOR-InnerConvolutions'!$A$449	4.00000E+03
44	'RIGOR-InnerConvolutions'!$B$447	1.25645E-14	'RIGOR-InnerConvolutions'!$A$446	2.00000E+03
45	'RIGOR-InnerConvolutions'!$B$437	0.00000E+00	'RIGOR-InnerConvolutions'!$A$436	1.00000E+00
46	'RIGOR-InnerConvolutions'!$B$436	0.00000E+00	'RIGOR-InnerConvolutions'!$A$435	0.00000E+00
47	'RIGOR-InnerConvolutions'!$B$436	0.00000E+00	'RIGOR-InnerConvolutions'!$A$435	0.00000E+00
48	'RIGOR-InnerConvolutions'!$B$436	0.00000E+00	'RIGOR-InnerConvolutions'!$A$435	0.00000E+00
49	'RIGOR-InnerConvolutions'!$B$436	0.00000E+00	'RIGOR-InnerConvolutions'!$A$435	0.00000E+00
50	'RIGOR-InnerConvolutions'!$B$436	0.00000E+00	'RIGOR-InnerConvolutions'!$A$435	0.00000E+00
51	'RIGOR-InnerConvolutions'!$B$436	0.00000E+00	'RIGOR-InnerConvolutions'!$A$435	0.00000E+00
52	'RIGOR-InnerConvolutions'!$B$436	0.00000E+00	'RIGOR-InnerConvolutions'!$A$435	0.00000E+00
53	'RIGOR-InnerConvolutions'!$B$436	0.00000E+00	'RIGOR-InnerConvolutions'!$A$435	0.00000E+00
54	'RIGOR-InnerConvolutions'!$B$436	0.00000E+00	'RIGOR-InnerConvolutions'!$A$435	0.00000E+00
55	'RIGOR-InnerConvolutions'!$B$436	0.00000E+00	'RIGOR-InnerConvolutions'!$A$435	0.00000E+00
56	'RIGOR-InnerConvolutions'!$B$436	0.00000E+00	'RIGOR-InnerConvolutions'!$A$435	0.00000E+00
57	'RIGOR-InnerConvolutions'!$B$436	0.00000E+00	'RIGOR-InnerConvolutions'!$A$435	0.00000E+00
58	'RIGOR-InnerConvolutions'!$B$436	0.00000E+00	'RIGOR-InnerConvolutions'!$A$435	0.00000E+00

	O	P	Q	R	S	T
1						
2						
3						
4						
5						
6						
7						
8	SAMPLE COLUMN O = ADDRESS($H10,1,1,TRUE,"RIGOR-InnerConvolutions"). This column facilitates interpolation of data from sheet RIGOR-InnerConvolutions.	SAMPLE COLUMN P = CELL("contents",INDIRECT($O10)). This column facilitates interpolation of data from sheet RIGOR-InnerConvolutions.	SAMPLE COLUMN Q = IF(($P10-$N10)>0,($C10-$N10)/($P10-$N10),0). This column facilitates interpolation of data from sheet RIGOR-InnerConvolutions.	SAMPLE COLUMN R = $J10+$Q10*($L10-$J10). This column is the interpolated data from sheet RIGOR-InnerConvolutions	SAMPLE COLUMN S = IF($B10<=$A$6,$A$3*$B$3*$D10*$F10*$R10,0)	T10 FORMULA = SUM($S10:$S133). This is the value returned by solution of Eq. 1 in AMR.
9	ADDRESS for Lower Index (t-tb) Bound	Lower Indexed (t-tb) Bound	Interpolation Factor	Interpolated Pb-g(t-tb)	delta(P0-g(t))	P0-g(t)
10	'RIGOR-InnerConvolutions'!$A$468	6.50000E+04	2.00000E-04	6.61058E-07	0.00000E+00	1.89337E-19
11	'RIGOR-InnerConvolutions'!$A$467	6.00000E+04	8.00200E-01	6.30684E-07	0.00000E+00	
12	'RIGOR-InnerConvolutions'!$A$467	6.00000E+04	6.00200E-01	6.00315E-07	0.00000E+00	
13	'RIGOR-InnerConvolutions'!$A$467	6.00000E+04	4.00200E-01	5.69946E-07	0.00000E+00	
14	'RIGOR-InnerConvolutions'!$A$467	6.00000E+04	2.00200E-01	5.39576E-07	0.00000E+00	
15	'RIGOR-InnerConvolutions'!$A$467	6.00000E+04	2.00000E-04	5.09207E-07	0.00000E+00	
16	'RIGOR-InnerConvolutions'!$A$466	5.50000E+04	8.00200E-01	4.83087E-07	0.00000E+00	
17	'RIGOR-InnerConvolutions'!$A$466	5.50000E+04	6.00200E-01	4.56971E-07	0.00000E+00	
18	'RIGOR-InnerConvolutions'!$A$466	5.50000E+04	4.00200E-01	4.30854E-07	0.00000E+00	
19	'RIGOR-InnerConvolutions'!$A$466	5.50000E+04	2.00200E-01	4.04738E-07	0.00000E+00	
20	'RIGOR-InnerConvolutions'!$A$466	5.50000E+04	2.00000E-04	3.78622E-07	0.00000E+00	
21	'RIGOR-InnerConvolutions'!$A$465	5.00000E+04	6.00200E-01	3.34934E-07	0.00000E+00	
22	'RIGOR-InnerConvolutions'!$A$465	5.00000E+04	2.00200E-01	2.91250E-07	0.00000E+00	
23	'RIGOR-InnerConvolutions'!$A$464	4.50000E+04	8.00200E-01	2.51775E-07	0.00000E+00	
24	'RIGOR-InnerConvolutions'!$A$464	4.50000E+04	4.00200E-01	2.16515E-07	0.00000E+00	
25	'RIGOR-InnerConvolutions'!$A$464	4.50000E+04	2.00000E-04	1.81256E-07	0.00000E+00	
26	'RIGOR-InnerConvolutions'!$A$463	4.00000E+04	6.00200E-01	1.54091E-07	0.00000E+00	
27	'RIGOR-InnerConvolutions'!$A$463	4.00000E+04	2.00200E-01	1.26930E-07	0.00000E+00	
28	'RIGOR-InnerConvolutions'!$A$462	3.50000E+04	8.00200E-01	1.03514E-07	0.00000E+00	
29	'RIGOR-InnerConvolutions'!$A$462	3.50000E+04	4.00200E-01	8.38505E-08	0.00000E+00	
30	'RIGOR-InnerConvolutions'!$A$462	3.50000E+04	2.00000E-04	6.41873E-08	0.00000E+00	
31	'RIGOR-InnerConvolutions'!$A$461	3.00000E+04	6.00200E-01	5.11316E-08	0.00000E+00	
32	'RIGOR-InnerConvolutions'!$A$461	3.00000E+04	2.00200E-01	3.80793E-08	0.00000E+00	
33	'RIGOR-InnerConvolutions'!$A$460	2.50000E+04	8.00200E-01	2.77400E-08	0.00000E+00	
34	'RIGOR-InnerConvolutions'!$A$460	2.50000E+04	4.00200E-01	2.01192E-08	0.00000E+00	
35	'RIGOR-InnerConvolutions'!$A$460	2.50000E+04	2.00000E-04	1.24983E-08	0.00000E+00	
36	'RIGOR-InnerConvolutions'!$A$459	2.00000E+04	2.00400E-01	8.06664E-09	0.00000E+00	
37	'RIGOR-InnerConvolutions'!$A$458	1.75000E+04	4.00400E-01	4.84205E-09	0.00000E+00	
38	'RIGOR-InnerConvolutions'!$A$457	1.50000E+04	6.00400E-01	2.62520E-09	0.00000E+00	
39	'RIGOR-InnerConvolutions'!$A$456	1.25000E+04	8.00400E-01	1.22187E-09	0.00000E+00	
40	'RIGOR-InnerConvolutions'!$A$456	1.25000E+04	4.00000E-04	4.42601E-10	0.00000E+00	
41	'RIGOR-InnerConvolutions'!$A$454	9.00000E+03	1.00000E-03	1.25247E-10	5.31893E-20	
42	'RIGOR-InnerConvolutions'!$A$452	7.00000E+03	1.00000E-03	2.07339E-11	1.11777E-19	
43	'RIGOR-InnerConvolutions'!$A$450	5.00000E+03	1.00000E-03	1.06719E-12	2.43218E-20	
44	'RIGOR-InnerConvolutions'!$A$447	2.50000E+03	2.00000E-03	7.88449E-16	4.85742E-23	
45	'RIGOR-InnerConvolutions'!$A$437	5.00000E+00	0.00000E+00	0.00000E+00	0.00000E+00	
46	'RIGOR-InnerConvolutions'!$A$436	1.00000E+00	0.00000E+00	0.00000E+00	0.00000E+00	
47	'RIGOR-InnerConvolutions'!$A$436	1.00000E+00	0.00000E+00	0.00000E+00	0.00000E+00	
48	'RIGOR-InnerConvolutions'!$A$436	1.00000E+00	0.00000E+00	0.00000E+00	0.00000E+00	
49	'RIGOR-InnerConvolutions'!$A$436	1.00000E+00	0.00000E+00	0.00000E+00	0.00000E+00	
50	'RIGOR-InnerConvolutions'!$A$436	1.00000E+00	0.00000E+00	0.00000E+00	0.00000E+00	
51	'RIGOR-InnerConvolutions'!$A$436	1.00000E+00	0.00000E+00	0.00000E+00	0.00000E+00	
52	'RIGOR-InnerConvolutions'!$A$436	1.00000E+00	0.00000E+00	0.00000E+00	0.00000E+00	
53	'RIGOR-InnerConvolutions'!$A$436	1.00000E+00	0.00000E+00	0.00000E+00	0.00000E+00	
54	'RIGOR-InnerConvolutions'!$A$436	1.00000E+00	0.00000E+00	0.00000E+00	0.00000E+00	
55	'RIGOR-InnerConvolutions'!$A$436	1.00000E+00	0.00000E+00	0.00000E+00	0.00000E+00	
56	'RIGOR-InnerConvolutions'!$A$436	1.00000E+00	0.00000E+00	0.00000E+00	0.00000E+00	
57	'RIGOR-InnerConvolutions'!$A$436	1.00000E+00	0.00000E+00	0.00000E+00	0.00000E+00	
58	'RIGOR-InnerConvolutions'!$A$436	1.00000E+00	0.00000E+00	0.00000E+00	0.00000E+00	

	U	V	W	X	Y
1					
2					
3					
4					
5					
6					
7					
8		SAMPLE COLUMN V = ADDRESS($G10,3,1,TRUE,"RIGOR-InnerConvolutions"). This column facilitates interpolation of data from sheet RIGOR-InnerConvolutions.	SAMPLE COLUMN W = CELL("contents",INDIRECT ($V10)). This column facilitates interpolation of data from sheet RIGOR-InnerConvolutions.	SAMPLE COLUMN X = ADDRESS($H10,3,1,TRUE,"RIGOR-InnerConvolutions"). This column facilitates interpolation of data from sheet RIGOR-InnerConvolutions.	SAMPLE COLUMN Y = CELL("contents",INDIRECT ($X10)). This column facilitates interpolation of data from sheet RIGOR-InnerConvolutions.
9		ADDRESS for Upper Index Pb-c Bound	Upper Indexed Pb-c Bound	ADDRESS for Lower Index Pb-c Bound	Lower Indexed Pb-c Bound
10		'RIGOR-InnerConvolutions'!$C$467	2.14991E-01	'RIGOR-InnerConvolutions'!$C$468	2.25171E-01
11		'RIGOR-InnerConvolutions'!$C$466	2.03733E-01	'RIGOR-InnerConvolutions'!$C$467	2.14991E-01
12		'RIGOR-InnerConvolutions'!$C$466	2.03733E-01	'RIGOR-InnerConvolutions'!$C$467	2.14991E-01
13		'RIGOR-InnerConvolutions'!$C$466	2.03733E-01	'RIGOR-InnerConvolutions'!$C$467	2.14991E-01
14		'RIGOR-InnerConvolutions'!$C$466	2.03733E-01	'RIGOR-InnerConvolutions'!$C$467	2.14991E-01
15		'RIGOR-InnerConvolutions'!$C$466	2.03733E-01	'RIGOR-InnerConvolutions'!$C$467	2.14991E-01
16		'RIGOR-InnerConvolutions'!$C$465	1.91259E-01	'RIGOR-InnerConvolutions'!$C$466	2.03733E-01
17		'RIGOR-InnerConvolutions'!$C$465	1.91259E-01	'RIGOR-InnerConvolutions'!$C$466	2.03733E-01
18		'RIGOR-InnerConvolutions'!$C$465	1.91259E-01	'RIGOR-InnerConvolutions'!$C$466	2.03733E-01
19		'RIGOR-InnerConvolutions'!$C$465	1.91259E-01	'RIGOR-InnerConvolutions'!$C$466	2.03733E-01
20		'RIGOR-InnerConvolutions'!$C$465	1.91259E-01	'RIGOR-InnerConvolutions'!$C$466	2.03733E-01
21		'RIGOR-InnerConvolutions'!$C$464	1.77407E-01	'RIGOR-InnerConvolutions'!$C$465	1.91259E-01
22		'RIGOR-InnerConvolutions'!$C$464	1.77407E-01	'RIGOR-InnerConvolutions'!$C$465	1.91259E-01
23		'RIGOR-InnerConvolutions'!$C$463	1.63608E-01	'RIGOR-InnerConvolutions'!$C$464	1.77407E-01
24		'RIGOR-InnerConvolutions'!$C$463	1.63608E-01	'RIGOR-InnerConvolutions'!$C$464	1.77407E-01
25		'RIGOR-InnerConvolutions'!$C$463	1.63608E-01	'RIGOR-InnerConvolutions'!$C$464	1.77407E-01
26		'RIGOR-InnerConvolutions'!$C$462	1.46538E-01	'RIGOR-InnerConvolutions'!$C$463	1.63608E-01
27		'RIGOR-InnerConvolutions'!$C$462	1.46538E-01	'RIGOR-InnerConvolutions'!$C$463	1.63608E-01
28		'RIGOR-InnerConvolutions'!$C$461	1.27512E-01	'RIGOR-InnerConvolutions'!$C$462	1.46538E-01
29		'RIGOR-InnerConvolutions'!$C$461	1.27512E-01	'RIGOR-InnerConvolutions'!$C$462	1.46538E-01
30		'RIGOR-InnerConvolutions'!$C$461	1.27512E-01	'RIGOR-InnerConvolutions'!$C$462	1.46538E-01
31		'RIGOR-InnerConvolutions'!$C$460	1.06332E-01	'RIGOR-InnerConvolutions'!$C$461	1.27512E-01
32		'RIGOR-InnerConvolutions'!$C$460	1.06332E-01	'RIGOR-InnerConvolutions'!$C$461	1.27512E-01
33		'RIGOR-InnerConvolutions'!$C$459	8.28706E-02	'RIGOR-InnerConvolutions'!$C$460	1.06332E-01
34		'RIGOR-InnerConvolutions'!$C$459	8.28706E-02	'RIGOR-InnerConvolutions'!$C$460	1.06332E-01
35		'RIGOR-InnerConvolutions'!$C$459	8.28706E-02	'RIGOR-InnerConvolutions'!$C$460	1.06332E-01
36		'RIGOR-InnerConvolutions'!$C$458	7.03039E-02	'RIGOR-InnerConvolutions'!$C$459	8.28706E-02
37		'RIGOR-InnerConvolutions'!$C$457	5.72535E-02	'RIGOR-InnerConvolutions'!$C$458	7.03039E-02
38		'RIGOR-InnerConvolutions'!$C$456	4.38611E-02	'RIGOR-InnerConvolutions'!$C$457	5.72535E-02
39		'RIGOR-InnerConvolutions'!$C$455	3.25504E-02	'RIGOR-InnerConvolutions'!$C$456	4.38611E-02
40		'RIGOR-InnerConvolutions'!$C$455	3.25504E-02	'RIGOR-InnerConvolutions'!$C$456	4.38611E-02
41		'RIGOR-InnerConvolutions'!$C$453	2.20699E-02	'RIGOR-InnerConvolutions'!$C$454	2.72495E-02
42		'RIGOR-InnerConvolutions'!$C$451	1.23958E-02	'RIGOR-InnerConvolutions'!$C$452	1.70852E-02
43		'RIGOR-InnerConvolutions'!$C$449	4.51425E-03	'RIGOR-InnerConvolutions'!$C$450	8.14081E-03
44		'RIGOR-InnerConvolutions'!$C$446	3.09015E-04	'RIGOR-InnerConvolutions'!$C$447	8.53700E-04
45		'RIGOR-InnerConvolutions'!$C$436	0.00000E+00	'RIGOR-InnerConvolutions'!$C$437	0.00000E+00
46		'RIGOR-InnerConvolutions'!$C$435	0.00000E+00	'RIGOR-InnerConvolutions'!$C$436	0.00000E+00
47		'RIGOR-InnerConvolutions'!$C$435	0.00000E+00	'RIGOR-InnerConvolutions'!$C$436	0.00000E+00
48		'RIGOR-InnerConvolutions'!$C$435	0.00000E+00	'RIGOR-InnerConvolutions'!$C$436	0.00000E+00
49		'RIGOR-InnerConvolutions'!$C$435	0.00000E+00	'RIGOR-InnerConvolutions'!$C$436	0.00000E+00
50		'RIGOR-InnerConvolutions'!$C$435	0.00000E+00	'RIGOR-InnerConvolutions'!$C$436	0.00000E+00
51		'RIGOR-InnerConvolutions'!$C$435	0.00000E+00	'RIGOR-InnerConvolutions'!$C$436	0.00000E+00
52		'RIGOR-InnerConvolutions'!$C$435	0.00000E+00	'RIGOR-InnerConvolutions'!$C$436	0.00000E+00
53		'RIGOR-InnerConvolutions'!$C$435	0.00000E+00	'RIGOR-InnerConvolutions'!$C$436	0.00000E+00
54		'RIGOR-InnerConvolutions'!$C$435	0.00000E+00	'RIGOR-InnerConvolutions'!$C$436	0.00000E+00
55		'RIGOR-InnerConvolutions'!$C$435	0.00000E+00	'RIGOR-InnerConvolutions'!$C$436	0.00000E+00
56		'RIGOR-InnerConvolutions'!$C$435	0.00000E+00	'RIGOR-InnerConvolutions'!$C$436	0.00000E+00
57		'RIGOR-InnerConvolutions'!$C$435	0.00000E+00	'RIGOR-InnerConvolutions'!$C$436	0.00000E+00
58		'RIGOR-InnerConvolutions'!$C$435	0.00000E+00	'RIGOR-InnerConvolutions'!$C$436	0.00000E+00

	Z	AA	AB	AC	AD	AE
1						
2						
3						
4						
5						
6						
7						
8	SAMPLE COLUMN Z = $W10+$Q10*($Y10-$W10). This is the interpolated data from sheet RIGOR-InnerConvolutions.	SAMPLE COLUMN AA = IF($B10<=$A$6,$A$3*$B$3*$D10*$F10*$Z10,0)	AB10 FORMULA = SUM($AA10:$AA133). This is a result for the integrations in Eq. 1 in AMR, except Pc-g is assigned constant value 1.		SAMPLE COLUMN AD = =IF($B10<=$A$6,$A$3*$B$3*$D10*$F10,0)	AE10 FORMULA = SUM($AD10:$AD133). This is a result for the integrations in Eq. 1 in AMR, except Pb-c and Pc-g are assigned the constant values 1.
9	Interpolated Pb-c(t-tb)	delta(P0-c(t))	P0-c(t)		delta(P0-b(t))	P0-b(t)
10	2.14993E-01	0.00000E+00	1.98296E-10		0.00000E+00	2.20763E-07
11	2.12742E-01	0.00000E+00			0.00000E+00	
12	2.10490E-01	0.00000E+00			0.00000E+00	
13	2.08239E-01	0.00000E+00			0.00000E+00	
14	2.05987E-01	0.00000E+00			0.00000E+00	
15	2.03736E-01	0.00000E+00			0.00000E+00	
16	2.01241E-01	0.00000E+00			0.00000E+00	
17	1.98746E-01	0.00000E+00			0.00000E+00	
18	1.96251E-01	0.00000E+00			0.00000E+00	
19	1.93756E-01	0.00000E+00			0.00000E+00	
20	1.91261E-01	0.00000E+00			0.00000E+00	
21	1.85721E-01	0.00000E+00			0.00000E+00	
22	1.80180E-01	0.00000E+00			0.00000E+00	
23	1.74650E-01	0.00000E+00			0.00000E+00	
24	1.69130E-01	0.00000E+00			0.00000E+00	
25	1.63611E-01	0.00000E+00			0.00000E+00	
26	1.56783E-01	0.00000E+00			0.00000E+00	
27	1.49955E-01	0.00000E+00			0.00000E+00	
28	1.42736E-01	0.00000E+00			0.00000E+00	
29	1.35126E-01	0.00000E+00			0.00000E+00	
30	1.27516E-01	0.00000E+00			0.00000E+00	
31	1.19044E-01	0.00000E+00			0.00000E+00	
32	1.10572E-01	0.00000E+00			0.00000E+00	
33	1.01644E-01	0.00000E+00			0.00000E+00	
34	9.22597E-02	0.00000E+00			0.00000E+00	
35	8.28753E-02	0.00000E+00			0.00000E+00	
36	7.28223E-02	0.00000E+00			0.00000E+00	
37	6.24789E-02	0.00000E+00			0.00000E+00	
38	5.19019E-02	0.00000E+00			0.00000E+00	
39	4.16035E-02	0.00000E+00			0.00000E+00	
40	3.25549E-02	0.00000E+00			0.00000E+00	
41	2.20751E-02	9.37478E-12			4.24677E-10	
42	1.24005E-02	6.68518E-11			5.39104E-09	
43	4.51788E-03	1.02965E-10			2.27905E-08	
44	3.10104E-04	1.91047E-11			6.16073E-08	
45	0.00000E+00	0.00000E+00			1.30549E-07	
46	0.00000E+00	0.00000E+00			0.00000E+00	
47	0.00000E+00	0.00000E+00			0.00000E+00	
48	0.00000E+00	0.00000E+00			0.00000E+00	
49	0.00000E+00	0.00000E+00			0.00000E+00	
50	0.00000E+00	0.00000E+00			0.00000E+00	
51	0.00000E+00	0.00000E+00			0.00000E+00	
52	0.00000E+00	0.00000E+00			0.00000E+00	
53	0.00000E+00	0.00000E+00			0.00000E+00	
54	0.00000E+00	0.00000E+00			0.00000E+00	
55	0.00000E+00	0.00000E+00			0.00000E+00	
56	0.00000E+00	0.00000E+00			0.00000E+00	
57	0.00000E+00	0.00000E+00			0.00000E+00	
58	0.00000E+00	0.00000E+00			0.00000E+00	

	A	B	C	D	E	F
59	2.00E+03	88000	0.00000E+00	2.27273E-02	0.565092093	0.00000E+00
60	2.00E+03	90000	0.00000E+00	2.22222E-02	0.587564949	0.00000E+00
61	2.00E+03	92000	0.00000E+00	2.17391E-02	0.609543856	0.00000E+00
62	2.00E+03	94000	0.00000E+00	2.12766E-02	0.631050061	0.00000E+00
63	2.00E+03	96000	0.00000E+00	2.08333E-02	0.65210347	0.00000E+00
64	2.00E+03	98000	0.00000E+00	2.04082E-02	0.672722758	0.00000E+00
65	2.00E+03	100000	0.00000E+00	2.00000E-02	0.692925465	0.00000E+00
66	1.00E+04	110000	0.00000E+00	9.09091E-02	0.788235645	0.00000E+00
67	1.00E+04	120000	0.00000E+00	8.33333E-02	0.875247022	0.00000E+00
68	1.00E+04	130000	0.00000E+00	7.69231E-02	0.955289729	0.00000E+00
69	1.00E+04	140000	0.00000E+00	7.14286E-02	1.029397702	0.00000E+00
70	1.00E+04	150000	0.00000E+00	6.66667E-02	1.098390573	0.00000E+00
71	1.00E+04	160000	0.00000E+00	6.25000E-02	1.162929094	0.00000E+00
72	1.00E+04	170000	0.00000E+00	5.88235E-02	1.223553716	0.00000E+00
73	1.00E+04	180000	0.00000E+00	5.55556E-02	1.28071213	0.00000E+00
74	1.00E+04	190000	0.00000E+00	5.26316E-02	1.334779351	0.00000E+00
75	1.00E+04	200000	0.00000E+00	5.00000E-02	1.386072646	0.00000E+00
76	1.00E+04	210000	0.00000E+00	4.76190E-02	1.43486281	0.00000E+00
77	1.00E+04	220000	0.00000E+00	4.54545E-02	1.481382825	0.00000E+00
78	1.00E+04	230000	0.00000E+00	4.34783E-02	1.525834588	0.00000E+00
79	1.00E+04	240000	0.00000E+00	4.16667E-02	1.568394202	0.00000E+00
80	1.00E+04	250000	0.00000E+00	4.00000E-02	1.609216197	0.00000E+00
81	1.00E+04	260000	0.00000E+00	3.84615E-02	1.64843691	0.00000E+00
82	1.00E+04	270000	0.00000E+00	3.70370E-02	1.686177238	0.00000E+00
83	1.00E+04	280000	0.00000E+00	3.57143E-02	1.722544882	0.00000E+00
84	1.00E+04	290000	0.00000E+00	3.44828E-02	1.757636202	0.00000E+00
85	1.00E+04	300000	0.00000E+00	3.33333E-02	1.791537754	0.00000E+00
86	1.00E+04	310000	0.00000E+00	3.22581E-02	1.824327576	0.00000E+00
87	1.00E+04	320000	0.00000E+00	3.12500E-02	1.856076275	0.00000E+00
88	1.00E+04	330000	0.00000E+00	3.03030E-02	1.886847933	0.00000E+00
89	1.00E+04	340000	0.00000E+00	2.94118E-02	1.916700897	0.00000E+00
90	1.00E+04	350000	0.00000E+00	2.85714E-02	1.945688433	0.00000E+00
91	1.00E+04	360000	0.00000E+00	2.77778E-02	1.97385931	0.00000E+00
92	1.00E+04	370000	0.00000E+00	2.70270E-02	2.001258285	0.00000E+00
93	1.00E+04	380000	0.00000E+00	2.63158E-02	2.027926532	0.00000E+00
94	1.00E+04	390000	0.00000E+00	2.56410E-02	2.053902018	0.00000E+00
95	1.00E+04	400000	0.00000E+00	2.50000E-02	2.079219826	0.00000E+00
96	1.00E+04	410000	0.00000E+00	2.43902E-02	2.103912439	0.00000E+00
97	1.00E+04	420000	0.00000E+00	2.38095E-02	2.12800999	0.00000E+00
98	1.00E+04	430000	0.00000E+00	2.32558E-02	2.151540488	0.00000E+00
99	1.00E+04	440000	0.00000E+00	2.27273E-02	2.174530006	0.00000E+00
100	1.00E+04	450000	0.00000E+00	2.22222E-02	2.197002862	0.00000E+00
101	1.00E+04	460000	0.00000E+00	2.17391E-02	2.218981768	0.00000E+00
102	1.00E+04	470000	0.00000E+00	2.12766E-02	2.240487974	0.00000E+00
103	1.00E+04	480000	0.00000E+00	2.08333E-02	2.261541383	0.00000E+00
104	1.00E+04	490000	0.00000E+00	2.04082E-02	2.28216067	0.00000E+00
105	1.00E+04	500000	0.00000E+00	2.00000E-02	2.302363377	0.00000E+00
106	1.00E+04	510000	0.00000E+00	1.96078E-02	2.322166005	0.00000E+00
107	1.00E+04	520000	0.00000E+00	1.92308E-02	2.341584091	0.00000E+00
108	1.00E+04	530000	0.00000E+00	1.88679E-02	2.360632286	0.00000E+00
109	1.00E+04	540000	0.00000E+00	1.85185E-02	2.379324419	0.00000E+00
110	1.00E+04	550000	0.00000E+00	1.81818E-02	2.397673557	0.00000E+00
111	1.00E+04	560000	0.00000E+00	1.78571E-02	2.415692063	0.00000E+00
112	1.00E+04	570000	0.00000E+00	1.75439E-02	2.43339164	0.00000E+00
113	1.00E+04	580000	0.00000E+00	1.72414E-02	2.450783383	0.00000E+00
114	1.00E+04	590000	0.00000E+00	1.69492E-02	2.467877816	0.00000E+00
115	1.00E+04	600000	0.00000E+00	1.66667E-02	2.484684934	0.00000E+00
116	2.00E+04	620000	0.00000E+00	3.22581E-02	2.517474757	0.00000E+00

	G	H	I	J
59	4.35000E+02	4.36000E+02	'RIGOR-InnerConvolutions'!$B$435	0.00000E+00
60	4.35000E+02	4.36000E+02	'RIGOR-InnerConvolutions'!$B$435	0.00000E+00
61	4.35000E+02	4.36000E+02	'RIGOR-InnerConvolutions'!$B$435	0.00000E+00
62	4.35000E+02	4.36000E+02	'RIGOR-InnerConvolutions'!$B$435	0.00000E+00
63	4.35000E+02	4.36000E+02	'RIGOR-InnerConvolutions'!$B$435	0.00000E+00
64	4.35000E+02	4.36000E+02	'RIGOR-InnerConvolutions'!$B$435	0.00000E+00
65	4.35000E+02	4.36000E+02	'RIGOR-InnerConvolutions'!$B$435	0.00000E+00
66	4.35000E+02	4.36000E+02	'RIGOR-InnerConvolutions'!$B$435	0.00000E+00
67	4.35000E+02	4.36000E+02	'RIGOR-InnerConvolutions'!$B$435	0.00000E+00
68	4.35000E+02	4.36000E+02	'RIGOR-InnerConvolutions'!$B$435	0.00000E+00
69	4.35000E+02	4.36000E+02	'RIGOR-InnerConvolutions'!$B$435	0.00000E+00
70	4.35000E+02	4.36000E+02	'RIGOR-InnerConvolutions'!$B$435	0.00000E+00
71	4.35000E+02	4.36000E+02	'RIGOR-InnerConvolutions'!$B$435	0.00000E+00
72	4.35000E+02	4.36000E+02	'RIGOR-InnerConvolutions'!$B$435	0.00000E+00
73	4.35000E+02	4.36000E+02	'RIGOR-InnerConvolutions'!$B$435	0.00000E+00
74	4.35000E+02	4.36000E+02	'RIGOR-InnerConvolutions'!$B$435	0.00000E+00
75	4.35000E+02	4.36000E+02	'RIGOR-InnerConvolutions'!$B$435	0.00000E+00
76	4.35000E+02	4.36000E+02	'RIGOR-InnerConvolutions'!$B$435	0.00000E+00
77	4.35000E+02	4.36000E+02	'RIGOR-InnerConvolutions'!$B$435	0.00000E+00
78	4.35000E+02	4.36000E+02	'RIGOR-InnerConvolutions'!$B$435	0.00000E+00
79	4.35000E+02	4.36000E+02	'RIGOR-InnerConvolutions'!$B$435	0.00000E+00
80	4.35000E+02	4.36000E+02	'RIGOR-InnerConvolutions'!$B$435	0.00000E+00
81	4.35000E+02	4.36000E+02	'RIGOR-InnerConvolutions'!$B$435	0.00000E+00
82	4.35000E+02	4.36000E+02	'RIGOR-InnerConvolutions'!$B$435	0.00000E+00
83	4.35000E+02	4.36000E+02	'RIGOR-InnerConvolutions'!$B$435	0.00000E+00
84	4.35000E+02	4.36000E+02	'RIGOR-InnerConvolutions'!$B$435	0.00000E+00
85	4.35000E+02	4.36000E+02	'RIGOR-InnerConvolutions'!$B$435	0.00000E+00
86	4.35000E+02	4.36000E+02	'RIGOR-InnerConvolutions'!$B$435	0.00000E+00
87	4.35000E+02	4.36000E+02	'RIGOR-InnerConvolutions'!$B$435	0.00000E+00
88	4.35000E+02	4.36000E+02	'RIGOR-InnerConvolutions'!$B$435	0.00000E+00
89	4.35000E+02	4.36000E+02	'RIGOR-InnerConvolutions'!$B$435	0.00000E+00
90	4.35000E+02	4.36000E+02	'RIGOR-InnerConvolutions'!$B$435	0.00000E+00
91	4.35000E+02	4.36000E+02	'RIGOR-InnerConvolutions'!$B$435	0.00000E+00
92	4.35000E+02	4.36000E+02	'RIGOR-InnerConvolutions'!$B$435	0.00000E+00
93	4.35000E+02	4.36000E+02	'RIGOR-InnerConvolutions'!$B$435	0.00000E+00
94	4.35000E+02	4.36000E+02	'RIGOR-InnerConvolutions'!$B$435	0.00000E+00
95	4.35000E+02	4.36000E+02	'RIGOR-InnerConvolutions'!$B$435	0.00000E+00
96	4.35000E+02	4.36000E+02	'RIGOR-InnerConvolutions'!$B$435	0.00000E+00
97	4.35000E+02	4.36000E+02	'RIGOR-InnerConvolutions'!$B$435	0.00000E+00
98	4.35000E+02	4.36000E+02	'RIGOR-InnerConvolutions'!$B$435	0.00000E+00
99	4.35000E+02	4.36000E+02	'RIGOR-InnerConvolutions'!$B$435	0.00000E+00
100	4.35000E+02	4.36000E+02	'RIGOR-InnerConvolutions'!$B$435	0.00000E+00
101	4.35000E+02	4.36000E+02	'RIGOR-InnerConvolutions'!$B$435	0.00000E+00
102	4.35000E+02	4.36000E+02	'RIGOR-InnerConvolutions'!$B$435	0.00000E+00
103	4.35000E+02	4.36000E+02	'RIGOR-InnerConvolutions'!$B$435	0.00000E+00
104	4.35000E+02	4.36000E+02	'RIGOR-InnerConvolutions'!$B$435	0.00000E+00
105	4.35000E+02	4.36000E+02	'RIGOR-InnerConvolutions'!$B$435	0.00000E+00
106	4.35000E+02	4.36000E+02	'RIGOR-InnerConvolutions'!$B$435	0.00000E+00
107	4.35000E+02	4.36000E+02	'RIGOR-InnerConvolutions'!$B$435	0.00000E+00
108	4.35000E+02	4.36000E+02	'RIGOR-InnerConvolutions'!$B$435	0.00000E+00
109	4.35000E+02	4.36000E+02	'RIGOR-InnerConvolutions'!$B$435	0.00000E+00
110	4.35000E+02	4.36000E+02	'RIGOR-InnerConvolutions'!$B$435	0.00000E+00
111	4.35000E+02	4.36000E+02	'RIGOR-InnerConvolutions'!$B$435	0.00000E+00
112	4.35000E+02	4.36000E+02	'RIGOR-InnerConvolutions'!$B$435	0.00000E+00
113	4.35000E+02	4.36000E+02	'RIGOR-InnerConvolutions'!$B$435	0.00000E+00
114	4.35000E+02	4.36000E+02	'RIGOR-InnerConvolutions'!$B$435	0.00000E+00
115	4.35000E+02	4.36000E+02	'RIGOR-InnerConvolutions'!$B$435	0.00000E+00
116	4.35000E+02	4.36000E+02	'RIGOR-InnerConvolutions'!$B$435	0.00000E+00

	K	L	M	N
59	'RIGOR-InnerConvolutions'!$B$436	0.00000E+00	'RIGOR-InnerConvolutions'!$A$435	0.00000E+00
60	'RIGOR-InnerConvolutions'!$B$436	0.00000E+00	'RIGOR-InnerConvolutions'!$A$435	0.00000E+00
61	'RIGOR-InnerConvolutions'!$B$436	0.00000E+00	'RIGOR-InnerConvolutions'!$A$435	0.00000E+00
62	'RIGOR-InnerConvolutions'!$B$436	0.00000E+00	'RIGOR-InnerConvolutions'!$A$435	0.00000E+00
63	'RIGOR-InnerConvolutions'!$B$436	0.00000E+00	'RIGOR-InnerConvolutions'!$A$435	0.00000E+00
64	'RIGOR-InnerConvolutions'!$B$436	0.00000E+00	'RIGOR-InnerConvolutions'!$A$435	0.00000E+00
65	'RIGOR-InnerConvolutions'!$B$436	0.00000E+00	'RIGOR-InnerConvolutions'!$A$435	0.00000E+00
66	'RIGOR-InnerConvolutions'!$B$436	0.00000E+00	'RIGOR-InnerConvolutions'!$A$435	0.00000E+00
67	'RIGOR-InnerConvolutions'!$B$436	0.00000E+00	'RIGOR-InnerConvolutions'!$A$435	0.00000E+00
68	'RIGOR-InnerConvolutions'!$B$436	0.00000E+00	'RIGOR-InnerConvolutions'!$A$435	0.00000E+00
69	'RIGOR-InnerConvolutions'!$B$436	0.00000E+00	'RIGOR-InnerConvolutions'!$A$435	0.00000E+00
70	'RIGOR-InnerConvolutions'!$B$436	0.00000E+00	'RIGOR-InnerConvolutions'!$A$435	0.00000E+00
71	'RIGOR-InnerConvolutions'!$B$436	0.00000E+00	'RIGOR-InnerConvolutions'!$A$435	0.00000E+00
72	'RIGOR-InnerConvolutions'!$B$436	0.00000E+00	'RIGOR-InnerConvolutions'!$A$435	0.00000E+00
73	'RIGOR-InnerConvolutions'!$B$436	0.00000E+00	'RIGOR-InnerConvolutions'!$A$435	0.00000E+00
74	'RIGOR-InnerConvolutions'!$B$436	0.00000E+00	'RIGOR-InnerConvolutions'!$A$435	0.00000E+00
75	'RIGOR-InnerConvolutions'!$B$436	0.00000E+00	'RIGOR-InnerConvolutions'!$A$435	0.00000E+00
76	'RIGOR-InnerConvolutions'!$B$436	0.00000E+00	'RIGOR-InnerConvolutions'!$A$435	0.00000E+00
77	'RIGOR-InnerConvolutions'!$B$436	0.00000E+00	'RIGOR-InnerConvolutions'!$A$435	0.00000E+00
78	'RIGOR-InnerConvolutions'!$B$436	0.00000E+00	'RIGOR-InnerConvolutions'!$A$435	0.00000E+00
79	'RIGOR-InnerConvolutions'!$B$436	0.00000E+00	'RIGOR-InnerConvolutions'!$A$435	0.00000E+00
80	'RIGOR-InnerConvolutions'!$B$436	0.00000E+00	'RIGOR-InnerConvolutions'!$A$435	0.00000E+00
81	'RIGOR-InnerConvolutions'!$B$436	0.00000E+00	'RIGOR-InnerConvolutions'!$A$435	0.00000E+00
82	'RIGOR-InnerConvolutions'!$B$436	0.00000E+00	'RIGOR-InnerConvolutions'!$A$435	0.00000E+00
83	'RIGOR-InnerConvolutions'!$B$436	0.00000E+00	'RIGOR-InnerConvolutions'!$A$435	0.00000E+00
84	'RIGOR-InnerConvolutions'!$B$436	0.00000E+00	'RIGOR-InnerConvolutions'!$A$435	0.00000E+00
85	'RIGOR-InnerConvolutions'!$B$436	0.00000E+00	'RIGOR-InnerConvolutions'!$A$435	0.00000E+00
86	'RIGOR-InnerConvolutions'!$B$436	0.00000E+00	'RIGOR-InnerConvolutions'!$A$435	0.00000E+00
87	'RIGOR-InnerConvolutions'!$B$436	0.00000E+00	'RIGOR-InnerConvolutions'!$A$435	0.00000E+00
88	'RIGOR-InnerConvolutions'!$B$436	0.00000E+00	'RIGOR-InnerConvolutions'!$A$435	0.00000E+00
89	'RIGOR-InnerConvolutions'!$B$436	0.00000E+00	'RIGOR-InnerConvolutions'!$A$435	0.00000E+00
90	'RIGOR-InnerConvolutions'!$B$436	0.00000E+00	'RIGOR-InnerConvolutions'!$A$435	0.00000E+00
91	'RIGOR-InnerConvolutions'!$B$436	0.00000E+00	'RIGOR-InnerConvolutions'!$A$435	0.00000E+00
92	'RIGOR-InnerConvolutions'!$B$436	0.00000E+00	'RIGOR-InnerConvolutions'!$A$435	0.00000E+00
93	'RIGOR-InnerConvolutions'!$B$436	0.00000E+00	'RIGOR-InnerConvolutions'!$A$435	0.00000E+00
94	'RIGOR-InnerConvolutions'!$B$436	0.00000E+00	'RIGOR-InnerConvolutions'!$A$435	0.00000E+00
95	'RIGOR-InnerConvolutions'!$B$436	0.00000E+00	'RIGOR-InnerConvolutions'!$A$435	0.00000E+00
96	'RIGOR-InnerConvolutions'!$B$436	0.00000E+00	'RIGOR-InnerConvolutions'!$A$435	0.00000E+00
97	'RIGOR-InnerConvolutions'!$B$436	0.00000E+00	'RIGOR-InnerConvolutions'!$A$435	0.00000E+00
98	'RIGOR-InnerConvolutions'!$B$436	0.00000E+00	'RIGOR-InnerConvolutions'!$A$435	0.00000E+00
99	'RIGOR-InnerConvolutions'!$B$436	0.00000E+00	'RIGOR-InnerConvolutions'!$A$435	0.00000E+00
100	'RIGOR-InnerConvolutions'!$B$436	0.00000E+00	'RIGOR-InnerConvolutions'!$A$435	0.00000E+00
101	'RIGOR-InnerConvolutions'!$B$436	0.00000E+00	'RIGOR-InnerConvolutions'!$A$435	0.00000E+00
102	'RIGOR-InnerConvolutions'!$B$436	0.00000E+00	'RIGOR-InnerConvolutions'!$A$435	0.00000E+00
103	'RIGOR-InnerConvolutions'!$B$436	0.00000E+00	'RIGOR-InnerConvolutions'!$A$435	0.00000E+00
104	'RIGOR-InnerConvolutions'!$B$436	0.00000E+00	'RIGOR-InnerConvolutions'!$A$435	0.00000E+00
105	'RIGOR-InnerConvolutions'!$B$436	0.00000E+00	'RIGOR-InnerConvolutions'!$A$435	0.00000E+00
106	'RIGOR-InnerConvolutions'!$B$436	0.00000E+00	'RIGOR-InnerConvolutions'!$A$435	0.00000E+00
107	'RIGOR-InnerConvolutions'!$B$436	0.00000E+00	'RIGOR-InnerConvolutions'!$A$435	0.00000E+00
108	'RIGOR-InnerConvolutions'!$B$436	0.00000E+00	'RIGOR-InnerConvolutions'!$A$435	0.00000E+00
109	'RIGOR-InnerConvolutions'!$B$436	0.00000E+00	'RIGOR-InnerConvolutions'!$A$435	0.00000E+00
110	'RIGOR-InnerConvolutions'!$B$436	0.00000E+00	'RIGOR-InnerConvolutions'!$A$435	0.00000E+00
111	'RIGOR-InnerConvolutions'!$B$436	0.00000E+00	'RIGOR-InnerConvolutions'!$A$435	0.00000E+00
112	'RIGOR-InnerConvolutions'!$B$436	0.00000E+00	'RIGOR-InnerConvolutions'!$A$435	0.00000E+00
113	'RIGOR-InnerConvolutions'!$B$436	0.00000E+00	'RIGOR-InnerConvolutions'!$A$435	0.00000E+00
114	'RIGOR-InnerConvolutions'!$B$436	0.00000E+00	'RIGOR-InnerConvolutions'!$A$435	0.00000E+00
115	'RIGOR-InnerConvolutions'!$B$436	0.00000E+00	'RIGOR-InnerConvolutions'!$A$435	0.00000E+00
116	'RIGOR-InnerConvolutions'!$B$436	0.00000E+00	'RIGOR-InnerConvolutions'!$A$435	0.00000E+00

	O	P	Q	R	S	T
59	'RIGOR-InnerConvolutions'!$A$436	1.00000E+00	0.00000E+00	0.00000E+00	0.00000E+00	
60	'RIGOR-InnerConvolutions'!$A$436	1.00000E+00	0.00000E+00	0.00000E+00	0.00000E+00	
61	'RIGOR-InnerConvolutions'!$A$436	1.00000E+00	0.00000E+00	0.00000E+00	0.00000E+00	
62	'RIGOR-InnerConvolutions'!$A$436	1.00000E+00	0.00000E+00	0.00000E+00	0.00000E+00	
63	'RIGOR-InnerConvolutions'!$A$436	1.00000E+00	0.00000E+00	0.00000E+00	0.00000E+00	
64	'RIGOR-InnerConvolutions'!$A$436	1.00000E+00	0.00000E+00	0.00000E+00	0.00000E+00	
65	'RIGOR-InnerConvolutions'!$A$436	1.00000E+00	0.00000E+00	0.00000E+00	0.00000E+00	
66	'RIGOR-InnerConvolutions'!$A$436	1.00000E+00	0.00000E+00	0.00000E+00	0.00000E+00	
67	'RIGOR-InnerConvolutions'!$A$436	1.00000E+00	0.00000E+00	0.00000E+00	0.00000E+00	
68	'RIGOR-InnerConvolutions'!$A$436	1.00000E+00	0.00000E+00	0.00000E+00	0.00000E+00	
69	'RIGOR-InnerConvolutions'!$A$436	1.00000E+00	0.00000E+00	0.00000E+00	0.00000E+00	
70	'RIGOR-InnerConvolutions'!$A$436	1.00000E+00	0.00000E+00	0.00000E+00	0.00000E+00	
71	'RIGOR-InnerConvolutions'!$A$436	1.00000E+00	0.00000E+00	0.00000E+00	0.00000E+00	
72	'RIGOR-InnerConvolutions'!$A$436	1.00000E+00	0.00000E+00	0.00000E+00	0.00000E+00	
73	'RIGOR-InnerConvolutions'!$A$436	1.00000E+00	0.00000E+00	0.00000E+00	0.00000E+00	
74	'RIGOR-InnerConvolutions'!$A$436	1.00000E+00	0.00000E+00	0.00000E+00	0.00000E+00	
75	'RIGOR-InnerConvolutions'!$A$436	1.00000E+00	0.00000E+00	0.00000E+00	0.00000E+00	
76	'RIGOR-InnerConvolutions'!$A$436	1.00000E+00	0.00000E+00	0.00000E+00	0.00000E+00	
77	'RIGOR-InnerConvolutions'!$A$436	1.00000E+00	0.00000E+00	0.00000E+00	0.00000E+00	
78	'RIGOR-InnerConvolutions'!$A$436	1.00000E+00	0.00000E+00	0.00000E+00	0.00000E+00	
79	'RIGOR-InnerConvolutions'!$A$436	1.00000E+00	0.00000E+00	0.00000E+00	0.00000E+00	
80	'RIGOR-InnerConvolutions'!$A$436	1.00000E+00	0.00000E+00	0.00000E+00	0.00000E+00	
81	'RIGOR-InnerConvolutions'!$A$436	1.00000E+00	0.00000E+00	0.00000E+00	0.00000E+00	
82	'RIGOR-InnerConvolutions'!$A$436	1.00000E+00	0.00000E+00	0.00000E+00	0.00000E+00	
83	'RIGOR-InnerConvolutions'!$A$436	1.00000E+00	0.00000E+00	0.00000E+00	0.00000E+00	
84	'RIGOR-InnerConvolutions'!$A$436	1.00000E+00	0.00000E+00	0.00000E+00	0.00000E+00	
85	'RIGOR-InnerConvolutions'!$A$436	1.00000E+00	0.00000E+00	0.00000E+00	0.00000E+00	
86	'RIGOR-InnerConvolutions'!$A$436	1.00000E+00	0.00000E+00	0.00000E+00	0.00000E+00	
87	'RIGOR-InnerConvolutions'!$A$436	1.00000E+00	0.00000E+00	0.00000E+00	0.00000E+00	
88	'RIGOR-InnerConvolutions'!$A$436	1.00000E+00	0.00000E+00	0.00000E+00	0.00000E+00	
89	'RIGOR-InnerConvolutions'!$A$436	1.00000E+00	0.00000E+00	0.00000E+00	0.00000E+00	
90	'RIGOR-InnerConvolutions'!$A$436	1.00000E+00	0.00000E+00	0.00000E+00	0.00000E+00	
91	'RIGOR-InnerConvolutions'!$A$436	1.00000E+00	0.00000E+00	0.00000E+00	0.00000E+00	
92	'RIGOR-InnerConvolutions'!$A$436	1.00000E+00	0.00000E+00	0.00000E+00	0.00000E+00	
93	'RIGOR-InnerConvolutions'!$A$436	1.00000E+00	0.00000E+00	0.00000E+00	0.00000E+00	
94	'RIGOR-InnerConvolutions'!$A$436	1.00000E+00	0.00000E+00	0.00000E+00	0.00000E+00	
95	'RIGOR-InnerConvolutions'!$A$436	1.00000E+00	0.00000E+00	0.00000E+00	0.00000E+00	
96	'RIGOR-InnerConvolutions'!$A$436	1.00000E+00	0.00000E+00	0.00000E+00	0.00000E+00	
97	'RIGOR-InnerConvolutions'!$A$436	1.00000E+00	0.00000E+00	0.00000E+00	0.00000E+00	
98	'RIGOR-InnerConvolutions'!$A$436	1.00000E+00	0.00000E+00	0.00000E+00	0.00000E+00	
99	'RIGOR-InnerConvolutions'!$A$436	1.00000E+00	0.00000E+00	0.00000E+00	0.00000E+00	
100	'RIGOR-InnerConvolutions'!$A$436	1.00000E+00	0.00000E+00	0.00000E+00	0.00000E+00	
101	'RIGOR-InnerConvolutions'!$A$436	1.00000E+00	0.00000E+00	0.00000E+00	0.00000E+00	
102	'RIGOR-InnerConvolutions'!$A$436	1.00000E+00	0.00000E+00	0.00000E+00	0.00000E+00	
103	'RIGOR-InnerConvolutions'!$A$436	1.00000E+00	0.00000E+00	0.00000E+00	0.00000E+00	
104	'RIGOR-InnerConvolutions'!$A$436	1.00000E+00	0.00000E+00	0.00000E+00	0.00000E+00	
105	'RIGOR-InnerConvolutions'!$A$436	1.00000E+00	0.00000E+00	0.00000E+00	0.00000E+00	
106	'RIGOR-InnerConvolutions'!$A$436	1.00000E+00	0.00000E+00	0.00000E+00	0.00000E+00	
107	'RIGOR-InnerConvolutions'!$A$436	1.00000E+00	0.00000E+00	0.00000E+00	0.00000E+00	
108	'RIGOR-InnerConvolutions'!$A$436	1.00000E+00	0.00000E+00	0.00000E+00	0.00000E+00	
109	'RIGOR-InnerConvolutions'!$A$436	1.00000E+00	0.00000E+00	0.00000E+00	0.00000E+00	
110	'RIGOR-InnerConvolutions'!$A$436	1.00000E+00	0.00000E+00	0.00000E+00	0.00000E+00	
111	'RIGOR-InnerConvolutions'!$A$436	1.00000E+00	0.00000E+00	0.00000E+00	0.00000E+00	
112	'RIGOR-InnerConvolutions'!$A$436	1.00000E+00	0.00000E+00	0.00000E+00	0.00000E+00	
113	'RIGOR-InnerConvolutions'!$A$436	1.00000E+00	0.00000E+00	0.00000E+00	0.00000E+00	
114	'RIGOR-InnerConvolutions'!$A$436	1.00000E+00	0.00000E+00	0.00000E+00	0.00000E+00	
115	'RIGOR-InnerConvolutions'!$A$436	1.00000E+00	0.00000E+00	0.00000E+00	0.00000E+00	
116	'RIGOR-InnerConvolutions'!$A$436	1.00000E+00	0.00000E+00	0.00000E+00	0.00000E+00	

	U	V	W	X	Y
59		'RIGOR-InnerConvolutions'!$C$435	0.00000E+00	'RIGOR-InnerConvolutions'!$C$436	0.00000E+00
60		'RIGOR-InnerConvolutions'!$C$435	0.00000E+00	'RIGOR-InnerConvolutions'!$C$436	0.00000E+00
61		'RIGOR-InnerConvolutions'!$C$435	0.00000E+00	'RIGOR-InnerConvolutions'!$C$436	0.00000E+00
62		'RIGOR-InnerConvolutions'!$C$435	0.00000E+00	'RIGOR-InnerConvolutions'!$C$436	0.00000E+00
63		'RIGOR-InnerConvolutions'!$C$435	0.00000E+00	'RIGOR-InnerConvolutions'!$C$436	0.00000E+00
64		'RIGOR-InnerConvolutions'!$C$435	0.00000E+00	'RIGOR-InnerConvolutions'!$C$436	0.00000E+00
65		'RIGOR-InnerConvolutions'!$C$435	0.00000E+00	'RIGOR-InnerConvolutions'!$C$436	0.00000E+00
66		'RIGOR-InnerConvolutions'!$C$435	0.00000E+00	'RIGOR-InnerConvolutions'!$C$436	0.00000E+00
67		'RIGOR-InnerConvolutions'!$C$435	0.00000E+00	'RIGOR-InnerConvolutions'!$C$436	0.00000E+00
68		'RIGOR-InnerConvolutions'!$C$435	0.00000E+00	'RIGOR-InnerConvolutions'!$C$436	0.00000E+00
69		'RIGOR-InnerConvolutions'!$C$435	0.00000E+00	'RIGOR-InnerConvolutions'!$C$436	0.00000E+00
70		'RIGOR-InnerConvolutions'!$C$435	0.00000E+00	'RIGOR-InnerConvolutions'!$C$436	0.00000E+00
71		'RIGOR-InnerConvolutions'!$C$435	0.00000E+00	'RIGOR-InnerConvolutions'!$C$436	0.00000E+00
72		'RIGOR-InnerConvolutions'!$C$435	0.00000E+00	'RIGOR-InnerConvolutions'!$C$436	0.00000E+00
73		'RIGOR-InnerConvolutions'!$C$435	0.00000E+00	'RIGOR-InnerConvolutions'!$C$436	0.00000E+00
74		'RIGOR-InnerConvolutions'!$C$435	0.00000E+00	'RIGOR-InnerConvolutions'!$C$436	0.00000E+00
75		'RIGOR-InnerConvolutions'!$C$435	0.00000E+00	'RIGOR-InnerConvolutions'!$C$436	0.00000E+00
76		'RIGOR-InnerConvolutions'!$C$435	0.00000E+00	'RIGOR-InnerConvolutions'!$C$436	0.00000E+00
77		'RIGOR-InnerConvolutions'!$C$435	0.00000E+00	'RIGOR-InnerConvolutions'!$C$436	0.00000E+00
78		'RIGOR-InnerConvolutions'!$C$435	0.00000E+00	'RIGOR-InnerConvolutions'!$C$436	0.00000E+00
79		'RIGOR-InnerConvolutions'!$C$435	0.00000E+00	'RIGOR-InnerConvolutions'!$C$436	0.00000E+00
80		'RIGOR-InnerConvolutions'!$C$435	0.00000E+00	'RIGOR-InnerConvolutions'!$C$436	0.00000E+00
81		'RIGOR-InnerConvolutions'!$C$435	0.00000E+00	'RIGOR-InnerConvolutions'!$C$436	0.00000E+00
82		'RIGOR-InnerConvolutions'!$C$435	0.00000E+00	'RIGOR-InnerConvolutions'!$C$436	0.00000E+00
83		'RIGOR-InnerConvolutions'!$C$435	0.00000E+00	'RIGOR-InnerConvolutions'!$C$436	0.00000E+00
84		'RIGOR-InnerConvolutions'!$C$435	0.00000E+00	'RIGOR-InnerConvolutions'!$C$436	0.00000E+00
85		'RIGOR-InnerConvolutions'!$C$435	0.00000E+00	'RIGOR-InnerConvolutions'!$C$436	0.00000E+00
86		'RIGOR-InnerConvolutions'!$C$435	0.00000E+00	'RIGOR-InnerConvolutions'!$C$436	0.00000E+00
87		'RIGOR-InnerConvolutions'!$C$435	0.00000E+00	'RIGOR-InnerConvolutions'!$C$436	0.00000E+00
88		'RIGOR-InnerConvolutions'!$C$435	0.00000E+00	'RIGOR-InnerConvolutions'!$C$436	0.00000E+00
89		'RIGOR-InnerConvolutions'!$C$435	0.00000E+00	'RIGOR-InnerConvolutions'!$C$436	0.00000E+00
90		'RIGOR-InnerConvolutions'!$C$435	0.00000E+00	'RIGOR-InnerConvolutions'!$C$436	0.00000E+00
91		'RIGOR-InnerConvolutions'!$C$435	0.00000E+00	'RIGOR-InnerConvolutions'!$C$436	0.00000E+00
92		'RIGOR-InnerConvolutions'!$C$435	0.00000E+00	'RIGOR-InnerConvolutions'!$C$436	0.00000E+00
93		'RIGOR-InnerConvolutions'!$C$435	0.00000E+00	'RIGOR-InnerConvolutions'!$C$436	0.00000E+00
94		'RIGOR-InnerConvolutions'!$C$435	0.00000E+00	'RIGOR-InnerConvolutions'!$C$436	0.00000E+00
95		'RIGOR-InnerConvolutions'!$C$435	0.00000E+00	'RIGOR-InnerConvolutions'!$C$436	0.00000E+00
96		'RIGOR-InnerConvolutions'!$C$435	0.00000E+00	'RIGOR-InnerConvolutions'!$C$436	0.00000E+00
97		'RIGOR-InnerConvolutions'!$C$435	0.00000E+00	'RIGOR-InnerConvolutions'!$C$436	0.00000E+00
98		'RIGOR-InnerConvolutions'!$C$435	0.00000E+00	'RIGOR-InnerConvolutions'!$C$436	0.00000E+00
99		'RIGOR-InnerConvolutions'!$C$435	0.00000E+00	'RIGOR-InnerConvolutions'!$C$436	0.00000E+00
100		'RIGOR-InnerConvolutions'!$C$435	0.00000E+00	'RIGOR-InnerConvolutions'!$C$436	0.00000E+00
101		'RIGOR-InnerConvolutions'!$C$435	0.00000E+00	'RIGOR-InnerConvolutions'!$C$436	0.00000E+00
102		'RIGOR-InnerConvolutions'!$C$435	0.00000E+00	'RIGOR-InnerConvolutions'!$C$436	0.00000E+00
103		'RIGOR-InnerConvolutions'!$C$435	0.00000E+00	'RIGOR-InnerConvolutions'!$C$436	0.00000E+00
104		'RIGOR-InnerConvolutions'!$C$435	0.00000E+00	'RIGOR-InnerConvolutions'!$C$436	0.00000E+00
105		'RIGOR-InnerConvolutions'!$C$435	0.00000E+00	'RIGOR-InnerConvolutions'!$C$436	0.00000E+00
106		'RIGOR-InnerConvolutions'!$C$435	0.00000E+00	'RIGOR-InnerConvolutions'!$C$436	0.00000E+00
107		'RIGOR-InnerConvolutions'!$C$435	0.00000E+00	'RIGOR-InnerConvolutions'!$C$436	0.00000E+00
108		'RIGOR-InnerConvolutions'!$C$435	0.00000E+00	'RIGOR-InnerConvolutions'!$C$436	0.00000E+00
109		'RIGOR-InnerConvolutions'!$C$435	0.00000E+00	'RIGOR-InnerConvolutions'!$C$436	0.00000E+00
110		'RIGOR-InnerConvolutions'!$C$435	0.00000E+00	'RIGOR-InnerConvolutions'!$C$436	0.00000E+00
111		'RIGOR-InnerConvolutions'!$C$435	0.00000E+00	'RIGOR-InnerConvolutions'!$C$436	0.00000E+00
112		'RIGOR-InnerConvolutions'!$C$435	0.00000E+00	'RIGOR-InnerConvolutions'!$C$436	0.00000E+00
113		'RIGOR-InnerConvolutions'!$C$435	0.00000E+00	'RIGOR-InnerConvolutions'!$C$436	0.00000E+00
114		'RIGOR-InnerConvolutions'!$C$435	0.00000E+00	'RIGOR-InnerConvolutions'!$C$436	0.00000E+00
115		'RIGOR-InnerConvolutions'!$C$435	0.00000E+00	'RIGOR-InnerConvolutions'!$C$436	0.00000E+00
116		'RIGOR-InnerConvolutions'!$C$435	0.00000E+00	'RIGOR-InnerConvolutions'!$C$436	0.00000E+00

	Z	AA	AB	AC	AD	AE
59	0.00000E+00	0.00000E+00			0.00000E+00	
60	0.00000E+00	0.00000E+00			0.00000E+00	
61	0.00000E+00	0.00000E+00			0.00000E+00	
62	0.00000E+00	0.00000E+00			0.00000E+00	
63	0.00000E+00	0.00000E+00			0.00000E+00	
64	0.00000E+00	0.00000E+00			0.00000E+00	
65	0.00000E+00	0.00000E+00			0.00000E+00	
66	0.00000E+00	0.00000E+00			0.00000E+00	
67	0.00000E+00	0.00000E+00			0.00000E+00	
68	0.00000E+00	0.00000E+00			0.00000E+00	
69	0.00000E+00	0.00000E+00			0.00000E+00	
70	0.00000E+00	0.00000E+00			0.00000E+00	
71	0.00000E+00	0.00000E+00			0.00000E+00	
72	0.00000E+00	0.00000E+00			0.00000E+00	
73	0.00000E+00	0.00000E+00			0.00000E+00	
74	0.00000E+00	0.00000E+00			0.00000E+00	
75	0.00000E+00	0.00000E+00			0.00000E+00	
76	0.00000E+00	0.00000E+00			0.00000E+00	
77	0.00000E+00	0.00000E+00			0.00000E+00	
78	0.00000E+00	0.00000E+00			0.00000E+00	
79	0.00000E+00	0.00000E+00			0.00000E+00	
80	0.00000E+00	0.00000E+00			0.00000E+00	
81	0.00000E+00	0.00000E+00			0.00000E+00	
82	0.00000E+00	0.00000E+00			0.00000E+00	
83	0.00000E+00	0.00000E+00			0.00000E+00	
84	0.00000E+00	0.00000E+00			0.00000E+00	
85	0.00000E+00	0.00000E+00			0.00000E+00	
86	0.00000E+00	0.00000E+00			0.00000E+00	
87	0.00000E+00	0.00000E+00			0.00000E+00	
88	0.00000E+00	0.00000E+00			0.00000E+00	
89	0.00000E+00	0.00000E+00			0.00000E+00	
90	0.00000E+00	0.00000E+00			0.00000E+00	
91	0.00000E+00	0.00000E+00			0.00000E+00	
92	0.00000E+00	0.00000E+00			0.00000E+00	
93	0.00000E+00	0.00000E+00			0.00000E+00	
94	0.00000E+00	0.00000E+00			0.00000E+00	
95	0.00000E+00	0.00000E+00			0.00000E+00	
96	0.00000E+00	0.00000E+00			0.00000E+00	
97	0.00000E+00	0.00000E+00			0.00000E+00	
98	0.00000E+00	0.00000E+00			0.00000E+00	
99	0.00000E+00	0.00000E+00			0.00000E+00	
100	0.00000E+00	0.00000E+00			0.00000E+00	
101	0.00000E+00	0.00000E+00			0.00000E+00	
102	0.00000E+00	0.00000E+00			0.00000E+00	
103	0.00000E+00	0.00000E+00			0.00000E+00	
104	0.00000E+00	0.00000E+00			0.00000E+00	
105	0.00000E+00	0.00000E+00			0.00000E+00	
106	0.00000E+00	0.00000E+00			0.00000E+00	
107	0.00000E+00	0.00000E+00			0.00000E+00	
108	0.00000E+00	0.00000E+00			0.00000E+00	
109	0.00000E+00	0.00000E+00			0.00000E+00	
110	0.00000E+00	0.00000E+00			0.00000E+00	
111	0.00000E+00	0.00000E+00			0.00000E+00	
112	0.00000E+00	0.00000E+00			0.00000E+00	
113	0.00000E+00	0.00000E+00			0.00000E+00	
114	0.00000E+00	0.00000E+00			0.00000E+00	
115	0.00000E+00	0.00000E+00			0.00000E+00	
116	0.00000E+00	0.00000E+00			0.00000E+00	

	A	B	C	D	E	F
117	2.00E+04	640000	0.00000E+00	3.12500E-02	2.549223455	0.00000E+00
118	2.00E+04	660000	0.00000E+00	3.03030E-02	2.579995114	0.00000E+00
119	2.00E+04	680000	0.00000E+00	2.94118E-02	2.609848077	0.00000E+00
120	2.00E+04	700000	0.00000E+00	2.85714E-02	2.638835614	0.00000E+00
121	2.00E+04	720000	0.00000E+00	2.77778E-02	2.667006491	0.00000E+00
122	2.00E+04	740000	0.00000E+00	2.70270E-02	2.694405465	0.00000E+00
123	2.00E+04	760000	0.00000E+00	2.63158E-02	2.721073712	0.00000E+00
124	2.00E+04	780000	0.00000E+00	2.56410E-02	2.747049199	0.00000E+00
125	2.00E+04	800000	0.00000E+00	2.50000E-02	2.772367007	0.00000E+00
126	2.00E+04	820000	0.00000E+00	2.43902E-02	2.797059619	0.00000E+00
127	2.00E+04	840000	0.00000E+00	2.38095E-02	2.821157171	0.00000E+00
128	2.00E+04	860000	0.00000E+00	2.32558E-02	2.844687668	0.00000E+00
129	2.00E+04	880000	0.00000E+00	2.27273E-02	2.867677186	0.00000E+00
130	2.00E+04	900000	0.00000E+00	2.22222E-02	2.890150042	0.00000E+00
131	2.00E+04	920000	0.00000E+00	2.17391E-02	2.912128949	0.00000E+00
132	2.00E+04	940000	0.00000E+00	2.12766E-02	2.933635154	0.00000E+00
133	2.00E+04	960000	0.00000E+00	2.08333E-02	2.954688563	0.00000E+00
134						
135						
136						
137						
138						
139						
140						
141						
142						
143						
144						
145						
146						
147						
148						
149						
150						
151						
153	DATA IN COLUMNS A,B,C and D; ROWS 158 TO 194 ARE OBTAINED BY VARIATION OF THE VALUE FOR TSCOPE IN CELL A6 TO PRODUCE ASSOCIATED VALUES FOR A7, C7 AND E7 AS TABULATED BELOW IN COLUMNS B,C AND D.					
154						
155						
156						
157	tscope	P0-g(tscope)	P0-c(tscope)	P0-b(tscope)		
158	0	0.00000E+00	0.00000E+00	0.00000E+00		
159	1	0.00000E+00	0.00000E+00	0.00000E+00		
160	5	0.00000E+00	0.00000E+00	0.00000E+00		
161	10	0.00000E+00	0.00000E+00	0.00000E+00		
162	50	0.00000E+00	0.00000E+00	0.00000E+00		
163	100	0.00000E+00	0.00000E+00	0.00000E+00		
164	300	0.00000E+00	0.00000E+00	0.00000E+00		
165	500	0.00000E+00	0.00000E+00	0.00000E+00		
166	1,000	0.00000E+00	0.00000E+00	0.00000E+00		
167	3,000	0.00000E+00	0.00000E+00	0.00000E+00		
168	5,000	0.00000E+00	0.00000E+00	0.00000E+00		
169	10,000	0.00000E+00	0.00000E+00	0.00000E+00		
170	30,000	0.00000E+00	0.00000E+00	0.00000E+00		
171	50,000	0.00000E+00	0.00000E+00	0.00000E+00		
172	60,000	1.88986E-19	1.98119E-10	9.02135E-08		
173	60,001	1.89337E-19	1.98296E-10		<- P0-b = 2.20762790653643E-07	
174	60,970	5.33156E-19	3.92300E-10		<- P0-b = 2.20762790653643E-07	

	G	H	I	J
117	4.35000E+02	4.36000E+02	'RIGOR-InnerConvolutions'!$B$435	0.00000E+00
118	4.35000E+02	4.36000E+02	'RIGOR-InnerConvolutions'!$B$435	0.00000E+00
119	4.35000E+02	4.36000E+02	'RIGOR-InnerConvolutions'!$B$435	0.00000E+00
120	4.35000E+02	4.36000E+02	'RIGOR-InnerConvolutions'!$B$435	0.00000E+00
121	4.35000E+02	4.36000E+02	'RIGOR-InnerConvolutions'!$B$435	0.00000E+00
122	4.35000E+02	4.36000E+02	'RIGOR-InnerConvolutions'!$B$435	0.00000E+00
123	4.35000E+02	4.36000E+02	'RIGOR-InnerConvolutions'!$B$435	0.00000E+00
124	4.35000E+02	4.36000E+02	'RIGOR-InnerConvolutions'!$B$435	0.00000E+00
125	4.35000E+02	4.36000E+02	'RIGOR-InnerConvolutions'!$B$435	0.00000E+00
126	4.35000E+02	4.36000E+02	'RIGOR-InnerConvolutions'!$B$435	0.00000E+00
127	4.35000E+02	4.36000E+02	'RIGOR-InnerConvolutions'!$B$435	0.00000E+00
128	4.35000E+02	4.36000E+02	'RIGOR-InnerConvolutions'!$B$435	0.00000E+00
129	4.35000E+02	4.36000E+02	'RIGOR-InnerConvolutions'!$B$435	0.00000E+00
130	4.35000E+02	4.36000E+02	'RIGOR-InnerConvolutions'!$B$435	0.00000E+00
131	4.35000E+02	4.36000E+02	'RIGOR-InnerConvolutions'!$B$435	0.00000E+00
132	4.35000E+02	4.36000E+02	'RIGOR-InnerConvolutions'!$B$435	0.00000E+00
133	4.35000E+02	4.36000E+02	'RIGOR-InnerConvolutions'!$B$435	0.00000E+00
134				
135				
136				
137				
138				
139				
140				
141				
142				
143				
144				
145				
146				
147				
148				
149				
150				
151				
153				
154				
155				
156				
157				
158				
159				
160				
161				
162				
163				
164				
165				
166				
167				
168				
169				
170				
171				
172				
173				
174				

	K	L	M	N
117	'RIGOR-InnerConvolutions'!$B$436	0.00000E+00	'RIGOR-InnerConvolutions'!$A$435	0.00000E+00
118	'RIGOR-InnerConvolutions'!$B$436	0.00000E+00	'RIGOR-InnerConvolutions'!$A$435	0.00000E+00
119	'RIGOR-InnerConvolutions'!$B$436	0.00000E+00	'RIGOR-InnerConvolutions'!$A$435	0.00000E+00
120	'RIGOR-InnerConvolutions'!$B$436	0.00000E+00	'RIGOR-InnerConvolutions'!$A$435	0.00000E+00
121	'RIGOR-InnerConvolutions'!$B$436	0.00000E+00	'RIGOR-InnerConvolutions'!$A$435	0.00000E+00
122	'RIGOR-InnerConvolutions'!$B$436	0.00000E+00	'RIGOR-InnerConvolutions'!$A$435	0.00000E+00
123	'RIGOR-InnerConvolutions'!$B$436	0.00000E+00	'RIGOR-InnerConvolutions'!$A$435	0.00000E+00
124	'RIGOR-InnerConvolutions'!$B$436	0.00000E+00	'RIGOR-InnerConvolutions'!$A$435	0.00000E+00
125	'RIGOR-InnerConvolutions'!$B$436	0.00000E+00	'RIGOR-InnerConvolutions'!$A$435	0.00000E+00
126	'RIGOR-InnerConvolutions'!$B$436	0.00000E+00	'RIGOR-InnerConvolutions'!$A$435	0.00000E+00
127	'RIGOR-InnerConvolutions'!$B$436	0.00000E+00	'RIGOR-InnerConvolutions'!$A$435	0.00000E+00
128	'RIGOR-InnerConvolutions'!$B$436	0.00000E+00	'RIGOR-InnerConvolutions'!$A$435	0.00000E+00
129	'RIGOR-InnerConvolutions'!$B$436	0.00000E+00	'RIGOR-InnerConvolutions'!$A$435	0.00000E+00
130	'RIGOR-InnerConvolutions'!$B$436	0.00000E+00	'RIGOR-InnerConvolutions'!$A$435	0.00000E+00
131	'RIGOR-InnerConvolutions'!$B$436	0.00000E+00	'RIGOR-InnerConvolutions'!$A$435	0.00000E+00
132	'RIGOR-InnerConvolutions'!$B$436	0.00000E+00	'RIGOR-InnerConvolutions'!$A$435	0.00000E+00
133	'RIGOR-InnerConvolutions'!$B$436	0.00000E+00	'RIGOR-InnerConvolutions'!$A$435	0.00000E+00
134				
135				
136				
137				
138				
139				
140				
141				
142				
143				
144				
145				
146				
147				
148				
149				
150				
151				
153				
154				
155				
156				
157				
158				
159				
160				
161				
162				
163				
164				
165				
166				
167				
168				
169				
170				
171				
172				
173				
174				

	O	P	Q	R	S	T
117	'RIGOR-InnerConvolutions'!$A$436	1.00000E+00	0.00000E+00	0.00000E+00	0.00000E+00	
118	'RIGOR-InnerConvolutions'!$A$436	1.00000E+00	0.00000E+00	0.00000E+00	0.00000E+00	
119	'RIGOR-InnerConvolutions'!$A$436	1.00000E+00	0.00000E+00	0.00000E+00	0.00000E+00	
120	'RIGOR-InnerConvolutions'!$A$436	1.00000E+00	0.00000E+00	0.00000E+00	0.00000E+00	
121	'RIGOR-InnerConvolutions'!$A$436	1.00000E+00	0.00000E+00	0.00000E+00	0.00000E+00	
122	'RIGOR-InnerConvolutions'!$A$436	1.00000E+00	0.00000E+00	0.00000E+00	0.00000E+00	
123	'RIGOR-InnerConvolutions'!$A$436	1.00000E+00	0.00000E+00	0.00000E+00	0.00000E+00	
124	'RIGOR-InnerConvolutions'!$A$436	1.00000E+00	0.00000E+00	0.00000E+00	0.00000E+00	
125	'RIGOR-InnerConvolutions'!$A$436	1.00000E+00	0.00000E+00	0.00000E+00	0.00000E+00	
126	'RIGOR-InnerConvolutions'!$A$436	1.00000E+00	0.00000E+00	0.00000E+00	0.00000E+00	
127	'RIGOR-InnerConvolutions'!$A$436	1.00000E+00	0.00000E+00	0.00000E+00	0.00000E+00	
128	'RIGOR-InnerConvolutions'!$A$436	1.00000E+00	0.00000E+00	0.00000E+00	0.00000E+00	
129	'RIGOR-InnerConvolutions'!$A$436	1.00000E+00	0.00000E+00	0.00000E+00	0.00000E+00	
130	'RIGOR-InnerConvolutions'!$A$436	1.00000E+00	0.00000E+00	0.00000E+00	0.00000E+00	
131	'RIGOR-InnerConvolutions'!$A$436	1.00000E+00	0.00000E+00	0.00000E+00	0.00000E+00	
132	'RIGOR-InnerConvolutions'!$A$436	1.00000E+00	0.00000E+00	0.00000E+00	0.00000E+00	
133	'RIGOR-InnerConvolutions'!$A$436	1.00000E+00	0.00000E+00	0.00000E+00	0.00000E+00	
134						
135						
136						
137						
138						
139						
140						
141						
142						
143						
144						
145						
146						
147						
148						
149						
150						
151						
153						
154						
155						
156						
157						
158						
159						
160						
161						
162						
163						
164						
165						
166						
167						
168						
169						
170						
171						
172						
173						
174						

	U	V	W	X	Y
117		'RIGOR-InnerConvolutions'!$C$435	0.00000E+00	'RIGOR-InnerConvolutions'!$C$436	0.00000E+00
118		'RIGOR-InnerConvolutions'!$C$435	0.00000E+00	'RIGOR-InnerConvolutions'!$C$436	0.00000E+00
119		'RIGOR-InnerConvolutions'!$C$435	0.00000E+00	'RIGOR-InnerConvolutions'!$C$436	0.00000E+00
120		'RIGOR-InnerConvolutions'!$C$435	0.00000E+00	'RIGOR-InnerConvolutions'!$C$436	0.00000E+00
121		'RIGOR-InnerConvolutions'!$C$435	0.00000E+00	'RIGOR-InnerConvolutions'!$C$436	0.00000E+00
122		'RIGOR-InnerConvolutions'!$C$435	0.00000E+00	'RIGOR-InnerConvolutions'!$C$436	0.00000E+00
123		'RIGOR-InnerConvolutions'!$C$435	0.00000E+00	'RIGOR-InnerConvolutions'!$C$436	0.00000E+00
124		'RIGOR-InnerConvolutions'!$C$435	0.00000E+00	'RIGOR-InnerConvolutions'!$C$436	0.00000E+00
125		'RIGOR-InnerConvolutions'!$C$435	0.00000E+00	'RIGOR-InnerConvolutions'!$C$436	0.00000E+00
126		'RIGOR-InnerConvolutions'!$C$435	0.00000E+00	'RIGOR-InnerConvolutions'!$C$436	0.00000E+00
127		'RIGOR-InnerConvolutions'!$C$435	0.00000E+00	'RIGOR-InnerConvolutions'!$C$436	0.00000E+00
128		'RIGOR-InnerConvolutions'!$C$435	0.00000E+00	'RIGOR-InnerConvolutions'!$C$436	0.00000E+00
129		'RIGOR-InnerConvolutions'!$C$435	0.00000E+00	'RIGOR-InnerConvolutions'!$C$436	0.00000E+00
130		'RIGOR-InnerConvolutions'!$C$435	0.00000E+00	'RIGOR-InnerConvolutions'!$C$436	0.00000E+00
131		'RIGOR-InnerConvolutions'!$C$435	0.00000E+00	'RIGOR-InnerConvolutions'!$C$436	0.00000E+00
132		'RIGOR-InnerConvolutions'!$C$435	0.00000E+00	'RIGOR-InnerConvolutions'!$C$436	0.00000E+00
133		'RIGOR-InnerConvolutions'!$C$435	0.00000E+00	'RIGOR-InnerConvolutions'!$C$436	0.00000E+00
134					
135					
136					
137					
138					
139					
140					
141					
142					
143					
144					
145					
146					
147					
148					
149					
150					
151					
153					
154					
155					
156					
157					
158					
159					
160					
161					
162					
163					
164					
165					
166					
167					
168					
169					
170					
171					
172					
173					
174					

	Z	AA	AB	AC	AD	AE
117	0.00000E+00	0.00000E+00			0.00000E+00	
118	0.00000E+00	0.00000E+00			0.00000E+00	
119	0.00000E+00	0.00000E+00			0.00000E+00	
120	0.00000E+00	0.00000E+00			0.00000E+00	
121	0.00000E+00	0.00000E+00			0.00000E+00	
122	0.00000E+00	0.00000E+00			0.00000E+00	
123	0.00000E+00	0.00000E+00			0.00000E+00	
124	0.00000E+00	0.00000E+00			0.00000E+00	
125	0.00000E+00	0.00000E+00			0.00000E+00	
126	0.00000E+00	0.00000E+00			0.00000E+00	
127	0.00000E+00	0.00000E+00			0.00000E+00	
128	0.00000E+00	0.00000E+00			0.00000E+00	
129	0.00000E+00	0.00000E+00			0.00000E+00	
130	0.00000E+00	0.00000E+00			0.00000E+00	
131	0.00000E+00	0.00000E+00			0.00000E+00	
132	0.00000E+00	0.00000E+00			0.00000E+00	
133	0.00000E+00	0.00000E+00			0.00000E+00	
134						
135						
136						
137						
138						
139						
140						
141						
142						
143						
144						
145						
146						
147						
148						
149						
150						
151						
153						
154						
155						
156						
157						
158						
159						
160						
161						
162						
163						
164						
165						
166						
167						
168						
169						
170						
171						
172						
173						
174						

	A	B	C	D	E	F
175	60,971	5.33514E-19	3.92525E-10	2.20763E-07		
176	75,000	2.12015E-15	8.20670E-08	6.93036E-06		
177	100,000	7.50160E-13	3.50982E-06	8.53779E-05		
178	150,000	9.56596E-11	7.28703E-05	6.86372E-04		
179	200,000	1.15293E-09	3.38836E-04	2.24490E-03		
180	250,000	5.45761E-09	8.52566E-04	4.57993E-03		
181	300,000	1.58425E-08	1.58816E-03	7.41784E-03		
182	350,000	3.44039E-08	2.48110E-03	1.04837E-02		
183	400,000	6.18030E-08	3.45808E-03	1.35539E-02		
184	450,000	9.72073E-08	4.45347E-03	1.64694E-02		
185	500,000	1.38639E-07	5.41626E-03	1.91309E-02		
186	550,000	1.83479E-07	6.31139E-03	2.14877E-02		
187	600,000	2.28948E-07	7.11813E-03	2.35248E-02		
188	650,000	2.72427E-07	7.79563E-03	2.52272E-02		
189	700,000	3.11538E-07	8.38821E-03	2.63782E-02		
190	750,000	3.44828E-07	8.89950E-03	2.77993E-02		
191	800,000	3.71543E-07	9.32648E-03	2.85686E-02		
192	850,000	3.91373E-07	9.68102E-03	2.94986E-02		
193	900,000	4.04367E-07	9.96906E-03	2.99927E-02		
194	950,000	4.10887E-07	1.02030E-02	3.05806E-02		
195						
196						
197						
198						
199						
200						
201						
202						
203						
204						
205						
206						
207						
208						
209						
210						
211						
212						
213						
214						
215						
216						
217						
218						
219						
220						
221						
222						
223						
224						
225						
226						
227						
228						

	A	B	C	D
1	NUMERICAL TREATMENT FOR CONVOLVED P(BCG) - InnerConvolutions			
2				M [kg]
3				11.43
4			C6 FORMULA =$A$6-$B$6	U [m^3/yr]
5	tscope [years]	tb[years]	tscope-tb [years]	0.15
6	100,000	1.00000E-10	1.00000E+05	
7	2.54301E-06	<-Pb-g(tscope-tb)	2.74771E-01	<-Pb-c(tscope-tb)
8			SAMPLE COLUMN C =IF($B10>0,$A10/$B10,0)	SAMPLE COLUMN D = IF(($C$6-$B10)>0,18+LOG10($D$3/252.22/$D$5/($C$6-$B10)),3E+99). This is the argument for Eq. 13 in AMR.
9	d(deltb) [years]	deltb [years]	Jacobian*d(deltb)=d(deltb)/deltb	18+log10[M/252.22/U/(t-tb-deltb)]
10	0	0	0.00000E+00	1.24802E+01
11	10	10	1.00000E+00	1.24802E+01
12	10	20	5.00000E-01	1.24803E+01
13	10	30	3.33333E-01	1.24803E+01
14	10	40	2.50000E-01	1.24803E+01
15	10	50	2.00000E-01	1.24804E+01
16	10	60	1.66667E-01	1.24804E+01
17	10	70	1.42857E-01	1.24805E+01
18	10	80	1.25000E-01	1.24805E+01
19	10	90	1.11111E-01	1.24806E+01
20	10	100	1.00000E-01	1.24806E+01
21	10	110	9.09091E-02	1.24807E+01
22	10	120	8.33333E-02	1.24807E+01
23	10	130	7.69231E-02	1.24807E+01
24	10	140	7.14286E-02	1.24808E+01
25	10	150	6.66667E-02	1.24808E+01
26	10	160	6.25000E-02	1.24809E+01
27	10	170	5.88235E-02	1.24809E+01
28	10	180	5.55556E-02	1.24810E+01
29	10	190	5.26316E-02	1.24810E+01
30	10	200	5.00000E-02	1.24810E+01
31	10	210	4.76190E-02	1.24811E+01
32	10	220	4.54545E-02	1.24811E+01
33	10	230	4.34783E-02	1.24812E+01
34	10	240	4.16667E-02	1.24812E+01
35	10	250	4.00000E-02	1.24813E+01
36	10	260	3.84615E-02	1.24813E+01
37	10	270	3.70370E-02	1.24813E+01
38	10	280	3.57143E-02	1.24814E+01
39	10	290	3.44828E-02	1.24814E+01
40	10	300	3.33333E-02	1.24815E+01
41	10	310	3.22581E-02	1.24815E+01
42	10	320	3.12500E-02	1.24816E+01
43	10	330	3.03030E-02	1.24816E+01
44	10	340	2.94118E-02	1.24817E+01
45	10	350	2.85714E-02	1.24817E+01
46	10	360	2.77778E-02	1.24817E+01
47	10	370	2.70270E-02	1.24818E+01
48	10	380	2.63158E-02	1.24818E+01
49	10	390	2.56410E-02	1.24819E+01
50	10	400	2.50000E-02	1.24819E+01
51	30	430	6.97674E-02	1.24820E+01
52	30	460	6.52174E-02	1.24822E+01
53	30	490	6.12245E-02	1.24823E+01
54	30	520	5.76923E-02	1.24824E+01

	E	F	G	H
1				
2	Alpha-flood	Alpha-Gdflush	Alpha-SS	M-SS [mm]
3	11.881	8.2038	4.852	9.525
4	Beta-flood	Beta-Gdflush	Beta-SS	
5	10.218	5.5416	4.041	
6	Theta-flood	Theta-Gdflush	Theta-SS	
7	0	0	4.605	
8	SAMPLE COLUMN E =IF(AND($D10>=$F$7,$D10<3E+99,LN($C$6)>=0),0.66*EXP(-(POWER((LN($C$6)-$E$7)/($E$3),$E$5)))*EXP(-(POWER(($D10-$F$7)/($F$3),$F$5))),0). This is Eq. 7 in AMR.	SAMPLE COLUMN F = IF(AND(-LN($H$3/($B10+1E-99))>=$G$7,$B10>0,$B10<=$C$6,$H$3/($B10+1E-99)<=1),WEIBULL((-LN($H$3/$B10)-$G$7),$G$5,$G$3,FALSE),0). This is a differential form of Eq. 6 in AMR.	SAMPLE COLUMN G = IF($B10<=$C$6,$C10*$E10*$F10,0)	H10 FORMULA = SUM($G10:$G410). This is the result of the 2 interior integrations in Eq. 1 in AMR.
9	Pc-g(t,tb,deltb)	pdf in ln(M/deltb) for P-SS	delta(Pb-g(t,tb))	Pb-g(t,tb)
10	1.15752E-05	0.00000E+00	0.00000E+00	2.54301E-06
11	1.15729E-05	0.00000E+00	0.00000E+00	
12	1.15706E-05	0.00000E+00	0.00000E+00	
13	1.15683E-05	0.00000E+00	0.00000E+00	
14	1.15661E-05	0.00000E+00	0.00000E+00	
15	1.15638E-05	0.00000E+00	0.00000E+00	
16	1.15615E-05	0.00000E+00	0.00000E+00	
17	1.15592E-05	0.00000E+00	0.00000E+00	
18	1.15569E-05	0.00000E+00	0.00000E+00	
19	1.15546E-05	0.00000E+00	0.00000E+00	
20	1.15524E-05	0.00000E+00	0.00000E+00	
21	1.15501E-05	0.00000E+00	0.00000E+00	
22	1.15478E-05	0.00000E+00	0.00000E+00	
23	1.15455E-05	0.00000E+00	0.00000E+00	
24	1.15432E-05	0.00000E+00	0.00000E+00	
25	1.15410E-05	0.00000E+00	0.00000E+00	
26	1.15387E-05	0.00000E+00	0.00000E+00	
27	1.15364E-05	0.00000E+00	0.00000E+00	
28	1.15341E-05	0.00000E+00	0.00000E+00	
29	1.15318E-05	0.00000E+00	0.00000E+00	
30	1.15296E-05	0.00000E+00	0.00000E+00	
31	1.15273E-05	0.00000E+00	0.00000E+00	
32	1.15250E-05	0.00000E+00	0.00000E+00	
33	1.15227E-05	0.00000E+00	0.00000E+00	
34	1.15205E-05	0.00000E+00	0.00000E+00	
35	1.15182E-05	0.00000E+00	0.00000E+00	
36	1.15159E-05	0.00000E+00	0.00000E+00	
37	1.15136E-05	0.00000E+00	0.00000E+00	
38	1.15113E-05	0.00000E+00	0.00000E+00	
39	1.15091E-05	0.00000E+00	0.00000E+00	
40	1.15068E-05	0.00000E+00	0.00000E+00	
41	1.15045E-05	0.00000E+00	0.00000E+00	
42	1.15022E-05	0.00000E+00	0.00000E+00	
43	1.15000E-05	0.00000E+00	0.00000E+00	
44	1.14977E-05	0.00000E+00	0.00000E+00	
45	1.14954E-05	0.00000E+00	0.00000E+00	
46	1.14931E-05	0.00000E+00	0.00000E+00	
47	1.14909E-05	0.00000E+00	0.00000E+00	
48	1.14886E-05	0.00000E+00	0.00000E+00	
49	1.14863E-05	0.00000E+00	0.00000E+00	
50	1.14840E-05	0.00000E+00	0.00000E+00	
51	1.14772E-05	0.00000E+00	0.00000E+00	
52	1.14704E-05	0.00000E+00	0.00000E+00	
53	1.14636E-05	0.00000E+00	0.00000E+00	
54	1.14567E-05	0.00000E+00	0.00000E+00	

	I	J	K	L	M	N
1						
2						
3						
4						
5						
6						
7						
8		SAMPLE COLUMN J = IF((LN($B10+1E-99)>=$E$7),0.66*EXP(-(POWER((LN($B10)-$E$7)/($E$3),$E$5))),0)	SAMPLE COLUMN K = IF($B10<=$C$6,$C10*$F10*$J10,0)	L10 FORMULA = SUM($K10:$K410). This is a result for the 2 interior integrations in Eq. 1 in AMR, except Pc-g is assigned constant value 1.		
9		Pfloodduntiltime=tb+deltb(t,tb)	delta(Pb-c(t,tb))	Pb-c(t,tb)		
10		0.00000E+00	0.00000E+00	2.74771E-01		
11		6.60000E-01	0.00000E+00			
12		6.59999E-01	0.00000E+00			
13		6.59998E-01	0.00000E+00			
14		6.59996E-01	0.00000E+00			
15		6.59992E-01	0.00000E+00			
16		6.59988E-01	0.00000E+00			
17		6.59982E-01	0.00000E+00			
18		6.59975E-01	0.00000E+00			
19		6.59968E-01	0.00000E+00			
20		6.59959E-01	0.00000E+00			
21		6.59949E-01	0.00000E+00			
22		6.59939E-01	0.00000E+00			
23		6.59928E-01	0.00000E+00			
24		6.59916E-01	0.00000E+00			
25		6.59903E-01	0.00000E+00			
26		6.59889E-01	0.00000E+00			
27		6.59875E-01	0.00000E+00			
28		6.59860E-01	0.00000E+00			
29		6.59844E-01	0.00000E+00			
30		6.59828E-01	0.00000E+00			
31		6.59811E-01	0.00000E+00			
32		6.59793E-01	0.00000E+00			
33		6.59775E-01	0.00000E+00			
34		6.59757E-01	0.00000E+00			
35		6.59738E-01	0.00000E+00			
36		6.59718E-01	0.00000E+00			
37		6.59698E-01	0.00000E+00			
38		6.59677E-01	0.00000E+00			
39		6.59656E-01	0.00000E+00			
40		6.59634E-01	0.00000E+00			
41		6.59612E-01	0.00000E+00			
42		6.59590E-01	0.00000E+00			
43		6.59567E-01	0.00000E+00			
44		6.59544E-01	0.00000E+00			
45		6.59520E-01	0.00000E+00			
46		6.59496E-01	0.00000E+00			
47		6.59471E-01	0.00000E+00			
48		6.59446E-01	0.00000E+00			
49		6.59421E-01	0.00000E+00			
50		6.59396E-01	0.00000E+00			
51		6.59317E-01	0.00000E+00			
52		6.59235E-01	0.00000E+00			
53		6.59151E-01	0.00000E+00			
54		6.59064E-01	0.00000E+00			

	A	B	C	D
55	30	550	5.45455E-02	1.24826E+01
56	30	580	5.17241E-02	1.24827E+01
57	30	610	4.91803E-02	1.24828E+01
58	30	640	4.68750E-02	1.24830E+01
59	30	670	4.47761E-02	1.24831E+01
60	30	700	4.28571E-02	1.24832E+01
61	30	730	4.10959E-02	1.24834E+01
62	30	760	3.94737E-02	1.24835E+01
63	30	790	3.79747E-02	1.24836E+01
64	30	820	3.65854E-02	1.24838E+01
65	30	850	3.52941E-02	1.24839E+01
66	30	880	3.40909E-02	1.24840E+01
67	30	910	3.29670E-02	1.24841E+01
68	30	940	3.19149E-02	1.24843E+01
69	30	970	3.09278E-02	1.24844E+01
70	30	1000	3.00000E-02	1.24845E+01
71	50	1050	4.76190E-02	1.24848E+01
72	50	1100	4.54545E-02	1.24850E+01
73	50	1150	4.34783E-02	1.24852E+01
74	50	1200	4.16667E-02	1.24854E+01
75	50	1250	4.00000E-02	1.24856E+01
76	50	1300	3.84615E-02	1.24859E+01
77	50	1350	3.70370E-02	1.24861E+01
78	50	1400	3.57143E-02	1.24863E+01
79	50	1450	3.44828E-02	1.24865E+01
80	50	1500	3.33333E-02	1.24867E+01
81	50	1550	3.22581E-02	1.24870E+01
82	50	1600	3.12500E-02	1.24872E+01
83	50	1650	3.03030E-02	1.24874E+01
84	50	1700	2.94118E-02	1.24876E+01
85	50	1750	2.85714E-02	1.24878E+01
86	50	1800	2.77778E-02	1.24881E+01
87	50	1850	2.70270E-02	1.24883E+01
88	50	1900	2.63158E-02	1.24885E+01
89	50	1950	2.56410E-02	1.24887E+01
90	50	2000	2.50000E-02	1.24889E+01
91	100	2100	4.76190E-02	1.24894E+01
92	100	2200	4.54545E-02	1.24898E+01
93	100	2300	4.34783E-02	1.24903E+01
94	100	2400	4.16667E-02	1.24907E+01
95	100	2500	4.00000E-02	1.24912E+01
96	100	2600	3.84615E-02	1.24916E+01
97	100	2700	3.70370E-02	1.24921E+01
98	100	2800	3.57143E-02	1.24925E+01
99	100	2900	3.44828E-02	1.24930E+01
100	100	3000	3.33333E-02	1.24934E+01
101	100	3100	3.22581E-02	1.24939E+01
102	100	3200	3.12500E-02	1.24943E+01
103	100	3300	3.03030E-02	1.24947E+01
104	100	3400	2.94118E-02	1.24952E+01
105	100	3500	2.85714E-02	1.24956E+01
106	100	3600	2.77778E-02	1.24961E+01
107	100	3700	2.70270E-02	1.24965E+01
108	100	3800	2.63158E-02	1.24970E+01
109	100	3900	2.56410E-02	1.24975E+01
110	100	4000	2.50000E-02	1.24979E+01
111	100	4100	2.43902E-02	1.24984E+01
112	100	4200	2.38095E-02	1.24988E+01
113	100	4300	2.32558E-02	1.24993E+01
114	100	4400	2.27273E-02	1.24997E+01
115	100	4500	2.22222E-02	1.25002E+01
116	100	4600	2.17391E-02	1.25006E+01
117	100	4700	2.12766E-02	1.25011E+01
118	100	4800	2.08333E-02	1.25015E+01
119	100	4900	2.04082E-02	1.25020E+01
120	100	5000	2.00000E-02	1.25025E+01

	E	F	G	H
55	1.14499E-05	0.00000E+00	0.00000E+00	
56	1.14431E-05	0.00000E+00	0.00000E+00	
57	1.14363E-05	0.00000E+00	0.00000E+00	
58	1.14295E-05	0.00000E+00	0.00000E+00	
59	1.14227E-05	0.00000E+00	0.00000E+00	
60	1.14159E-05	0.00000E+00	0.00000E+00	
61	1.14090E-05	0.00000E+00	0.00000E+00	
62	1.14022E-05	0.00000E+00	0.00000E+00	
63	1.13954E-05	0.00000E+00	0.00000E+00	
64	1.13886E-05	0.00000E+00	0.00000E+00	
65	1.13818E-05	0.00000E+00	0.00000E+00	
66	1.13750E-05	0.00000E+00	0.00000E+00	
67	1.13682E-05	0.00000E+00	0.00000E+00	
68	1.13614E-05	0.00000E+00	0.00000E+00	
69	1.13546E-05	3.59982E-08	1.26417E-14	
70	1.13479E-05	7.03273E-07	2.39419E-13	
71	1.13365E-05	5.78023E-06	3.12037E-12	
72	1.13252E-05	1.89059E-05	9.73243E-12	
73	1.13139E-05	4.28140E-05	2.10606E-11	
74	1.13026E-05	7.94917E-05	3.74360E-11	
75	1.12913E-05	1.30347E-04	5.88715E-11	
76	1.12800E-05	1.96340E-04	8.51813E-11	
77	1.12687E-05	2.78085E-04	1.16062E-10	
78	1.12574E-05	3.75931E-04	1.51144E-10	
79	1.12462E-05	4.90022E-04	1.90030E-10	
80	1.12349E-05	6.20345E-04	2.32317E-10	
81	1.12236E-05	7.66767E-04	2.77609E-10	
82	1.12123E-05	9.29063E-04	3.25531E-10	
83	1.12011E-05	1.10694E-03	3.75726E-10	
84	1.11898E-05	1.30006E-03	4.27867E-10	
85	1.11786E-05	1.50805E-03	4.81652E-10	
86	1.11673E-05	1.73049E-03	5.36804E-10	
87	1.11561E-05	1.96697E-03	5.93072E-10	
88	1.11448E-05	2.21706E-03	6.50231E-10	
89	1.11336E-05	2.48032E-03	7.08075E-10	
90	1.11224E-05	2.75632E-03	7.66423E-10	
91	1.10999E-05	3.34483E-03	1.76797E-09	
92	1.10775E-05	3.97919E-03	2.00362E-09	
93	1.10551E-05	4.65617E-03	2.23802E-09	
94	1.10327E-05	5.37269E-03	2.46981E-09	
95	1.10104E-05	6.12586E-03	2.69791E-09	
96	1.09880E-05	6.91296E-03	2.92152E-09	
97	1.09657E-05	7.73146E-03	3.14003E-09	
98	1.09434E-05	8.57901E-03	3.35297E-09	
99	1.09211E-05	9.45341E-03	3.56005E-09	
100	1.08988E-05	1.03526E-02	3.76104E-09	
101	1.08765E-05	1.12748E-02	3.95582E-09	
102	1.08543E-05	1.22181E-02	4.14433E-09	
103	1.08321E-05	1.31809E-02	4.32656E-09	
104	1.08099E-05	1.41617E-02	4.50256E-09	
105	1.07877E-05	1.51592E-02	4.67238E-09	
106	1.07656E-05	1.61720E-02	4.83612E-09	
107	1.07434E-05	1.71988E-02	4.99390E-09	
108	1.07213E-05	1.82386E-02	5.14583E-09	
109	1.06992E-05	1.92903E-02	5.29207E-09	
110	1.06771E-05	2.03529E-02	5.43276E-09	
111	1.06550E-05	2.14255E-02	5.56805E-09	
112	1.06330E-05	2.25073E-02	5.69809E-09	
113	1.06110E-05	2.35973E-02	5.82304E-09	
114	1.05890E-05	2.46950E-02	5.94305E-09	
115	1.05670E-05	2.57995E-02	6.05829E-09	
116	1.05450E-05	2.69103E-02	6.16890E-09	
117	1.05231E-05	2.80267E-02	6.27504E-09	
118	1.05011E-05	2.91482E-02	6.37685E-09	
119	1.04792E-05	3.02742E-02	6.47447E-09	
120	1.04573E-05	3.14041E-02	6.56806E-09	

	I	J	K	L	M	N
55		6.58974E-01	0.00000E+00			
56		6.58883E-01	0.00000E+00			
57		6.58789E-01	0.00000E+00			
58		6.58693E-01	0.00000E+00			
59		6.58595E-01	0.00000E+00			
60		6.58496E-01	0.00000E+00			
61		6.58395E-01	0.00000E+00			
62		6.58292E-01	0.00000E+00			
63		6.58187E-01	0.00000E+00			
64		6.58081E-01	0.00000E+00			
65		6.57974E-01	0.00000E+00			
66		6.57865E-01	0.00000E+00			
67		6.57755E-01	0.00000E+00			
68		6.57643E-01	0.00000E+00			
69		6.57530E-01	7.32059E-10			
70		6.57417E-01	1.38703E-08			
71		6.57224E-01	1.80900E-07			
72		6.57029E-01	5.64624E-07			
73		6.56831E-01	1.22268E-06			
74		6.56631E-01	2.17486E-06			
75		6.56428E-01	3.42253E-06			
76		6.56222E-01	4.95548E-06			
77		6.56015E-01	6.75659E-06			
78		6.55805E-01	8.80491E-06			
79		6.55594E-01	1.10778E-05			
80		6.55380E-01	1.35521E-05			
81		6.55165E-01	1.62051E-05			
82		6.54948E-01	1.90152E-05			
83		6.54729E-01	2.19621E-05			
84		6.54509E-01	2.50266E-05			
85		6.54287E-01	2.81913E-05			
86		6.54064E-01	3.14403E-05			
87		6.53840E-01	3.47590E-05			
88		6.53614E-01	3.81342E-05			
89		6.53387E-01	4.15541E-05			
90		6.53159E-01	4.50079E-05			
91		6.52699E-01	1.03960E-04			
92		6.52236E-01	1.17971E-04			
93		6.51768E-01	1.31945E-04			
94		6.51297E-01	1.45801E-04			
95		6.50822E-01	1.59474E-04			
96		6.50345E-01	1.72916E-04			
97		6.49864E-01	1.86089E-04			
98		6.49381E-01	1.98966E-04			
99		6.48896E-01	2.11527E-04			
100		6.48408E-01	2.23757E-04			
101		6.47918E-01	2.35649E-04			
102		6.47426E-01	2.47197E-04			
103		6.46933E-01	2.58398E-04			
104		6.46438E-01	2.69255E-04			
105		6.45941E-01	2.79770E-04			
106		6.45443E-01	2.89947E-04			
107		6.44943E-01	2.99791E-04			
108		6.44442E-01	3.09309E-04			
109		6.43940E-01	3.18508E-04			
110		6.43437E-01	3.27395E-04			
111		6.42933E-01	3.35980E-04			
112		6.42427E-01	3.44269E-04			
113		6.41921E-01	3.52271E-04			
114		6.41415E-01	3.59994E-04			
115		6.40907E-01	3.67447E-04			
116		6.40399E-01	3.74638E-04			
117		6.39890E-01	3.81575E-04			
118		6.39381E-01	3.88267E-04			
119		6.38871E-01	3.94720E-04			
120		6.38361E-01	4.00943E-04			

	A	B	C	D
121	100	5100	1.96078E-02	1.25029E+01
122	100	5200	1.92308E-02	1.25034E+01
123	100	5300	1.88679E-02	1.25038E+01
124	100	5400	1.85185E-02	1.25043E+01
125	100	5500	1.81818E-02	1.25047E+01
126	100	5600	1.78571E-02	1.25052E+01
127	100	5700	1.75439E-02	1.25057E+01
128	100	5800	1.72414E-02	1.25061E+01
129	100	5900	1.69492E-02	1.25066E+01
130	100	6000	1.66667E-02	1.25070E+01
131	100	6100	1.63934E-02	1.25075E+01
132	100	6200	1.61290E-02	1.25080E+01
133	100	6300	1.58730E-02	1.25084E+01
134	100	6400	1.56250E-02	1.25089E+01
135	100	6500	1.53846E-02	1.25094E+01
136	100	6600	1.51515E-02	1.25098E+01
137	100	6700	1.49254E-02	1.25103E+01
138	100	6800	1.47059E-02	1.25108E+01
139	100	6900	1.44928E-02	1.25112E+01
140	100	7000	1.42857E-02	1.25117E+01
141	100	7100	1.40845E-02	1.25122E+01
142	100	7200	1.38889E-02	1.25126E+01
143	100	7300	1.36986E-02	1.25131E+01
144	100	7400	1.35135E-02	1.25136E+01
145	100	7500	1.33333E-02	1.25140E+01
146	100	7600	1.31579E-02	1.25145E+01
147	100	7700	1.29870E-02	1.25150E+01
148	100	7800	1.28205E-02	1.25154E+01
149	100	7900	1.26582E-02	1.25159E+01
150	100	8000	1.25000E-02	1.25164E+01
151	100	8100	1.23457E-02	1.25169E+01
152	100	8200	1.21951E-02	1.25173E+01
153	100	8300	1.20482E-02	1.25178E+01
154	100	8400	1.19048E-02	1.25183E+01
155	100	8500	1.17647E-02	1.25188E+01
156	100	8600	1.16279E-02	1.25192E+01
157	100	8700	1.14943E-02	1.25197E+01
158	100	8800	1.13636E-02	1.25202E+01
159	100	8900	1.12360E-02	1.25207E+01
160	100	9000	1.11111E-02	1.25211E+01
161	100	9100	1.09890E-02	1.25216E+01
162	100	9200	1.08696E-02	1.25221E+01
163	100	9300	1.07527E-02	1.25226E+01
164	100	9400	1.06383E-02	1.25230E+01
165	100	9500	1.05263E-02	1.25235E+01
166	100	9600	1.04167E-02	1.25240E+01
167	100	9700	1.03093E-02	1.25245E+01
168	100	9800	1.02041E-02	1.25250E+01
169	100	9900	1.01010E-02	1.25255E+01
170	100	10000	1.00000E-02	1.25259E+01
171	500	10500	4.76190E-02	1.25284E+01
172	500	11000	4.54545E-02	1.25308E+01
173	500	11500	4.34783E-02	1.25332E+01
174	500	12000	4.16667E-02	1.25357E+01
175	500	12500	4.00000E-02	1.25382E+01
176	500	13000	3.84615E-02	1.25407E+01
177	500	13500	3.70370E-02	1.25432E+01
178	500	14000	3.57143E-02	1.25457E+01
179	500	14500	3.44828E-02	1.25482E+01
180	500	15000	3.33333E-02	1.25508E+01
181	500	15500	3.22581E-02	1.25533E+01
182	500	16000	3.12500E-02	1.25559E+01
183	500	16500	3.03030E-02	1.25585E+01
184	500	17000	2.94118E-02	1.25611E+01
185	500	17500	2.85714E-02	1.25637E+01
186	500	18000	2.77778E-02	1.25664E+01

	E	F	G	H
121	1.04354E-05	3.25376E-02	6.65774E-09	
122	1.04136E-05	3.36742E-02	6.74364E-09	
123	1.03917E-05	3.48135E-02	6.82591E-09	
124	1.03699E-05	3.59550E-02	6.90465E-09	
125	1.03481E-05	3.70985E-02	6.98000E-09	
126	1.03264E-05	3.82435E-02	7.05207E-09	
127	1.03046E-05	3.93898E-02	7.12097E-09	
128	1.02829E-05	4.05369E-02	7.18682E-09	
129	1.02611E-05	4.16847E-02	7.24971E-09	
130	1.02394E-05	4.28329E-02	7.30975E-09	
131	1.02178E-05	4.39812E-02	7.36703E-09	
132	1.01961E-05	4.51293E-02	7.42166E-09	
133	1.01744E-05	4.62771E-02	7.47372E-09	
134	1.01528E-05	4.74243E-02	7.52329E-09	
135	1.01312E-05	4.85708E-02	7.57047E-09	
136	1.01096E-05	4.97162E-02	7.61534E-09	
137	1.00881E-05	5.08605E-02	7.65797E-09	
138	1.00665E-05	5.20035E-02	7.69844E-09	
139	1.00450E-05	5.31450E-02	7.73682E-09	
140	1.00235E-05	5.42848E-02	7.77318E-09	
141	1.00020E-05	5.54229E-02	7.80759E-09	
142	9.98052E-06	5.65590E-02	7.84011E-09	
143	9.95907E-06	5.76931E-02	7.87082E-09	
144	9.93764E-06	5.88250E-02	7.89976E-09	
145	9.91623E-06	5.99547E-02	7.92699E-09	
146	9.89483E-06	6.10820E-02	7.95258E-09	
147	9.87346E-06	6.22067E-02	7.97657E-09	
148	9.85211E-06	6.33289E-02	7.99902E-09	
149	9.83077E-06	6.44484E-02	8.01997E-09	
150	9.80946E-06	6.55652E-02	8.03949E-09	
151	9.78816E-06	6.66791E-02	8.05760E-09	
152	9.76689E-06	6.77901E-02	8.07437E-09	
153	9.74563E-06	6.88981E-02	8.08982E-09	
154	9.72439E-06	7.00031E-02	8.10402E-09	
155	9.70318E-06	7.11049E-02	8.11698E-09	
156	9.68198E-06	7.22036E-02	8.12876E-09	
157	9.66080E-06	7.32990E-02	8.13939E-09	
158	9.63964E-06	7.43911E-02	8.14891E-09	
159	9.61850E-06	7.54799E-02	8.15735E-09	
160	9.59738E-06	7.65654E-02	8.16475E-09	
161	9.57628E-06	7.76474E-02	8.17113E-09	
162	9.55520E-06	7.87259E-02	8.17654E-09	
163	9.53414E-06	7.98009E-02	8.18100E-09	
164	9.51310E-06	8.08724E-02	8.18455E-09	
165	9.49208E-06	8.19404E-02	8.18720E-09	
166	9.47108E-06	8.30047E-02	8.18900E-09	
167	9.45009E-06	8.40654E-02	8.18996E-09	
168	9.42913E-06	8.51224E-02	8.19011E-09	
169	9.40819E-06	8.61757E-02	8.18947E-09	
170	9.38727E-06	8.72254E-02	8.18808E-09	
171	9.28295E-06	9.24173E-02	4.08526E-08	
172	9.17912E-06	9.75141E-02	4.06861E-08	
173	9.07579E-06	1.02515E-01	4.04522E-08	
174	8.97295E-06	1.07418E-01	4.01607E-08	
175	8.87062E-06	1.12224E-01	3.98200E-08	
176	8.76878E-06	1.16934E-01	3.94373E-08	
177	8.66744E-06	1.21548E-01	3.90189E-08	
178	8.56661E-06	1.26067E-01	3.85702E-08	
179	8.46628E-06	1.30492E-01	3.80958E-08	
180	8.36646E-06	1.34824E-01	3.76000E-08	
181	8.26715E-06	1.39065E-01	3.70861E-08	
182	8.16834E-06	1.43216E-01	3.65575E-08	
183	8.07004E-06	1.47280E-01	3.60167E-08	
184	7.97226E-06	1.51256E-01	3.54663E-08	
185	7.87499E-06	1.55148E-01	3.49082E-08	
186	7.77823E-06	1.58957E-01	3.43445E-08	

	I	J	K	L	M	N
121		6.37850E-01	4.06944E-04			
122		6.37338E-01	4.12729E-04			
123		6.36827E-01	4.18305E-04			
124		6.36315E-01	4.23680E-04			
125		6.35803E-01	4.28861E-04			
126		6.35291E-01	4.33852E-04			
127		6.34778E-01	4.38662E-04			
128		6.34265E-01	4.43296E-04			
129		6.33752E-01	4.47759E-04			
130		6.33239E-01	4.52058E-04			
131		6.32726E-01	4.56198E-04			
132		6.32213E-01	4.60183E-04			
133		6.31700E-01	4.64020E-04			
134		6.31186E-01	4.67712E-04			
135		6.30673E-01	4.71266E-04			
136		6.30160E-01	4.74684E-04			
137		6.29647E-01	4.77972E-04			
138		6.29133E-01	4.81134E-04			
139		6.28620E-01	4.84174E-04			
140		6.28107E-01	4.87096E-04			
141		6.27595E-01	4.89903E-04			
142		6.27082E-01	4.92599E-04			
143		6.26569E-01	4.95188E-04			
144		6.26057E-01	4.97673E-04			
145		6.25545E-01	5.00058E-04			
146		6.25033E-01	5.02345E-04			
147		6.24521E-01	5.04538E-04			
148		6.24009E-01	5.06639E-04			
149		6.23498E-01	5.08651E-04			
150		6.22987E-01	5.10578E-04			
151		6.22476E-01	5.12421E-04			
152		6.21965E-01	5.14184E-04			
153		6.21455E-01	5.15868E-04			
154		6.20945E-01	5.17477E-04			
155		6.20435E-01	5.19012E-04			
156		6.19926E-01	5.20475E-04			
157		6.19417E-01	5.21869E-04			
158		6.18908E-01	5.23196E-04			
159		6.18399E-01	5.24458E-04			
160		6.17891E-01	5.25656E-04			
161		6.17384E-01	5.26793E-04			
162		6.16876E-01	5.27871E-04			
163		6.16369E-01	5.28891E-04			
164		6.15862E-01	5.29854E-04			
165		6.15356E-01	5.30763E-04			
166		6.14850E-01	5.31619E-04			
167		6.14345E-01	5.32424E-04			
168		6.13839E-01	5.33178E-04			
169		6.13335E-01	5.33885E-04			
170		6.12830E-01	5.34544E-04			
171		6.10315E-01	2.68589E-03			
172		6.07810E-01	2.69410E-03			
173		6.05317E-01	2.69799E-03			
174		6.02835E-01	2.69814E-03			
175		6.00366E-01	2.69503E-03			
176		5.97909E-01	2.68908E-03			
177		5.95464E-01	2.68065E-03			
178		5.93033E-01	2.67006E-03			
179		5.90614E-01	2.65759E-03			
180		5.88208E-01	2.64348E-03			
181		5.85815E-01	2.62795E-03			
182		5.83435E-01	2.61117E-03			
183		5.81069E-01	2.59332E-03			
184		5.78716E-01	2.57454E-03			
185		5.76376E-01	2.55496E-03			
186		5.74049E-01	2.53469E-03			

	A	B	C	D
187	500	18500	2.70270E-02	1.25690E+01
188	500	19000	2.63158E-02	1.25717E+01
189	500	19500	2.56410E-02	1.25744E+01
190	500	20000	2.50000E-02	1.25771E+01
191	500	20500	2.43902E-02	1.25798E+01
192	500	21000	2.38095E-02	1.25825E+01
193	500	21500	2.32558E-02	1.25853E+01
194	500	22000	2.27273E-02	1.25881E+01
195	500	22500	2.22222E-02	1.25909E+01
196	500	23000	2.17391E-02	1.25937E+01
197	500	23500	2.12766E-02	1.25965E+01
198	500	24000	2.08333E-02	1.25994E+01
199	500	24500	2.04082E-02	1.26022E+01
200	500	25000	2.00000E-02	1.26051E+01
201	500	25500	1.96078E-02	1.26080E+01
202	500	26000	1.92308E-02	1.26109E+01
203	500	26500	1.88679E-02	1.26139E+01
204	500	27000	1.85185E-02	1.26169E+01
205	500	27500	1.81818E-02	1.26198E+01
206	500	28000	1.78571E-02	1.26228E+01
207	500	28500	1.75439E-02	1.26259E+01
208	500	29000	1.72414E-02	1.26289E+01
209	500	29500	1.69492E-02	1.26320E+01
210	500	30000	1.66667E-02	1.26351E+01
211	500	30500	1.63934E-02	1.26382E+01
212	500	31000	1.61290E-02	1.26413E+01
213	500	31500	1.58730E-02	1.26445E+01
214	500	32000	1.56250E-02	1.26477E+01
215	500	32500	1.53846E-02	1.26509E+01
216	500	33000	1.51515E-02	1.26541E+01
217	500	33500	1.49254E-02	1.26574E+01
218	500	34000	1.47059E-02	1.26606E+01
219	500	34500	1.44928E-02	1.26639E+01
220	500	35000	1.42857E-02	1.26673E+01
221	500	35500	1.40845E-02	1.26706E+01
222	500	36000	1.38889E-02	1.26740E+01
223	500	36500	1.36986E-02	1.26774E+01
224	500	37000	1.35135E-02	1.26808E+01
225	500	37500	1.33333E-02	1.26843E+01
226	500	38000	1.31579E-02	1.26878E+01
227	500	38500	1.29870E-02	1.26913E+01
228	500	39000	1.28205E-02	1.26948E+01
229	500	39500	1.26582E-02	1.26984E+01
230	500	40000	1.25000E-02	1.27020E+01
231	1000	41000	2.43902E-02	1.27093E+01
232	1000	42000	2.38095E-02	1.27167E+01
233	1000	43000	2.32558E-02	1.27243E+01
234	1000	44000	2.27273E-02	1.27320E+01
235	1000	45000	2.22222E-02	1.27398E+01
236	1000	46000	2.17391E-02	1.27478E+01
237	1000	47000	2.12766E-02	1.27559E+01
238	1000	48000	2.08333E-02	1.27642E+01
239	1000	49000	2.04082E-02	1.27726E+01
240	1000	50000	2.00000E-02	1.27812E+01
241	1000	51000	1.96078E-02	1.27900E+01
242	1000	52000	1.92308E-02	1.27989E+01
243	1000	53000	1.88679E-02	1.28081E+01
244	1000	54000	1.85185E-02	1.28174E+01
245	1000	55000	1.81818E-02	1.28270E+01
246	1000	56000	1.78571E-02	1.28367E+01
247	1000	57000	1.75439E-02	1.28467E+01
248	1000	58000	1.72414E-02	1.28569E+01
249	1000	59000	1.69492E-02	1.28674E+01
250	1000	60000	1.66667E-02	1.28781E+01
251	1000	61000	1.63934E-02	1.28891E+01
252	1000	62000	1.61290E-02	1.29004E+01

	E	F	G	H
187	7.68199E-06	1.62684E-01	3.37766E-08	
188	7.58627E-06	1.66331E-01	3.32061E-08	
189	7.49106E-06	1.69900E-01	3.26341E-08	
190	7.39638E-06	1.73392E-01	3.20619E-08	
191	7.30222E-06	1.76810E-01	3.14903E-08	
192	7.20859E-06	1.80154E-01	3.09203E-08	
193	7.11548E-06	1.83426E-01	3.03527E-08	
194	7.02290E-06	1.86628E-01	2.97880E-08	
195	6.93085E-06	1.89762E-01	2.92269E-08	
196	6.83933E-06	1.92828E-01	2.86699E-08	
197	6.74834E-06	1.95829E-01	2.81174E-08	
198	6.65788E-06	1.98765E-01	2.75699E-08	
199	6.56796E-06	2.01638E-01	2.70276E-08	
200	6.47858E-06	2.04450E-01	2.64910E-08	
201	6.38973E-06	2.07202E-01	2.59602E-08	
202	6.30143E-06	2.09895E-01	2.54354E-08	
203	6.21367E-06	2.12531E-01	2.49169E-08	
204	6.12645E-06	2.15110E-01	2.44049E-08	
205	6.03978E-06	2.17635E-01	2.38993E-08	
206	5.95365E-06	2.20105E-01	2.34005E-08	
207	5.86807E-06	2.22522E-01	2.29084E-08	
208	5.78305E-06	2.24889E-01	2.24231E-08	
209	5.69857E-06	2.27204E-01	2.19447E-08	
210	5.61465E-06	2.29470E-01	2.14733E-08	
211	5.53128E-06	2.31688E-01	2.10087E-08	
212	5.44848E-06	2.33859E-01	2.05512E-08	
213	5.36623E-06	2.35983E-01	2.01006E-08	
214	5.28454E-06	2.38062E-01	1.96570E-08	
215	5.20341E-06	2.40096E-01	1.92203E-08	
216	5.12284E-06	2.42087E-01	1.87905E-08	
217	5.04285E-06	2.44036E-01	1.83677E-08	
218	4.96342E-06	2.45943E-01	1.79517E-08	
219	4.88455E-06	2.47809E-01	1.75425E-08	
220	4.80626E-06	2.49635E-01	1.71401E-08	
221	4.72855E-06	2.51422E-01	1.67445E-08	
222	4.65140E-06	2.53170E-01	1.63555E-08	
223	4.57483E-06	2.54881E-01	1.59731E-08	
224	4.49884E-06	2.56555E-01	1.55973E-08	
225	4.42343E-06	2.58193E-01	1.52280E-08	
226	4.34860E-06	2.59796E-01	1.48651E-08	
227	4.27436E-06	2.61364E-01	1.45086E-08	
228	4.20069E-06	2.62898E-01	1.41584E-08	
229	4.12762E-06	2.64399E-01	1.38144E-08	
230	4.05513E-06	2.65867E-01	1.34766E-08	
231	3.91193E-06	2.68708E-01	2.56382E-08	
232	3.77111E-06	2.71425E-01	2.43708E-08	
233	3.63267E-06	2.74025E-01	2.31498E-08	
234	3.49664E-06	2.76511E-01	2.19740E-08	
235	3.36302E-06	2.78887E-01	2.08423E-08	
236	3.23184E-06	2.81157E-01	1.97534E-08	
237	3.10311E-06	2.83327E-01	1.87062E-08	
238	2.97683E-06	2.85398E-01	1.76996E-08	
239	2.85304E-06	2.87375E-01	1.67325E-08	
240	2.73173E-06	2.89262E-01	1.58037E-08	
241	2.61293E-06	2.91061E-01	1.49122E-08	
242	2.49664E-06	2.92776E-01	1.40569E-08	
243	2.38289E-06	2.94409E-01	1.32367E-08	
244	2.27169E-06	2.95964E-01	1.24507E-08	
245	2.16305E-06	2.97443E-01	1.16979E-08	
246	2.05699E-06	2.98849E-01	1.09773E-08	
247	1.95351E-06	3.00185E-01	1.02880E-08	
248	1.85264E-06	3.01453E-01	9.62902E-09	
249	1.75438E-06	3.02655E-01	8.99954E-09	
250	1.65876E-06	3.03794E-01	8.39866E-09	
251	1.56577E-06	3.04871E-01	7.82556E-09	
252	1.47545E-06	3.05889E-01	7.27940E-09	

	I	J	K	L	M	N
187		5.71735E-01	2.51384E-03			
188		5.69435E-01	2.49249E-03			
189		5.67148E-01	2.47072E-03			
190		5.64874E-01	2.44862E-03			
191		5.62612E-01	2.42623E-03			
192		5.60364E-01	2.40361E-03			
193		5.58129E-01	2.38082E-03			
194		5.55906E-01	2.35790E-03			
195		5.53697E-01	2.33490E-03			
196		5.51500E-01	2.31184E-03			
197		5.49315E-01	2.28876E-03			
198		5.47143E-01	2.26569E-03			
199		5.44984E-01	2.24265E-03			
200		5.42837E-01	2.21967E-03			
201		5.40702E-01	2.19676E-03			
202		5.38580E-01	2.17395E-03			
203		5.36469E-01	2.15125E-03			
204		5.34371E-01	2.12868E-03			
205		5.32284E-01	2.10624E-03			
206		5.30210E-01	2.08396E-03			
207		5.28147E-01	2.06183E-03			
208		5.26095E-01	2.03988E-03			
209		5.24056E-01	2.01810E-03			
210		5.22028E-01	1.99650E-03			
211		5.20011E-01	1.97509E-03			
212		5.18006E-01	1.95387E-03			
213		5.16011E-01	1.93286E-03			
214		5.14028E-01	1.91204E-03			
215		5.12056E-01	1.89143E-03			
216		5.10095E-01	1.87102E-03			
217		5.08145E-01	1.85083E-03			
218		5.06206E-01	1.83085E-03			
219		5.04277E-01	1.81108E-03			
220		5.02359E-01	1.79152E-03			
221		5.00451E-01	1.77217E-03			
222		4.98554E-01	1.75304E-03			
223		4.96668E-01	1.73413E-03			
224		4.94791E-01	1.71542E-03			
225		4.92925E-01	1.69693E-03			
226		4.91069E-01	1.67865E-03			
227		4.89223E-01	1.66059E-03			
228		4.87387E-01	1.64273E-03			
229		4.85561E-01	1.62508E-03			
230		4.83744E-01	1.60764E-03			
231		4.80141E-01	3.14677E-03			
232		4.76575E-01	3.07987E-03			
233		4.73047E-01	3.01458E-03			
234		4.69557E-01	2.95085E-03			
235		4.66103E-01	2.88867E-03			
236		4.62685E-01	2.82799E-03			
237		4.59303E-01	2.76878E-03			
238		4.55955E-01	2.71101E-03			
239		4.52642E-01	2.65465E-03			
240		4.49362E-01	2.59967E-03			
241		4.46116E-01	2.54602E-03			
242		4.42903E-01	2.49368E-03			
243		4.39722E-01	2.44261E-03			
244		4.36573E-01	2.39278E-03			
245		4.33456E-01	2.34415E-03			
246		4.30369E-01	2.29671E-03			
247		4.27313E-01	2.25041E-03			
248		4.24287E-01	2.20522E-03			
249		4.21291E-01	2.16112E-03			
250		4.18324E-01	2.11807E-03			
251		4.15386E-01	2.07605E-03			
252		4.12476E-01	2.03503E-03			

	A	B	C	D
253	1000	63000	1.58730E-02	1.29120E+01
254	1000	64000	1.56250E-02	1.29239E+01
255	1000	65000	1.53846E-02	1.29361E+01
256	1000	66000	1.51515E-02	1.29487E+01
257	1000	67000	1.49254E-02	1.29617E+01
258	1000	68000	1.47059E-02	1.29750E+01
259	1000	69000	1.44928E-02	1.29888E+01
260	1000	70000	1.42857E-02	1.30031E+01
261	1000	71000	1.40845E-02	1.30178E+01
262	1000	72000	1.38889E-02	1.30330E+01
263	1000	73000	1.36986E-02	1.30488E+01
264	1000	74000	1.35135E-02	1.30652E+01
265	1000	75000	1.33333E-02	1.30822E+01
266	1000	76000	1.31579E-02	1.31000E+01
267	1000	77000	1.29870E-02	1.31184E+01
268	1000	78000	1.28205E-02	1.31378E+01
269	1000	79000	1.26582E-02	1.31580E+01
270	1000	80000	1.25000E-02	1.31791E+01
271	1000	81000	1.23457E-02	1.32014E+01
272	1000	82000	1.21951E-02	1.32249E+01
273	1000	83000	1.20482E-02	1.32497E+01
274	1000	84000	1.19048E-02	1.32761E+01
275	1000	85000	1.17647E-02	1.33041E+01
276	1000	86000	1.16279E-02	1.33340E+01
277	1000	87000	1.14943E-02	1.33662E+01
278	1000	88000	1.13636E-02	1.34010E+01
279	1000	89000	1.12360E-02	1.34388E+01
280	1000	90000	1.11111E-02	1.34802E+01
281	1000	91000	1.09890E-02	1.35259E+01
282	1000	92000	1.08696E-02	1.35771E+01
283	1000	93000	1.07527E-02	1.36351E+01
284	1000	94000	1.06383E-02	1.37020E+01
285	1000	95000	1.05263E-02	1.37812E+01
286	1000	96000	1.04167E-02	1.38781E+01
287	1000	97000	1.03093E-02	1.40031E+01
288	1000	98000	1.02041E-02	1.41791E+01
289	1000	99000	1.01010E-02	1.44802E+01
290	1000	100000	1.00000E-02	3.00000E+99
291	5000	105000	4.76190E-02	3.00000E+99
292	5000	110000	4.54545E-02	3.00000E+99
293	5000	115000	4.34783E-02	3.00000E+99
294	5000	120000	4.16667E-02	3.00000E+99
295	5000	125000	4.00000E-02	3.00000E+99
296	5000	130000	3.84615E-02	3.00000E+99
297	5000	135000	3.70370E-02	3.00000E+99
298	5000	140000	3.57143E-02	3.00000E+99
299	5000	145000	3.44828E-02	3.00000E+99
300	5000	150000	3.33333E-02	3.00000E+99
301	5000	155000	3.22581E-02	3.00000E+99
302	5000	160000	3.12500E-02	3.00000E+99
303	5000	165000	3.03030E-02	3.00000E+99
304	5000	170000	2.94118E-02	3.00000E+99
305	5000	175000	2.85714E-02	3.00000E+99
306	5000	180000	2.77778E-02	3.00000E+99
307	5000	185000	2.70270E-02	3.00000E+99
308	5000	190000	2.63158E-02	3.00000E+99
309	5000	195000	2.56410E-02	3.00000E+99
310	5000	200000	2.50000E-02	3.00000E+99
311	5000	205000	2.43902E-02	3.00000E+99
312	5000	210000	2.38095E-02	3.00000E+99
313	5000	215000	2.32558E-02	3.00000E+99
314	5000	220000	2.27273E-02	3.00000E+99
315	5000	225000	2.22222E-02	3.00000E+99
316	5000	230000	2.17391E-02	3.00000E+99
317	5000	235000	2.12766E-02	3.00000E+99
318	5000	240000	2.08333E-02	3.00000E+99

	E	F	G	H
253	1.38779E-06	3.06850E-01	6.75940E-09	
254	1.30281E-06	3.07756E-01	6.26479E-09	
255	1.22052E-06	3.08608E-01	5.79479E-09	
256	1.14093E-06	3.09408E-01	5.34870E-09	
257	1.06406E-06	3.10159E-01	4.92578E-09	
258	9.89909E-07	3.10861E-01	4.52535E-09	
259	9.18490E-07	3.11516E-01	4.14673E-09	
260	8.49810E-07	3.12126E-01	3.78926E-09	
261	7.83877E-07	3.12693E-01	3.45229E-09	
262	7.20698E-07	3.13217E-01	3.13520E-09	
263	6.60276E-07	3.13700E-01	2.83738E-09	
264	6.02617E-07	3.14144E-01	2.55822E-09	
265	5.47722E-07	3.14549E-01	2.29714E-09	
266	4.95592E-07	3.14917E-01	2.05355E-09	
267	4.46225E-07	3.15249E-01	1.82691E-09	
268	3.99618E-07	3.15546E-01	1.61664E-09	
269	3.55766E-07	3.15810E-01	1.42221E-09	
270	3.14659E-07	3.16041E-01	1.24306E-09	
271	2.76286E-07	3.16240E-01	1.07867E-09	
272	2.40631E-07	3.16409E-01	9.28510E-10	
273	2.07676E-07	3.16548E-01	7.92041E-10	
274	1.77396E-07	3.16658E-01	6.68738E-10	
275	1.49763E-07	3.16741E-01	5.58070E-10	
276	1.24740E-07	3.16796E-01	4.59501E-10	
277	1.02285E-07	3.16826E-01	3.72489E-10	
278	8.23478E-08	3.16830E-01	2.96480E-10	
279	6.48676E-08	3.16810E-01	2.30906E-10	
280	4.97727E-08	3.16765E-01	1.75181E-10	
281	3.69781E-08	3.16698E-01	1.28691E-10	
282	2.63824E-08	3.16609E-01	9.07926E-11	
283	1.78656E-08	3.16498E-01	6.08004E-11	
284	1.12842E-08	3.16366E-01	3.79780E-11	
285	6.46650E-09	3.16214E-01	2.15242E-11	
286	3.20639E-09	3.16042E-01	1.05557E-11	
287	1.25525E-09	3.15851E-01	4.08732E-12	
288	3.13306E-10	3.15641E-01	1.00910E-12	
289	2.41931E-11	3.15414E-01	7.70792E-14	
290	0.00000E+00	0.00000E+00	0.00000E+00	
291	0.00000E+00	0.00000E+00	0.00000E+00	
292	0.00000E+00	0.00000E+00	0.00000E+00	
293	0.00000E+00	0.00000E+00	0.00000E+00	
294	0.00000E+00	0.00000E+00	0.00000E+00	
295	0.00000E+00	0.00000E+00	0.00000E+00	
296	0.00000E+00	0.00000E+00	0.00000E+00	
297	0.00000E+00	0.00000E+00	0.00000E+00	
298	0.00000E+00	0.00000E+00	0.00000E+00	
299	0.00000E+00	0.00000E+00	0.00000E+00	
300	0.00000E+00	0.00000E+00	0.00000E+00	
301	0.00000E+00	0.00000E+00	0.00000E+00	
302	0.00000E+00	0.00000E+00	0.00000E+00	
303	0.00000E+00	0.00000E+00	0.00000E+00	
304	0.00000E+00	0.00000E+00	0.00000E+00	
305	0.00000E+00	0.00000E+00	0.00000E+00	
306	0.00000E+00	0.00000E+00	0.00000E+00	
307	0.00000E+00	0.00000E+00	0.00000E+00	
308	0.00000E+00	0.00000E+00	0.00000E+00	
309	0.00000E+00	0.00000E+00	0.00000E+00	
310	0.00000E+00	0.00000E+00	0.00000E+00	
311	0.00000E+00	0.00000E+00	0.00000E+00	
312	0.00000E+00	0.00000E+00	0.00000E+00	
313	0.00000E+00	0.00000E+00	0.00000E+00	
314	0.00000E+00	0.00000E+00	0.00000E+00	
315	0.00000E+00	0.00000E+00	0.00000E+00	
316	0.00000E+00	0.00000E+00	0.00000E+00	
317	0.00000E+00	0.00000E+00	0.00000E+00	
318	0.00000E+00	0.00000E+00	0.00000E+00	

	I	J	K	L	M	N
253		4.09594E-01	1.99498E-03			
254		4.06740E-01	1.95588E-03			
255		4.03913E-01	1.91770E-03			
256		4.01113E-01	1.88042E-03			
257		3.98339E-01	1.84401E-03			
258		3.95592E-01	1.80844E-03			
259		3.92870E-01	1.77370E-03			
260		3.90174E-01	1.73977E-03			
261		3.87503E-01	1.70661E-03			
262		3.84857E-01	1.67422E-03			
263		3.82235E-01	1.64257E-03			
264		3.79638E-01	1.61163E-03			
265		3.77064E-01	1.58140E-03			
266		3.74514E-01	1.55185E-03			
267		3.71987E-01	1.52297E-03			
268		3.69482E-01	1.49473E-03			
269		3.67001E-01	1.46712E-03			
270		3.64542E-01	1.44013E-03			
271		3.62105E-01	1.41373E-03			
272		3.59689E-01	1.38791E-03			
273		3.57295E-01	1.36266E-03			
274		3.54923E-01	1.33797E-03			
275		3.52571E-01	1.31381E-03			
276		3.50240E-01	1.29017E-03			
277		3.47930E-01	1.26705E-03			
278		3.45640E-01	1.24442E-03			
279		3.43369E-01	1.22228E-03			
280		3.41119E-01	1.20061E-03			
281		3.38888E-01	1.17940E-03			
282		3.36676E-01	1.15864E-03			
283		3.34483E-01	1.13832E-03			
284		3.32310E-01	1.11842E-03			
285		3.30154E-01	1.09894E-03			
286		3.28017E-01	1.07987E-03			
287		3.25899E-01	1.06119E-03			
288		3.23798E-01	1.04290E-03			
289		3.21715E-01	1.02498E-03			
290		3.19649E-01	0.00000E+00			
291		3.09578E-01	0.00000E+00			
292		2.99916E-01	0.00000E+00			
293		2.90641E-01	0.00000E+00			
294		2.81733E-01	0.00000E+00			
295		2.73173E-01	0.00000E+00			
296		2.64943E-01	0.00000E+00			
297		2.57026E-01	0.00000E+00			
298		2.49407E-01	0.00000E+00			
299		2.42072E-01	0.00000E+00			
300		2.35006E-01	0.00000E+00			
301		2.28198E-01	0.00000E+00			
302		2.21634E-01	0.00000E+00			
303		2.15305E-01	0.00000E+00			
304		2.09199E-01	0.00000E+00			
305		2.03306E-01	0.00000E+00			
306		1.97617E-01	0.00000E+00			
307		1.92124E-01	0.00000E+00			
308		1.86817E-01	0.00000E+00			
309		1.81689E-01	0.00000E+00			
310		1.76732E-01	0.00000E+00			
311		1.71940E-01	0.00000E+00			
312		1.67305E-01	0.00000E+00			
313		1.62821E-01	0.00000E+00			
314		1.58482E-01	0.00000E+00			
315		1.54283E-01	0.00000E+00			
316		1.50217E-01	0.00000E+00			
317		1.46280E-01	0.00000E+00			
318		1.42467E-01	0.00000E+00			

	A	B	C	D
319	5000	245000	2.04082E-02	3.00000E+99
320	5000	250000	2.00000E-02	3.00000E+99
321	5000	255000	1.96078E-02	3.00000E+99
322	5000	260000	1.92308E-02	3.00000E+99
323	5000	265000	1.88679E-02	3.00000E+99
324	5000	270000	1.85185E-02	3.00000E+99
325	5000	275000	1.81818E-02	3.00000E+99
326	5000	280000	1.78571E-02	3.00000E+99
327	5000	285000	1.75439E-02	3.00000E+99
328	5000	290000	1.72414E-02	3.00000E+99
329	5000	295000	1.69492E-02	3.00000E+99
330	5000	300000	1.66667E-02	3.00000E+99
331	5000	305000	1.63934E-02	3.00000E+99
332	5000	310000	1.61290E-02	3.00000E+99
333	5000	315000	1.58730E-02	3.00000E+99
334	5000	320000	1.56250E-02	3.00000E+99
335	5000	325000	1.53846E-02	3.00000E+99
336	5000	330000	1.51515E-02	3.00000E+99
337	5000	335000	1.49254E-02	3.00000E+99
338	5000	340000	1.47059E-02	3.00000E+99
339	5000	345000	1.44928E-02	3.00000E+99
340	5000	350000	1.42857E-02	3.00000E+99
341	5000	355000	1.40845E-02	3.00000E+99
342	5000	360000	1.38889E-02	3.00000E+99
343	5000	365000	1.36986E-02	3.00000E+99
344	5000	370000	1.35135E-02	3.00000E+99
345	5000	375000	1.33333E-02	3.00000E+99
346	5000	380000	1.31579E-02	3.00000E+99
347	5000	385000	1.29870E-02	3.00000E+99
348	5000	390000	1.28205E-02	3.00000E+99
349	5000	395000	1.26582E-02	3.00000E+99
350	5000	400000	1.25000E-02	3.00000E+99
351	10000	410000	2.43902E-02	3.00000E+99
352	10000	420000	2.38095E-02	3.00000E+99
353	10000	430000	2.32558E-02	3.00000E+99
354	10000	440000	2.27273E-02	3.00000E+99
355	10000	450000	2.22222E-02	3.00000E+99
356	10000	460000	2.17391E-02	3.00000E+99
357	10000	470000	2.12766E-02	3.00000E+99
358	10000	480000	2.08333E-02	3.00000E+99
359	10000	490000	2.04082E-02	3.00000E+99
360	10000	500000	2.00000E-02	3.00000E+99
361	10000	510000	1.96078E-02	3.00000E+99
362	10000	520000	1.92308E-02	3.00000E+99
363	10000	530000	1.88679E-02	3.00000E+99
364	10000	540000	1.85185E-02	3.00000E+99
365	10000	550000	1.81818E-02	3.00000E+99
366	10000	560000	1.78571E-02	3.00000E+99
367	10000	570000	1.75439E-02	3.00000E+99
368	10000	580000	1.72414E-02	3.00000E+99
369	10000	590000	1.69492E-02	3.00000E+99
370	10000	600000	1.66667E-02	3.00000E+99
371	10000	610000	1.63934E-02	3.00000E+99
372	10000	620000	1.61290E-02	3.00000E+99
373	10000	630000	1.58730E-02	3.00000E+99
374	10000	640000	1.56250E-02	3.00000E+99
375	10000	650000	1.53846E-02	3.00000E+99
376	10000	660000	1.51515E-02	3.00000E+99
377	10000	670000	1.49254E-02	3.00000E+99
378	10000	680000	1.47059E-02	3.00000E+99
379	10000	690000	1.44928E-02	3.00000E+99
380	10000	700000	1.42857E-02	3.00000E+99
381	10000	710000	1.40845E-02	3.00000E+99
382	10000	720000	1.38889E-02	3.00000E+99
383	10000	730000	1.36986E-02	3.00000E+99
384	10000	740000	1.35135E-02	3.00000E+99

	E	F	G	H
319	0.00000E+00	0.00000E+00	0.00000E+00	
320	0.00000E+00	0.00000E+00	0.00000E+00	
321	0.00000E+00	0.00000E+00	0.00000E+00	
322	0.00000E+00	0.00000E+00	0.00000E+00	
323	0.00000E+00	0.00000E+00	0.00000E+00	
324	0.00000E+00	0.00000E+00	0.00000E+00	
325	0.00000E+00	0.00000E+00	0.00000E+00	
326	0.00000E+00	0.00000E+00	0.00000E+00	
327	0.00000E+00	0.00000E+00	0.00000E+00	
328	0.00000E+00	0.00000E+00	0.00000E+00	
329	0.00000E+00	0.00000E+00	0.00000E+00	
330	0.00000E+00	0.00000E+00	0.00000E+00	
331	0.00000E+00	0.00000E+00	0.00000E+00	
332	0.00000E+00	0.00000E+00	0.00000E+00	
333	0.00000E+00	0.00000E+00	0.00000E+00	
334	0.00000E+00	0.00000E+00	0.00000E+00	
335	0.00000E+00	0.00000E+00	0.00000E+00	
336	0.00000E+00	0.00000E+00	0.00000E+00	
337	0.00000E+00	0.00000E+00	0.00000E+00	
338	0.00000E+00	0.00000E+00	0.00000E+00	
339	0.00000E+00	0.00000E+00	0.00000E+00	
340	0.00000E+00	0.00000E+00	0.00000E+00	
341	0.00000E+00	0.00000E+00	0.00000E+00	
342	0.00000E+00	0.00000E+00	0.00000E+00	
343	0.00000E+00	0.00000E+00	0.00000E+00	
344	0.00000E+00	0.00000E+00	0.00000E+00	
345	0.00000E+00	0.00000E+00	0.00000E+00	
346	0.00000E+00	0.00000E+00	0.00000E+00	
347	0.00000E+00	0.00000E+00	0.00000E+00	
348	0.00000E+00	0.00000E+00	0.00000E+00	
349	0.00000E+00	0.00000E+00	0.00000E+00	
350	0.00000E+00	0.00000E+00	0.00000E+00	
351	0.00000E+00	0.00000E+00	0.00000E+00	
352	0.00000E+00	0.00000E+00	0.00000E+00	
353	0.00000E+00	0.00000E+00	0.00000E+00	
354	0.00000E+00	0.00000E+00	0.00000E+00	
355	0.00000E+00	0.00000E+00	0.00000E+00	
356	0.00000E+00	0.00000E+00	0.00000E+00	
357	0.00000E+00	0.00000E+00	0.00000E+00	
358	0.00000E+00	0.00000E+00	0.00000E+00	
359	0.00000E+00	0.00000E+00	0.00000E+00	
360	0.00000E+00	0.00000E+00	0.00000E+00	
361	0.00000E+00	0.00000E+00	0.00000E+00	
362	0.00000E+00	0.00000E+00	0.00000E+00	
363	0.00000E+00	0.00000E+00	0.00000E+00	
364	0.00000E+00	0.00000E+00	0.00000E+00	
365	0.00000E+00	0.00000E+00	0.00000E+00	
366	0.00000E+00	0.00000E+00	0.00000E+00	
367	0.00000E+00	0.00000E+00	0.00000E+00	
368	0.00000E+00	0.00000E+00	0.00000E+00	
369	0.00000E+00	0.00000E+00	0.00000E+00	
370	0.00000E+00	0.00000E+00	0.00000E+00	
371	0.00000E+00	0.00000E+00	0.00000E+00	
372	0.00000E+00	0.00000E+00	0.00000E+00	
373	0.00000E+00	0.00000E+00	0.00000E+00	
374	0.00000E+00	0.00000E+00	0.00000E+00	
375	0.00000E+00	0.00000E+00	0.00000E+00	
376	0.00000E+00	0.00000E+00	0.00000E+00	
377	0.00000E+00	0.00000E+00	0.00000E+00	
378	0.00000E+00	0.00000E+00	0.00000E+00	
379	0.00000E+00	0.00000E+00	0.00000E+00	
380	0.00000E+00	0.00000E+00	0.00000E+00	
381	0.00000E+00	0.00000E+00	0.00000E+00	
382	0.00000E+00	0.00000E+00	0.00000E+00	
383	0.00000E+00	0.00000E+00	0.00000E+00	
384	0.00000E+00	0.00000E+00	0.00000E+00	

	I	J	K	L	M	N
319		1.38772E-01	0.00000E+00			
320		1.35192E-01	0.00000E+00			
321		1.31722E-01	0.00000E+00			
322		1.28358E-01	0.00000E+00			
323		1.25096E-01	0.00000E+00			
324		1.21933E-01	0.00000E+00			
325		1.18864E-01	0.00000E+00			
326		1.15886E-01	0.00000E+00			
327		1.12997E-01	0.00000E+00			
328		1.10193E-01	0.00000E+00			
329		1.07471E-01	0.00000E+00			
330		1.04827E-01	0.00000E+00			
331		1.02261E-01	0.00000E+00			
332		9.97677E-02	0.00000E+00			
333		9.73460E-02	0.00000E+00			
334		9.49932E-02	0.00000E+00			
335		9.27068E-02	0.00000E+00			
336		9.04847E-02	0.00000E+00			
337		8.83248E-02	0.00000E+00			
338		8.62250E-02	0.00000E+00			
339		8.41834E-02	0.00000E+00			
340		8.21979E-02	0.00000E+00			
341		8.02669E-02	0.00000E+00			
342		7.83886E-02	0.00000E+00			
343		7.65612E-02	0.00000E+00			
344		7.47832E-02	0.00000E+00			
345		7.30530E-02	0.00000E+00			
346		7.13690E-02	0.00000E+00			
347		6.97300E-02	0.00000E+00			
348		6.81344E-02	0.00000E+00			
349		6.65809E-02	0.00000E+00			
350		6.50682E-02	0.00000E+00			
351		6.21603E-02	0.00000E+00			
352		5.94013E-02	0.00000E+00			
353		5.67824E-02	0.00000E+00			
354		5.42954E-02	0.00000E+00			
355		5.19326E-02	0.00000E+00			
356		4.96870E-02	0.00000E+00			
357		4.75518E-02	0.00000E+00			
358		4.55208E-02	0.00000E+00			
359		4.35882E-02	0.00000E+00			
360		4.17486E-02	0.00000E+00			
361		3.99969E-02	0.00000E+00			
362		3.83283E-02	0.00000E+00			
363		3.67382E-02	0.00000E+00			
364		3.52226E-02	0.00000E+00			
365		3.37774E-02	0.00000E+00			
366		3.23990E-02	0.00000E+00			
367		3.10838E-02	0.00000E+00			
368		2.98286E-02	0.00000E+00			
369		2.86303E-02	0.00000E+00			
370		2.74860E-02	0.00000E+00			
371		2.63929E-02	0.00000E+00			
372		2.53484E-02	0.00000E+00			
373		2.43502E-02	0.00000E+00			
374		2.33958E-02	0.00000E+00			
375		2.24833E-02	0.00000E+00			
376		2.16104E-02	0.00000E+00			
377		2.07753E-02	0.00000E+00			
378		1.99762E-02	0.00000E+00			
379		1.92112E-02	0.00000E+00			
380		1.84788E-02	0.00000E+00			
381		1.77775E-02	0.00000E+00			
382		1.71057E-02	0.00000E+00			
383		1.64621E-02	0.00000E+00			
384		1.58453E-02	0.00000E+00			

	A	B	C	D
385	10000	750000	1.33333E-02	3.00000E+99
386	10000	760000	1.31579E-02	3.00000E+99
387	10000	770000	1.29870E-02	3.00000E+99
388	10000	780000	1.28205E-02	3.00000E+99
389	10000	790000	1.26582E-02	3.00000E+99
390	10000	800000	1.25000E-02	3.00000E+99
391	10000	810000	1.23457E-02	3.00000E+99
392	10000	820000	1.21951E-02	3.00000E+99
393	10000	830000	1.20482E-02	3.00000E+99
394	10000	840000	1.19048E-02	3.00000E+99
395	10000	850000	1.17647E-02	3.00000E+99
396	10000	860000	1.16279E-02	3.00000E+99
397	10000	870000	1.14943E-02	3.00000E+99
398	10000	880000	1.13636E-02	3.00000E+99
399	10000	890000	1.12360E-02	3.00000E+99
400	10000	900000	1.11111E-02	3.00000E+99
401	10000	910000	1.09890E-02	3.00000E+99
402	10000	920000	1.08696E-02	3.00000E+99
403	10000	930000	1.07527E-02	3.00000E+99
404	10000	940000	1.06383E-02	3.00000E+99
405	10000	950000	1.05263E-02	3.00000E+99
406	10000	960000	1.04167E-02	3.00000E+99
407	10000	970000	1.03093E-02	3.00000E+99
408	10000	980000	1.02041E-02	3.00000E+99
409	10000	990000	1.01010E-02	3.00000E+99
410	10000	1000000	1.00000E-02	3.00000E+99
411				
412				
413				
414				
415				
416				
417				
418				
419				
420				
421				
422				
423				
424				
425				
426				
427				
428				
429				
430	DATA IN COLUMNS A,B and C; ROWS 435 TO 505 ARE OBTAINED BY VARIATION			
431	OF THE VALUE FOR TSCOPE IN CELL A6 TO PRODUCE ASSOCIATED VALUES FOR A7 AND C7 AS TABULATED BELOW IN COLUMNS B AND C.			
432				
433				
434	(tscope-tb)	Pb-g(t,tb) = Pb-g(tscope-tb)	Pb-c(t-tb)=Pb-c(tscope-tb)	
435	0	0.00000E+00	0.00000E+00	
436	1	0.00000E+00	0.00000E+00	
437	5	0.00000E+00	0.00000E+00	
438	10	0.00000E+00	0.00000E+00	
439	100	0.00000E+00	0.00000E+00	
440	500	0.00000E+00	0.00000E+00	
441	750	0.00000E+00	0.00000E+00	
442	970	0.00000E+00	0.00000E+00	
443	971	1.35600E-38	7.32059E-10	
444	1,000	1.77505E-27	7.32059E-10	
445	1,500	4.97600E-18	3.91749E-05	
446	2,000	7.64850E-16	3.09015E-04	
447	2,500	1.25645E-14	8.53700E-04	
448	3,000	8.33711E-14	1.78267E-03	

	E	F	G	H
385	0.00000E+00	0.00000E+00	0.00000E+00	
386	0.00000E+00	0.00000E+00	0.00000E+00	
387	0.00000E+00	0.00000E+00	0.00000E+00	
388	0.00000E+00	0.00000E+00	0.00000E+00	
389	0.00000E+00	0.00000E+00	0.00000E+00	
390	0.00000E+00	0.00000E+00	0.00000E+00	
391	0.00000E+00	0.00000E+00	0.00000E+00	
392	0.00000E+00	0.00000E+00	0.00000E+00	
393	0.00000E+00	0.00000E+00	0.00000E+00	
394	0.00000E+00	0.00000E+00	0.00000E+00	
395	0.00000E+00	0.00000E+00	0.00000E+00	
396	0.00000E+00	0.00000E+00	0.00000E+00	
397	0.00000E+00	0.00000E+00	0.00000E+00	
398	0.00000E+00	0.00000E+00	0.00000E+00	
399	0.00000E+00	0.00000E+00	0.00000E+00	
400	0.00000E+00	0.00000E+00	0.00000E+00	
401	0.00000E+00	0.00000E+00	0.00000E+00	
402	0.00000E+00	0.00000E+00	0.00000E+00	
403	0.00000E+00	0.00000E+00	0.00000E+00	
404	0.00000E+00	0.00000E+00	0.00000E+00	
405	0.00000E+00	0.00000E+00	0.00000E+00	
406	0.00000E+00	0.00000E+00	0.00000E+00	
407	0.00000E+00	0.00000E+00	0.00000E+00	
408	0.00000E+00	0.00000E+00	0.00000E+00	
409	0.00000E+00	0.00000E+00	0.00000E+00	
410	0.00000E+00	0.00000E+00	0.00000E+00	
411				
412				
413				
414				
415				
416				
417				
418				
419				
420				
421				
422				
423				
424				
425				
426				
427				
428				
429				
430				
431				
432				
433				
434				
435				
436				
437				
438				
439				
440				
441				
442				
443				
444				
445				
446				
447				
448				

	I	J	K	L	M	N
385		1.52541E-02	0.00000E+00			
386		1.46874E-02	0.00000E+00			
387		1.41439E-02	0.00000E+00			
388		1.36227E-02	0.00000E+00			
389		1.31227E-02	0.00000E+00			
390		1.26430E-02	0.00000E+00			
391		1.21827E-02	0.00000E+00			
392		1.17408E-02	0.00000E+00			
393		1.13166E-02	0.00000E+00			
394		1.09093E-02	0.00000E+00			
395		1.05181E-02	0.00000E+00			
396		1.01424E-02	0.00000E+00			
397		9.78146E-03	0.00000E+00			
398		9.43463E-03	0.00000E+00			
399		9.10131E-03	0.00000E+00			
400		8.78093E-03	0.00000E+00			
401		8.47292E-03	0.00000E+00			
402		8.17678E-03	0.00000E+00			
403		7.89198E-03	0.00000E+00			
404		7.61806E-03	0.00000E+00			
405		7.35456E-03	0.00000E+00			
406		7.10104E-03	0.00000E+00			
407		6.85708E-03	0.00000E+00			
408		6.62230E-03	0.00000E+00			
409		6.39631E-03	0.00000E+00			
410		6.17874E-03	0.00000E+00			
411						
412						
413						
414						
415						
416						
417						
418						
419						
420						
421						
422						
423						
424						
425						
426						
427						
428						
429						
430						
431						
432						
433						
434						
435						
436						
437						
438						
439						
440						
441						
442						
443						
444						
445						
446						
447						
448						

	A	B	C	D
449	4,000	1.06239E-12	4.51425E-03	
450	5,000	5.85723E-12	8.14081E-03	
451	6,000	2.06988E-11	1.23958E-02	
452	7,000	5.57338E-11	1.70852E-02	
453	8,000	1.25125E-10	2.20699E-02	
454	9,000	2.46831E-10	2.72495E-02	
455	10,000	4.42212E-10	3.25504E-02	
456	12,500	1.41630E-09	4.38611E-02	
457	15,000	3.42980E-09	5.72535E-02	
458	17,500	6.95690E-09	7.03039E-02	
459	20,000	1.24945E-08	8.28706E-02	
460	25,000	3.15466E-08	1.06332E-01	
461	30,000	6.41775E-08	1.27512E-01	
462	35,000	1.13335E-07	1.46538E-01	
463	40,000	1.81238E-07	1.63608E-01	
464	45,000	2.69387E-07	1.77407E-01	
465	50,000	3.78596E-07	1.91259E-01	
466	55,000	5.09177E-07	2.03733E-01	
467	60,000	6.61023E-07	2.14991E-01	
468	65,000	8.33686E-07	2.25171E-01	
469	70,000	1.02644E-06	2.34395E-01	
470	75,000	1.23833E-06	2.42770E-01	
471	80,000	1.46826E-06	2.50388E-01	
472	90,000	1.97728E-06	2.63668E-01	
473	100,000	2.54301E-06	2.74771E-01	
474	110,000	3.15437E-06	2.84655E-01	
475	120,000	3.79988E-06	2.92177E-01	
476	130,000	4.46940E-06	2.98584E-01	
477	140,000	5.15396E-06	3.04066E-01	
478	150,000	5.84556E-06	3.08776E-01	
479	160,000	6.53714E-06	3.12839E-01	
480	170,000	7.22255E-06	3.16357E-01	
481	180,000	7.89651E-06	3.19412E-01	
482	190,000	8.55454E-06	3.22075E-01	
483	200,000	9.19291E-06	3.24402E-01	
484	225,000	1.06842E-05	3.29045E-01	
485	250,000	1.20026E-05	3.32434E-01	
486	275,000	1.31329E-05	3.34940E-01	
487	300,000	1.40724E-05	3.36816E-01	
488	325,000	1.48267E-05	3.38234E-01	
489	350,000	1.54065E-05	3.39317E-01	
490	375,000	1.58258E-05	3.40151E-01	
491	400,000	1.61002E-05	3.40798E-01	
492	425,000	1.62456E-05	3.41202E-01	
493	450,000	1.62777E-05	3.41680E-01	
494	475,000	1.62115E-05	3.41931E-01	
495	500,000	1.60612E-05	3.42232E-01	
496	550,000	1.55593E-05	3.42586E-01	
497	600,000	1.48612E-05	3.42816E-01	
498	650,000	1.40381E-05	3.42969E-01	
499	700,000	1.31442E-05	3.43072E-01	
500	750,000	1.22206E-05	3.43142E-01	
501	800,000	1.12969E-05	3.43190E-01	
502	850,000	1.03944E-05	3.43224E-01	
503	900,000	9.52728E-06	3.43247E-01	
504	950,000	8.70495E-06	3.43264E-01	
505	1,000,000	7.93284E-06	3.43276E-01	

ATTACHMENT III

SCOPING CALCULATIONS FOR IN-PACKAGE MASS TRANSPORT ENHANCEMENTS BY NATURAL CONVECTION

ATTACHMENT III

SCOPING CALCULATIONS FOR IN-PACKAGE MASS TRANSPORT ENHANCEMENTS BY NATURAL CONVECTION : WORKSHEET DT_Scope IN MICROSOFT EXCEL 97 SR-2 SPREADSHEET CodispNatCirc.xls

	A	B	C	D
1	18"DOE TRIGA SNF CANISTER IN CODISPOSAL WP	ΔT = 18	ΔT = 12	ΔT = 8
2	Screening Analysis for In-Package Buoyant Circulation			
3				
4				
5	*Parameter Specifications*			
6	Outer Diameter [m] (Do, Inside of WP)	1.8800E+00	1.8800E+00	1.8800E+00
7	Inner Diameter [m] (Di, Outside of DOE SNF Canister)	4.5720E-01	4.5720E-01	4.5720E-01
8	Fluid Kinematic Viscosity [m^2/s] (nu, SAE 50 oil)	5.7000E-04	5.7000E-04	5.7000E-04
9	Thermal Diffusivity [m^2/s] (alpha, from Pr for water and oil viscosity)	3.2000E-04	3.2000E-04	3.2000E-04
10	Schmidt Number (Sc, for Benzoic Acid)	9.1300E+02	9.1300E+02	9.1300E+02
11	Volumetric Coefficient of Fluid Thermal Expansion [1/K] (beta, Water)	7.5010E-04	7.5010E-04	7.5010E-04
12	Temperature Drop [ΔT, Centigrade]	1.8000E+01	1.2000E+01	8.0000E+00
13	Acceleration Due to Gravity [m/s^2] (g)	9.8067E+00	9.8067E+00	9.8067E+00
14	Degradation Product Hydrodynamic Permeability [m^2] (K, upper bound for wire crimps)	1.0000E-04	1.0000E-04	1.0000E-04
15				
16	*Calculations*			
17	Annular Gap Dimension, delta =(Do - Di)/2	0.7114	0.7114	0.7114
18				
19	*Ra for Clear Fluid*			
20	Ra	2.6136E+05	1.7424E+05	1.1616E+05
21				
22	*Intrinsic Ra for Porous Degradation Product Mixture*			
23	Ra-poros	5.1642E+01	3.4428E+01	2.2952E+01
24				
25	*Geometric Correction*			
26	Correction Factor	0.178579097	0.178579097	0.178579097
27				
28	*Corrected Ra and Sh for Clear Fluid*			
29	Ra-ann	4.6673E+04	3.1115E+04	2.0743E+04

	E	F	G	H
1	ΔT = 4	ΔT = 2	ΔT = 1	ΔT = 0.5
2				
3				
4				
5				
6	1.8800E+00	1.8800E+00	1.8800E+00	1.8800E+00
7	4.5720E-01	4.5720E-01	4.5720E-01	4.5720E-01
8	5.7000E-04	5.7000E-04	5.7000E-04	5.7000E-04
9	3.2000E-04	3.2000E-04	3.2000E-04	3.2000E-04
10	9.1300E+02	9.1300E+02	9.1300E+02	9.1300E+02
11	7.5010E-04	7.5010E-04	7.5010E-04	7.5010E-04
12	4.0000E+00	2.0000E+00	1.0000E+00	5.0000E-01
13	9.8067E+00	9.8067E+00	9.8067E+00	9.8067E+00
14	1.0000E-04	1.0000E-04	1.0000E-04	1.0000E-04
15				
16				
17	0.7114	0.7114	0.7114	0.7114
18				
19				
20	5.8079E+04	2.9039E+04	1.4520E+04	7.2599E+03
21				
22				
23	1.1476E+01	5.7380E+00	2.8690E+00	1.4345E+00
24				
25				
26	0.178579097	0.178579097	0.178579097	0.178579097
27				
28				
29	1.0372E+04	5.1858E+03	2.5929E+03	1.2965E+03

	I	J
1	SYMBOLIC REPRESENTATION	SAMPLE EXCEL INSTRUCTION
2	OF MANIPULATION PERFORMED	PERFORMED AT THIS ROW
3	AT THIS ROW	
4		
5		
6	USER INPUT	N/A
7	USER INPUT	N/A
8	USER INPUT	N/A
9	USER INPUT	N/A
10	USER INPUT	N/A
11	USER INPUT	N/A
12	USER INPUT	N/A
13	USER INPUT	N/A
14	USER INPUT	N/A
15		
16		
17	delta =(Do - Di)/2	=(B$6-B$7)/2
18		
19		
20	Ra = (beta*ΔT*g*(delta)^3)/(nu*alpha) : Eq. 23 in AMR	=(B$11*B$12*B$13*B$17^3)/(B$8*B$9)
21		
22		
23	Ra-porous = (beta*ΔT*g*K*delta)/(nu*alpha) : Eq. 24 in AMR	=(B$11*B$12*B$13*B$14*B$17)/(B$8*B$9)
24		
25		
26	Correction Factor =(ln(Do/Di))^4/((delta)^3*(Do$^{-3/5}$ + Di$^{-3/5}$)^5) : Eq. 22 in AMR	=(LN(B$6/B$7))^4/((B$17^3)*(B$6^(-(3/5))+B$7^(-(3/5)))^5)
27		
28		
29	Ra-ann = Ra*Correction Factor : Eq. 22 in AMR	=B$20*B$26

	A	B	C	D
30	Eta	5.672185769	5.125398426	4.631320287
31	Sh	5.672185769	5.125398426	4.631320287
32				
33	Corected Ra and Sh for Porous Degradation Product Mixture			
34	Ra-ann-porous	9.2222E+00	6.1481E+00	4.0988E+00
35	Eta-porous	0.6725019	0.607674064	0.549095502
36	Sh-porous	1	1	1
37				
38				
39				
40	*Tabular Results for Graph*	ΔT [Centigrade]	Sh	Sh-porous
41		5.0000E-01	2.3157E+00	1.0000E+00
42		1.0000E+00	2.7538E+00	1.0000E+00
43		2.0000E+00	3.2748E+00	1.0000E+00
44		4.0000E+00	3.8945E+00	1.0000E+00
45		8.0000E+00	4.6313E+00	1.0000E+00
46		1.2000E+01	5.1254E+00	1.0000E+00
47		1.8000E+01	5.6722E+00	1.0000E+00

	E	F	G	H
30	3.894460627	3.274837981	2.753799518	2.315660143
31	3.894460627	3.274837981	2.753799518	2.315660143
32				
33				
34	2.0494E+00	1.0247E+00	5.1234E-01	2.5617E-01
35	0.461732439	0.388269153	0.326494139	0.274547751
36	1	1	1	1
37				
38				
39				
40				
41				
42				
43				
44				
45				
46				
47				

	I	J
30	Eta = $0.386*(Sc/(Sc+0.861))^{1/4}*(Ra\text{-}ann)^{1/4}$: Eq. 21 in AMR	=0.386*((B$10/(B$10+0.861))^(0.25))*(B$29)^(0.25)
31	IF Eta > 1, THEN Sh = Eta ; ELSE Sh = 1 : Eq. 20 in AMR	=IF(B$30>1,B$30,1)
32		
33		
34	Ra-ann-porous = Ra-porous*Correction Factor : Eq. 22 in AMR	=B$23*B$26
35	Eta-porous = $0.386*(Sc/(Sc+0.861))^{1/4}*(Ra\text{-}ann\text{-}porous)^{1/4}$: Eq. 21 in AMR	=0.386*((B$10/(B$10+0.861))^(0.25))*(B$34)^(0.25)
36	IF Eta-porous > 1, THEN Sh-porous = Eta-porous ; ELSE Sh-porous = 1 : Eq. 20 in AMR	=IF(B$35>1,B$35,1)
37		
38		
39		
40		
41	COPY RESULTS FROM COLUMN H ; ROWS 12, 31 and 36	=$H$31
42	COPY RESULTS FROM COLUMN G ; ROWS 12, 31 and 36	=$G$31
43	COPY RESULTS FROM COLUMN F ; ROWS 12, 31 and 36	=$F$31
44	COPY RESULTS FROM COLUMN E ; ROWS 12, 31 and 36	=$E$31
45	COPY RESULTS FROM COLUMN D ; ROWS 12, 31 and 36	=$D$31
46	COPY RESULTS FROM COLUMN C ; ROWS 12, 31 and 36	=$C$31
47	COPY RESULTS FROM COLUMN B ; ROWS 12, 31 and 36	=$B$31

ATTACHMENT IV

GEOMETRY CALCULATIONS FOR TRIGA SNF

ATTACHMENT IV

Geometry Calculations for TRIGA SNF

IV-1 Ratio of Cross-sectional Areas of Constituents

The cross sectional area of the different constituents (fuel, basket, DOE-SNF canister) has been utilized to obtain the area fractions (CRWMS M&O 2000a, Sections 2.1.3 and 2.1.4). Most of the dimensions are shown in figure below

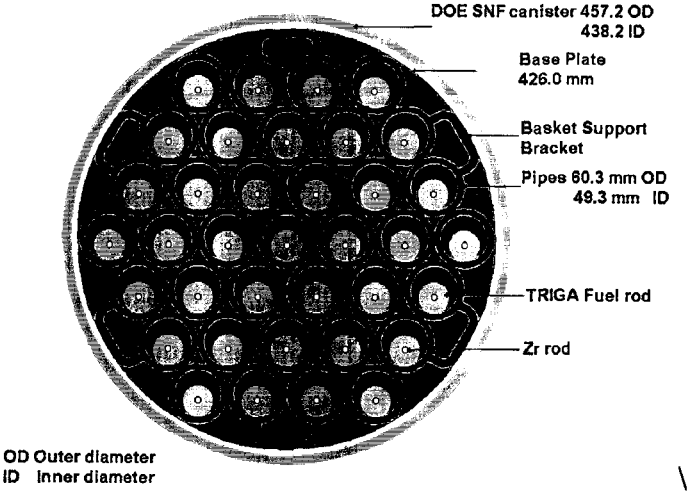

Cross sectional area of DOE-SNF canister:
$A_{DOE\text{-}SNF} = \pi\cdot(ID_{DOE\text{-}SNF})^2/4 = \pi\cdot 438.2^2/4$
$A_{DOE\text{-}SNF} = 1508\ cm^2$

Cross sectional area of basket tubes:
For one tube, $A_{tube} = \pi\cdot(OD_{tube})^2/4 - \pi\cdot(IDtube)^2/4$
$= \pi \cdot (6.03^2\text{-}4.93^2)/4 = 9.469\ cm^2$.

There are 37 tubes in the basket structure, thus:
$A_{Basket} = 37 \cdot A_{tube} = 37\cdot 9.469 = 350.3\ cm^2$

Cross sectional area of fuel rods:
$A_{rod} = \pi\cdot(D_{rod})^2/4 = \pi\cdot 3.754^2/4 = 11.07\ cm^2$

There are 37 fuel rods in the cross section, thus:
$A_{rod\text{-}total} = 37 \cdot 11.07 = 409.5\ cm^2$

For degraded mode assume that there is a volumetric expansion of basket structure of 2 times. This requires that area of the basket structure is 2 times the value given above, i.e.,
$A_{Degraded\text{-}basket} = 2 \cdot 350.3 = 701\ cm^2$

IV-2 Ratio of Cross-sectional Areas of Constituents (i.e., area fraction for fuel)

$= A_{rod\text{-}total}/(A_{Degraded\text{-}basket}+A_{rod\text{-}total}) = 410\ cm^2/(701\ cm^2 + 410\ cm^2)$ = approx **0.36** (actual value is 0.369 but lower rounding is used to account for basket brackets shown in figure above).

IV-3 Cross sectional area of DOE-SNF canister

$A_{DOE\text{-}SNF} = \pi\cdot(ID_{DOE\text{-}SNF})^2/4 = \pi\cdot 438.2^2/4$
$A_{DOE\text{-}SNF} =$ **1508 cm^2**

IV-4 Area of 37 Fuel Rods and Basket Tubes

Cross sectional area of basket tubes: for one tube $A_{tube} = \pi\cdot(OD_{tube})^2/4 - \pi\cdot(IDtube)^2/4$
$= \pi \cdot (6.03^2-4.93^2)/4 = 9.469\ cm^2$.

There are 37 tubes in the basket structure, thus:
$A_{Basket} = 37 \cdot A_{tube} = 37\cdot 9.469 = 350.3\ cm^2$

Cross sectional area of fuel rods:
$A_{rod} = \pi\cdot(D_{rod})^2/4 = \pi\cdot 3.754^2/4 = 11.07\ cm^2$

There are 37 fuel rods in the cross section, thus:
$A_{rod\text{-}total} = 37 \cdot 11.07 = 409.5\ cm^2$

Area of 37 fuel rods and basket tubes = $A_{rod\text{-}total} + A_{Basket} = 409.5 + 350.3 =$ **759.8 cm^2**